Cell dynamics and genetic regulation in the zebrafish hindbrain morphogenesis

Mageshi Kamaraj

université
PARIS-SACLAY

Dynamique cellulaire et régulation génétique de la morphogenèse du cerveau postérieur du poisson zèbre

Cell dynamics and genetic regulation of zebrafish hindbrain morphogenesis

Thèse de doctorat de l'université Paris-Saclay

École doctorale n° 568 , signalisations et réseaux intégratifs en biologie (Biosigne)
Spécialité de doctorat : aspects moléculaires et cellulaires de la biologie
Graduate School : Life Sciences and Health Référent : Faculté de médecine

Thèse préparée dans l'unité de recherche **BioEmergences** (Université Paris-Saclay, CNRS) et **Institut des Neurosciences Paris-Saclay** (Université Paris-Saclay**,** CNRS), 91400 sous la direction de **Monique FRAIN**

Thèse soutenue à Paris, le 09 Mars 2022, par

Mageshi KAMARAJ

Composition du Jury

Sophie CREUZET DR, CNRS, NeuroPSI, Saclay	Présidente
Claudio ARAYA Assistant Professor, Universidad Astral de Chile	Rapporteur & Examinateur
Cristina PUJADES Professor, Universitat Pompeu Fabra, Barcelona	Rapportrice & Examinatrice
Paula ALEXANDRE Group leader, University College London	Examinatrice
Anne-Hélène MONSORO-BURQ Professor, Université Paris-Saclay	Examinatrice
Monique FRAIN CR, CNRS, MSC, Paris	Directrice de thèse

THÈSE DE DOCTORAT

NNT : 2022UPASL015

Acknowledgements

I would like to thank everyone I met during this journey!

First, I would like to thank Nadine for giving me the opportunity and resources to pursue a PhD in BioEmergences lab and for all the scientific discussions. My sincere thanks to my PhD supervisor, Monique. She has been very supportive and provided great guidance on the thesis project. I have learnt a lot from her from paying attention to details in science to some great life advice. Merci Monique! Beyond PhD, she lent her help through personal challenges I encountered during my stay in France. It means a lot to me. I would also like to thank my thesis committee members, Dr David Bensimon and Dr Paula Alexandre for being encouraging and for valuable feedback during the annual review meetings and thesis defense. I thank very much the reviewers of my thesis manuscript, Dr Cristina Pujades and Dr Claudio Araya and examiners Dr Anne-Hélène Monsoro-Burq and Dr Sophie Crezuet for the insightful discussion and suggestions during the defense.

I am happy to have met all the past and present BioEmergences lab members during my PhD study. Thanks a bunch to Thierry for all the cool algorithms and beautiful movies and caring for the students beyond PhD life. I thank Antonio and Fanny most warmly for introducing me to all lab approaches. They are excellent teachers and great labmates. Hanh and Svetlana were always there for any help related to work and life in France. All the car rides and the travel time for out-of-station meetings were fun-filled. Cheers and many thanks to them. Big thanks to Maxime for fish lab assistance and his sweet and quick effort to learn English to help us. I wish to thank Mark for helping us with the workflow and being a nice officemate, Sylvia for always being a positive energy and for her advice on microscopy and Elena for her guidance with photo-conversion experiments and for her support during the course of PhD. I would like to thank my colleagues in Neuro-PSI building and MSC, Paris (during last six months) for providing me the friendly environment and all the members of fish facility.

I am thankful to Dr Daniel Boujard for providing the extension of my PhD funding due to the Covid-19 pandemic. I am also thankful to all the administrative people especially Amparo and Marwa who helped me with the paperwork I had to deal with CNRS and as a foreigner in France. I sincerely appreciate the experience I had with ImageInlife ITN program. It has personally helped me to have a view on the global and scientific world. Thanks a lot to Dr Karol Mikula and the lab members especially Seol ah for the warm welcome during my one month secondment in Bratislava. I thank Balaz (STUBA) and Joel (MMU) for the collaboration work. I am grateful to Antonio, Aswini, Manoj, Sourav and Kartik for proof-reading and having helped me improve the thesis manuscript. Thanks

to Nandha and Pratik for their assistance on statistical analysis and Vignesh for illustrator tricks and his big moral support.

I acknowledge Maison de l'inde (CIUP) and friends there for giving me a residence with lively environment for the past four years. All the cultural exchanges with students from all over the world and different states of India helped me grow into a better person. I am grateful to Raj, Jerda, my little angel, Brenda, Sourav, Shweta, Kartik and my cutie pie, Thea for being a home away from home. Thanks to Jahnavi, Gentle, Biji and Shweta D for all the fun times and care. Cheers to Shruti for all the pleasant chats we had during the writing phase of our PhD theses.

I am thankful to Dr Chetana Sachidanandan, my previous lab PI, for inspiring me on many levels including pursuing a PhD. I take this opportunity to express my gratitude to my dear friends from school, college, IGIB (Delhi) and other places for putting up with all the frustrations and joys of PhD life and for constantly checking up on me and lending moral support all these years despite the hundreds/thousands of miles distance. Special thanks to Roja for all the weekly calls. I can't thank Moulee enough for being there during some of the toughest times in my life during PhD and his immense support during the writing process.

I am grateful to my family for having a strong belief in me and my decisions throughout my academic life. My PhD study was made possible because of my parents' value in education and their sincere effort in providing that to me and my brother.

Abstract

The brain is often considered the most complex organ. During embryonic development, the brain is classically divided into three functional and anatomical units namely, fore, mid and hindbrain. Hindbrain, the posterior part utilises segmentation as a strategy to organise its diverse range of cranial nerves and the streams of neural crest cells. The transient segmentation of hindbrain leads to 7/8 repeated cellular units of segments in the antero-posterior axis (AP) called rhombomeres. Hindbrain segmentation patterns the head and is conserved among vertebrates. Molecular mechanisms that underlie hindbrain segmentation have been vastly investigated. We aim to study the formation of the rhombomeres at cellular level in zebrafish, a vertebrate model at the forefront of developmental biology. We need the precise fate map and the cell dynamics that lead from the progenitors' domains to the organ. The current fate map of the zebrafish central nervous system (CNS) at early and late gastrula stages was published in 1995. It was obtained through sparse lineage tracing with a fluorescent dye. The precise border of the rhombomere progenitor domains and the cell dynamics that shape the hindbrain are unknown. Utilising advanced microscopy imaging of transgenic zebrafish lines and automated image processing tools, we developed a method to reconstruct the cell lineage of rhombomeres r2-r6 from mid-gastrulation through early neurulation. We provide a finer and dynamic fate map of zebrafish hindbrain from 6hpf till 15hpf. The rhombomere progenitor domains are aligned along the AP and dorso-ventral (DV) axes as early as the shield stage. Rhombomere progenitor domains exhibit AP organisation parallel to the blastoderm margin. The DV segregation of the rhombomeres is set by distribution of the progenitors along the DV axis at the shield stage. Progenitors located at the most dorsal part of the blastoderm will form the ventral domain of the rhombomeres. Our study gives insights into the clonal origin, cell proliferation and migration paths of hindbrain's rhombomere progenitors throughout the early steps of the organ morphogenesis.

We used our method to explore the role of the signalling pathways Retinoic acid (RA) and Fibroblast Growth Factor (FGF) in hindbrain morphogenesis. RA and FGF morphogen gradients are thought to specify and pattern the hindbrain primordia into seven segments with different identities. RA inhibition upon drug treatment leads to progressive loss of posterior rhombomeres in a concentration dependent manner. Concomitantly, there is a loss of expression of their molecular markers. It is presumed the expansion of anterior rhombomeres happens at the expense of the posterior ones. How the morphogenesis of the progenitor domains leads to this phenotypic defect is not known. We investigate the cellular events, cell proliferation and cell movements from the dynamic fate map under RA-null condition. We identified the progenitor domains whose organisation is in correspondence with the position and size of the modified segments i.e. the expansion

of anterior progenitors' domains. We also observed a delayed convergence movement that is an early consequence of the altered RA gradient. Consequently, it results in ectopic neural progenitor accumulations and neural tube defects. Our phenotype is reminiscent of the *trilobite* mutant of *vangl2,* that is a component of planer cell polarity (PCP) pathway. It was shown in mouse *Raldh2-/-* embryo that RA deficiency causes a strong downregulation of *Vangl2* and *Fzd3* at the level of hindbrain and spinal cord. Altogether our data suggests that neural tube defects in zebrafish RA-null embryo is due to the alteration in the PCP signalling. We demonstrated the community effect of RA signalling on target genes and hindbrain morphogenesis. Optogenetic restoration of RA in r5 progenitors at mid-gastrulation on one half of the embryo rescued the whole posterior rhombomere formation.

Résumé

Au cours du développement embryonnaire, le cerveau est classiquement divisé en trois unités fonctionnelles et anatomiques, à savoir le cerveau antérieur, moyen et postérieur. Le cerveau postérieur utilise la segmentation comme stratégie pour organiser les nerfs crâniens et les flux de cellules de la crête neurale. La segmentation transitoire du cerveau postérieur conduit à 7/8 unités cellulaires répétées le long de l'axe antéro-postérieur (AP) appelés rhombomères (r). Ce processus conservé au cours de l'évolution établit le plan de la tête des vertébrés. Les mécanismes moléculaires sous-jacents à la segmentation du cerveau postérieur ont été largement étudiés. Notre objectif est d'étudier la formation des r au niveau cellulaire chez le poisson zèbre, un modèle vertébré star de la biologie. Nous avons besoin de la carte précise du destin et de la dynamique cellulaire qui mène du domaine des progéniteurs à l'organe. La carte actuelle du destin du système nerveux central du poisson aux stades précoce et tardif de la gastrula a été publiée en 1995. Elle a été obtenue par une reconstruction partielle du lignage grâce à un colorant fluorescent. La frontière précise des domaines de progéniteurs des r et les dynamiques cellulaire qui façonnent le cerveau postérieur sont inconnues. En utilisant l'imagerie par microscopie de pointe de poissons transgéniques et des outils de traitement d'image automatisés, nous avons reconstruit le lignage de r2-r6 de la mi gastrulation à la neurulation précoce. Nous fournissons une carte du destin plus fine et dynamique du cerveau postérieur de 6 à 15hpf. Les domaines de progéniteurs sont alignés le long des axes AP et dorso-ventral (DV) dès le stade du bouclier embryonnaire. Ils présentent une organisation AP parallèle à la marge du blastoderme. La ségrégation DV des r est établie par une distribution des progéniteurs le long de l'axe DV tel que ceux situés dans la partie dorsale du blastoderme vont former le domaine ventral des r. Notre étude donne un aperçu de l'origine clonale, de la prolifération cellulaire et des voies de migration des progéniteurs au cours de la mise en place du rhombencéphale.

Nous avons exploré le rôle des voies de signalisation de l'acide rétinoïque (AR) et du facteur de croissance des fibroblastes (FGF) dans la morphogenèse du cerveau postérieur. On pense que les gradients des morphogènes AR et FGF spécifient et modèlent les ébauches du cerveau postérieur en sept segments d'identités distinctes. L'inhibition de l'AR à l'aide de drogue entraîne une perte progressive des r postérieurs, dépendante de sa concentration. De même, il y a une perte d'expression de leurs marqueurs moléculaires. On suppose que l'expansion des r antérieurs se fait au détriment des postérieurs. Nous ne savons pas comment la morphogenèse des

domaines de progéniteurs conduit à ce défaut. Nous avons établi la carte dynamique du destin du cerveau postérieur de l'embryon AR nul. L'organisation des domaines de progéniteurs est en correspondance avec la position et la taille des segments modifiés, i.e. l'expansion des domaines des progéniteurs antérieurs. De plus, le mouvement de convergence des cellules est retardé ce qui est une conséquence précoce du gradient AR altéré. Il en résulte des accumulations ectopiques de progéniteurs neuraux et des anomalies du tube neural. Notre phénotype rappelle celui du mutant *trilobite* de *Vangl2* acteur dans la voie de signalisation de polarité cellulaire planaire (PCP). Il a été montré dans l'embryon de souris *Raldh2-/-* que le déficit en AR provoque une forte inhibition de *Vangl2* et *Fzd3* au niveau du cerveau postérieur et de la moelle épinière. Dans l'ensemble, nos données suggèrent que les défauts du tube neural dans l'embryon AR nul sont dus à l'altération de la signalisation PCP. De plus, nous avons démontré l'effet de communauté de l'AR sur les gènes cibles et la morphogenèse du cerveau postérieur par la restauration optogénétique du morphogène dans l'embryon vivant.

Résumé détaillé

Introduction

Le développement embryonnaire se définit par la construction de l'ensemble du corps animal à partir d'une seule cellule, peu après la fécondation d'un ovule par un spermatozoïde. Les cellules se divisent et meurent, se déplacent, s'intercalent, changent de forme et migrent sur de grandes distances pour sculpter l'embryon dans sa forme et sa taille finales de manière spécifique à l'espèce. Les cellules se déplacent et se différencient en réponse à des signaux afin de se modeler et de construire divers organes dans une forme spécifique à leur position déterminée (Ashe et Briscoe, 2006 ; Kerszberg et Wolpert, 2007). Les organismes multicellulaires possèdent des organes aux structures complexes pour exécuter des fonctions très fines et complexes. Souvent, ils utilisent une feuille de route simple pour construire les structures complexes avec une diversité régionale qui finalement facilite leur fonction. La segmentation est l'une des stratégies largement employée au cours du développement embryonnaire (Lawrence et Struhl, 1996). Le cerveau est l'organe le plus complexe avec une énorme variété de neurones. Au cours de l'embryogenèse, le cerveau forme trois vésicules principales : le cerveau antérieur, le cerveau moyen et le cerveau postérieur. Chez les vertébrés, peu après la fin de la gastrulation, l'ébauche du cerveau postérieur se subdivise transitoirement en sept ou huit segments répétés le long de l'axe antéro-postérieur (AP). Chaque segment est appelé rhombomère (r). L'organisation segmentée du cerveau postérieur détermine et organise l'émergence des neurones et leurs connexions avec la tête. Les flux de crête neurale dépendent également de la segmentation du cerveau postérieur. La plupart des structures craniofaciales, le système nerveux périphérique et le tissu conjonctif sont dérivés des cellules de crête neurale qui émergent de la partie dorsale du tube neural.

Les mécanismes moléculaires qui sous-tendent la segmentation du cerveau postérieur ont été largement étudiés. Notre objectif est d'étudier la formation des rhombomères à l'échelle de la cellule chez le poisson zèbre, un modèle de vertébré à la pointe de la biologie du développement. L'état de l'art de la carte dynamique du destin du cerveau postérieur du poisson zèbre provient d'une reconstruction partielle du lignage cellulaire par une méthode conventionnelle, réalisé en 1995. Elle ne définit pas précisément les frontières des domaines de progéniteurs des rhombomères. Il manque les dynamiques cellulaires qui sous-tendent la formation des segments. Le réseau de régulation génétique impliqué dans le processus a été largement élucidé au travers d'expériences de perte et gain de fonction de gènes et de l'analyse consécutive des gènes en aval. L'approche cellulaire devrait permettre d'élucider les comportements cellulaires qui conduisent à des défauts phénotypiques lors de conditions pathologiques. Elle devrait fournir des informations sur les dynamiques, les lignages et les mouvements cellulaires. Les paramètres quantitatifs

du comportement cellulaire tels que la prolifération, la vitesse, la direction et la persistance du voisinage seront utilisés pour caractériser les tout premiers effets phénotypiques d'une perturbation génétique. L'intégration des processus cellulaires avec la régulation génétique est essentielle pour la compréhension complète des processus morphogénétiques qui sous-tendent la segmentation du cerveau postérieur.

Objectifs de la thèse

Dans ma thèse, nous cherchons à comprendre la morphogenèse du cerveau postérieur du poisson zèbre au travers de la visualisation, la quantification et la reconstruction du lignage cellulaire des rhombomères individuels, de la mi-gastrulation au début de la neurulation, dans des conditions normales et pathologiques telles que l'inhibition des voies de signalisation AR et FGF. Nous réaliserons une imagerie *in vivo* 3D+temps d'embryons de poisson zèbre par microscopie 2-photon. Nous utiliserons la lignée de poisson transgénique spécifique du cerveau postérieur, *krox20:eGFP-Hras*, qui marque les rhombomères présomptifs r3 et r5. Elle sert de marqueur précoce de formation de ces rhombomères avant l'apparition morphologique des segments. Comme il s'agit des rhombomères centraux, elle nous permet de localiser également les rhombomères adjacents. Nous utiliserons la chaîne de traitements d'image, workflow BioEmergences, pour reconstruire l'arbre du lignage cellulaire des rhombomères r2-r6 depuis la mi-gastrulation jusqu'en début de neurulation, à partir des données d'imagerie 3D+temps. Les jeux de données d'imagerie permettront également d'analyser le comportement des cellules progénitrices au cours de ce processus morphogénétique. Ainsi, les objectifs spécifiques de la thèse sont les suivants:

1) Établir la carte du destin du cerveau postérieur et sa dynamique cellulaire en condition normale depuis la mi-gastrulation jusqu'à la neurulation précoce.
2) Définir le rôle de l'AR dans la morphogenèse du cerveau postérieur à l'échelle de la cellule par l'inhibition de la signalisation de l'AR en utilisant un inhibiteur chimique (DEAB), par l'établissement de la carte du destin et l'analyse du comportement cellulaire. De plus, nous évaluons l'effet de communauté de la signalisation AR pendant la morphogenèse du cerveau postérieur en utilisant des approches optogénétiques.
3) Définir le rôle du FGF dans la morphogenèse du cerveau postérieur à l'échelle de la cellule par l'inhibition de la signalisation FGF en utilisant un inhibiteur chimique (SU5402), par l'établissement d'une carte du destin du rhombencéphale et l'analyse du comportement de ses progeniteurs.

Observation et discussion

Carte dynamique du destin des rhombomères r2-r6

Nous avons établi une méthode pour étudier quantitativement la morphogenèse du cerveau postérieur chez le poisson zèbre, depuis la mi-gastrulation jusqu'au début de la neurulation, grâce à l'imagerie 3D+temps d'embryon transgénique vivant spécifique du cerveau postérieur. Nous avons fourni une carte dynamique du destin du cerveau postérieur chez le poisson zèbre avec une plus grande précision comparé à l'état de l'art en tirant parti d'avancées techniques. Nous avons démontré que l'engagement clonal des progéniteurs de rhombomère est atteint vers 8 hpf. L'origine clonale du rhombomère ainsi définie est en accord avec les expériences de transplantation montrant que l'engagement de l'identité neurale régionale se produit à 80% d'épibolie (Woo et Fraser, 1995). Les progéniteurs dorsaux et ventraux du rhombencéphale sont localisés en position plus latérale et médiale respectivement par rapport au bouclier embryonnaire à la mi-gastrulation. Les deux populations se déplacent dans la même direction vers la ligne médiane, cependant à 11 hpf les cellules médiales subissent une migration postérieure et suivent ensuite un mouvement vers l'avant. En même temps, elles subissent également un mouvement vers l'intérieur pour s'internaliser. Les cellules latérales qui sont loin de la ligne médiane commencent à accélérer et convergent directement vers la ligne médiane. De cette façon, elles se placent au-dessus des cellules médiales qui se déplacent vers l'intérieur. Ainsi, nous avons montré que les progéniteurs empruntent des voies de migration distinctes pour orchestrer la structure de la quille neurale en 3D à partir de cellules de la plaque neurale en 2D avec une mesure quantitative des comportements cellulaires

Le rôle du RA dans la morphogenèse du cerveau postérieur

L'AR, qui est impliqué dans la postériorisation du neurectoderme, est synthétisé par la RALDH dans la couche du mésoderme à proximité de la marge dès la fin du stade blastula de l'embryon de poisson zèbre (Schier et Talbot, 2005). Afin d'établir la base de l'intégration de la signalisation moléculaire et des comportements cellulaires dans la mise en place du cerveau postérieur et dans la spécification de l'identité cellulaire, nous avons reconstruit les lignages cellulaires dans des embryons témoins et dans un fond de signalisation AR nulle en présence de la drogue diéthylaminobenzaldéhyde (DEAB). Nous avons obtenu la carte du destin du cerveau postérieur après inhibition de l'AR. Elle montre que l'antériorisation du cerveau postérieur est dûe à un changement d'identité des progéniteurs postérieurs, sans augmentation du taux de prolifération cellulaire. Nous avons constaté que les domaines antérieurs r3 et r4 ont augmenté de 200% après

traitement par le DEAB, par la mesure du volume via une segmentation semi-automatique et une forte réduction du domaine r5. Nous n'avons pas trouvé de changement significatif du taux de prolifération/la longueur du cycle cellulaire après inhibition de l'AR. Cela suggère fortement que les progéniteurs des rhombomères postérieurs adoptent un destin antérieur en raison du déplacement du gradient du morphogène AR et du destin cellulaire correspondant. La segmentation des domaines et leur reconstruction 3D ont montré que le domaine r5 réduit se limite à la partie dorsale du tube neural, ce qui suggère que les cellules ventrales sont plus sensibles à la perturbation de l'AR. Nous avons montré que les progéniteurs des cellules ventrales au résidu r5 ont acquis l'identité r4 en suivant à rebours ces cellules qui n'expriment pas *krox20*. Dans l'ensemble, notre étude dissèque le phénotype d'antériorisation du cerveau postérieur après inhibition de la voie AR.

Nous avons constaté que la convergence est retardée après inhibition de l'AR, par mesure du taux de compaction du neurectoderme. En conséquence, nous observons un défaut de morphologie du tube neural chez 20 à 40 % des embryons de deux lignées transgéniques établies en fonds *casper* et WT/Tü. Ce défaut est très réminiscent de celui des mutants *vangl2-/-* dans lesquels la convergence est retardée. La signalisation PCP établit la polarité des cellules durant les mouvements de convergence extension. Une convergence retardée conduit à une plaque neurale plus large. La division de type C (division cellulaire avec franchissement de la ligne médiane par la cellule fille) qui est une activité intrinsèque dépendante du temps, se produit dans la région latérale de la plaque neurale et conduit à la formation d'une double ligne médiane apicale et, par conséquent, à la duplication du tube neural. Nous avons également recherché une potentielle interaction entre les voies AR et PCP. Il a été démontré que dans les embryons de souris *Raldh2-/-*, vangl2 et fzd3, qui sont nécessaires à la signalisation PCP, sont fortement inhibés dans le cerveau postérieur et la moelle épinière aux stades E8.25-E8.75 (Tuduce et al., 2009). Nos résultats suggèrent pour la première fois que l'acide rétinoïque pourrait contrôler la voie de signalisation PCP dans la morphogenèse du rhombencéphale chez le poisson zèbre.

Les gradients de morphogènes ne se forment pas seulement par simple diffusion mais par le transport actif de molécules de morphogènes à travers la matrice extracellulaire sur de longues distances (Rogers et Schier, 2011a). Pour comprendre la nature du gradient du morphogène AR et à quelle distance il agit dans le neuroectoderme présomptif, nous avons cherché à restaurer l'AR sélectivement dans des progéniteurs du rhombencéphale et avons analysé le sauvetage du rhombomère r5 qui en résulte. La photo-isomérisation de la forme inactive 13-cis RA en forme active all-trans-RA a été utilisée pour développer le contrôle spatio-temporel de l'activité AR (Xu et al., 2012). La même étude a montré que si l'AR était activé localement dans la région de la tête avant le stade bud, il était possible de corriger les défauts du cerveau postérieur chez les

embryons traités par le DEAB. Dans notre expérience, nous avons restauré l'AR spécifiquement dans les progéniteurs de r5 sur un côté de l'embryon au stade du bouclier par une illumination aux UV par microscopie confocale. Nous avons observé le sauvetage de l'ensemble du domaine r5 c.a.d de part et d'autre de l'axe AP du tube neural. Ce résultat indique que l'AR restauré dans les cellules est rapidement séquestré sur une longue distance et renforce l'idée d'un effet de communauté de l'AR sur ses gènes cibles et la morphogenèse du cerveau postérieur.

Le rôle des FGFs dans la morphogenèse du cerveau postérieur

Les FGFs contrôlent la spécification du mésoderme et les mouvements morphogénétiques au cours de la gastrulation. Ils établissent l'identité segmentaire dans l'ensemble du rhombencéphale. Le dernier rôle a été bien établi dans plusieurs études (Maves, Jackman et Kimmel, 2002 ; Walshe et al., 2002). Au stade précoce, FGF est nécessaire et doit être activé avant 5 hpf pour induire l'expression de nombreux gènes de patterning du cerveau postérieur (Roy et Sagerström, 2004). Nous montrons que l'inhibition de FGF de 4 à 6 hpf est suffisante pour perturber la mise en place du cerveau postérieur. Nous observons une réduction de r3 et r5 dans ces embryons. FGF est connu pour réguler les mouvements de convergence extension du mésoderme. L'inhibition de FGF chez l'embryon de poisson zèbre de 4 à 6 hpf affecte l'extension du plan du corps de l'embryon selon l'axe AP. Ainsi nous avons opté pour une nouvelle position de montage de l'embryon au stade de bouclier afin de capturer le développement du cerveau postérieur lors de nos imageries. Les jeux de données d'imagerie obtenus après traitement avec SU5402, inhibiteur de l'activité des récepteurs FGFs, seront exploités pour comprendre le rôle des FGFs au cours de la gastrulation en analysant le mouvement coordonné du mésendoderme et de l'ectoderme, grâce à l'analyse de divers paramètres cellulaires tels que la vitesse, les mouvements directionnels et autres. Les données d'imagerie recueillies peuvent être explorées en détail afin de comprendre le rôle des FGFs dans la formation du cerveau postérieur à l'échelle de la cellule grâce à l'obtention de la carte du destin des rhombomères individuels dans l'embryon traité au 5402.

La construction et l'utilisation de spécimens numériques à partir de données 3D+temps et de leurs équivalents simulés pour mettre en évidence la boîte noire des processus morphogénétiques reliant le génotype et le phénotype est actuellement à l'avant-garde d'une approche transdiciplinaire du développement embryonnaire.

Table of Contents

List of Figures

List of publication figures

List of appendix figures

List of tables

List of Movies

List of publication movies

List of abbreviations

3D	3 Dimensional
AP	Antero-posterior
BMP	Bone morphogenetic protein
CE	Convergent Extension
CNS	Central Nervous system
Cyp	Cytochrome P450
DEAB	N,N-diethylaminobenzaldehyde
DMSO	Dimethyl Sulfoxide
DoG	Difference of Gaussian
DV	Dorso-ventral
eGFP	enhanced Green Fluorescent Protein
Egr2	Early growth response 2
EVL	Enveloping Layer
FGF	Fibroblast Growth Factor
GRN	Gene Regulatory Network
Hox	Homeobox
hpf	hours post-fertilisation
mg	microgram
ml	millilitre
mM	millimolar
mRNA	messenger Ribo-Nucleic Acid
NA	Numerical Aperture
NCC	Neural Crest Cells
nm	nanometre
PCP	Planar Cell Polarity
r	rhombomere
RA	Retinoic Acid
RAR	Retinoic Acid Receptor
RARE	DNA elements that bind to retinoic acid (RA) receptors
RXR	Retinoid X Receptor
SU5402	2-[(1,2-dihydro-2-oxo-3H-indol-3-ylidene)methyl]-4-methyl-1H-pyrrole-3-propanoic acid
T	Time step
UV	Ultra-Violet
WNT	Wingless/Integrated gene
WT	Wild Type
YSL	Yolk Syncytial Layer
µg	Microgram
µl	Microlitre
µM	micromolar

Overview

In this thesis, we aim to study cellular mechanisms that underlie early hindbrain patterning using zebrafish as a model organism. Further, we aim to understand the role of signalling pathways Retinoic acid (RA) and Fibroblast Growth Factor (FGF) in the early cellular events of hindbrain segmentation. The thesis is divided into parts as follows,

-An introduction to zebrafish as a model, an overview of zebrafish early morphogenesis with emphasis on neural tube formation and the current CNS fate map at gastrula stages. It also provides comprehensive details, the signalling pathways involved during hindbrain segmentation and current model of Gene Regulatory Network (GRN). Further, I discuss the current approaches to study morphogenesis and finally, I state the aims of my PhD thesis.

-The methodology we established to perform long term *in vivo* imaging of early hindbrain morphogenesis in transgenic zebrafish reporter line using two-photon microscopy and reconstruction of cell lineages at individual rhombomere. Then, I explain the method to perform optogenetic restoration of RA in selective progenitors of RA-null embryos.

-The result section contains two parts: 1) The manuscript (in preparation) titled "Segmental organization of hindbrain progenitors during gastrulation: Implication of RA role in hindbrain patterning at cellular level". Fate map of hindbrain rhombomeres r2- r6 is established. The manuscript describes the cell behaviours during early hindbrain morphogenesis; AP segmental organization of rhombomeres and DV segregation of rhombomere cells from the shield stage. Further, the RA role in hindbrain morphogenesis at cellular level is elucidated. Restoration of RA in RA-null embryos using optogenetic tools demonstrated the community effect of RA on target gene and hindbrain morphogenesis. 2) The study of FGF role in hindbrain morphogenesis. It outlines the standardisation of chemical treatment to inhibit FGF signalling and imaging protocol for capturing early hindbrain morphogenesis upon FGF inhibition are presented. Further, the expected analysis is presented.

-The general discussion and perspective of the results. We aim to model hindbrain morphogenesis with quantitative parameters obtained from our 3D+time imaging data.

1. Introduction

1.1. Zebrafish as a model

Zebrafish (*Danio rerio*) is a tropical fish that belongs to teleost family. It has been a powerful vertebrate model especially in the field of developmental biology since 1980s (Veldman and Lin, 2008; Basu and Sachidanandan, 2013). Zebrafish are small, about 4-5cm (Figure 1.1) and require low cost and low maintenance. After the divergence of fish and mammals, whole genome duplication occurred in the lineage, leading to the teleost family (Gebo, 1988). Thus, zebrafish possesses two paralogue genes of their many mammalian counterpart orthologues. 71.4% of human genes have at least one zebrafish orthologue which makes it fairly comparable to humans (Howe *et al.*, 2013). High genome similarities and conserved physiology between humans and zebrafish make it an excellent model to study genetic diseases including developmental disorders. Developmental stages of zebrafish are well characterized (Kimmel *et al.*, 1995; Karlstrom and Kane, 1996). Zebrafish undergo ex-utero fertilization and embryonic development which makes it more accessible to investigate developmental events than mammalian models such as mice and rabbits which develop in-utero. Its high fecundity is advantageous for genetic manipulation and chemical drug screening experiments which require a large sample size. Additional advantages such as transparent nature of embryos at early stages and rapid embryonic development complemented with readily available transgenesis tools (Driever *et al.*, 1994; Suster *et al.*, 2009) make it an ideal model to visualise the individual cell movements and sub-cellular processes during morphogenesis using simple to advanced microscopes. Combined advanced microscopic techniques and computational tools are being used to perform reconstruction of cell lineages and further to dissect various morphogenetic events (Keller *et al.*, 2008; Wan *et al.*, 2019).

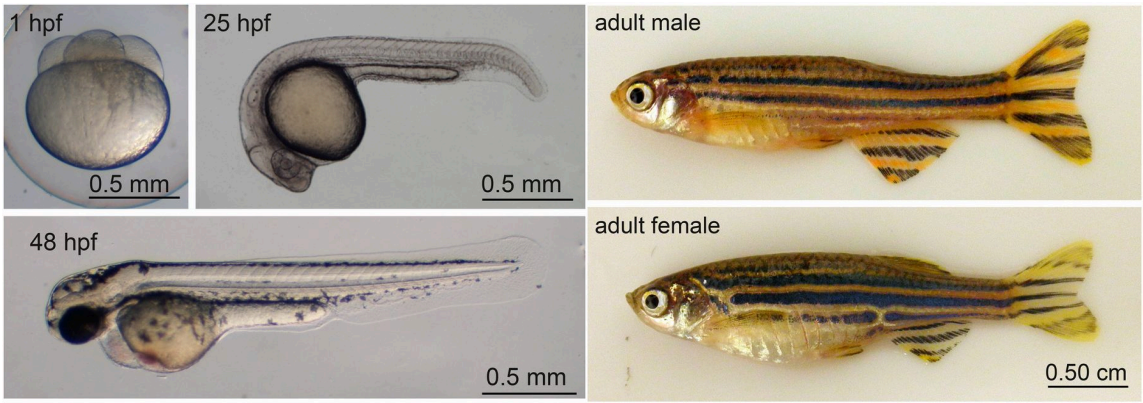

Figure 1. 1. Embryonic and adult stages of zebrafish.

Embryo and larva stages (left). Adult male and female zebrafish (right). Figure from (Holtzman *et al.*, 2016).

1.2. Zebrafish early morphogenesis : Emphasis on neural tube formation

1.2.1. Gastrulation

Gastrulation is a fundamental process of animal embryogenesis, where specification and formation of distinct germ layers occur. Further, anteroposterior (AP) and dorsoventral (DV) embryonic axes are established. In triploblastic animals, three germ layers are formed namely, ectoderm (outer), mesoderm (middle) and endoderm (inner). Ectoderm gives rise to nervous system and epidermis. Mesoderm gives rise to muscles, bones and circulatory system. Endoderm will develop into gastrointestinal tract and associated organs. Major morphogenetic movements that shape the embryo from a simple uniform mass of cells, the blastula to multi-layered gastrula are epiboly, internalisation, convergence and extension (Solnica-Krezel and Sepich, 2012). Epiboly enables thinning and spreading of blastoderm cells. During internalisation, the endoderm and mesoderm cells separate from ectoderm and internalise beneath the ectoderm. Convergence helps narrow the germ layers dorsoventrally. Concurrent extension elongates them antero-posteriorly. These morphogenetic components are evolutionarily conserved although there is species-specific differences in the underlying cell behaviours (Williams and Solnica-Krezel, 2020).

1.2.1.2. Zebrafish gastrulation

Morphogenesis of zebrafish embryo starts with the epiboly movement. During which, all three regions of the blastula stage embryo, the enveloping layer (EVL), deep cells and the yolk syncytial layer (YSL) spread towards the vegetal pole (Figure 1.2) (Pinheiro and Heisenberg, 2020). The progression of epiboly movement pauses briefly at 50% epiboly stage when other gastrulation movements begin and eventually completes at 10 hpf after engulfing the entire yolk. This event marks the end of gastrulation (Figure 1.2)(Bruce and Heisenberg, 2020). Zebrafish gastrulation starts at 5.3 hpf (50% epiboly) and lasts till 10 hpf (100% epiboly) (Warga and Kimmel, 1990). At 50% epiboly, cells start to accumulate at the embryonic margin and form a transient thickening called the germ ring. Internalization of mesendoderm cells beneath the ectoderm occurs first on the dorsal side of the germ ring margin and then proceeds at all points around the margin. On the dorsal side, it makes a prominent structure called the shield. Internalisation movements result in the formation of two layers namely epiblast and hypoblast (Figure 1.2B, C). The epiblast consists of ectoderm and pre-internalisation mesendoderm progenitors and hypoblast consists of internalised mesendoderm cells. Soon after internalisation, mesendoderm differentiates into mesoderm or endoderm progenitors. Endoderm cells engage in random walking over the yolk. The dorsal internalized mesoderm continues to migrate towards animal pole until the end of gastrulation and facilitates the formation of AP axis and head morphogenesis (Figure 1.2A). Cells on the

ventral side change direction at mid-gastrulation and move towards vegetal pole, where they will contact the dorsal mesoderm cells (Figure 1.2). Together, they contribute to tail morphogenesis. At 70% epiboly, all germ layer cells in the lateral regions start convergence and extension movements towards dorsal side which leads to AP extension of animal body axis, along with continued epiboly and anterior migration (Solnica-Krezel and Sepich, 2012; Pinheiro and Heisenberg, 2020a; Williams and Solnica-Krezel, 2020).

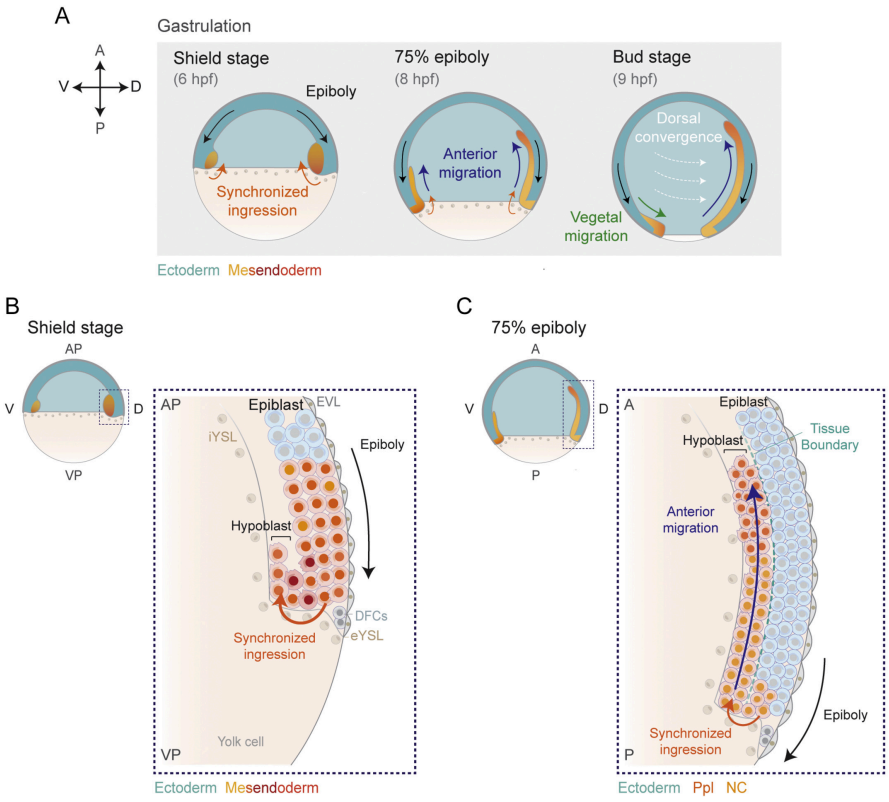

Figure 1. 2. Gastrulation movements in zebrafish embryo.

Schematic representation of the four major morphogenetic movements A) Cross section of the embryos at three gastrula stage are shown with animal pole up and the dorsal side to the right. Black and orange arrows indicate epiboly and internalization movements respectively. Mesendoderm progenitors in orange and red and the prospective ectoderm in light and dark blue. Following internalization, mesendoderm cells migrate towards the animal pole (blue arrows) and ventral-derived mesoderm progenitors eventually change direction and move towards vegetal pole (green arrows). White arrows indicates convergence and extension movement. (B) Mesendoderm internalization at shield stage. The magnified representation of the boxed area above shows that the onset of internalization movements gives rise to the formation of two cell layers—the hypoblast, composed of post-involution mesendoderm progenitors and the epiblast, which consists of ectoderm progenitors and pre-involution mesendoderm progenitors. (C) The magnified representation of the boxed area above highlights anterior migration of the dorsal axial mesendoderm and the characteristic separation of the germ layers at the epiblast/ hypoblast boundary at 75% epiboly. AP, Animal pole; VP, Vegetal pole; A, Anterior axis; P, Posterior axis; D, Dorsal side; V, Ventral side; EVL, Enveloping layer; YSL, Yolk syncytial layer (iYSL refers to internal YSL, eYSL designates the external YSL); DFCs, Dorsal Forerunner cells; Ppl, Prechordal plate; NC, Notochord. hpf- hours post-fertilization. Figure from (Pinheiro and Heisenberg, 2020).

1.2.1.3. Convergence and extension of neuroectoderm

After the completion of mesendoderm internalization, blastoderm cells that present on the surface of the embryo but beneath the enveloping layer constitute the ectoderm cells (Figure 1.2). Dorsal ectoderm cells give rise to neural tissue and the ventral cells develop into non-neural ectoderm such as the epidermis (Warga and Kimmel, 1990; Williams and Solnica-Krezel, 2020). During epiboly movement, neuroectoderm cells move towards vegetal pole. At mid-gastrulation, cells start to simultaneously undergo convergent extension towards the embryonic midline where they form the neural plate. Neuroectoderm cells exhibit similar movements of convergence extension with the underlying mesoderm cells. Cell behaviours such as directed migration, cell elongation and mediolateral intercalation underlie the convergence and extension of neuroectoderm cells to the embryonic dorsal midline. Polarised protrusions of neurectoderm cells drive their dorsal migration. Mediolateral intercalation facilitates narrowing and extension for the axis formation.

Regulation of neuroectoderm movements

BMP and FGF signalling gradients are known to specify various cell fates and morphogenetic movements during gastrulation. BMP (Bone morphogenetic protein) signalling specifies the ventral fate of the embryo and inhibits convergence and extension movement of ventral cells. High Bmp levels limits convergence and extension movement through negative regulation of genes involved in Planar Cell Polarity (PCP) such as *wnt11* and *wnt5a* (Myers, Sepich and Solnica-Krezel, 2002). The low BMP signalling in the dorsal cells restrict convergence and promote extension. BMP gradient also negatively regulates cell adhesion molecules and establish directional cell migrations during dorsal convergence of lateral cells (von der Hardt *et al.*, 2007). The cell behaviours of lateral region of gastrulating embryos are regulated by PCP signalling components such as vangl2 and wnt5b, extra-cellular matrix (ECM) organisation, and adhesion molecules such as N-cadherin (Jessen *et al.*, 2002; Kilian *et al.*, 2003; Love, Prince and Jessen, 2018). It is shown that wnt5b mediated activation of PCP signalling regulates cell elongation and convergent extension movements of neuroectoderm cells (Kilian *et al.*, 2003). Wnt11 also regulates convergence and extension movements of lateral cells during zebrafish gastrulation (Heisenberg *et al.*, 2000). In the *vangl2* mutant fishes, mediolateral intercalation and cell elongation of neuroectoderm cells are disrupted, resulting in short and wider neural plate (Jessen *et al.*, 2002). ECM, enriched with fibronectin and laminin proteins, is formed between the mesoderm and ectoderm during late gastrulation. Their recent study showed that the vangl2 expression at the cell surface depends on fibronectin and regulates the protrusive activity of cells, necessary for dorsal convergence (Love, Prince and Jessen, 2018). Furthermore, prechordal plate mesoderm (anterior axial mesoderm)

which migrates towards animal pole directly affects the opposite movement of the overlying neurectoderm moving towards vegetal pole. E-cadherin-mediated friction forces which are generated at their interface are critical for the neuroectoderm movements (Smutny *et al.*, 2017).

1.2.2. Vertebrate Neurulation

Neurulation is a period during which the formation of neural tube occurs. The morphogenetic events of neurulation start at the end of gastrulation and leads to formation of 3D neural tube structure from 2D neural plate cells. The neural tube is a hollow tube located on the dorsal side of the embryo which runs along antero-posterior axis of the embryonic body (Figure 1.3). Later neural tube structure develops into brain anteriorly and spinal cord posteriorly; the central lumen will form their ventricular system (Clarke, 2009). The neural tube is an epithelial structure with a strong apico-basal polarity. Vertebrate neurulation occurs by two distinct mechanisms namely, primary and secondary neurulation. Primary neurulation occurs in head and trunk regions of birds and mammals. The key events in primary neurulation is columnarisation of the ectoderm cells to form the epithelial neural plate, thickening of the edges of the neural plate to form the neural folds, convergent extension of the neural plate cells that facilitates bending to form the neural groove and elongates the neural tube, and closure of the groove to form the neural tube (Figure1.3A) (Lowery and Sive, 2004).

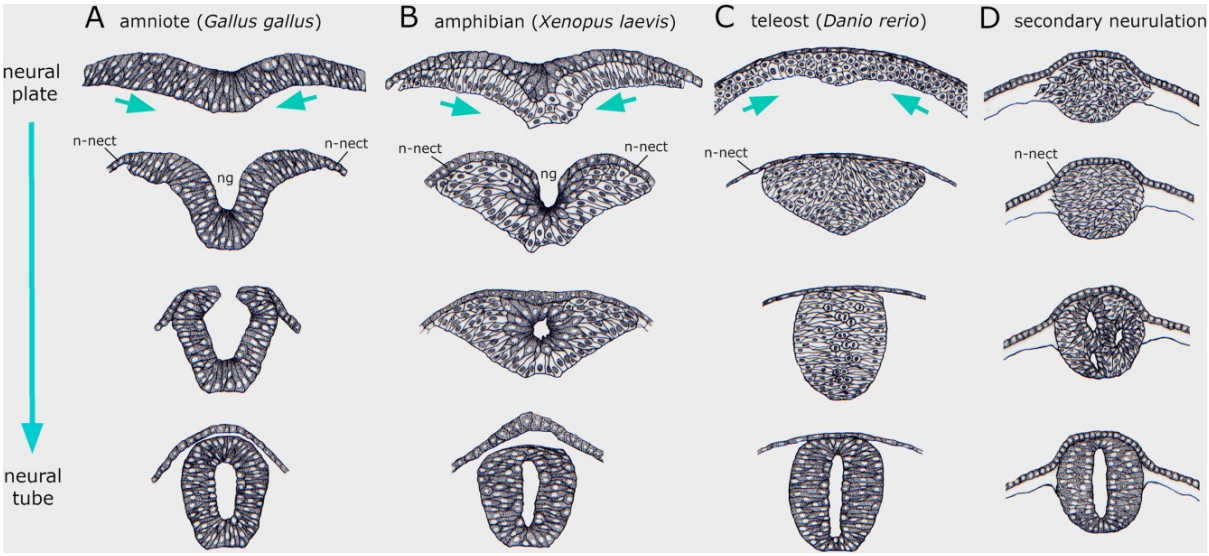

Figure 1. 3. Vertebrate neural tube formation.

Neural ectoderm (neural plate) and nonneural ectoderm (n-nect) tissues are shown. **A:** Classical primary neurulation in the chick embryo. This involves the invagination of an existing epithelium at the midline and lumen formation by folding up to form the neural tube **B:** Neurulation in the frog. This involves the invagination of a bi-layered neural plate and the formation of a central lumen by tissue invagination. **C:** Teleost neurulation in the zebrafish embryo. Here, the neural

plate converges and internalises to form solid keel and subsequently rod primordia. **D:** Classical secondary neurulation in the chick embryo. ng-neural groove. This is characterised by condensation of mesenchyme cells to form a solid primordium which then undergoes an epithelial transition to generate multiple lumen, which finally coalesce to form a continuous apical surface at the neural tube stage. Gray cells with white nuclei represent a polarized epithelial organization while white cells with gray nuclei represent nonpolarized tissue. Arrows indicate tissue movements. Figure from (Araya *et al.*, 2016).

In amphibians, neural tube closure occurs at all axial levels at the same time whereas in birds and mammals, the closure points varies along the AP axis (Figure 1.3B). Secondary neurulation occurs in more posterior, lumbosacral region of birds and mammals. Here, a group of mesenchymal cells condenses to form a transitory solid rod that eventually cavitates into an epithelial tube. Subsequently, a lumen (in the case of mouse) or a small number of cavities (in the case of chicken) generates, that coalesce to form proper neural tube structure (Figure 1.3D).

1.2.2.1. Zebrafish neurulation

Zebrafish neurulation does not entirely fit into either of these mechanisms, yet utilise similar strategies to construct the neural tube (Figure 1.3C). Unlike in mice and frog, where the neural plate cells are single or bi-layered respectively, zebrafish is comprised of multi-layer neural plate, 3-6 layers in the brain region and single layer in spinal cord region (Hong and Brewster, 2006; Araya *et al.*, 2016). Neural plate cells are less tightly associated than typical epithelial but more organized than a mesenchymal tissue, thus it is called pseudo-epithelium (Lowery and Sive, 2004). Around 10–11 hpf, neural plate cells from both sides of AP axis converge toward the dorsal embryonic midline and interdigitate with each other (Figure 1.4A) (Araya *et al.*, 2016). Medial cells internalize at the midline and move ventrally (deeper) while the incoming lateral cells move towards dorsal midline and intercalate. This forms a solid neural keel structure by 12-13 hpf (Figure 1.4A). Around 15–17 hpf, the solid keel forms a cylindrical-like structure called the neural rod (Figure1.4A). Slowly the neural rod acquires apico-basal polarity with opposing apical surfaces of cells along the midline. A lumen is generated at the midline but not in anterior to posterior sequence, which transforms neural rod into a hollow neural tube by 24 hpf. Rather, the opening is initiated in rhombomeres in a stereotypical manner along the AP length and coalesce to form the lumen (Gutzman and Sive, 2010). The mediolateral position of cells in neural plate correspond to dorsoventral organisation of the neural tube which is shown through sparse lineage tracing and 3D+time live imaging of early neurulation stages (Papan and Campos-Ortega, 1994; Hong and Brewster, 2006; Araya *et al.*, 2019).

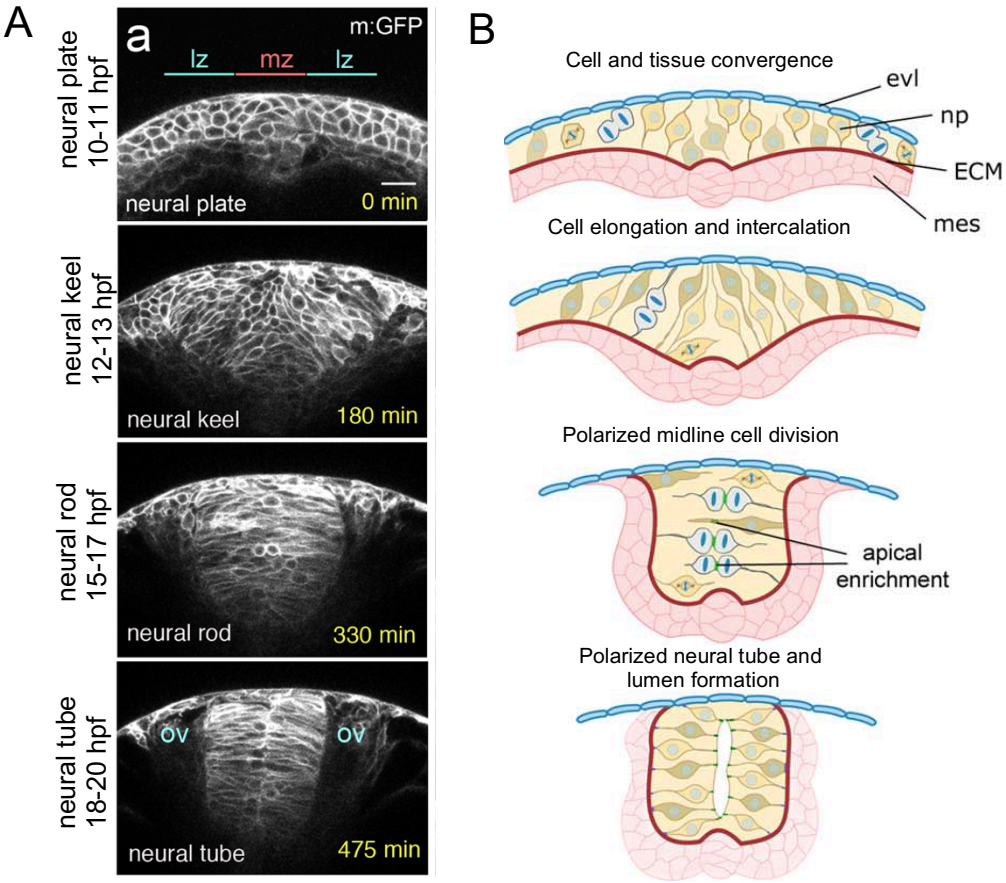

Figure 1. 4. Cell and tissue organisation of zebrafish neurulation.

A) Confocal images show the neural plate, keel, rod and tube stages of zebrafish neurulation at hindbrain levels (transverse view). Cells membranes labelled with CAAX-GFP. OV indicates otic vesicle. mz- medial zone and lz- lateral zone of the neural plate. Scale: 20 µm wide. B) Schematics of cell and tissue organisation at the four stages. At neural plate steps, neural cells are organised within the superficial deep axis of the neural anlage. By neural keel stages, neural cells undergo elongation and intercalation within its superficial-deep axis. At neural rod stages, neural progenitors change its mitotic spindle orientation in 90 degrees and polarised undergo crossing cell division. By neural tube stages, neural cells show well-established apical and basal polarity and a central lumen is formed. Green dots indicates midline apical deposition in neural cells prior the midline-crossing division. Apical (green) and basal (purple) polarity. Dividing cells (gray). Figure from (Araya *et al.*, 2016, 2019).

An interesting feature of zebrafish neurulation is the midline crossing cell division called C-division. During neural keel and rod stages, cell divisions occur predominantly across the midline (Figure1.4B). The orientation of the division is 90° angle to the AP axis (Geldmacher-Voss *et al.*, 2003). This stereotypical division underlies the proper formation of apical midline (Quesada-Hernández *et al.*, 2010). Approximately 90% of neural progenitor cells undergo C-division which deposit one daughter cell into each side of the AP axis. Following the division, daughter cells

elongate across the apico-basal extent of the left and right neuroepithelium. Ultimately, the dividing "mother" cell remains on its ipsilateral side while the midline crossing "daughter" integrates into the contralateral side of the neural rod with mirror-image apico-basal polarity (Figure 1.5A) (Tawk *et al.*, 2007). Further, it is shown that the pard3, apical polarizing protein is specifically localized in the cleavage furrow of cells prior to C-division and equally inherited to daughter cells in order to acquire mirror-symmetric apical polarity (Figure 1.5B). This ensures the position of apical ends of daughter cells at the midline and marks the future lumen. C-division has a powerful morphogenetic influence during zebrafish neural tube development. It was shown that the ectopic C-division leads to a spectrum of neural tube disorganization from a presence of "ectopic mass of disorganized cells in the neuroepithelium" to more dramatic "duplicated neural tube" (Ciruna *et al.*, 2006; Tawk *et al.*, 2007). In case of delayed convergence, as in PCP pathway mutant (trilobite), C-divisions occurs at lateral regions of the wider neural keel instead of the midline. This gives rise to bilateral ectopic apical planes which in turn results in duplicated neural tube (Figure 1.5C) (Tawk *et al.*, 2007). Misoriented C-divisions results in lack of coordination of cells across the midline and therefore, exhibit abnormal hindbrain architecture with a discontinuous lumen (Quesada-Hernández *et al.*, 2010; Žigman *et al.*, 2011; Zigman *et al.*, 2014). Independent of apical-basal polarity and PCP components, Hoxb1b and miR430 (microRNA through target genes) are also shown to control oriented cell division (Zigman *et al.*, 2014; Takacs and Giraldez, 2016). It is interesting to note that the role of Hox genes in orienting mitotic spindle formation during cell division at the hindbrain level. However, C-division is dispensable for lumen formation as blocking cell division do not abolish lumen formation. Acquisition of apical polarity at the midline is independent of C-division (Buckley *et al.*, 2013).

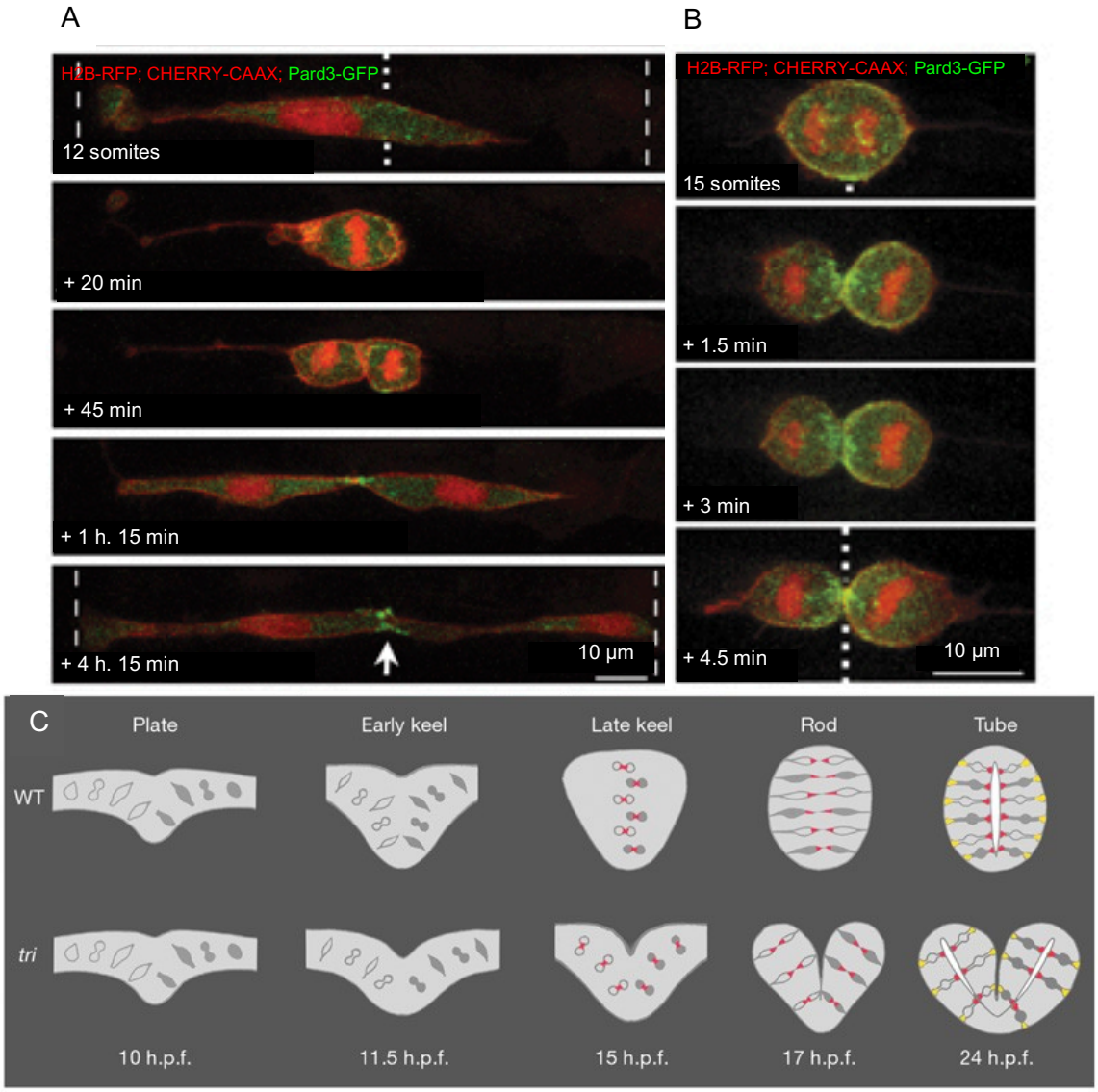

Figure 1. 5. C-divisions during zebrafish neurulation.

A) Time-lapse sequence shows a neural rod cell prior to, during and following C-division. Cells are shown with Pard3-GFP, a nuclear label (H2B-RFP) and a membrane label (Cherry-CAAX). Apical surface (arrow). The of an apical cell polarity at the tissue midline is observed prior to cytokinesis. Dotted lines: midlines. Dashed lines: basal edges. B) Pard3–GFP puncta localise to the cleavage furrow in cells diving very close to the midline. C) A schematic of developing neural tube in transverse sections is shown with the mirror-symmetric C-divisions in WT and trilobite mutant. Pard3 localization is shown in red and basal marker (GFAP) is shown in yellow. Figures from (Buckley *et al.*, 2013) and (Tawk *et al.*, 2007).

1.2.2.2. Molecular regulation of neurulation movements

Convergence movements of neural plate cells to the dorsal midline is partly controlled by planar cell polarity (PCP) pathway. In general, PCP signalling specifies cells with uniform orientation within a plane of tissue (Davey and Moens, 2017). The pathway is highly conserved from invertebrates to vertebrates. The core components of PCP signalling includes Van Gogh/Strabismus, Prickle, Dishevelled, Frizzled and Flamingo/Stan (Figure 1.6). Asymmetrical intracellular distribution of the components confer the planar polarity of the cells. Downstream signalling of PCP regulates cytoskeleton rearrangement, cell polarity and cell adhesion. These properties facilitate cell migration and other morphogenetic movements. The asymmetric localization of PCP components Prickle1 and Vangl2 in anterior edges of neuroectoderm cells establishes anterior-posterior polarity, thus restricts cell mixing along AP axis during convergence (Ciruna *et al.*, 2006; Roszko *et al.*, 2015). Loss of zebrafish Vangl2 in trilobite mutants eliminates the polarization of neural keel cells following C-division. This leads to poor re-intercalation of daughter cells into the neuroepithelium and accumulation of ectopic neural progenitors (Ciruna *et al.*, 2006). Cell-cell adhesion molecules, N-cadherin (cdh2) and Protocadherin-19 (pcdh19) play a critical role during internalization of neural keel stages as their absence causes disrupted neural cell movements and aberrant neural tube morphology despite normal initial convergence (Hong and Brewster, 2006; Biswas, Emond and Jontes, 2010; Araya *et al.*, 2016). Cell shape changes during internalization is influenced by Myosin II contractility, which is enriched transiently in superficial surface of medial cells and N-Cadherin regulates their localization (Araya *et al.*, 2019). This highlights that similar strategy of typical epithelial remodelling is used by zebrafish during internalisation.

Neuroectoderm cell movements are highly coordinated in terms of speed and direction with the underlying mesoderm movements during convergence and internalization stages. It is shown that in the absence of mesoderm in nodal mutant fishes, internalization of neural plate cells and formation of neural tube are severely disturbed due to the loss of coordinated movements, but not as a direct effect of loss of nodal signalling (Araya *et al.*, 2014). The extracellular matrix proteins, laminin and fibronectin present in the basal lamina between the two germ layers starting at 10hpf, couple the convergence of these two layers during the morphogenetic movements of neurulation (Araya, Carmona-Fontaine and Clarke, 2016).

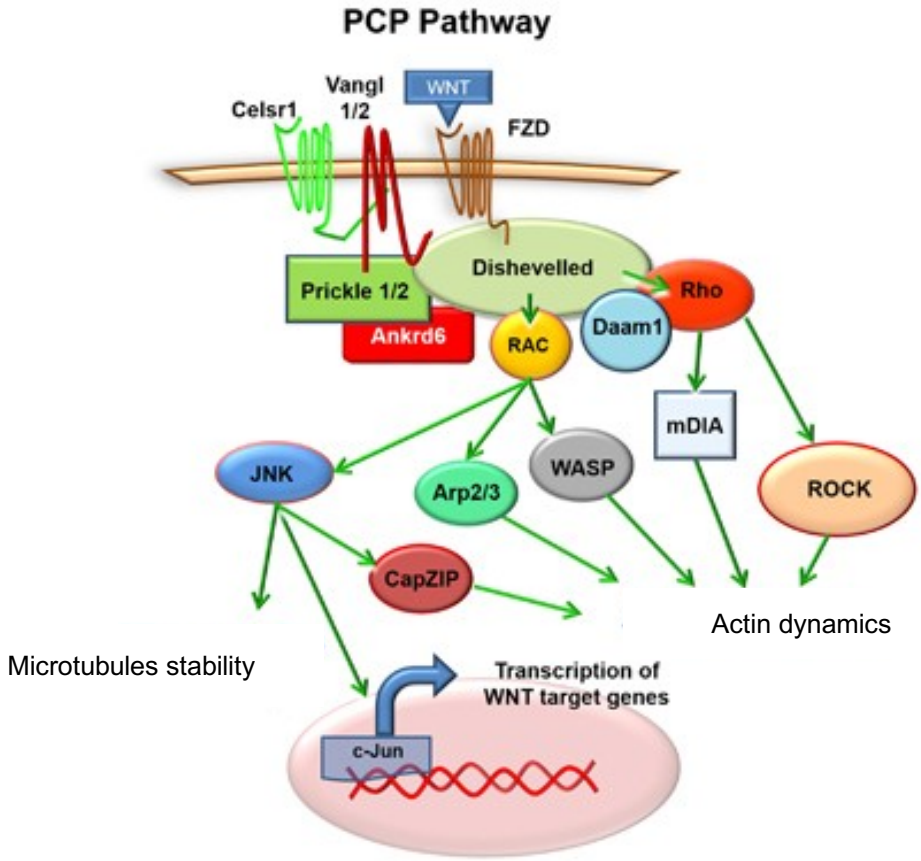

Figure 1. 6. Non-canonical/WNT pathway.

The various core components of the pathway are illustrated. The non-canonical/WNT pathway leads to microtubules stability, actin dynamics and transcription of WNT target genes. Figure from (Corda and Sala, 2017).

1.2.3. Zebrafish fate maps

1.2.3.1. Classical fate map

Historically, the fate mapping method has been used to study the reorganization of cells from one stage to a later stage of embryonic development (Clarke and Tickle, 1999; England and Adams, 2007). Fate maps give useful information such as cell rearrangement and cell migration processes that are necessary to build the tissue or organ in its size, shape and position. A cell or a distinct group of cells is labelled with dyes in a defined region of the embryo. The labelled cells and their progenies are identified at a later stage that gives the information about the contribution of the cell's descendants to a structure or organ. A repeatable pattern of cell location in several embryos studied is used to build the fate map. Fate maps of various species including zebrafish were established (Figure 1.7) (Keller, 1975; Kimmel, Warga and Schilling, 1990; Woo, Shih and Fraser, 1995). Despite geometrical differences, topological fate relationships at the stage of gastrulation are conserved between mammals, birds, amphibians, and zebrafish (Buckingham and Meilhac, 2011). Fate maps are instrumental to design the grafts and explants experiments and to interpret the function of molecular markers.

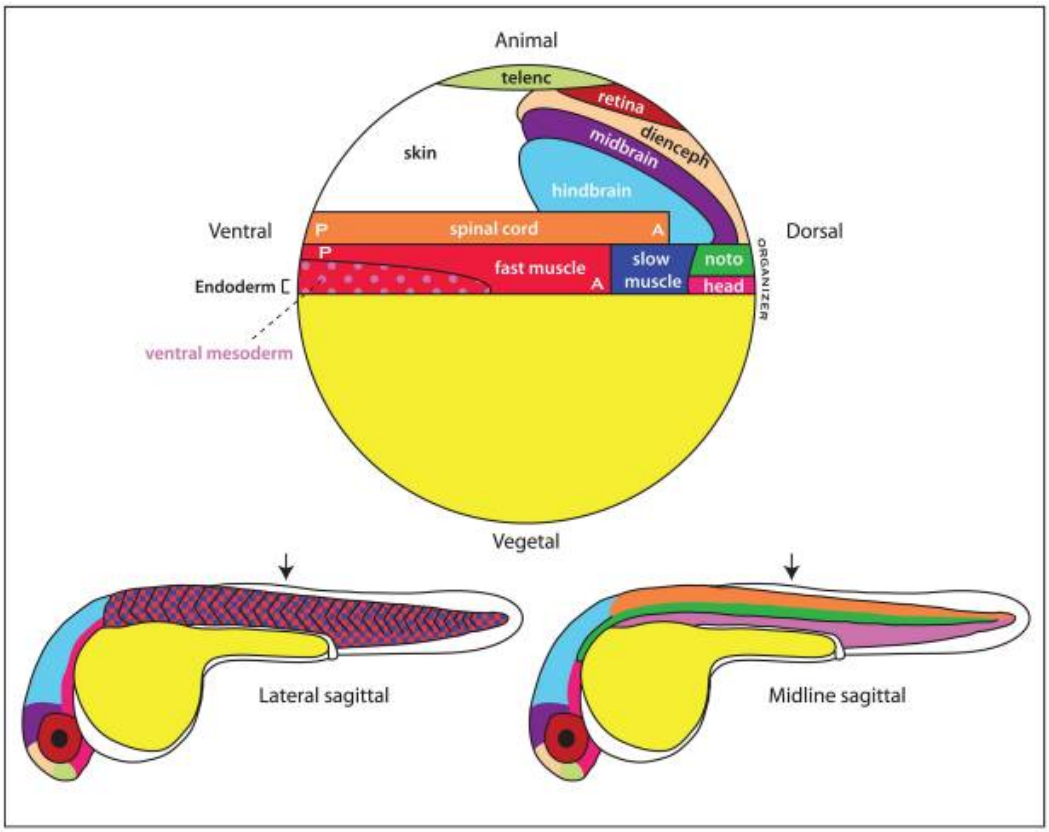

Figure 1. 7. Fate map of the zebrafish embryo.

A fate map of the zebrafish embryo at the early gastrula stage is presented (top). The organiser is at the equator, on the dorsal side of the embryo. 31 hpf embryos with lateral and midline sagittal views are shown (bottom). Figure from (Kimelman and Martin, 2012).

Intra-species (transplantation of labelled cells into the host of same species) and inter-species transplantation were also used to construct a fate map. Chick-quail chimeras were made based on the morphological difference in the nuclei of these two species and development of species-specific monoclonal antibodies (Le Douarin, 1973). Studies in these chimeras were invaluable in identifying various derivatives of neural crest cells. However, fate mapping of cells does not provide the information on cell fate commitment. It can be established only through experimental challenges such as transplantation. It is inferred whether the cell has acquired a restricted cell fate potential depending on the transplanted cells that adapt fate according to either the origin or its new environment (Buckingham and Meilhac, 2011). The Spemann and Mangold 's organiser graft led us to the understanding of neural commitment occurring at late gastrulation and of the concept of embryonic induction.

1.2.3.2. CNS fate map state-of-the-art

Zebrafish CNS fate map which consists of the various sub-divisions telencephalon, diencephalon, retina, midbrain and hindbrain was obtained at 6 hpf and 10 hpf (Figure 1.8A)(Woo and Fraser, 1995). The method involves injection of fluorescein-dextran or rhodamine dextran dye into a single cell in the superficial layers of 5-6 hpf embryos followed by scoring the position of labelled cells at later stages 6 hpf and 10 hpf using epi-fluorescent microscopy. In the study, they found that the presumptive neuroectoderm at 6 hpf displays a predictable organization that reflects the future anterior-posterior and dorso-ventral order of the CNS. The basic order of the neural tube is evident by 10 hpf (Figure 1.8B). Through time-lapse imaging of the embryo with labelled cells, authors were able to dissect the cell rearrangements during gastrulation. The neuroectoderm cells undergo highly ordered cell movements. The cells near the dorsal midline at 6 hpf consist of forebrain progenitors display anterior-directed migration while more laterally positioned midbrain and hindbrain progenitors converge at the midline prior to anterior ward migration. In summary, the fate map established by (Woo and Fraser, 1995) remains the current state-of-the-art zebrafish CNS.

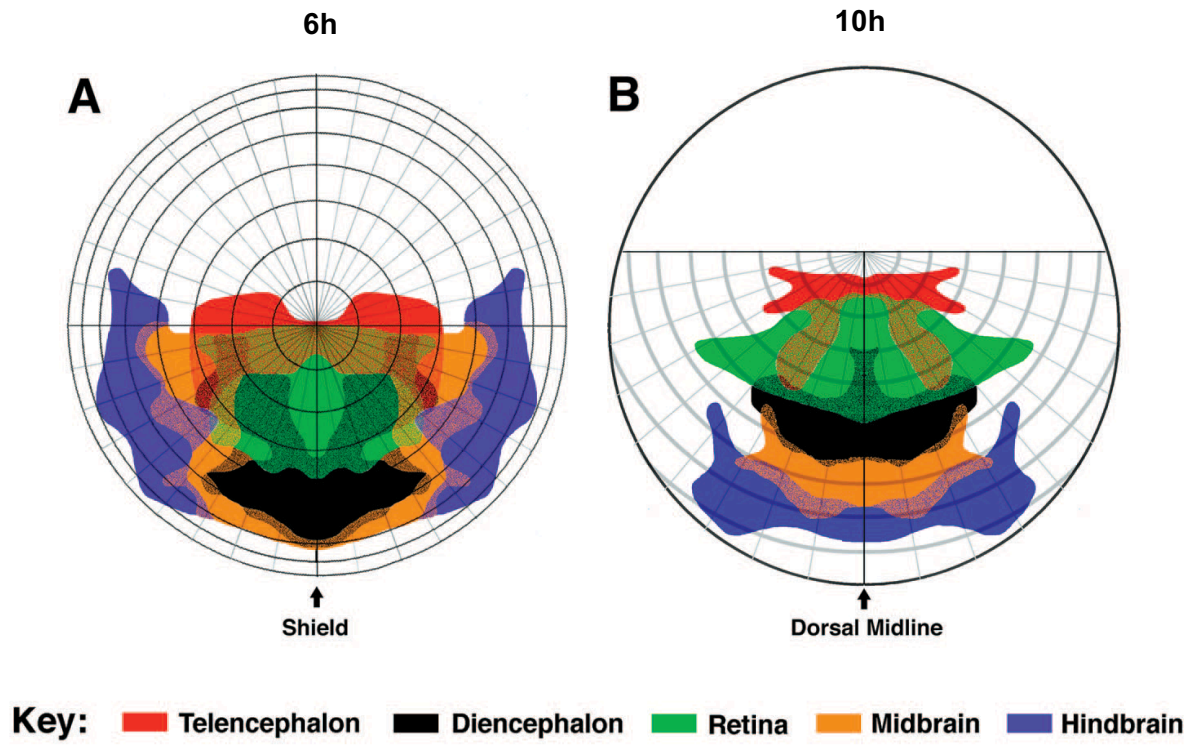

Figure 1. 8. Organization of the zebrafish central nervous system.

(A,B) Schematics of CNS fate map at 6h and 10h, respectively. A) Animal pole view with the shield positioned bottom B) Dorsal view with the advancing hypoblast on top.. Domains occupied by progenitors of each brain subdivisions are coded with their representative colours, as shown in the key. Shaded colours with a mixture of colours of any two domains indicate their respective overlapping region. Figure from (Woo and Fraser, 1995).

1.6.3.2. Limitations of the fate map

However, the fate map lacks precision of borders due to the limited number of cells analysed. Importantly, it targets only superficial layers of the embryo, 1-2 cell layers due to the inability to penetrate into deeper layers through injection. The embryo consists of 3-4 cell layers in animal pole and 5-6 cell layers in germ ring. It does not provide the entire cell dynamics of hindbrain progenitors throughout the gastrulation stages. Nevertheless, the fate map of hindbrain's individual rhombomeres and their clonal analysis have not been performed.

1.3. Hindbrain segmentation

1.3.1. Sub-divisions of brain

During neurulation, the developing brain is primarily divided into forebrain, midbrain and hindbrain with antero-posterior characteristics. They exhibit as major swellings at morphological level. The most anterior, forebrain (prosencephalon) is further classified into diencephalon and telencephalon. In the adult brain, telencephalon develops into cerebrum and diencephalon into thalamus, hypothalamus, pineal gland and optic vesicles of the eye. The middle, midbrain (mesencephalon) is composed of the tectum and the tegmentum and develops sensory and motor control. The most caudal, hindbrain (rhombencephalon) develops into cerebellum and pons (Metencephalon) and medulla oblongata (Myelencephalon)(Figure 1.9A). Medulla and pons together with midbrain are usually termed as the brainstem.

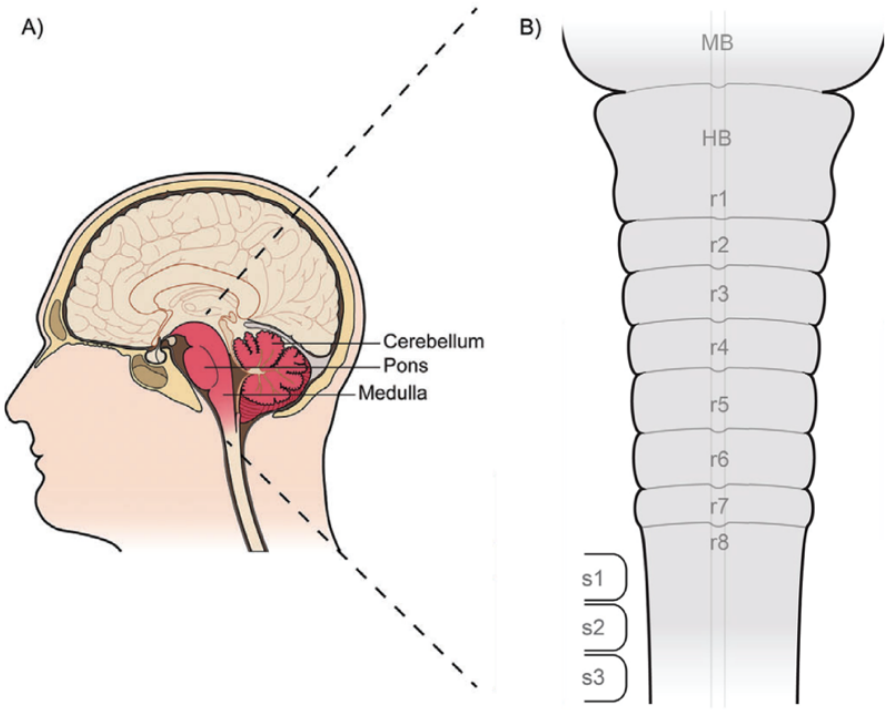

Figure 1. 9. Hindbrain derivatives in adult brain.

A) Anatomy of the human brain, with the hindbrain derivatives highlighted in red. B) Depiction of the mouse embryonic hindbrain with rhombomeres annotated (r1–r8). s-somite. Figure modified from (Parker, Bronner and Krumlauf, 2016).

1.3.2. Function of hindbrain

In the Central Nervous System (CNS), the hindbrain is a key coordination centre for many physiological processes and behaviours. Eight of the 12 cranial nerves emanate from the hindbrain. These cranial nerves (somatic and branchiomotor) are involved in receiving sensory information from various organs in the head and providing output motor signals to the facial muscles. Thus, they are responsible for sensations of taste, touch and hearing. They control movement of eye, head and face and also secretion of saliva and tears in higher vertebrates. Reticulospinal interneurons in the brainstem function as a motor-command for the execution of motor co-ordination during locomotion and posture (Peterson, 1979). Complex network of cell groups termed reticular formation in the brainstem are involved in blood circulation and wakefulness. Neural circuits in the hindbrain provide rhythmic-pace timing that is necessary for breathing, swallowing and vocalization. All these core functions along with their underlying neuroanatomy are common features in vertebrate brain. Hindbrain is one of the most evolutionarily conserved part of brain in vertebrates (Alexander, Nolte and Krumlauf, 2009; Parker, Bronner and Krumlauf, 2014).

1.3.3. Hindbrain segmentation

Segmentation is initially defined in the drosophila body plan and wing disc (Garcia-Bellido, Ripoll and Morata, 1973; Lawrence, 1973). In general, segmentation refers to the repetition of units along the AP body axis that leads to regional diversity. Segmental events that occur during vertebrate embryonic development are somitic segmentation (vertebral column), pharyngeal arches and hindbrain segmentation (Kimmel, Sepich and Trevarrow, 1988; Graham *et al.*, 2014). These segmental events are thought to have evolved independently (Graham *et al.*, 2014). Thus, there is no common molecular mechanisms that underlie different segmental events.

Shortly after the end of gastrulation, hindbrain territory starts to transiently subdivide into 7 or 8 repeated segments along the antero-posterior axis. However, the segments do not have obvious correspondence to the final contour of adult hindbrain structures (Figure 1.9). The segments are called rhombomeres. Segmentation is the mode of hindbrain morphogenesis in all studied vertebrates including chick, mice, xenopus, zebrafish (Gilland and Baker, 1993). These segments were initially and long thought to be inconsequential buckling as a result of mechanical constraints in the growing neuroepithelium (Vaage, 1969). But later, rhombomeres are identified as true segments. They are units of cell lineage restriction and of specific gene expression. It was first demonstrated in chick through elegant cell-labelling and transplantation analyses (Fraser, Keynes and Lumsden, 1990) and later in mice and zebrafish through genetic labelling (Jimenez-Guri *et al.*, 2010; Calzolari, Terriente and Pujades, 2014). Hindbrain segmentation exhibits a striking resemblance to the embryo body plan of drosophila, in the sense that progressive antero-

posterior sub-regionalization of the embryo results in segments which will each give rise to a specific part of the adult fly. In hindbrain, each segment expresses unique set of gene expression patterns and promote segment-specific cell fates, differentiation of neurons and discrete cranial neural crest streams (Kiecker and Lumsden, 2005).

Hindbrain segmentation manifests as visible morphological swellings along the AP length of hindbrain neuroepithelium. In zebrafish, the morphological segments appear from 18-20 hpf (Figure 1.10A) (Kimmel *et al.*, 1995). Unlike somitic segmentation, where the formation of somite is sequential and progressive, hindbrain segmentation does not follow sequential order and the order is species dependent (Lumsden, 1990). Also, the sub-divisions occur in the pre-existing hindbrain neuroepithelium. The formation of rhombomere boundaries is visualised with time-lapse analysis of Bodipy-ceramide–stained embryos during early somite stages in zebrafish (Moens *et al.*, 1998) and chick embryos (Lumsden and Keynes, 1989). In zebrafish, r4 domain is first defined with the appearance of the boundary between r3 and r4 (r3/4) and then the r4/5 boundary, followed by the r1/2, r2/3, and r6/7 boundaries (Figure 1.10B,C).

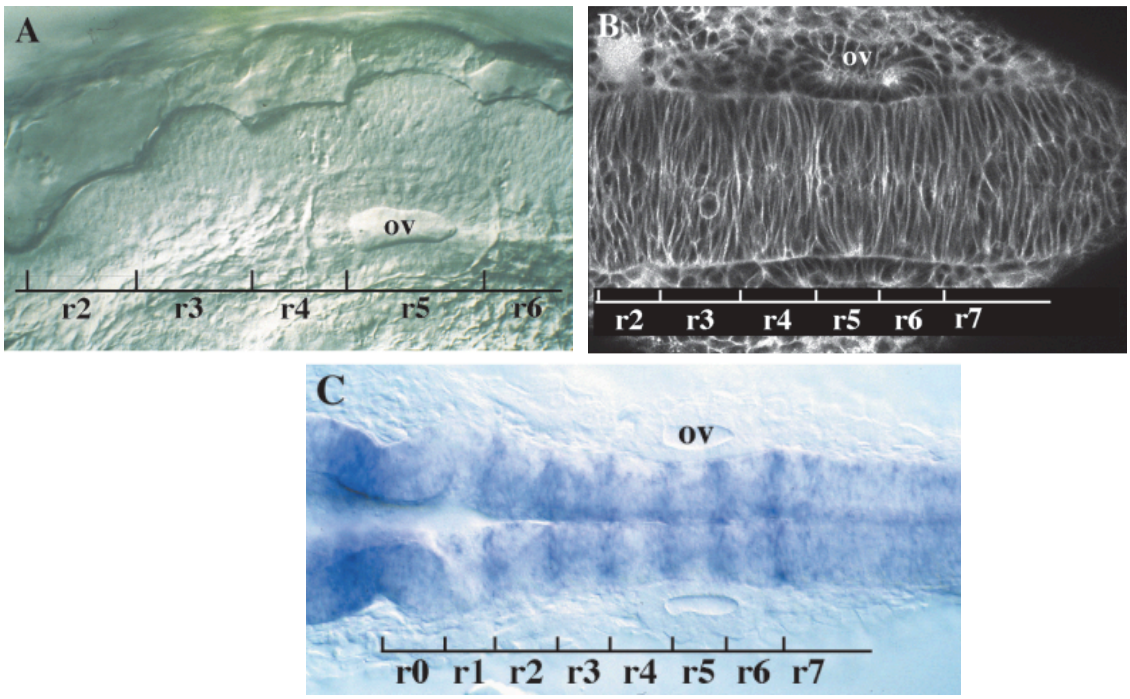

Figure 1. 10. The zebrafish hindbrain is organized into segmental rhombomeres.

A) The rhombomeres are visible as a series of bulges along the anterior-posterior axis of the hindbrain at 18 hpf (lateral view). The otic vesicle (ov) is present adjacent to r5. B) The cellular architecture of the hindbrain and rhombomere boundaries are visualised at 15 hpf (12-somite stage) with Bodipy-ceramide staining of intercellular spaces. C) RNA in situ hybridization with *mariposa/foxb1.2* shows boundary-specific expression in the r1/2–r6/7 boundaries at 20 hpf. Anterior is to the left. Figure from (Moens and Prince, 2002).

Molecular boundaries with rhombomere-specific gene expression precede the morphological appearance of segments. It was first shown with the segmental expression of *krox20* gene in presumptive r3 and r5 of mice (Wilkinson *et al.*, 1989). Initially the ragged expression of these genes seen at 11 hpf sharpens and straightens over a short period by the time of morphological appearance at 13 hpf. Some cells with different molecular-rhombomere identity intermingle between the rhombomere segments at early stages due to the challenge faced by cell intercalation during convergent-extension movements of neural progenitors. They do not inter cross between rhombomeres once the boundaries are established (Fraser, Keynes and Lumsden, 1990; Jimenez-Guri *et al.*, 2010; Calzolari, Terriente and Pujades, 2014). Cell identity switch of intermingled cells at early stages and cell segregation between odd and even numbered rhombomeres at the borders at later stages ensure the homogeneity of the rhombomere cells within the segments (Figure1.11) (Xu and Wilkinson, 2013). Cell adhesion within the rhombomeres and repulsion between odd and even-numbered segments restrict cell movements between rhombomeres (Wizenmann and Lumsden, 1997; Xu *et al.*, 1999). Studies in zebrafish showed that the actomyosin cytoskeletal components are enriched at inter-rhombomeric boundaries and prevent cell mixing between adjacent rhombomeres (Calzolari, Terriente and Pujades, 2014; Cayuso *et al.*, 2019).

Boundary-specific gene expression are shown to be induced between odd and even-numbered rhombomeres by increased cortical tension at the border (Cayuso *et al.*, 2019). The boundary region is composed of a two-cell layer throughout the dorsal-ventral axis. Boundary cells have distinct cellular properties compared to cells present within the rhombomeres (Heyman, Kent and Lumsden, 1993). In zebrafish, boundary cells are triangular/club-shaped with larger apical side while cells within segments are spindle-shaped with smaller apical side (Gutzman and Sive, 2010; Voltes *et al.*, 2019). They express specific molecular markers such as *wnt1* and *wnt8b* at early stages *and, foxb1* and radical fringe *(rfng)* at later stages (Figure1.10C). Boundary cells act as signalling centres to pattern the differentiation of neurons in the segment, exerted in part through coordinate modulation of notch and Wnt signalling pathways (Kiecker and Lumsden, 2005a). Wnt1 at the boundary cells promote neurogenesis in the non-boundary regions in zebrafish (Amoyel *et al.*, 2005). Neurogenesis is prevented in boundary cells in response to notch activation that helps maintain the boundary cell population. It is shown that the Yap/Taz mechano-transduction maintains boundary cells as proliferative progenitors till 40 hpf (Voltes *et al.*, 2019). Later, boundary cells switch to participate in neurogenesis. In contrast to zebrafish, boundary cells in chick exhibit decreased proliferation and differential spatial regulation of gene expression emphasising that species-specific differences exist in the role of boundary cells and that lead to the corresponding features in their neuroanatomy (Pujades, 2020).

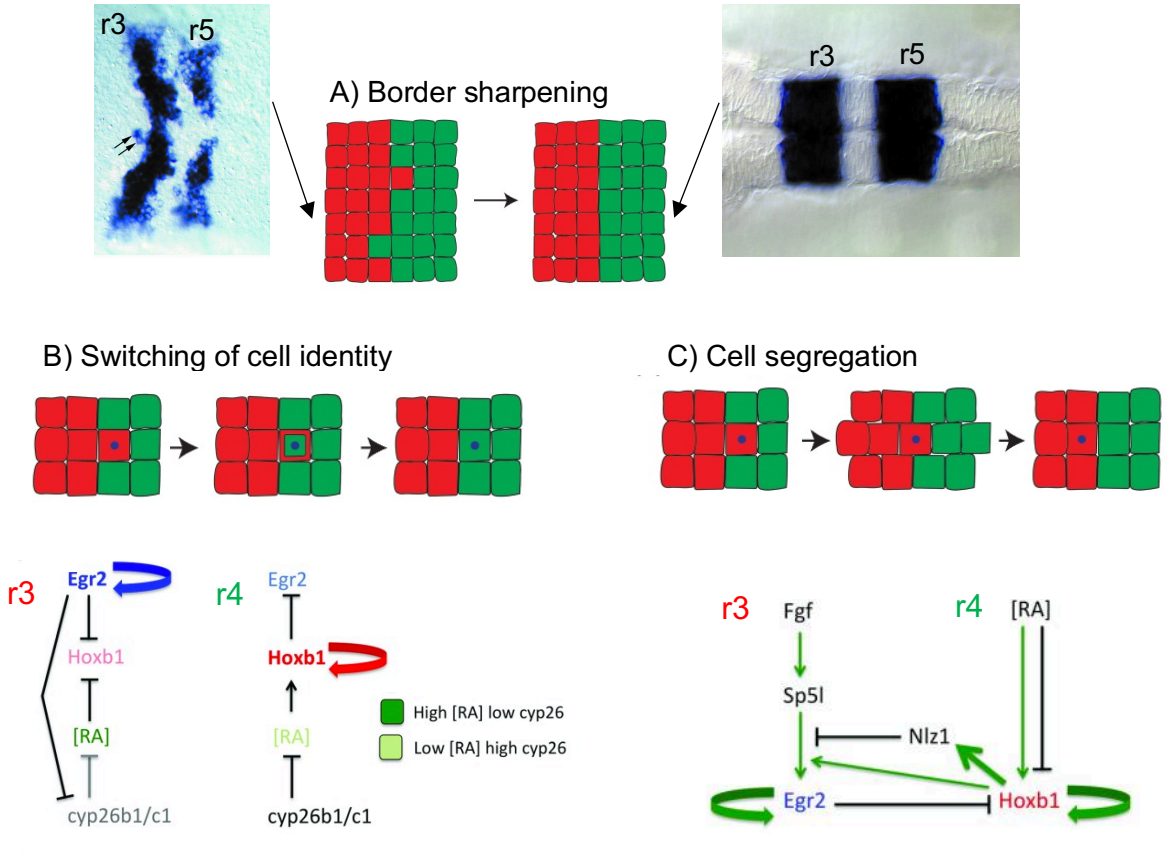

Figure 1. 11. Mechanisms involved in rhombomere border sharpening.

A) The initial fuzzy border of segments (distinct cell identity indicated with red vs green) becomes a sharp and straight border. *krox20* expression in pre-r3 and r5 at 11 hpf with ragged boundaries (top left) and the boundaries of *krox20* are razor shaped by 18 hpf (top right) in zebrafish. Two mechanisms can contribute to such sharpening: B) Switching of identity of ectopic cells to match to their predominant neighbours C) Segregation of cells into territory that has the same identity. Bottom, models of switching of cell identity and of cell segregation involving their signalling pathways and gene regulatory network. Adapted from (Moens and Prince, 2002; Xu and Wilkinson, 2013; Wilkinson, 2018).

Hindbrain segments also follow two segment periodicity meaning alternative segments having similar cellular properties and gene expression patterns. Odd-numbered rhombomeres have different cell adhesion properties than the even-numbered rhombomeres (Wizenmann and Lumsden, 1997). Cell repulsion exists between two rhombomeres. Among segmentation genes, *krox-20* is expressed in alternate rhombomeres r3 and r5 (Wilkinson *et al.*, 1989; Oxtoby and Jowett, 1993). Two-segment periodicity is also exhibited by the formation and organisation of branchiomotor nerves. Each nerve is derived from alternating pairs of even- and odd-numbered segments but exit to the periphery from only the even-numbered segments (Moens and Prince, 2002).

1.3.4. Significance of hindbrain segmentation

Construction of vertebrate head depends crucially on the transient hindbrain segmentation by two main means 1) Neuronal organisation: Segmentation enables the embryo to organize progenitor cells that define the organization of birth of neurons, neuronal differentiation and neural circuit connections during brain development. 2) Craniofacial patterning: Guides the segment-specific migration paths of neural crest cells to specific pharyngeal arches, that give rise to various craniofacial features (Lumsden and Keynes, 1989).

1.3.4.1. Neuronal organisation

In the developing hindbrain, segmental patterns of proliferation and neurogenesis give rise to repeated neuronal population, which differentiate in a rhombomere-specific manner. For example in zebrafish, each rhombomere contains a similar set of reticulospinal interneurons, yet there are differences in size, number, and projections within each segment (Higashijima, Hotta and Okamoto, 2000). In chick and fish, it is shown that the neurons of the trigeminal (V), facial (VII) and glossopharyngeal (IX) branchiomotor nerves arise first in even-numbered rhombomeres r2, r4 and r6, subsequently differentiate in odd-numbered segments (r3, r5 and r7). Their axons exit from even numbered rhombomeres to innervate the corresponding pharyngeal arches b1, b2 and b3 respectively (Figure 1.12) (Lumsden and Keynes, 1989; Higashijima, Hotta and Okamoto, 2000; Chandrasekhar, 2004). Further, the timing of neuronal differentiation is also shown to be delayed in odd-numbered rhombomeres (Lumsden and Keynes, 1989). Disruption of morphological segmentation leads to neuronal patterning defects, such as fusion of motor nuclei and loss of specificity in target innervation (Parker, Bronner and Krumlauf, 2016). The segmental organization of neurons and of the hindbrain is lost during subsequent growth and morphogenesis of brain. However, it acts as a common structural and functional plan of neuronal connection that persists throughout adult life (Moens and Prince, 2002).

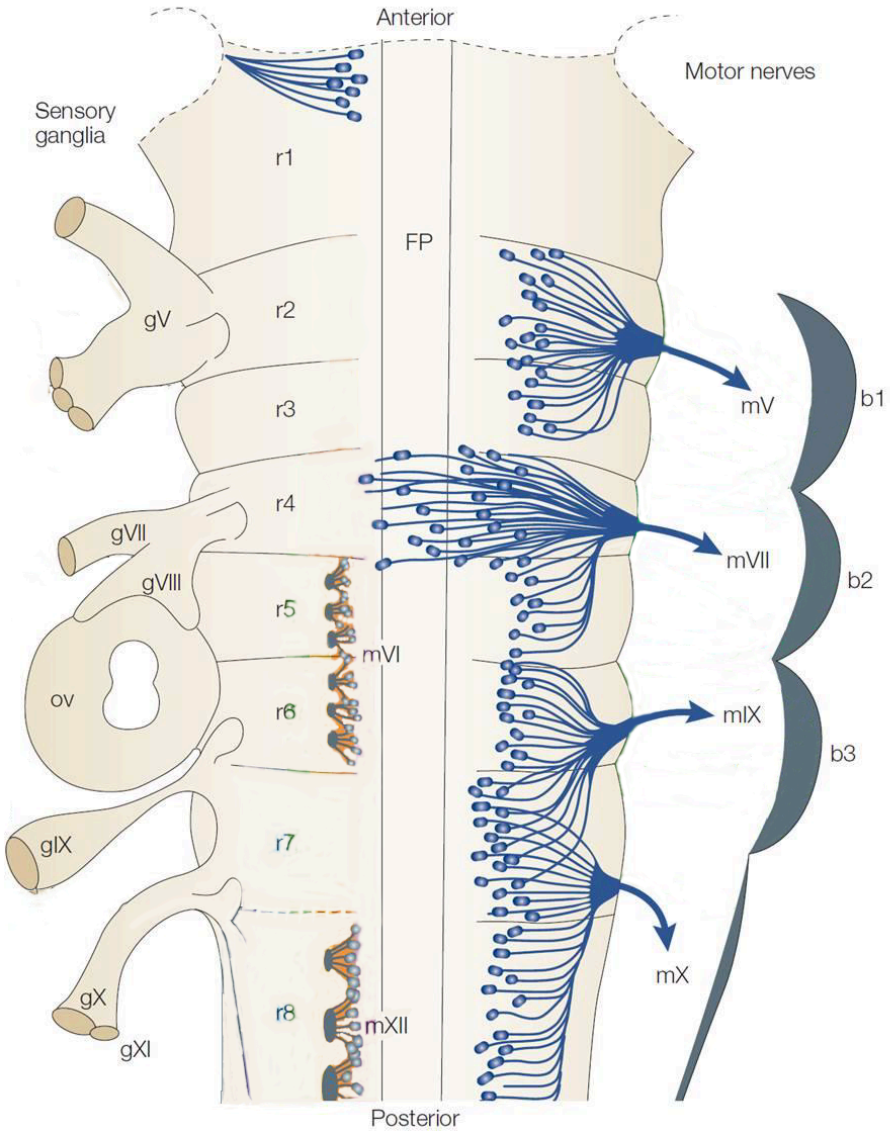

Figure 1. 12. Schematic representation of a vertebrate hindbrain (chick) in dorsal view.

The reiterative formation of motor nuclei and the exit points of their efferent nerves from rhombomeres 2, 4, 6 and 7 (r2, r4, r6 and r7) are indicated on the right side. The trigeminal (mV), facial (mVII) and glossopharyngeal cranial (mIX) nerves project into the first (b1), second (b2) and third (b3) branchial arches, respectively, and the vagus nerve (mX) innervates a large part of the body. The positions of the cranial sensory ganglia (gV and gVII–gXI) and the otic vesicles (ov) are indicated on the left side. FP, floor plate; mVI, mXII, somatic motor neurons. Figure modified from (Kiecker and Lumsden, 2005).

1.3.4.2. Migration paths of neural crest cells

Neural crest cells (NCC) are often classified as fourth germ layer because of their enormous potential to contribute to diverse structures including pigment cells, peripheral neurons, glia, cartilages and bones (Le Douarin and Kalcheim, 1999; Hall, 2000; Simões-Costa and Bronner, 2015). Neural plate border cells (neural ectoderm) give rise to NCCs around the time of vertebrate neural tube closure. They are broadly classified into cranial, vagal, trunk and sacral neural crest based on the location where they originate from along the AP neural axis.

The cranial neural crest emanating from forebrain, midbrain and hindbrain gives rise to craniofacial skeleton, connective tissue, pigment cells and cranial ganglia (Schilling and Kimmel, 1994; Couly *et al.*, 1998; Martik and Bronner, 2017). At the level of posterior midbrain and whole hindbrain, they migrate latero-ventrally in three discrete streams. Their migration paths are dictated by the segmental organisation of the hindbrain (Lumsden, Sprawson and Graham, 1991; Knecht and Bronner-Fraser, 2002). All rhombomere segments contribute to populate pharyngeal arches but not equally (Figure1.13B). In the zebrafish embryo, the first stream is composed of cells from posterior midbrain and hindbrain segments r1-r2, contributing to mandibular arch primordia (PA1). The second stream originates mainly from r4 and a few cells from r3 and r5 and contributes to hyoid arch primordia (PA2). The third stream that populates branchial arches primordia (PA3-6) comes from r6 and r7, but fewer cells come from r5 as well (Schilling and Kimmel, 1994). R3 and r5 regions are considered as nearly crest-free zones. In zebrafish, cranial NCCs migration from hindbrain starts at 13 hpf and follows an AP progression in timing (Rocha *et al.*, 2020) (Figure1.13A). Disruption of the segmental organisation of hindbrain will lead to cranial neural crest development and migration defects. The segregation of cranial neural crest cells into distinct streams is necessary to prevent fusions of the cranial ganglia and skeletal elements and also mixing of neural crest cells with other cell types (Golding *et al.*, 2000; Golding, Dixon and Gassmann, 2002).

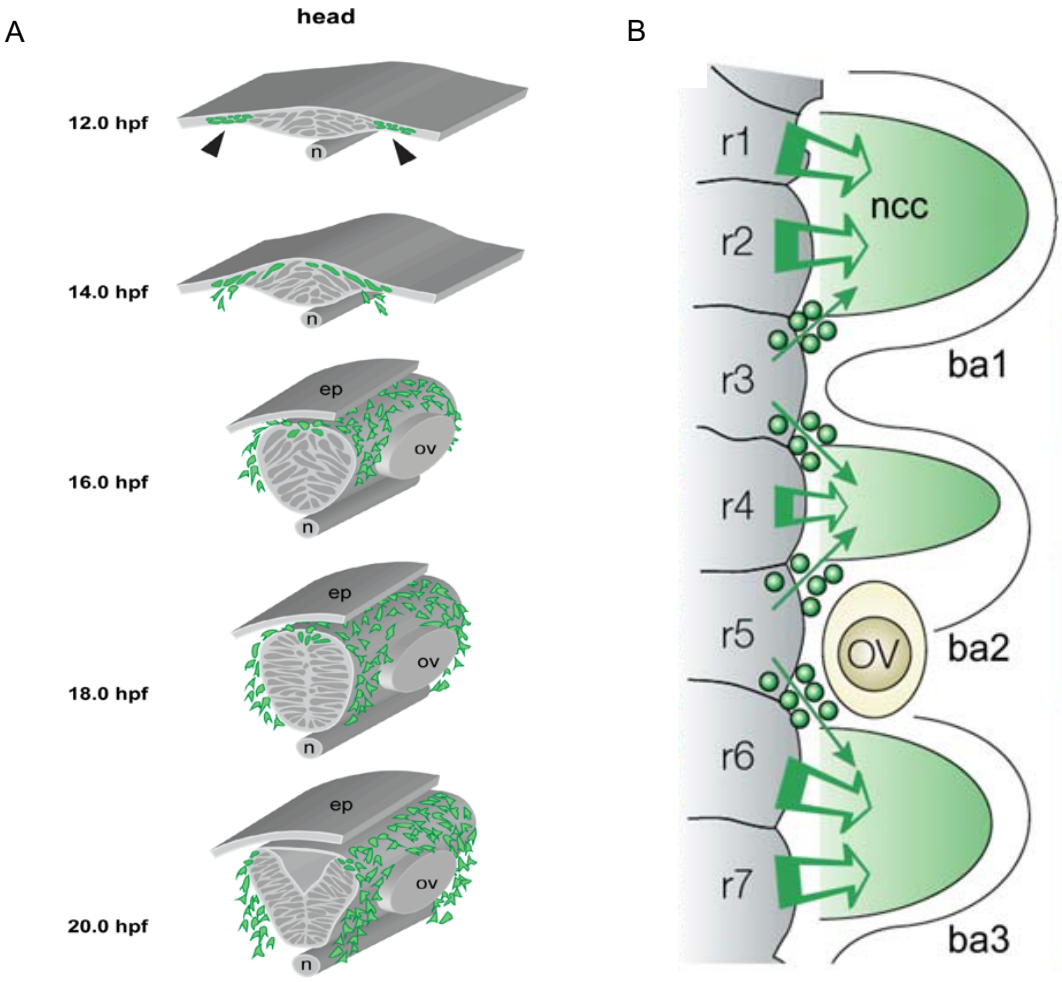

Figure 1. 13. Migration of cranial neural crest cells.

A) Schematics of cranial neurulation and neural crest migration at the rhombomere 4-6 level, displaying neural crest cells (green) migrating anterior and posterior of the otic vesicle towards branchial arches. Arrowhead indicates the laterally segregated cells. Stages are indicated. n: notochord; ep: epidermis; ov: otic vesicle B) Streams of neural crest cell migration: Neural crest cells derived from the hindbrain (large green arrows) migrate ventrolaterally in three segmental streams adjacent to the even-numbered rhombomeres and into the branchial arches. Nccs derived from the odd-numbered rhombomeres do not migrate laterally, rather they migrate anteriorly or posteriorly to join the even-numbered neural crest streams. OV: otic vesicle; ba: branchial arch; ncc: neural crest cells. Figures from (Rocha *et al.*, 2020) and (Trainor, 2003) respectively.

1.4. Molecular mechanisms underlying hindbrain segmentation

The current dogma holds "activation-transformation" model (Niewkoop, 1999) for the induction of neural tissue. In this model, the naïve ectoderm is initially activated to general anterior neural tissue (forebrain) and a subset is subsequently transformed to posterior fate (hindbrain and spinal cord) through the secretion of caudalizing factors. In zebrafish, activator signal BMP antagonists: noggin, chordin, and follistatin proteins come from the mesodermal lip "organiser". Posteriorising signals such as FGF, RA and canonical Wnt pathways emanate from paraxial mesoderm present adjacent to the posterior neuroectoderm (Woo and Fraser, 1997; Begemann *et al.*, 2001; Kudoh, Wilson and Dawid, 2002). However, recent studies challenge the activation-transformation model, show the axial position (A-P) determines cell fate prior to neural induction (Metzis *et al.*, 2018) and further argue that two separate mechanisms act behind induction of anterior (brain) and posterior (spinal cord) neural tissue (Polevoy *et al.*, 2019). Nonetheless, it is established through many studies in several vertebrate systems that Fgf, Wnt and RA have roles as posteriorizing factors and are involved in hindbrain induction. Three morphogen gradients, FGF, RA and Wnt and a complex network of transcription factors control the regulation of early hindbrain specification and patterning (Frank and Sela-Donenfeld, 2019).

1.4.1. Morphogen gradients

A morphogen is a signalling molecule, mostly polypeptides but non-peptide molecules such as retinoic acid exist as well. Morphogen gradients are thought to give positional cues to a uniform field of cells and drive distinct cell fates in a concentration-dependent manner (Rogers and Schier, 2011). It is described by Lewis Wolpert's "French Flag", where different thresholds of an unique morphogen- concentration gradient gives distinct cell fates. Morphogens can also direct cell behaviour such as movement directly. Generally, gradients are produced at a source and transported towards the degrading sink. The spatial distribution is achieved not just through a simple diffusion but involves active transport mechanisms through the extracellular space toward neighbouring cells (Kerszberg and Wolpert, 1998). Responding to the signal at threshold levels, cells activate different sets of target genes, thus initiate the patterning processes and ultimately dictates cell fate (Rogers and Schier, 2011). Mechanisms leading to different cell states with different concentrations of morphogen are currently being elucidated. Cis-regulatory modules (enhancer) with different affinity for morphogen molecules provide insight into the mechanisms of action of Dorsal (Dl) and Bicoid (Bcd) morphogens in patterning *Drosophila* embryos (Irizarry and Stathopoulos, 2021). The challenges of simple concentration-dependent morphogen gradient are interpretation of noisy morphogen gradient by the cells at the border and how growing tissues incorporate morphogen gradient during morphogenesis.

Hindbrain segmentation utilises such positional signalling information to pattern the neuroepithelium into seven segments. Latest modelling with two morphogens FGF and RA and transcription factors such as krox20, hoxb1b, also taking into account the morphogenetic movements simulated the formation of r2-r6 with sharp boundaries at correct size (Qiu *et al.*, 2021). Following sections explain the known roles of RA and FGF morphogen gradients in hindbrain induction and patterning.

1.4.1.1. RA signalling

Retinoic acid is an active metabolite of vitamin A. It is a small lipophilic molecule which acts as a signalling ligand. It is a key player in chordate axial patterning. During embryogenesis, it plays several key roles such as anteroposterior patterning of hindbrain and heart, neuronal differentiation of spinal cord neurons, formation of early somites, optic cup, anterior eye and kidney, induction of forelimb, lung, pancreas and also meiosis (Duester, 2008). Embryos deficient in vitamin A (vitamin A deficiency syndrome or VAD) fail to complete development and exhibit patterning defects in the CNS, circulatory system, hematopoietic system, limbs, and trunk. But when given in excess or in ectopic places, RA is a potent teratogen. Thus, the appropriate pattern of RA activity is necessary for a successful embryonic development. Local control of synthesis and degradation creates the necessary balance in RA signalling (Dobbs-McAuliffe, Zhao and Linney, 2004).

Synthesis and degradation: Retinoic acid is synthesized from vitamin A precursor, which is available through diet as beta-carotene and retinyl esters from plant and animal sources respectively. During embryonic development, it is provided from the mother through placenta and yolk sac in mammalian embryos, while in other vertebrates such as zebrafish, it is contained in the egg yolk. RA is then derived from vitamin A precursor through two consecutive enzymatic steps (Figure 1.14a). Vitamin A, (retinol) is oxidised to retinaldehyde by either alcohol dehydrogenases (Adhs) or retinol dehydrogenases (RDHs) and then to retinoic acid by retinaldehyde dehydrogenases (Raldh1, Raldh2 and Raldh3) enzymes (Duester, 2008). On the other hand, RA undergoes oxidative degradation by cytochrome P450 (Cyp26) enzymes (Cyp26a1, Cyp26b1 and Cyp26c1). Intra and extra-cellular transportation of RA is mediated by binding proteins Retinol-Binding Protein (RBP4) and Cellular Retinol-Binding Proteins (CRBP 1 and 2) respectively. Several isomeric forms of RA such as all trans, 13-cis RA and 9-cis RA exist; however all-trans RA is the primary ligand acting during embryonic development and 9-cis RA is only detectable when vitamin A is in excess (Cunningham and Duester, 2015).

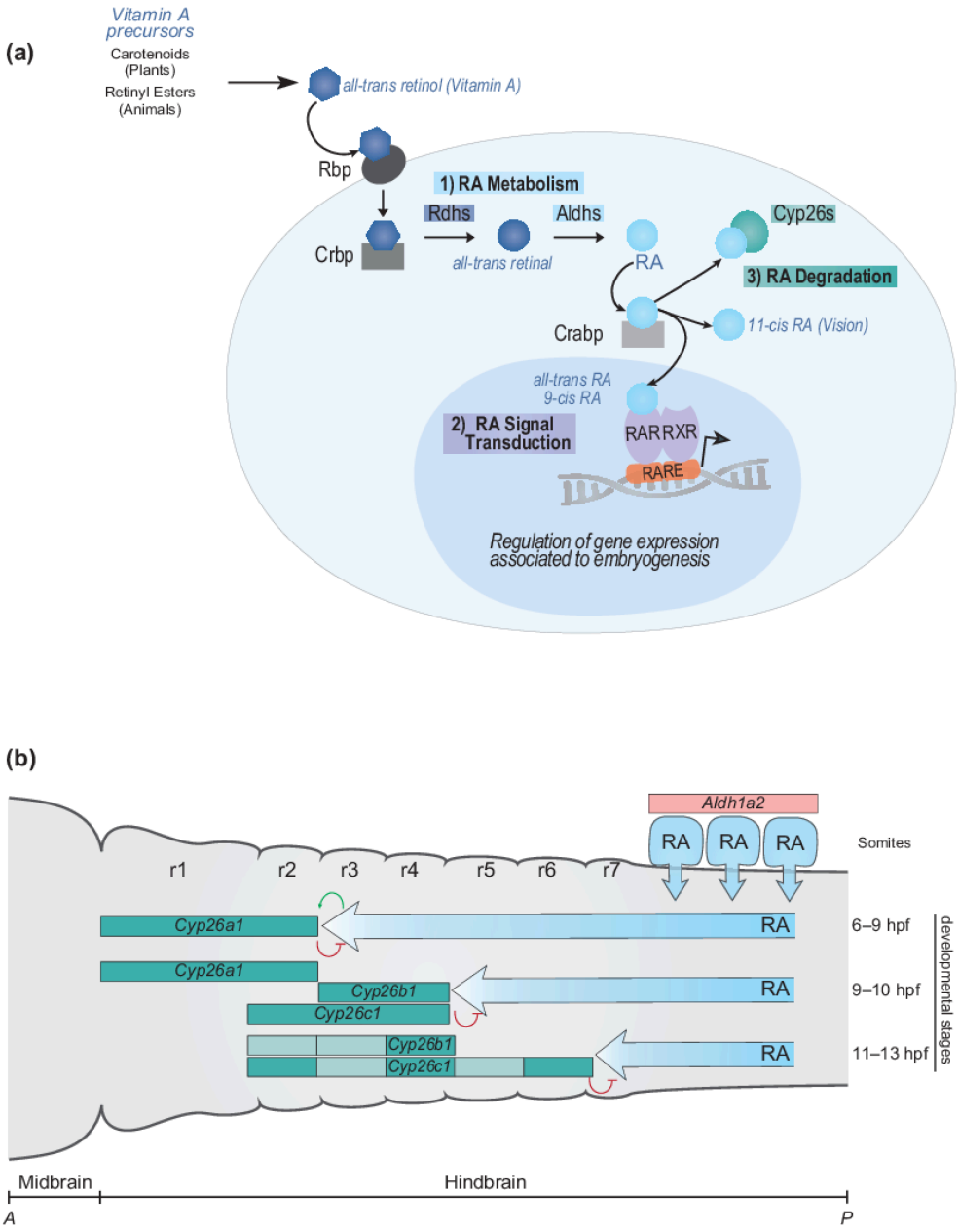

Figure 1. 14. RA signal transduction and RA morphogen gradient during zebrafish hindbrain development.

(a) Schematic representation of major steps of the RA signalling pathway and main components of the RA machinery. The RA signalling pathway converts Vitamin A to RA following three important steps: (1) RA metabolism, (2) RA signal transduction and (3) RA degradation. The RA machinery includes main actors of the signalling pathway: RA synthesizing and degrading enzymes (Rdhs; Aldhs; Cyp26s), transport proteins (Rbp; Crbp; Crabp), nuclear hormone receptors (RAR-RXRs), and Retinoic Acid Response Elements (RAREs). (b) Schematic depiction of the dynamic regulation of endogenous levels of RA during hindbrain development. Aldh1a2 expressed in presomitic mesoderm and somites induces the synthesis of RA which then diffuses into the adjacent neural tube. The anterior limit of RA signalling activity in the neural tube is progressively restricted by the dynamic segmental expression of Cyp26a1, Cyp26b1 and Cyp26c1 which encode the cyp degrading enzymes. The developmental time points correspond to zebrafish development. A, anterior; P, posterior; r, rhombomere. Figure from (Bedois, Parker and Krumlauf, 2021).

Mode of action: CRABP (cellular RA-binding protein) protein transports RA to the nucleus. Thus, unlike other signalling molecules such as FGF, and Wnt, which act through membrane receptors, RA directly enters nucleus and regulates transcription of target genes via two nuclear receptors namely, retinoic acid receptors (RARs) which bind all trans RA and retinoid X receptors (RXRs) which bind the isomer 9-cis RA. RAR α-γ (specific to RA) interacts with RXR α-γ (common dimeric factor) to form a dimer. The binding of RA ligand to RAR present in the RAR-RXR dimer forms a complex, which in turn binds directly to the specific DNA motifs, called retinoic acid response element (RAREs). RAREs are found in the regulatory regions of target genes. In the absence of RA ligand, RAR-RXR dimers can bind to RAREs and partner with transcriptional repressors to inhibit target gene expression. Binding of RA ligands to RAR-RXR dimers induces a conformational change and results in the replacement of the associated repressor complexes with co-activators (NCOA) and facilitates the activation of target genes. In this way, RA modulates the expression of downstream genes (Duester, 2008; Bedois, Parker and Krumlauf, 2021).

RA in hindbrain patterning: RA morphogen gradient primarily lays down the segmental Hox code in hindbrain primordia. The roles of RA have been elucidated from studies performed in various animal models mainly rats, mice, chick and zebrafish through causing vitamin A deficiency, excess RA treatment, mutants and morphants of various genes involved in RA synthesis and degradation pathways and their target genes and treatment of embryos with chemical inhibitors of RA synthesis.

RA forms shifting morphogen gradient: The shifting boundaries of RA morphogen gradient over time is depicted in zebrafish model (Figure 1.14b). The feedback mechanism between synthesis and degradation gives rise to a temporally dynamic concentration gradient of RA during hindbrain segmentation. Several ligands, receptors and antagonists of RA signalling pathway are expressed in region-specific manner at different time windows. This regulates the robust and dynamic RA morphogen gradient (White and Schilling, 2008; Frank and Sela-Donenfeld, 2019). In zebrafish, *cyp26a1* expression is initially induced in the mesendoderm, adjacent to the future hindbrain, by low levels of RA. During mid-gastrulation stages (6–9 hpf), FGF activity from the midbrain induces *cyp26a1* expression in the prospective r1–r2 domain of the hindbrain (White *et al.*, 2007) (Figure 1.14). Degradation of RA in r1 and r2 by *cyp26a1* initially sets a sharp anterior limit of RA signalling activity at the r2/r3 boundary of the hindbrain. Towards the end of gastrulation (9 to 10 hpf), *cyp26b1* is further induced in r3 and r4 and *cyp26c1* in r2 to r4, which alters the anterior limit of RA activity to the r4/r5 boundary. By 11–13 hpf, the *cyp26b1* and *cyp26c1* expression domains spread and collectively cover r2 to r6 domain, which results in another shift of the anterior limit of RA activity to the r6/r7 boundary. In support of the view, endogenous RA

gradient is also directly visualised *in vivo* during zebrafish gastrulation and hindbrain segmentation using Fluorescence Resonance Energy Transfer (FRET) based RA reporters (Shimozono *et al.*, 2013).

Downstream effectors of RA during hindbrain patterning: Many genes from the regulatory network controlling hindbrain segmentation such as *hoxa1*, *hoxb1*, *vhnf1, cdx1*, *hoxb4,* and *hoxd4* contain RARE elements in their enhancer regions. These RAREs respond to the RA morphogen gradient at different time windows and spatial positions along the A-P axis, leading to the generation of ordered gene expression domains (Figure 1.15). The domains are subsequently shaped by interactions with other patterning genes. The regulatory mechanisms underlying differential RA responsiveness are currently being understood with the discovery of cis-regulatory elements of various genes (Tümpel, Wiedemann and Krumlauf, 2009; Parker and Krumlauf, 2020).

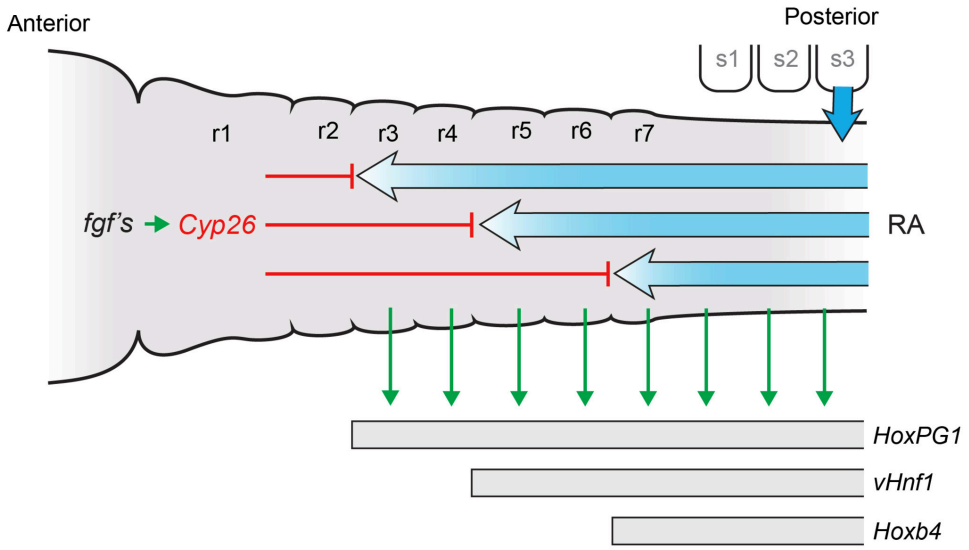

Figure 1. 15. Direct target genes of RA Signalling during hindbrain segmental patterning.

Depiction of the hindbrain is shown in dorsal view with anterior to the left. The shifting boundaries of *Cyp26* expression and RA responsiveness are illustrated for three sequential phases, as characterized in the zebrafish hindbrain at pre-rhombomeric and rhombomeric stages. RA activates directly the expression of key genes in the hindbrain, *Hox paralogue group1*, *vHnf1* and *Hoxb4*. Figure from (Parker and Krumlauf, 2020).

1.5.1.6. Effects of RA manipulation

In general, dietary depletion of vitamin A in chick embryos, loss-of-function mutations in Aldh1a2, both in mice and zebrafish, *aldha2* morphants in zebrafish and injection of dominant negative Retinoic Acid Receptors (dnRA) lead to a loss of posterior rhombomeres and expansion of anterior rhombomeres (Figure 1.16A) (Niederreither *et al.*, 2000; Begemann *et al.*, 2001, 2004). It is also exhibited with the loss of posteriorly expressed genes, such as *hoxb1*, *fgf3*, and *val*, together with caudal expansion of the r3 stripe of *krox20* (Figure1.16B). In contrast, embryos treated with exogenous RA exhibit expansion of posterior rhombomeres at the expense of anterior ones. Notably, both loss- and gain-of-function approaches are dose dependent. Higher doses of pharmacological inhibitors of RA signalling such as DEAB and BMS493 or exogeneous RA treatments lead to progressively more severe anteriorization or posteriorization, respectively (Maves and Kimmel, 2005). Challenging the morphogen gradients, continuous treatment of RA-deficient embryos with a uniform concentration of exogenous RA fully rescues hindbrain patterning within a wide concentration range. Interestingly, it is shown that the degradation enzymes Cyp26 play a crucial role in quickly converting any uniform extracellular concentration of RA into an intracellular concentration gradient that facilitates the rescue of hindbrain patterning (Hernandez *et al.*, 2007; White *et al.*, 2007; White and Schilling, 2008). Furthermore, a global transient exposure of RA via all-trans RA (active isomer) treatment or photoisomerization of 13-cis RA (inactive) into all-trans RA rescues hindbrain patterning in RA-deficient embryos. This indicates that all-trans-RA is sequestrated in the exposed embryo (Xu *et al.*, 2012).

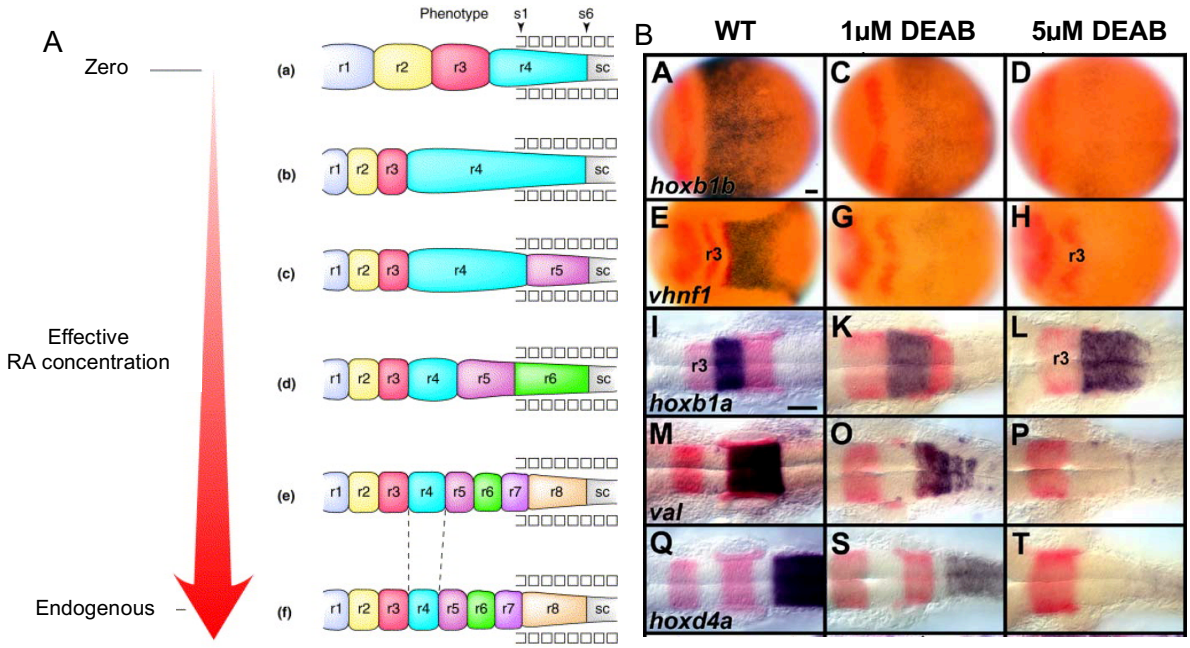

Figure 1. 16. Posterior rhombomere need progressively higher levels of RA signalling.

A) Schematics of hindbrain patterning with decreasing levels of RA, achieved by inhibition with varying concentration of pan-RAR synthetic retinoid antagonist (BMS493) in chick. Various concentration of the drug was applied at the primitive streak stage before the RA requirement for hindbrain patterning sets in, lead to a spectrum of phenotypes, ranging from a fully RA-deficient phenotype (a) to essentially wild type (f). r: rhombomere; s: somite; sc: spinal cord. B) Loss of posterior rhombomere markers upon DEAB treatment (µM), inhibitor of RA synthesis in zebrafish. In-situ hybridization of brain markers in wild type (A, E, I, M, Q) and DEAB-treated zebrafish embryos at various developmental stages. Embryos stained in blue for hoxb1b at 10 hpf (A, C, D), vhnf1 at 10.5 hpf (E, G, H) at 18 hpf, hoxb1a (I, K, L), val (M,O,P) and hoxd4a (Q, S, T). Other markers in red are pax2a to label MHB (A, C, E, G, H) and *krox20* (in all other panels). DEAB-treated embryos show severe reduction of *hoxb1a* and *hoxd4a* expression, loss of vhnf1 expression, krox20 in r5, val in r5-r6, and expansion of domains of krox20 in r3 and *hoxb1a* in r4. In situ hybridization of labelled genes, *hoxb1b*, *vhnf1*, *hoxb1a*, *val*, *hoxd4a* and *krox20* at respective stages. Dorsal view of zebrafish embryos with anterior to the left. Scale bar: 50µm. Figure from (Gavalas, 2002) and (Maves and Kimmel, 2005) respectively.

1.4.1.2. Fibroblast Growth Factor (FGF) signalling

FGF family consists of a several structurally related proteins that are found in various organisms from drosophila to mice and humans (Ornitz and Itoh, 2001). FGFs play regulatory roles in diverse cellular processes including cell migration, differentiation, cell survival, and apoptosis. During embryonic development, FGF signalling plays a crucial role in the induction and maintenance of mesoderm and neuroectoderm, the control of morphogenetic movements, anteroposterior (AP) patterning, somitogenesis and the development of various organs (Dorey and Amaya, 2010). There are 22 FGF ligands that have been characterised in humans and mice. FGFs are further classified into subfamilies based sequence similarity and biochemical properties. FGFs bind to heparan sulfate proteoglycans (hpcg). This acts as an accessory molecule to activate the cell surface receptors called FGFR. FGFRs are tyrosine kinase receptors that contain a heparin-binding sequence, three extracellular immunoglobulin-like domains, a hydrophobic transmembrane domain, and a split intracellular tyrosine kinase domain (Eswarakumar, Lax and Schlessinger, 2005). Four FGF receptors (FGFR1-FGFR4) are reported in all vertebrates. The differential binding affinities between FGFs and FGFRs and the complex and dynamic expressions of Fgf ligands and receptors provide the correct FGF signalling transduction for a variety of biological functions. Feedback inhibitors such as the Sproutys, Sef and MAP kinase phosphatase 3 are responsible for the attenuation of FGF signals restricting FGF activities spatio-temporally (Thisse and Thisse, 2005).

The FGF signalling cascade is initiated by the binding of FGF ligands and hspg to the extracellular ligand domain of FGFR, which in turn induces receptor dimerization, activation and autophosphorylation of multiple tyrosine residues in the cytoplasmic domain of the receptor molecule. A variety of signalling proteins are phosphorylated in response to FGF activation that initiate various intracellular signalling pathways and mediate changes in gene expression and cell behaviour. The FGF system is associated with several downstream signalling pathways such as RAS/mitogen-activating protein (MAP) kinase pathway, the phosphoinositide 3 (PI3) kinase/protein kinase B (PKB) pathway, and the phospholipase C gamma (PLCγ)/protein kinase C (PKC)/Ca^{2+} pathway (Figure 1.17) (Dorey and Amaya, 2010).

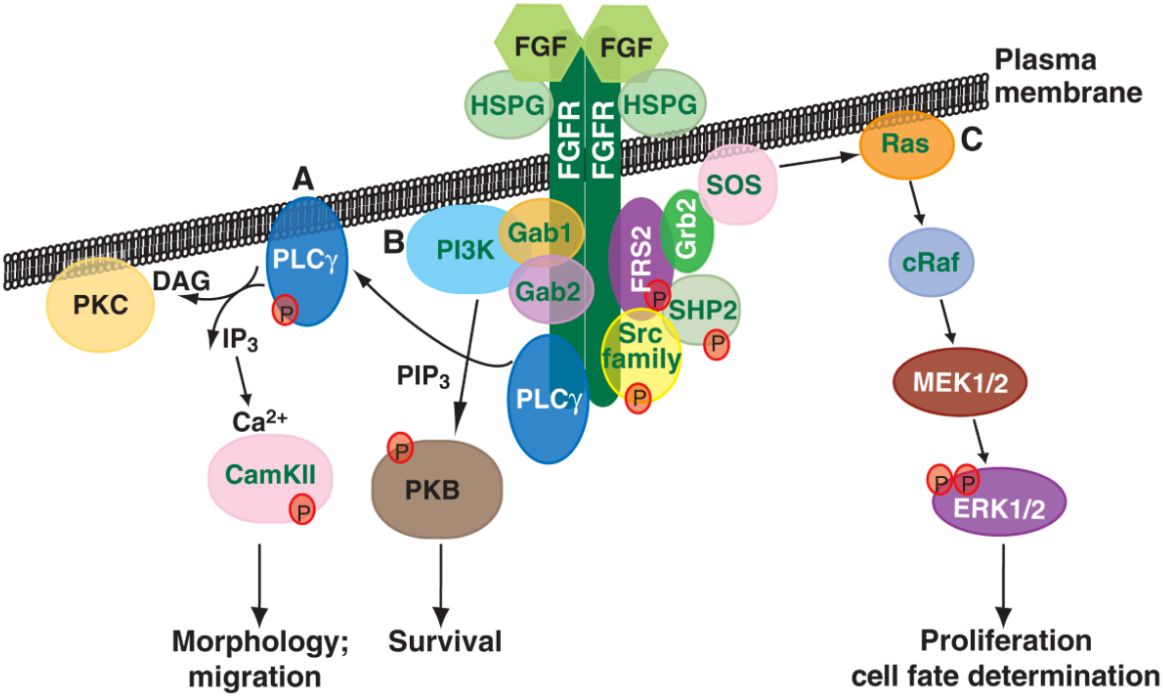

Figure 1. 17. Downstream pathways of FGF signalling.

FGF signalling is initiated by ligand-dependent dimerisation of the FGFR, which leads to the cross-phosphorylation (P) of tyrosine residues in the intracellular domain of the receptor tyrosine kinase (not shown). These phosphorylated residues are then bound specifically by several intracellular signal transduction proteins, including phospholipase C gamma (PLCγ), Fibroblast growth factor receptor substrate-2 (FRS2) and Sarcoma proto-oncogene tyrosine kinase (Src) family members. These initiate several intracellular signalling pathways, including the (A) PLCγ pathway, (B) protein kinase C/ Protein kinase B (PI3K/PKB) pathway and (C) the rat-sarcoma/extracellular-signal-regulated kinase (Ras/ERK) pathway. The cell responses to these three pathways are indicated. Figure from (Dorey and Amaya, 2010).

FGF in gastrulation movements: FGF is well known for its role in mesoderm specification and their morphogenetic movements during gastrulation. The role of FGF in controlling morphogenetic movements is highly conserved through evolution and it is shown in sea urchin, frog, drosophila, c.elegans, chick and mice (Dorey and Amaya, 2010). It regulates multiple cellular events, including cell shape change and migration. During mid-late gastrula stages of Xenopus, Spred protein, a FGF modulator indirectly activates FGF's PLCγ/PKCδ/Ca2+ pathway (Sivak, Petersen and Amaya, 2005). The pathway instructs the mesoderm cells to undergo morphogenetic movements, which occur after the specification of mesoderm cells by FGF. FGF interacts with Wnt/PCP pathway to control the cell movements such as convergent extension during gastrulation. Convergent extension requires the reorganization of cytoskeletal elements, that enables cells to become polarized along a similar axis. Polarized cells intercalate with one another, which causes the overall tissue layer to extend along the AP axis. FGF is shown to act as both chemoattractant and chemorepellent to organise the migratory events in chick (Yang *et al.*, 2002).

FGF in hindbrain induction and patterning: During hindbrain development, FGFs are first utilised as one of the posteriorizing factors of the neural ectoderm, together with RA and Wnt (Doniach, 1995). From mid-gastrulation to segmentation stages, FGFs are redeployed in several organizing centres such as Midbrain-Hindbrain Boundary (MHB) and mid-hindbrain (r4) to regulate further subdivision of the hindbrain (Mason, 2007).

FGF exerts its role in early AP patterning of neuroectoderm via the regulation of Hox genes. Increasing FGF concentrations lead to expression of progressively more posterior Hox genes (Doniach, 1995). It is also shown that ectopic FGF expression in developing central nervous systems can convert anterior neural tissue to more posterior neural cell types. Thus, it acts as an early posteriorizing factor on the neuroectoderm. Later, FGF signalling from the MHB inhibits *Hox* gene expression in r1 and sets the anterior limit of *Hoxa2* expression in r2. This regulation is required for development of r1. *Fgf3* and *fg8* are initially expressed in zebrafish hindbrain territory from 80%-90% epiboly stages. During late gastrulation, fgf3 and fgf8 are induced by Hoxb1a in presumptive r4 that in turn influence r5-r6 patterning (Figure 1.18)(Maves, Jackman and Kimmel, 2002). Vhnf1, which is initiated by RA, cooperates with Fgf3 and Fgf8 to activate the expression of *valentine (val)/Kreisler/MafB* in r5 and r6. Thus, FGF and RA signalling are proposed to be integrated to pattern the caudal hindbrain (Hernandez *et al.*, 2004; Chomette *et al.*, 2006). Val is required along with vhnf1 and Fgf for *krox20* induction in r5 (Wiellette and Sive, 2003). pea3 and erm are identified as the transcriptional factor target of fgf8 to activate *krox20* expression in r5 (Roehl and Nüsslein-Volhard, 2001). Ffg3 is also known to induce the expression of pax6 in r3 and r5 that indirectly inhibits krox20 expression via *nab1* induction (Kayam *et al.*, 2013). Through regulating both krox20 and pax6, which mutually repress each other, Fgf3 helps

achieve sharp rhombomere borders in the posterior hindbrain. In contrast to r4 signalling centre in zebrafish, in chicken embryos, r2 and r4 function as local signalling centres in the hindbrain where FGF signalling is necessary to maintain the expression of EphA4 in r3 and r5 (Cambronero *et al.*, 2020).

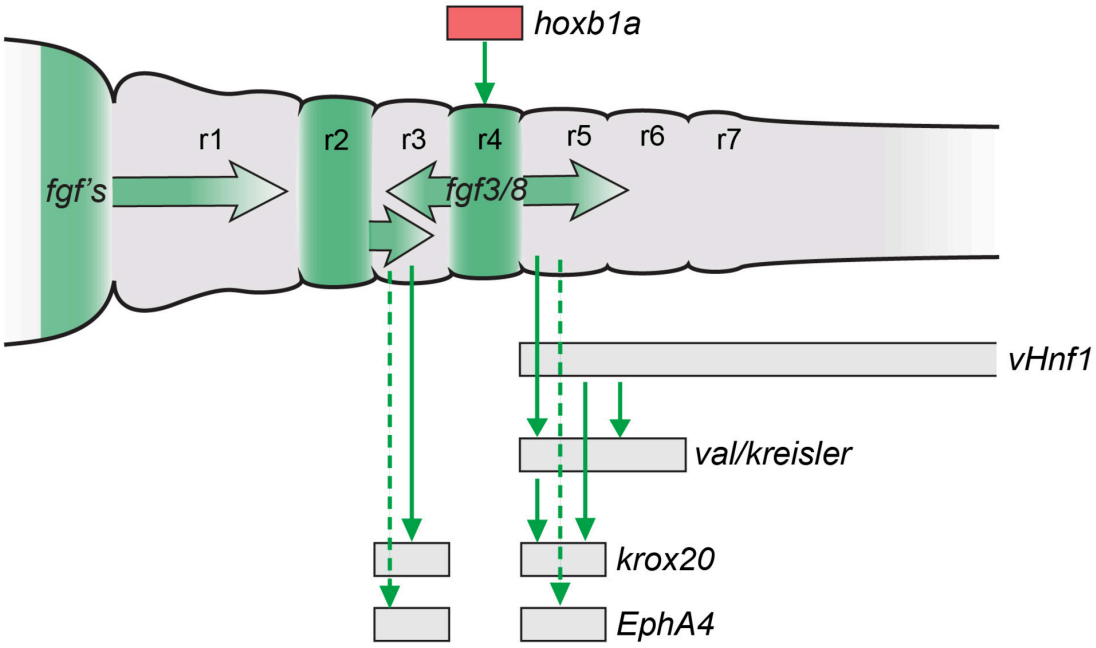

Figure 1. 18. FGF signalling during hindbrain patterning.

FGF signalling centres (green shading) characterized in the zebrafish or chick hindbrain. In zebrafish, *hoxb1a* activates expression of *fgf3/8* to create an r4 signalling centre, which influences expression of *val/Kreisler* and *krox20* in conjunction with *vHnf1*. The isthmic organizer is a source of FGF signals that pattern r1 and restrict anterior *Hox* expression. In chick, FGF signalling from r2 and r4 influences expression of *EphA4* in r3 and r5, either directly (dashed arrows) or via *Krox20*. r, rhombomere; s, somite. Figure from (Parker and Krumlauf, 2020).

Zebrafish ace mutant (fgf8) is hypomorphic and exhibits mild hindbrain defects but lacks cerebellum and the midbrain-hindbrain boundary organizer (Reifers *et al.*, 1998). Loss of FGF signalling through a competitive chemical inhibitor, SU5402 during gastrulation causes loss of posterior rhombomere formation along with the loss of gene expression in r5 and r6 (Roy and Sagerström, 2004). Also, fgf3 and fgf8 appear to act redundantly since gene expression in r5 and r6 is lost only in zebrafish embryos co-injected with morpholino oligonucleotides (MO) of both genes (Walshe *et al.*, 2002). Krox20 expression in r3 is also reduced in these morphants.

1.4.2. GRN of hindbrain segmentation

Many developmental genes are expressed in restricted domains of prospective hindbrain that reflect and underlie the development of future morphological segments. The key players are *Hox* genes. Zebrafish has seven Hox clusters, comprising of 48 Hox genes while mammals such as mouse and humans have four clusters with 39 described genes (Amores *et al.*, 1998). Hox genes play a crucial and ancient role in providing A-P identity to hindbrain segments. Hox gene expression is coupled to hindbrain segmentation and its regulatory elements are highly conserved till lamprey, which is at the base of vertebrates (Parker, Bronner and Krumlauf, 2014). Hox genes from the Paralogue Group (PG1-4) display nested and ordered segment-specific patterns of expression along the AP axis, in response to FGF and RA gradients. They position, sharpen, and maintain other segmental gene expression. Thereby, rhombomere-specific gene regulatory network is formed and commits cells to distinct segmental fates. Mis-specification of Hox code causes homoeotic transformation of rhombomere identity. For example, in mouse and zebrafish, ectopic expression of *Hoxa1* and *hoxb1b* respectively causes a homeotic transformation of r2 to r4 identity both in terms of molecular markers and neuroanatomy (Zhang *et al.*, 1994; McClintock *et al.*, 2001).

The latest GRN model of hindbrain patterning is constructed from the experimental data including analyses of gene expression, phenotypes and perturbation of gene expressions in mutants and morphants and characterisation of cis-regulatory elements performed in many vertebrate models, primarily in mice, zebrafish and chick. The network is found to be widely conserved as the overall hindbrain structure and function across vertebrate species are remarkably similar too (Parker, Bronner and Krumlauf, 2016; Parker and Krumlauf, 2020). However, the diversity of craniofacial features and hindbrain among different vertebrate species might have evolved due to the differential role of GRN genes at later stages and/or the difference in the downstream genes of this network (Krumlauf and Wilkinson, 2021). Comparative studies of nature of downstream genes in different species are required to further our understanding.

The “hypothetical” GRN is described in progressive series of modules with an example of mouse hindbrain. The different elements involved in each step is given in (Figure 1.19) and it is evident that many elements play multiple roles during hindbrain segmentation. The gene regulatory network in three progressive modules is depicted in (Figure 1.20).

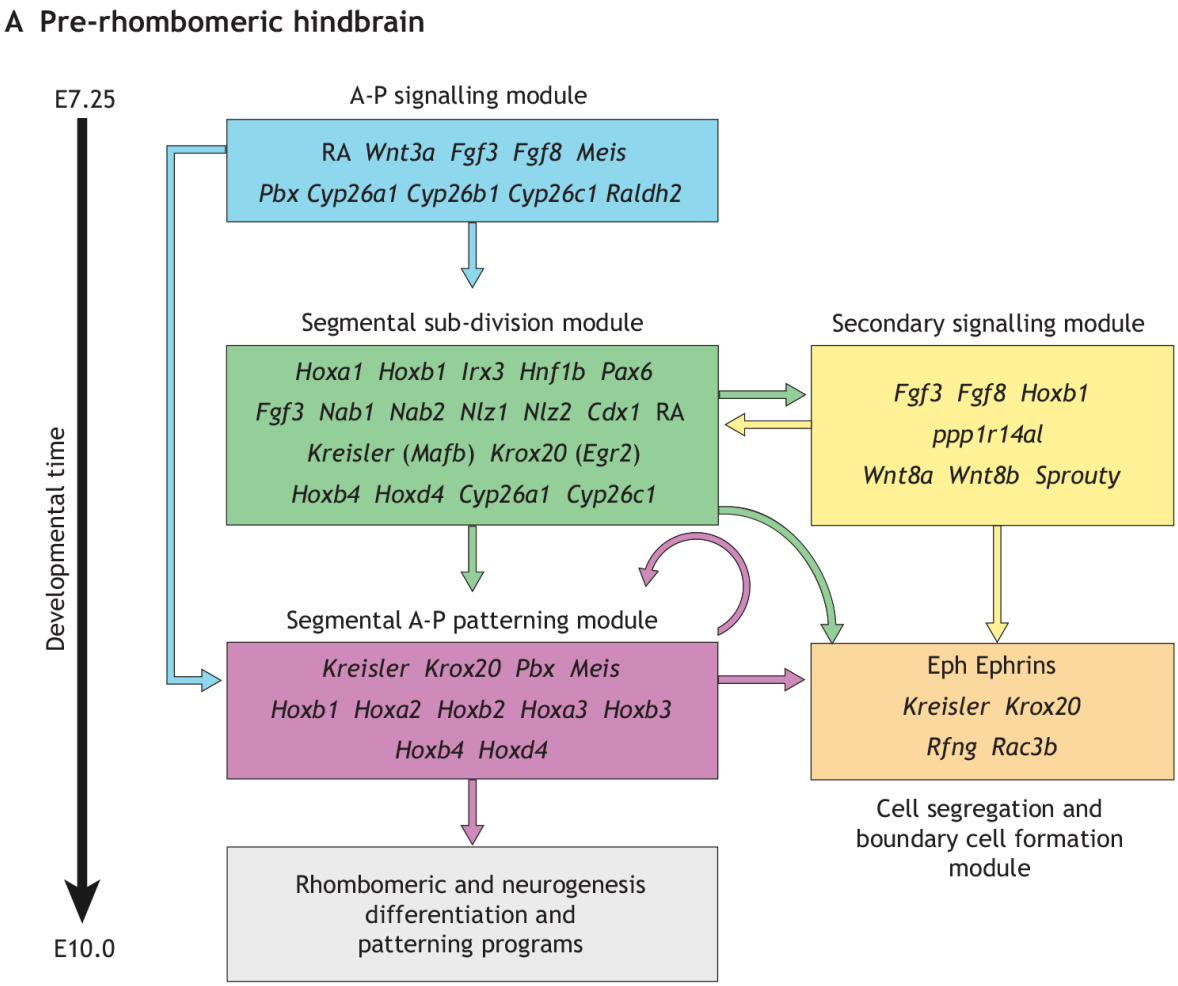

Figure 1. 19. Gene regulatory network (GRN) governing hindbrain segmentation.

A framework of the GRN model is depicted as a progressive series of modules associated with underlying cell and developmental processes in the mouse hindbrain between E7.25 and E10.0. Each module (coloured box) has its regulatory circuits and components. Key genes and signals are inside each box. The gene names correspond to mouse. The arrows indicate the flow of regulatory information between modules. Figure from (Krumlauf and Wilkinson, 2021).

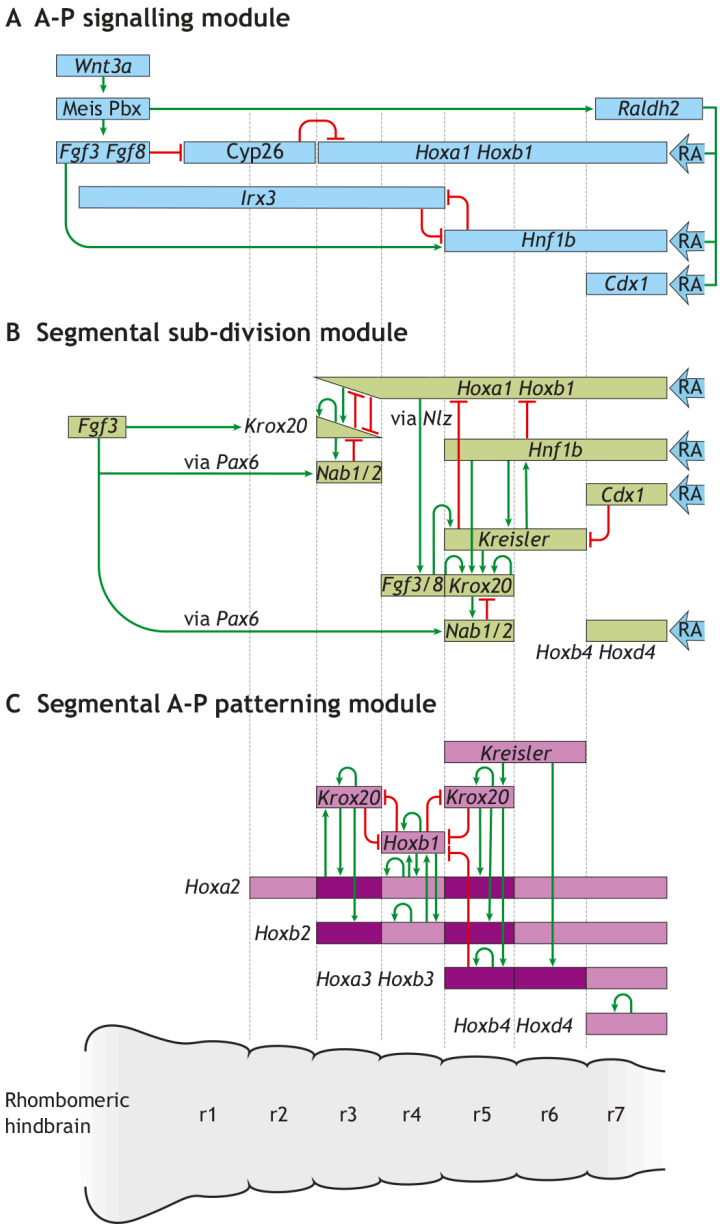

Figure 1. 20. Three modules governing successive steps in the hindbrain segmentation GRN.

(A) The A-P signalling module initiates the process of segmentation in the pre-rhombomeric hindbrain through combined inputs and cooperative interaction between Fgf, Wnt and RA signalling pathways. This establishes restricted domains of spatially restricted enzymes, signals and transcription factors (blue rectangles) that trigger the next step (B) The segmental sub-division module represents regulatory interactions that establish sharp expression domains of segmentation genes (green rectangles) through auto- and cross-regulation involving mutual repression and activation. This provides a transcriptional code that sub-divides the hindbrain into segments (C) The segmental A-P patterning module activate rhombomere-restricted domains of Hox expression (purple rectangles) to specify identity of individual segments. Darker shades of colour indicate higher levels of respective hox expression in specific rhombomeres. In A-C, the interactions depicted within each module do not imply a specific temporal or hierarchical order, but represent cumulative interactions associated with each module. r, rhombomere. RA-Retinoic acid, FGF- Fibroblast Growth Factor. Figure from (Krumlauf and Wilkinson, 2021).

1.4.2.1. A-P signalling module

In the initial A-P signalling module, signalling pathways such as RA, FGF and Wnt are constituted and involved in the induction of various Hox and other transcription factors, enzymes and signals in restricted domains in the neuroectoderm (Figure 1.20A). In mouse, Wnt3a activates Meis and Pbx genes which in turn activates the expression of Fgf3 and Fgf8 and the synthesis of RA in presomitic mesoderm, adjacent to the posterior hindbrain. Synthesised RA diffuses to the presumptive neuroectoderm till the level of r3 beyond that the FGF induced Cyp26a1 which degrades RA (Sirbu *et al.*, 2005). Thus, it forms the morphogen gradient in the prospective hindbrain with posterior RA [high] and anterior RA [low] levels. Hox PG1 genes, Hoxa1 and Hoxb1 are initially induced by RA with the anterior limit at r2/r3 boundary. Vhnf1/Hnf1b and Cdx1 are also induced by RA in prospective r5 and r6 and r7 domains respectively (Houle *et al.*, 2000; Hernandez *et al.*, 2004).

1.4.2.2. Segment sub-division module

In the segment sub-division module, the initiated transcription factors in the previous step in turn activate a network of spatially restricted transcription factors in the segmental sub-division module. Hoxb1 directly activates *Fgfs* in r4. Fgf and Vhnf1 together initiate the expression of *Kreisler* in r5 and r6 and *Krox20* in r5 (Wiellette and Sive, 2003). Later, the shifted RA gradient activates the Hox PG4 genes, Hoxb4 and Hoxd4 in prospective r7 domain (Gould, Itasaki, and Krumlauf 1998; F. Zhang, Nagy Kovács, and Featherstone 2000). Key segmentation genes such as Hoxa1 and Hoxb1 in r4, Vhnf1 in r5 and r6, Krox20 in r3 and r5, Kreisler/Valentino in r5 and r6 and Cdx1 in r7 with tight A-P expression domains are formed (Figure 1.20B). The segmental pattern of gene expression prefigures rhombomere boundaries. These genes have direct cross-regulatory properties among each other and form spatially restricted domains of the gene expression. For example, Hoxb1 in r4 and Krox20 in r3 and r5 repress each other and it establishes sharp borders of r3/r4 and r4/r5 (Chomette *et al.*, 2006; Labalette *et al.*, 2015). Cdx1 represses Kreisler in r7 thereby restricting Kreisler expression to r6/r7 border (Sturgeon *et al.*, 2011). Further, spatially restricted expression domains sharpen and maintain through positive-feedback loops. This ultimately provides the segment-specific "Hox code" to divide the hindbrain region into seven segments with unique identity (Parker and Krumlauf 2020).

1.4.2.3. Segment A-P patterning module

In the segment A-P patterning module, transcription factors directly regulate the spatially restricted expression of Hox genes. Krox20 regulates Hoxa2 and Hoxb2 in r3 and r5. Kreisler activates Hoxa3 and Hoxb3 in r5 and r6. The expression of Hox genes are confined and maintained

in specific rhombomeres through various auto- and cross-regulation among themselves (Figure 1.20C). Fox example, Hoxa3 in r5 and r6 is maintained by a conserved auto- and cross regulatory region, dependent on Hoxa3 and Hoxb3 and Pbx and Prep/Meis cofactors (Manzanares *et al.*, 2001). Hoxa2 is the only Hox expressed in r2 and regulates r2 development. Thereby, an "Hox code" is attributed to each individual segment. The "Hox code" gives A-P positional identity to each segment that facilitates regional diversity in the hindbrain primordia (Hunt and Krumlauf, 1991). Hox genes initiate and regulate rhombomere-specific genes necessary for neurogenesis, differentiation and patterning. The patterning cues must mediate dorsoventral, mediolateral, and temporal regulation to drive restricted expression of the target genes. The regulatory network imparted by Hox genes on their target genes is currently being elucidated. Hox target genes are identified with various techniques such as microarray and Chip seq (Rohrschneider, Elsen and Prince, 2007; Amin *et al.*, 2015). Rhombomere-specific single cell sequencing at three stages 16 hpf, 24 hpf and 44 hpf during zebrafish hindbrain segmentation further promises to identity downstream genes that are in relation with Hox (Appendix Figure 1) (Tambalo, Mitter and Wilkinson, 2020).

1.4.2.4. Secondary signals

Secondary signals such as Wnt and FGF form within the hindbrain in order to further subdivide the region (Figure 1.19). Segmentation sub-division module restricts Hoxb1 in r4 that induces the expression of fgf3 and fgf8 in the presumptive r4. Thus, for zebrafish, Fgf3 and fgf8 form a secondary local signalling centre (r4) where FGF signals act at short range to pattern the posterior hindbrain by regulating the expression of Hoxb1, Krox20 and Kreisler (Val/MafB) and specifies posterior rhombomeres r4-r7 (Mason, 2007). Wnt signalling centres form at the rhombomere boundaries that further regulate the precise metameric patterning in the zebrafish hindbrain (Riley *et al.*, 2004).

1.4.2.5. Cell segregation and boundary cell formation module

The sharp expression domains of transcription factors together with secondary signalling module regulate the cell segregation and border formation processes (Figure 1.19). Eph-Ephrin signalling plays a crucial role in cell segregation and boundary formation. Eph receptors (tyrosine kinase) are expressed in r3 and r5, whereas membrane-bound ephrins are expressed in r2, r4, and r6 (Figure 1.21A). Segmentation gene *krox20* directly regulates *ephA4* expression in r3 and r5. In the caudal region, hox4 proteins regulate cell segregation between r6 and r7, mediated through Ephrin B2 (Prin *et al.*, 2014). Ephb4 is regulated downstream of Val (Cooke *et al.*, 2001). The Ephs and ephrins forms bidirectional signalling pathway, meaning that interaction between cells expressing ephrin with those expressing Eph can lead to the transduction of signals in both cells

(Figure 1.21B). In this way, Eph/ephrin pathway serves to create cell adhesion between cells inside the segment and repulsion between cell populations of adjacent segments (Xu *et al.*, 1999; Cooke, Kemp and Moens, 2005). This leads to cell sorting between adjacent cell populations. The Eph-Ephrin is also involved in the formation of mechanical barriers at inter-rhombomeric boundaries (Calzolari, Terriente and Pujades, 2014). Cell identity switch is also shown to occur in intermingled cells of different rhombomere identity. Recent study showed that different levels of RA signalling in segments are directly coupled to segment identity of cells in respective segments. This enables cell identity switch of intermingled cells in a given segment to maintain homogenous segmental identity (Addison *et al.*, 2018; Wilkinson, 2018). Computer simulations have shown that both cell segregation and cell identity switch are necessary to maintain homogenous segments (Wang *et al.*, 2017). Furthermore, It is shown that rapid convergence of neural plate cells together with identity regulation by RA and FGF morphogen gradients contribute to border sharpening of the adjacent rhombomeres (Qiu *et al.*, 2021).

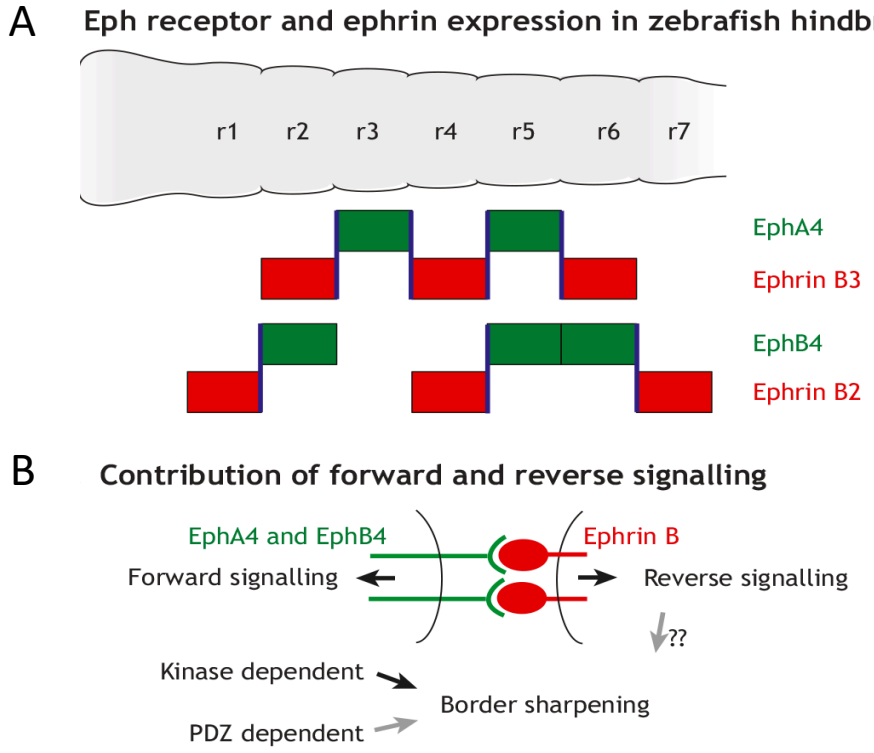

Figure 1. 21. Eph-ephrin signalling in hindbrain border sharpening.

A) Depiction of the segmental expression of Eph receptors and ephrins in the zebrafish hindbrain. EphA4 has high affinity for ephrin B2 and ephrin B3, whereas EphB4 binds selectively to ephrin B2. The segmental expression of high-affinity Eph-ephrin pairs is complementary, such that strong activation (blue lines) occurs at segment borders. B) Eph receptors are activated upon interacting with membrane-bound ephrins, which mediate signal transduction, leading to forward and reverse signalling with Eph-expressing cell and ephrin-expressing cell respectively. Figure from (Krumlauf and Wilkinson, 2021).

1.4.2.6. Transcription factor krox20/egr2b

The gene regulatory network (GRN) which underlies the hindbrain segmentation includes genes that encode transcription factors restricted to specific rhombomeres. The earliest genes expression in prospective hindbrain are *Hoxa1*, *Hoxb1*, *Vhnf1* and *Krox20*. *Krox20*, also known as *egr2*, encodes for a transcription factor member that belongs to zinc finger family proteins. It is the first identified molecular marker that proved the molecular segmentation of hindbrain (Wilkinson *et al.*, 1989; Schneider-Maunoury *et al.*, 1997). In zebrafish, it is expressed in presumptive hindbrain at 10 and 11 hpf that prefigures rhombomere 3 and 5 domains respectively (Figure1.22) (Oxtoby and Jowett, 1993). Krox20 confers r3 and r5 identity and is essential for the formation of these segments (Schneider-Maunoury *et al.*, 1993). Krox20 activates directly *Hox PG 2* and *3* genes such as *Hoxa2*, *Hoxb2* and *Hoxb3* in r3 and r5, and in r5, respectively whereas it represses the *Hox PG1* gene *Hoxb1*. Targeted *Krox20* gene inactivation in mice leads to disappearance of r3 and r5 domains and subsequently their neuronal formation. Krox20 in r3 is controlled by transcriptional enhancer occupied by Hox/Pbx and Meis factors (Wassef *et al.*, 2008) and FGF mediators (Labalette *et al.*, 2015). *Krox20* in r5 is induced by Vhnf1 and Mafb/Val/Kreisler which in turn are induced by RA and FGF signalling (Hernandez *et al.*, 2004; Labalette *et al.*, 2011). Thus, induction of *Krox20* needs synergism between RA and FGF signalling via their downstream mediators Vhnf1. Three enhancer elements (A-C) had been identified for *Krox20* regulation in mouse and chick (Chomette *et al.*, 2006) with element A having autoregulatory property. Recently, it was shown that there are six enhancer elements present in zebrafish which includes the three previous conserved elements (Torbey *et al.*, 2018).

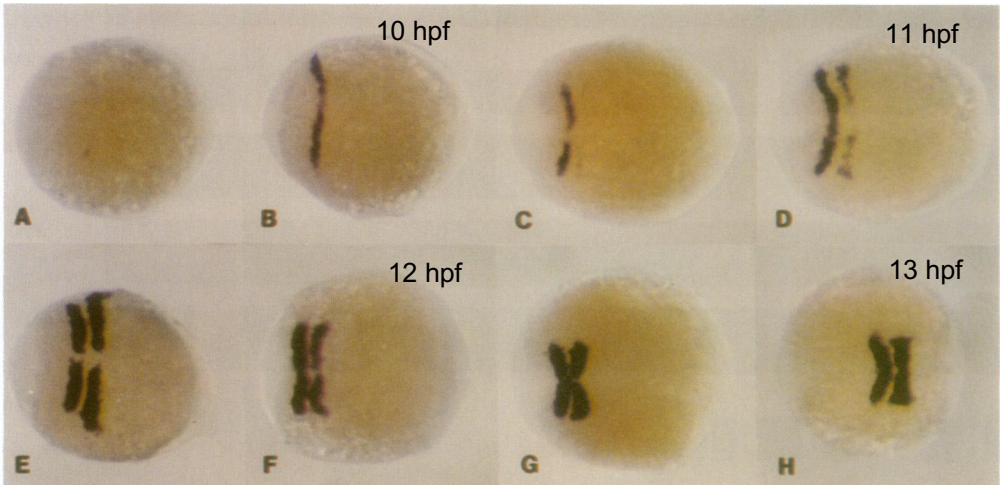

Figure 1. 22. *Krox20* expression in zebrafish embryo at early developmental stages.

A-D: 100% epiboly; E-H: Segmentation stage. Dorsal view of the embryos oriented with anterior end to the left. In-situ hybridisation on whole mount embryos reveals the expression of *krox20* in two segments of the hindbrain that constrict as segmentation progresses along the neuraxis. Figure from (Oxtoby and Jowett, 1993).

1.5. Approaches to study morphogenesis

1.5.1. Constructing dynamic fate maps and digitalising life

In order to understand the cellular mechanisms during morphogenesis, establishment of dynamic fate map is necessary. In such approach, the trajectory of each cell is followed and a complete record of the reorganisation of cells from the progenitor level to the organ formation is made. The technological advances in microscopy and computing methods made the constructions of such dynamic fate maps possible (Buckingham and Meilhac, 2011). The major components of obtaining dynamic fate map is cell lineage tracing via cell labelling, 3D+ live imaging, cell tracking tools and quantitative analysis of dynamic fate maps (England and Adams, 2007).

Vital dye labelling has been replaced by genetic labelling with the discovery of fluorescent proteins. Genetic labelling is performed through integration of fusion protein coding sequence into the genome through transgenesis (Köster and Fraser, 2004). Fusion proteins can permanently label the cells either ubiquitously or tissue-specifically. It can give further details such as mitotic status and cell shape dynamics by specifically targeting them to nucleus and membrane respectively. The mRNAs encoding fusion fluorescent proteins can be injected to label cells systemically that lasts for a short period of development. Photoconvertible fluorescent proteins (causing a shift in the wavelength and consequently colour of emitted light after illumination) such as Kaede and nls-Eos offer a spatial and temporal control of precise labelling (Hatta, Tsujii and Omura, 2006). Heat shock inducible promoter is also available to activate a gene at a specific stage along with the labelling of activated cells (Halloran *et al.*, 2000). Once the suitable labelling is achieved, live imaging can be performed upon optimum embryo growth condition and immobilisation. Advanced microscopes depend on the intensity of fluorescent labelling. It records image as a stack or z-series of optical sections. It can therefore capture the 3-D volume of the embryo at any time. Repeated imaging in a time-lapse or continuous mode over a period captures a 3D record of embryonic development. The positions of individual cells and their progeny over time can be stored as series of cartesian coordinates, can therefore be visualised and animated. Automated cell tracking tools make use of the isolated nuclei nature from neighbours and track them over time. Quantitative analysis of cell behaviours including trajectories, speed and mechanical cues provides biomechanical understanding of the integrated mechanisms of development (Megason and Fraser, 2007).

1.5.2. 3D+time live imaging

During embryo morphogenesis, cells are rearranged to form various tissues and organs in distinct shapes. Morphogenesis involves cell divisions and cell death, along with larger cell movements, cell-cell intercalation, cell shape changes and collective cell migration. It is a highly dynamic process at spatio-temporal levels. Visualising the embryo growth and obtaining quantitative measurements of these cell behaviours and reconstruction of the entire cell lineage is critical for our understanding of underlying biological mechanisms (Keller, 2013). In addition to cell dynamics, obtaining information such as change of gene expression, protein dynamics and physical forces acting during embryonic development in parallel is essential for our complete understanding of morphogenesis (Behrndt *et al.*, 2012; Maître *et al.*, 2012; Tsai *et al.*, 2020). Live imaging is a way to obtain such information quantitively with high spatio-temporal details (Megason and Fraser, 2007; Keller, 2013).

Progress in microscopic techniques and discovery of fluorescent proteins and subsequent transgenesis methods made it now possible to perform *in toto* imaging of early embryonic development and the reconstruction of cell lineages in many higher invertebrates *Drosophila* (McMahon *et al.*, 2008; Krzic *et al.*, 2012), *C. elegans* (Bao *et al.*, 2006; Wu *et al.*, 2011), sea urchin/*Paracentrotus lividus* (Villoutreix *et al.*, 2016), ascidie/*Phallusia mammillata* (Guignard *et al.*, 2020) and vertebrates models such as zebrafish/*Danio rerio* (Keller *et al.*, 2008; Faure *et al.*, 2016) and pre- and post-implantation developmental stages of mammalian models, mouse/ *Mus musculus* (McDole *et al.*, 2011, 2018; Strnad *et al.*, 2016) and pre-implantation stages of rabbit/ *Oryctolagus cuniculus* (Fabrèges *et al.*, 2018). Together with advances in computation tools such as image processing and automated cell tracking tools, almost every cell in the embryos can be tracked and reconstructed across the early developmental stages (Pastor-Escuredo and del Álamo, 2020). However, accurate automated reconstruction of all cells for a long period of morphogenesis is still a great challenge given the complexity and magnitude of cell numbers involved during vertebrate embryonic development.

1.5.2.1. Microscopy

Confocal, two-photon point scanning and light sheet (1-photon and 2-photon) microscopes are now routinely used for 3D+time live imaging of either embryo or organogenesis. Each of them provides several advantages and disadvantages. The choice of microscope depends on the specific objective, balancing the main competing parameters; embryo health, spatial and temporal resolution and signal-noise ratio (Figure 1.23) (Keller, 2013). Living cells and tissues in the developing embryo are sensitive to light exposure and results in cellular damage, also known as

phototoxicity. Therefore, embryo should be exposed to minimum light so that the health of the embryo is not compromised which allows long term live imaging. Optimum spatial resolution is important to observe cellular and sub-cellular processes. The acquisition speed should be high enough to capture and interpret certain fast morphogenetic events, like cell division. Signal-noise ratio is required for automated image processing to analyse the large amount of imaging data.

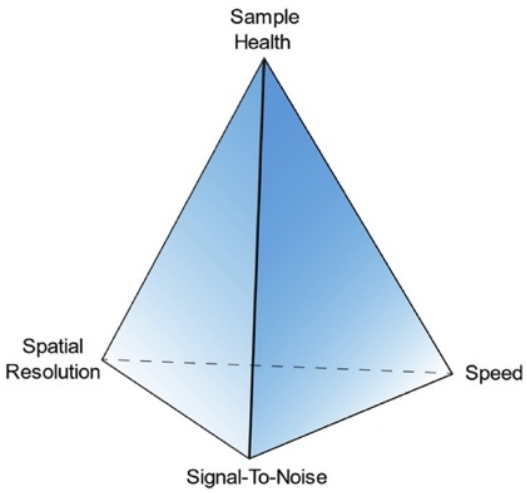

Figure 1. 23. Competing parameters during live-cell imaging in modern light microscopy.

The choice of the microscope depends on the priority of the competing parameters. Figure from (Lemon and McDole, 2020).

1.5.2.2. Confocal microscopy

Confocal point scanning microscopy is a highly used imaging system to obtain optical sectioning of 3D structures of the embryos and adult tissues (Keller, 2013). In confocal microscopy, laser beam is focused into a small focal spot of the biological specimen that excites the fluorescent molecule (Figure 1.24A). The specimen is scanned through the 3D volume and the corresponding images are recorded voxel by voxel from the signal obtained at each focus point. A pinhole is used in the detection system to reject fluorescence arising from outside of the focal spot (out-of-focus). The usage of pinhole provides 3D images with good contrast.

However, the drawback of the system is very inefficient use of light and fluorescent proteins as most of the light is rejected with the use of pinhole. It requires high laser power to produce an adequate signal which in turn exposes the specimen to more light. Due to these factors, photobleaching and phototoxicity remain a big issue. Further sequential acquisition of signal limits the imaging speed. The imaging depth is also limited with the usage of light at the spectrum of visible wavelength (Keller, 2013; Pantazis and Supatto, 2014).

1.5.2.3. Two-photon scanning microscopy

Two photons of longer wavelength can be absorbed by fluorescent molecules in a single event when power densities are high enough. Two-photon scanning microscopy works in this principle, two photons of longer wavelength (usually infrared range) from a femtosecond-pulsed laser source excite the fluorescent molecule (Benninger and Piston, 2013). The use of longer wavelength photons offers deeper penetration into tissues and less phototoxicity compared to ultraviolet range excitation light used in confocal microscopy. Fluorescence is usually generated within the focal volume and therefore pinhole is not required to prevent out-of-focus light (Figure 1.24 C,D). Also, it reduces photobleaching. Two-photon microscopy is a top choice to image larger depth of thick tissues such as neuronal architecture. However, it uses the same point scanning approach as confocal microscopes, thus limitations in speed and signal-to-noise ratio remain an issue.

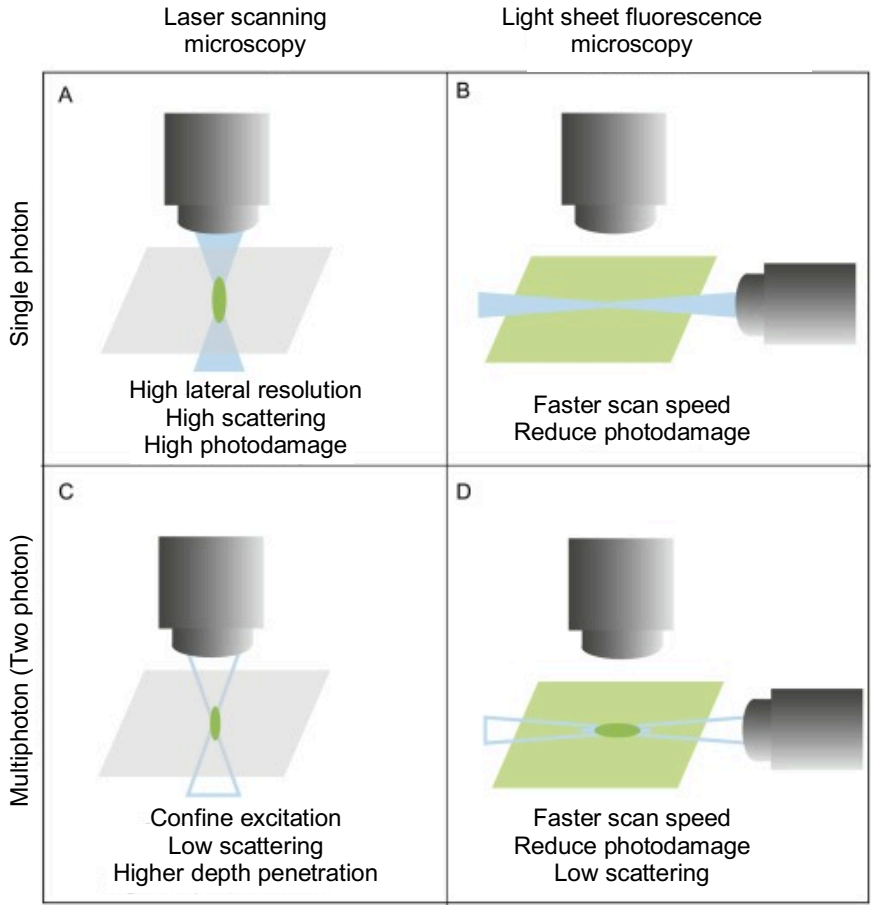

Figure 1. 24. Microscopy choices for capturing cell and tissue dynamics.

(A and C) Geometry of laser scanning microscopy (LSM) and (B and D) light-sheet fluorescence microscopy (LSFM), with (A-B) single (confocal) or (C-D) multiphoton excitation. For LSFM, fluorescence is collected with a widefield camera perpendicular to the excitation beam resulting in faster scanning rate and reduced photo damage. The main specifications are listed for the four imaging set ups. Figure from (Trinh and Fraser, 2015).

1.5.2.4. Light sheet microscopy

Light sheet microscopy provides solutions to the limitations faced by the point scanning approach. In light sheet microscopy, a micrometre-thin volume of the sample is illuminated with a plane of laser light entering from the objective placed on the side (Figure 1.24 B,D) (Wan, McDole and Keller, 2019). The emitted fluorescence is collected using another objective which is oriented at a right angle to the light sheet. In this way, other structures of the specimen outside the plane of illumination are not illuminated, hence the light exposure to the specimen is minimized. High speed is achieved as it uses a camera that records the thin sheet of volume of the specimen directly from the collected fluorescence. The 3D volume is captured faster by moving the light sheet through the sample along the detection axis. Therefore, it is suitable to image embryonic development for long term at high spatial and temporal resolution.

However, light sheet microscopy requires a special microscope set up and unconventional mounting procedure. The system-sample geometry limits the range of samples that can be imaged practically. Depth limit with one photon light sheet microscopy is mitigated with two-photon light sheet microscopy. The size of data generated by light-sheet setups is orders of magnitude greater than that of confocal and two-photon scanning microscopes as it ranges to a few tera bytes. Storage is a big challenge for routine applications. Thus, microscopy choice depends on the priority of the parameters required for the study by considering advantages and disadvantages provided by several microscopy techniques (Table1.1).

Properties	Confocal microscopy	Multiphoton microscopy	Light-sheet microscopy*	Advanced light-sheet microscopy‡
Standard imaging speed (pixel rate)	<1 MHz	<1 MHz§	>10–100 MHz	>10–100 MHz
Standard spatial resolution	<0.4 µm (lateral) and <2 µm (axial)	<0.5 µm (lateral)‖ and <3 µm (axial)¶	<0.5 µm (lateral)# and <3 µm (axial)**	Up to <0.5 µm (lateral) and up to <0.5 µm (axial)
Imaging depth‡‡	Limited	Best	Limited	Improved
Photodamage (photobleaching and phototoxicity)§§	Strong	Medium‖‖	Low	Low
Detection	Point detector	Point detector	Widefield detector	Widefield detector
Sample preparation	Standard for upright and inverted microscope	Standard for upright and inverted microscope	Unusual mounting procedure that depends on the geometry of the scope (needs access from at least two orthogonal directions)	Unusual mounting procedure that depends on the geometry of the scope (needs access from at least two orthogonal directions)
Commercial availability	Yes	Yes	Yes	No
Main limitations	Imaging speed, imaging depth and photodamage	Imaging speed and potential nonlinear photodamage	Imaging depth and inhomogeneity of image quality	Advances are not yet commercially available
Main advantages	Accessible in most imaging facilities	Imaging depth	Combined imaging speed, large field of view, low photodamage and quasi-isotropic spatial resolution can be obtained	Optimal compromise between signal to noise ratio, imaging speed, field of view, spatial resolution, imaging depth and photodamage

Table 1.1. Properties of different microscopy techniques for whole-embryo imaging.

Properties of different microscopy techniques for whole-embryo imaging.. * commercially available using Gaussian beam illumination and one-photon excited fluorescence. ‡ with recent developments, such as confocal detection, multiphoton excitation of Bessel beam illumination. Table from (Pantazis and Supatto, 2014).

1.5.1.5. Live imaging in zebrafish

Zebrafish provides optical transparency, rapid and external embryonic growth which are highly suitable for live imaging. Reconstruction of cell lineages during early 24 hours of development was made possible (Keller *et al.*, 2008; Olivier *et al.*, 2010). Global cell movements involved in germ layer formation during zebrafish gastrulation was further examined (Shah *et al.*, 2019). Apart from that, specific tissue and organ morphogenesis such as pectoral fin, inner ear, spinal cord neurons, forebrain among others were also imaged and their morphogenesis were investigated in detail (England *et al.*, 2006; Dyballa *et al.*, 2017; Nguyen *et al.*, 2019; Sharma *et al.*, 2019; Wan *et al.*, 2019). In collaboration with our lab, hindbrain morphogenesis during the end of gastrulation has been examined in a recent study (Araya *et al.*, 2019). This study provides insights into the formation of 3D neural tube from 2D neural plate stages in terms of cell rearrangement and cell shape changes.

1.5.3. Cell lineage reconstruction

Several methods that involve genetic tracers such as DNA barcoding and single-cell RNA sequencing are now available for cell lineage reconstruction (Woodworth, Girskis and Walsh, 2017; Zhang *et al.*, 2020). However, changes in cell behaviours can be only observed from direct visualisation of cells through microscopy data. Automated processing of 3D+time images provide precise data about cell positions, trajectories, divisions, nucleus and cell shapes. Thus, reconstruction of cell lineages during early development is feasible. The first standard tracking algorithm was established for *C. elegans* early development (Bao *et al.*, 2006). Further, it is applied to more complex organisms such as zebrafish (Keller *et al.*, 2008; Faure *et al.*, 2016), *Drosophila* (McMahon *et al.*, 2008) and recently in post implantation stages of mouse embryos (McDole *et al.*, 2018). Reconstruction of cell lineages are being performed with a few globally available tracking algorithms such as Tracking with Gaussian Mixture Models (TGMM) (Amat *et al.*, 2014), Trackmate (Tinevez *et al.*, 2017), Imaris and others (Faure *et al.*, 2016) (Table 1.2).

	Notes	2D/3D images	Detection/segmentation	Cell division	Linking/tracking	Available as	Open source	Citations/ references	Visualization/ curation	URL
Amira	Visualization and analysis	2D+3D	–	–	Linking based on proximity and intensity	Stand-alone software (Windows)	No	Jaqaman et al., 2008	Yes/No	https://tinyurl.com/47a322az
arivis Vision4D	Tracking with interactive TrackEditor	2D+3D	Proprietary	Proprietary	Proprietary	Stand-alone software (Windows)	No		Yes/Yes	https://imaging.arivis.com/en/imaging-science/arivis-vision4d
Bayesian Tracker (btrack)	Deep learning for segmentation and cell phase prediction	2D	Semantic segmentation with neural networks	Links track segments and identifies divisions based on appearance, motion and predicted cell phase	Generate track segments with Kalman filter	Napari plugin (OS X, Linux and Win10)	Yes	Ulicna et al., 2020 preprint	Yes/No	https://github.com/quantumjot/BayesianTracker
CellProfiler Tracer	Diverse set of pipelines	2D	Requires other software	Requires other software	Linking based on overlap, distance and measurements (e.g. intensity)	Stand-alone software	Yes	Lamprecht et al., 2007	Yes/No	https://cellprofiler.org/tracer
Elephant	Interactive training	3D	CNN for nucleus centre detection; cells are modelled as ellipsoids	Manual	Nearest neighbour linking; corrects for optical flow (CNN)	Client: (Windows/ Mac/Linux). Server: Linux	Yes	Sugawara et al., 2021 preprint	Yes/Yes	https://elephant-track.github.io/#/v0.1/
ilastik	Interactive training	2D+3D	Pixel-based classifier	Pixel-based classifier	Distance-based linking; considers all frames together to find a tracking solution	Stand-alone software (Windows/Mac/ Linux)	Yes	Berg et al., 2019	Yes/Yes	https://www.ilastik.org/
Imaris	Interactive microscopy image analysis software	2D+3D	Proprietary	Proprietary	Proprietary	Stand-alone software (Windows/ Mac)	No		Yes/No	https://imaris.oxinst.com/products/imaris-for-tracking
KNIME	Build analysis pipelines	2D	Various	–	TrackMate	Stand-alone software	Yes	Berthold, 2009	No/No	https://www.knime.com/
Lineage Mapper	Interactive training	2D	Requires other software	Based on roundness, size and daughter size	Hungarian matching based on overlap, distance and size change	Fiji/ImageJ plugin	Yes	Chalfoun, 2016	Yes/No	https://pages.nist.gov/Lineage-Mapper/
Lineage Tracker	Designed for fluorescence microscopy	2D	Seeded growth segmentation	–	Based on correlation of object features (e.g. mean intensity)	Fiji/ImageJ plugin	Yes	Downey et al., 2011	Yes/No	https://warwick.ac.uk/fac/sci/dcs/people/till_bretschneider/lineagetracker/
MaMuT (BigDataViewer and TrackMate)	Manual tracking and track editing	2D+3D	Manual; cells are modelled as ellipsoids	Manual	Semi-automated tracking	Fiji/ImageJ plugin	Yes	Wolff et al., 2017 preprint	Yes/Yes	https://imagej.net/MaMuT
Mastodon	Large-scale manual tracking and track editing	2D+3D	Manual; semi-automatic or custom plugin	Manual	Semi- and automated tracking	Stand-alone software (Windows/Mac/ Linux)	Yes		Yes/Yes	https://github.com/mastodon-sc/mastodon
MorphoGraphX	Ideal for subdividing geometry in two and three dimensions	3D	Watershed segmentation	Manual	Manual	Stand-alone software (Windows/Mac/ Linux)	Yes	Reuille et al., 2015	Yes/Yes	https://morphographx.org/
TGMM	Large 3D volume (typically lightsheet) GPU accelerated	3D	Fit of a 3D Gaussian mixture model	Pretrained CNN for division detection	Linking based on propagating Gaussian mixture models	Stand-alone software (Windows/ Linux)	Yes	Amat, 2014	No/No	https://figshare.com/s/0400896db2d17a63278c
TrackMate	Simple user interface for fast annotation and exploration	2D+3D	Various detection methods (can be extended and customized)	Manual	Semi-automated tracking	Fiji/ImageJ plugin	Yes	Tinevez, 2017	Yes/Yes	https://imagej.net/plugins/trackmate/

Software packages are categorised by their image domains (2D/3D) and availability. The algorithmic procedures of automatic lineage trackers are listed and focus on the key distinguishing factors of cell detection, division detection and linking.

Table 1.2. Overview of a selection of lineage-tracking tools.

Software packages available to perform automated lineage tracking are listed with their features. Table from (Wolf, Wan and McDole, 2021).

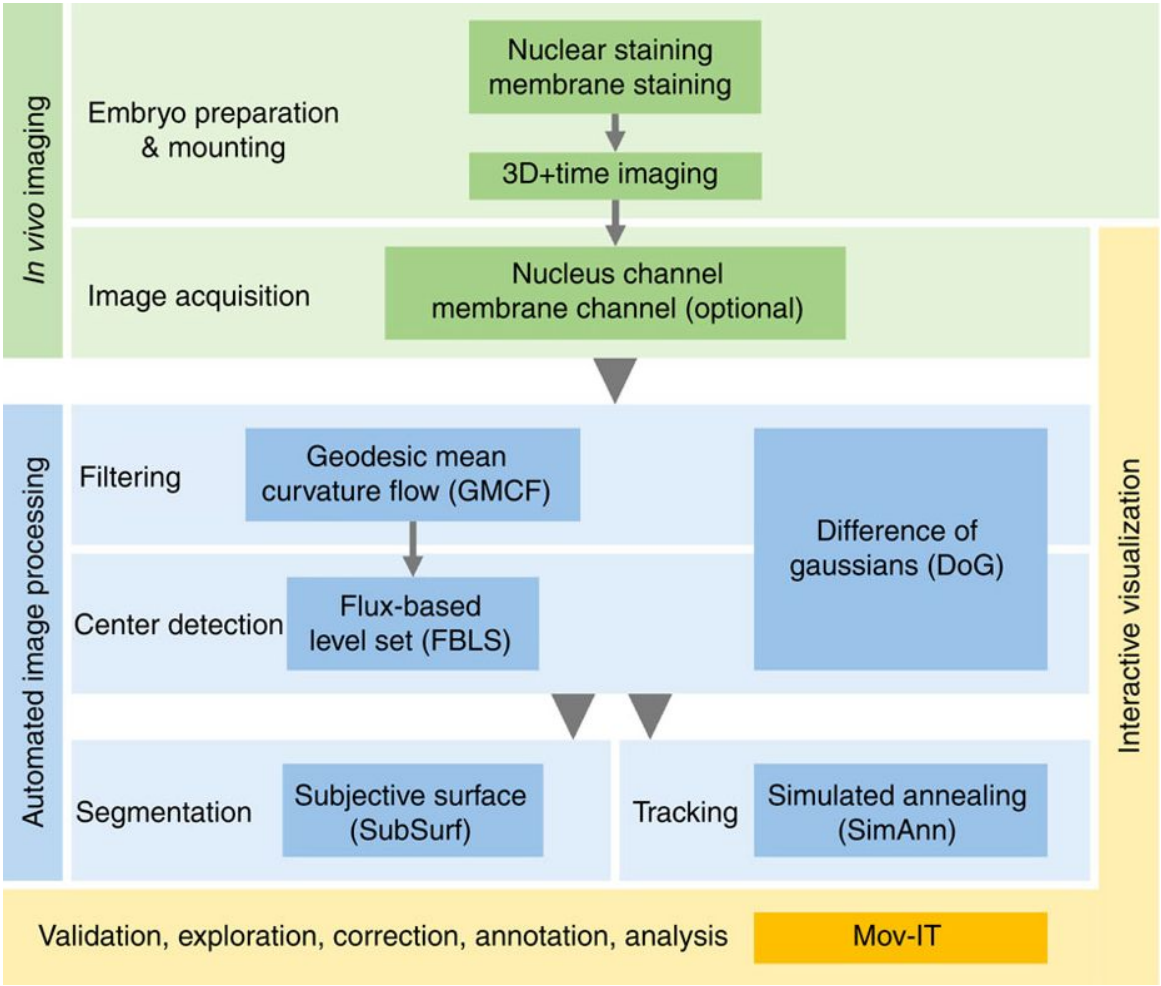

Figure 1. 25. The BioEmergences workflow for reconstruction of cell lineages.

Successive steps starting from embryo preparation and leading to the reconstructed data are depicted. It proposes two alternative nuclear centre detection methods, GMCF and DoG. Processed datasets are readily available for visualisation and analysis by the interactive visualization tool Mov-IT. Figure from (Faure *et al.*, 2016).

Our methodology: BioEmergences workflow

The BioEmergences platform was established by our laboratory (Faure *et al.*, 2016). The workflow has two channel detection workflow, one channel is nuclei, crucial for cell tracking and another is membrane channel which is optional. Algorithms integrated in the workflow perform image filtering, nucleus centre detection, nucleus and membrane segmentation, and nuclei-based cell tracking (Figure 1.25). Centre detection software allows us to manually apply parameters to detect maximum centres of nuclei. Upon processing of live imaging datasets through workflow, it is automatically transferred to Mov-IT software, a custom-made visualisation interface. Mov-IT allows us to perform validation and correction of nucleus detection and cell lineage by superimposing reconstructed data on the raw data. It provides several tools including 3D volume rendering, 2D orthoslice views, cell lineage and segmentation display.

The performance of the workflow has been measured by lineage score which determines nuclei centre sensitivity and linkage sensitivity. An average 'lineage score' reaches 96% and the average mitosis sensitivity is about 67% in the data set of zebrafish gastrulation (Faure *et al.*, 2016). During later stages, however the performance is decreased. Thus, the automated reconstruction of cell lineages during early neurulation (densely packed cells of neuroectoderm) is challenging and thereby requiring intense manual correction. Instead of Simulated Annealing (SimAnn) tracking algorithm originally described in the workflow (Figure 1.25), Expectation-Maximisation (EM) tracking, which is the iteration of SimAnn algorithm, is currently being used for improved automated cell tracking (Faure *et al.*, 2016). BioEmergences workflow is currently being adapted to process large data such as one from light sheet microscopy.

Deep learning has been increasingly used to improve various domains of image processing such as image segmentation, cell detection and tracking. Thereby, new methods of automated lineage reconstruction with higher performance are being developed including in our lab by Thierry Savy among others (Moen *et al.*, 2019; Malin-Mayor *et al.*, 2021; Sugawara, Cevrim and Averof, 2021).

1.5.4. Optogenetics approaches

Optogenetics means light-induced manipulation of gene or biological function. Light responsive proteins such as rhodopsin are naturally available from bacteria to humans (Joshi, Rubart and Zhu, 2020). The optogenetic approach utilises them where light responsive proteins are engineered into genetically encoded protein switches, in order to manipulate specific biological function non-invasively. Biological functions include activation of signalling pathway and gene expression, protein localization such as moving organelles, chromatin modification, and protein function (Rogers and Müller, 2020). The optogenetic approaches provide tunability and high

spatial and temporal control which is not usually achieved with genetic and pharmacological manipulation. Initially, optogenetics tools were introduced to activate or inhibit specific set of neurons. It is now widely employed to study embryogenesis. Signalling molecules pattern the embryo. To understand the mechanisms of signalling pathways such as how molecules spread, where and when the signalling is needed, the response of cells to different signalling amplitudes, signalling dynamics, noise and integration of various signalling pathways, optogenetics tools are being used (Rogers and Müller, 2020).

Optogenetic tool to manipulate RA signalling

To manipulate RA signalling during embryogenesis, isomerisation of RA at a specific wavelength of light serves as a principle (Figure 1.26). Different isomers of RA exist such as 13-cis RA, all-trans RA and 9-cis RA. Each of them has binding affinity to different RA receptors. During early embryonic development, only all-trans RA which binds to RARs is shown to be a key player. Photo isomerisation of biologically inactive 13-cis RA generates at steady state ~20-25% of the active all-trans RA and also 30-35% 9-cis and 20-25% 13-cis RA stereoisomers upon UV exposure. Therefore, this photo conversion allows us to have spatiotemporal controlled activation of RA signalling using confocal and two-photon scanning microscopy (Xu *et al.*, 2012).

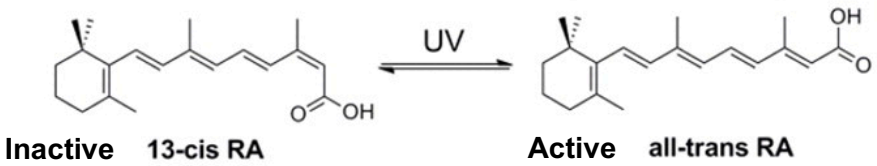

Figure 1. 26. Isomerization reaction of 13-cis RA into all-trans RA (and vice versa).

Figure from (Xu *et al.*, 2012).

Photo activation of caged RA (RA ester) is shown to be useful in manipulating RA signal in zebrafish embryo, however the concentration of RA released is less precise in this case (Neveu *et al.*, 2008).

1.6. Aims of the PhD thesis

The state-of-the-art of zebrafish hindbrain's fate map comes from the conventional sparse lineage tracing, performed in 1995. It does not precisely show the borders of the rhombomere progenitor domains. It lacks cell dynamics that underlie the formation of segments. The gene regulatory network involved in the process is extensively understood from loss and gain of gene function and consequent analysis of downstream genes. The cellular approach is anticipated to elucidate cell behaviours that lead to phenotypic defects upon pathological conditions. It should provide cell dynamics, lineages and movements. Quantitative parameters of cell behaviour such as proliferation, speed, direction and neighbourhood persistence will be used to characterise the early phenotypic effects of genetic perturbation. Integration of cellular processes with genetic regulation is essential for the complete understanding of morphogenetic processes underlying hindbrain segmentation.

In this PhD thesis, we aim to understand zebrafish hindbrain morphogenesis through visualisation, quantification, and reconstruction of cell lineages of individual rhombomeres from mid-gastrulation till early neurulation under normal and pathological conditions such as inhibition of RA and FGF signalling pathways. We will perform *in vivo* 3D+time imaging of zebrafish embryos using two-photon microscopy. We will use the hindbrain-specific transgenic reporter fish line, *krox20:eGFP-Hras* which labels prospective rhombomeres r3 and r5. It serves as an early marker of rhombomere before the morphological appearance of segments. Being the central rhombomeres, it enables us to label the flanking rhombomeres as well. We will use BioEmergences workflow to reconstruct the cell lineage tree of r2-r6 rhombomeres from mid-gastrulation till early neurulation from 3D+time imaging data. The imaging datasets will also provide the analysis of the progenitor cell behaviour during this morphogenetic process. Thus, the specific goals of the thesis are as follows:

1) Establish the hindbrain fate map and its cell dynamics in normal condition from mid-gastrulation through early neurulation.
2) Define the role of RA in hindbrain morphogenesis at cellular level by RA signalling inhibition using a chemical inhibitor (DEAB) through the establishment of fate map and analysis of the cellular behaviour. Further, we assess the community effect of RA signalling during hindbrain morphogenesis using optogenetic approaches.
3) Define the role of FGF in hindbrain morphogenesis at cellular level by FGF signalling inhibition using a chemical inhibitor (SU5402) through the establishment of fate map and analysis of the cellular behaviour.

2. Material and methods

2.1. Quantitative 3D live Imaging and cell lineage reconstruction of zebrafish hindbrain segment formation from mid-gastrulation through early neurulation

2.1.1. Introduction

The state-of-the art of zebrafish CNS fate map, including hindbrain at gastrula stages was obtained through sparse dye labelling (Woo and Fraser, 1995). However, it lacks precision of borders and cell dynamics through the hindbrain morphogenesis, further leaves a scope for precision of hindbrain fate map. Therefore, we utilised the advancement in microscopy techniques, genetic manipulation (transgenesis) and automated cell tracking tools and developed a protocol to perform quantitative 3D+ time imaging of early hindbrain development (via segmentation) and acquire dynamic fate map of rhombomeres r2-r6 from mid-gastrula stage. We further investigated their progenitor cells' behaviour from mid-gastrulation (6 hpf) till early neurulation (15 hpf).

We constructed transgenic fish line *krox20:eGFP-Hras* in *casper* background, double mutant for *nacre* and *roy* genes which is devoid of pigments (White *et al.*, 2008). We imaged the transgenic embryo from mid-gastrulation till early neurulation using two-photon laser scanning microscopy. The transgenic reporter fish initiate the labelling of rhombomeres 3 and 5 in cell membrane with a slight delay compared to *krox20* endogenous expression in r3 and r5 at 10 hpf and 11 hpf respectively. Ubiquitous nuclei staining of the embryo from ~3 hpf onwards was achieved through the injection of H2B-mCherry mRNA at one-cell stage. Cells of r3 and r5 domain (nuclei) can be identified through membranous eGFP expression upon their formation at the early neurula stages. Back tracking the cells based on nuclei staining provided the location of their progenitors at mid-gastrula stage. For that, we used BioEmergences workflow/pipeline which performs image filtering, nucleus centre detection, nucleus and membrane segmentation, and cell tracking on captured imaging data (Faure *et al.*, 2016). For the reconstruction of cell lineages and further analysis, digital embryos were made by the registration of all nuclei centres. The Mov-IT software was used to annotate and correct the automated cell tracking, and analyse the cell behaviours during early hindbrain morphogenesis.

2.1.2. Material

Zebrafish line	Tg *krox20:eGFP-Hras*
Molecular biology	mMessage mMachine mRNA transcription kit (Invitrogen), plasmid containing the sequence encoding fusion protein, H2B-mCherry
Chemicals	Embryo medium, Tricaine (Sigma), 0.5% Low melting point agarose (Sigma), Injection needle (glass capillaries 1.0 mm OD GC 100-10, Harvard apparatus)
Tools	Microinjection of mRNA: Microinjector (Femtojet), Injection plate at 2% Agarose (Sigma) Imaging chamber: 35 mm Petri dish (Nunc), Cover slip, Teflon ring
Imaging tools	Mounting and screening: Fluorescent stereo microscope (Nikon SMZ1000, Leica MZ16) 3D live imaging: Two-photon scanning microscopes (Zeiss LSM780 and Leica sp5) equipped with laser 980nm and 1030nm Temperature control system: Okolab H101
Software	BioEmergences workflow and Mov-IT software

2.1.3. Experimental designs

The experimental design for this study consists of four major parts: Embryo preparation, 3D+time imaging, data processing (automated reconstruction of cell lineage) and data analysis.

2.1.3.1. Embryo preparation

The basics of our method was to utilise ubiquitous labelling of all cell nuclei from the beginning of imaging and hindbrain specific reporter (membrane) to identify the hindbrain rhombomeres nuclei after their initiation of expression. In this study, we used H2B-mCherry nuclei staining through mRNA injection at one-cell stage which labels all nuclei in red starting from 3hpf. We used hindbrain specific reporter line Tg *Krox20:eGFP-Hras* in *casper* background which labels developing rhombomeres' (r3 and r5) cell membrane in green.

2.1.3.1.1. Characterization of krox20 reporter transgenic line

Krox20 is expressed in the rhombomeres r3 and r5 (Wilkinson *et al.*, 1989; Oxtoby and Jowett, 1993, p. 20) and is required for their specification and development. Its expression starts at 10 hpf/tailbud in pre-r3 and 11 hpf/0-1ss in pre-r5 as two stripes in both sides of the neural plate.

Then their territories are expanded and formed as two blocks/segments initially with ragged expression and sharp boundaries are formed by 6ss/12hpf (Addison *et al.*, 2018). Then the expression is downregulated around 26 hpf in r3 and later in r5 around 30 hpf (Oxtoby and Jowett, 1993).

There are three enhancer element reported for regulation of *krox20* expression in r3 and r5 in chick (Chomette *et al.*, 2006). They are conserved between chick, mouse and human. Element B is responsible of the initiation of *krox20* expression in r5 while element C is active from r3-r5 region. Element A is involved in the autoregulation/maintenance of *krox20* expression. Element A in zebrafish is conserved in position and function, but its sequence is not fully conserved (Chomette *et al.*, 2006). In our lab, we constructed the transgenic line Tg *krox20:eGFP-Hras* carrying the eGFP-Hras fusion. sequence driven by the chick element A. In our transgenic reporter line, GFP expression starts to be visible at 11 hpf in pre-r3 and at around 12hpf30 in pre-r5 due to the delay in maturation of eGFP (Figure 2.1). It spatially recapitulates *krox20* expression and thus used for our study.

2.1.3.1.2. Nuclei staining

H2bmCherry was transcribed *in vitro* using mMessage mMachine T7 transcription kit and stored at -80°C. H2B-mCherry mRNA at 75 ng/ul was injected at one-cell stage in Tg *krox20*:eGFP embryos. Embryos were collected immediately 15 minutes after they are spawn. A batch of embryos was injected with H2bmCherry mRNA carefully at the centre of the cell to ensure homogenous staining of mCherry in all nuclei. Embryos were kept in 28.5ºC incubator after injection. At around 4 hpf of development, embryos were screened for homogenous and bright staining of H2bmCherry using fluorescent stereo microscope and selected for live imaging experiments. Optimal bright staining allows the use of a low laser power which limits cell damage. Homogenous staining is necessary for efficient automated reconstruction of cell tracking.

Microinjection protocol is demonstrated **here (MOOC)**.

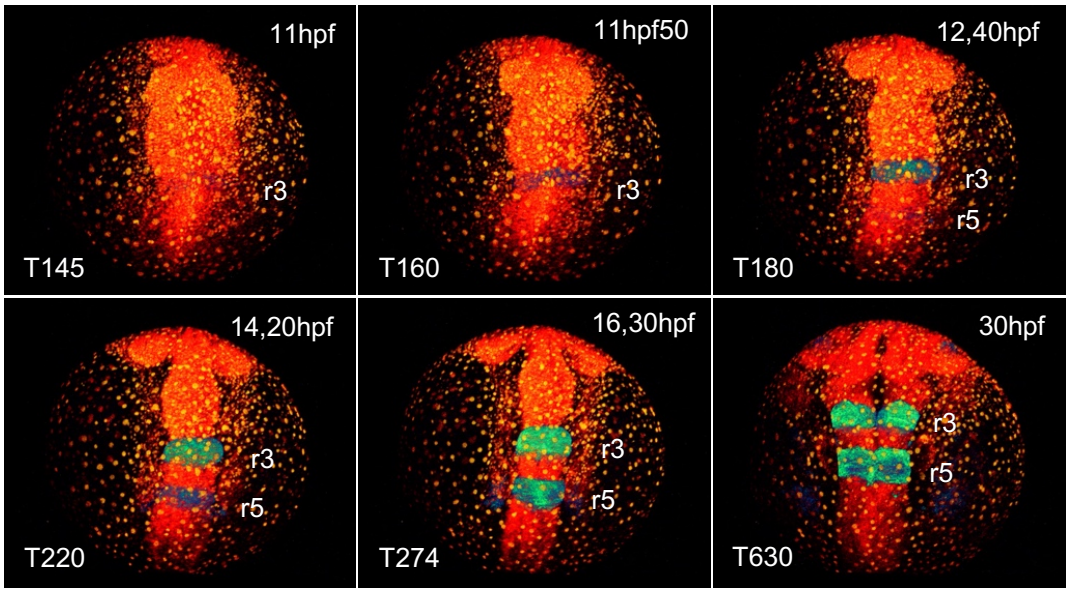

Figure 2. 1: Tg *krox20:eGFP-Hras* embryo recapitulates *krox20* expression in rhombomeres 3 and 5.

3D rendering of the raw data at different developmental stages/time steps acquired with 2-photon microscopy show the formation of rhombomeres 3 and 5 in transgenic embryo injected with *H2bmCherry* mRNA at one-cell stage. T: Time step, hpf- hour post fertilisation.

2.1.3.2. Mounting of a zebrafish embryo at the shield stage

The aim was to mount the embryo at shield stage in a desired position with the addition of low melting agarose which allow the development of hindbrain in the field of view during long term live imaging. Meanwhile, the embryo should develop normally. Therefore, we established a mounting procedure of the embryo at the shield stage for 3D+ live imaging from early gastrulation (6 hpf) till late neurulation stage (15 hpf and beyond) using an upright microscope.

Imaging chamber

A custom-made imaging chamber was made using a 35mm petri dish (Nunc TM). A hole of 1.55millimetre wide is made at centre of the petri dish. A Teflon ring (ALPHAnov) with a 850µm large hole is placed at the centre of the dish, and a glass coverslip is sealed at the bottom. This imaging chamber should be regularly cleaned up once in a month of usage by removing the teflon ring and rinsing with distilled water. (Figure 2.2)

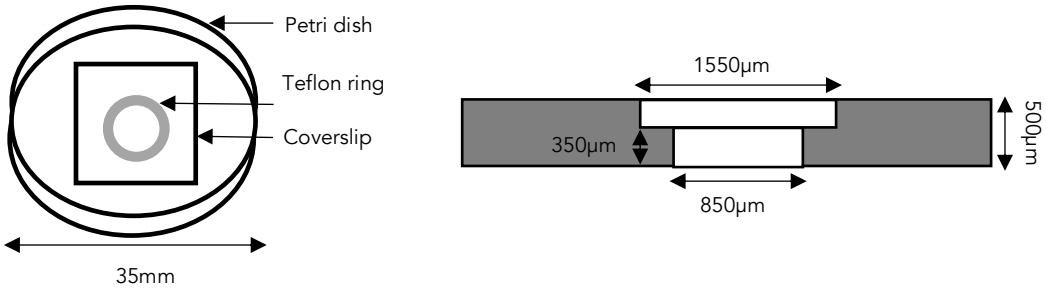

Figure 2. 2. Construction of the imaging chamber.

Teflon mold (ring) set up which has cover slip sealed bottom to a petri dish. Teflon ring (grey) is sealed on the glass at the centre of the petri dish. Taken from BioEmergences' lab protocol.

Embryo mounting procedure

- The imaging chamber was filled up with Embryo Medium, supplemented with an anaesthetic, Tricaine at 0.033%.
- Using 20µl pipette, 2-3µl of 0.5% low melting point agarose at lukewarm temperature was poured into the teflon ring to make an agarose bed in order to place the embryo on it.
- The embryo was brought into the teflon ring using embryo pipette, dechorionated using very fine and clean forceps and the chorion was removed from the dish.
- The animal pole was placed on top first and then tilted up/positioned making the shield at approximately 30° (1/3rd) from the central axis of the field of view using forceps as shown (Figure a 2.2).
- About 20-40µl of warmed 0.5% Low Melting Point agarose was poured slowly on top of the embryo to secure this proper orientation and prevent the movement during image acquisition.
- The agarose was let to solidify for 5 to 10 minutes before transferring the chamber to the microscope.

Additional steps for DEAB-treated embryo mounting,

- DEAB solution was made at 10µM from 10mM stock and applied to the embryos in a petri dish in dark gradually in two steps at 4 hpf and incubated in the same solution from 4 hpf onwards.
- Embryos were then incubated at 28.5°C in the petri dish wrapped in aluminium foil.
- Screening for homogenous and bright staining of H2B-mCherry was performed at 6 hpf.

- The imaging chamber was filled up with DEAB solution, supplemented with an anaesthetic, Tricaine at 0.033%.

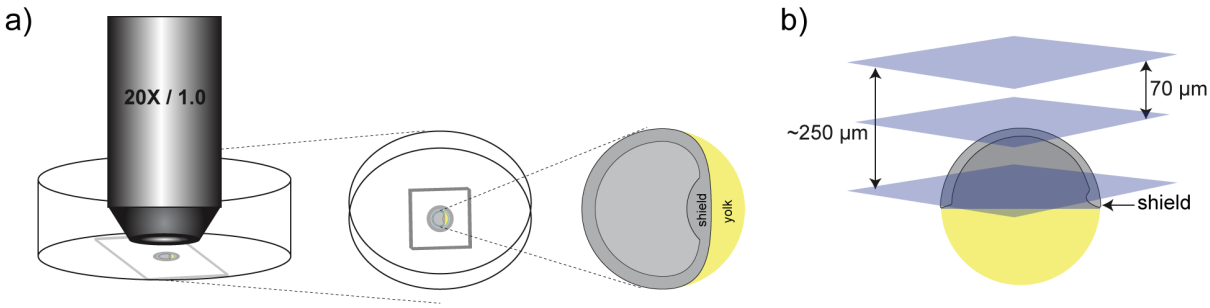

Figure 2. 3. Mounting of embryo at shield stage.

a) Objective 20X 1NA immersed in the imaging chamber filled with embryo medium. Position of the shield stage embryo with animal pole on top and tilted up to 20-30 degree angle. b) schematics of shield stage embryo under scanning.

Mounting of embryo and imaging is demonstrated **here (MOOC).**

2.1.4. 3D+time imaging

Our focus was not to image whole embryo but to capture all hindbrain progenitors r2-r6 from 6 to ~15 hpf of development. Hindbrain progenitors, the dorsal neuroectoderm cells from both sides of the embryo converge (narrow) to midline and undergoes AP extension to construct the rhombomere segments. It is a highly dynamic process which involves larger global movement of cells in a short time. Initial movements do not require scanning at higher depth, but it is needed during the neural keel and neural rod stages where the cells are tightly packed in ~100 µm thickness of the neuroepithelium. Suitable spatial and temporal resolution should be achieved throughout the imaging period for automated cell tracking. Phototoxicity should be minimal to allow proper embryo growth and cell movements. Two-photon microscopy provides good penetration, minimal phototoxicity and photobleaching compared to classic confocal microscopy. Thus, we opted for two-photon microscopy that allows the 3D+time long term imaging of zebrafish embryos from 6 hpf till 15 hpf and more. In order to obtain good signal-to-noise ratio for proper image segmentation and subsequent tracking, careful adjustment of the following parameters were made; objective, spatial and temporal sampling, field of view, laser power and wavelength.

2.1.4.1. Imaging condition

Two-photon imaging was performed on Zeiss LSM780 and Leica SP5 upright microscopes, equipped with 20X 1.0NA water dipping lens objective. Shield stage embryo was visualised with H2BmCherry staining in all nuclei. The parameters that we standardised for imaging with the two set ups are given in Table (2.1). The field size was kept at no more than 700x700 μm^2 in the x, y dimension and 260µm in the z dimension. We scanned 70 µm above the surface of animal pole to ensure that we do not lose hindbrain progenitors and cells in the scanning depth during the course of development (Figure 2.2 b). A spatial sampling of ~1.16 per pixel in x,y,z direction appeared sufficient. However, spatial scaling of z at 1 µm makes the hand correction of cell tracking easier. The temporal resolution is critical for error-free cell tracking. Thus, we chose Δt to be around 2 min30s at most. Image acquisition was continuously made over 12 hours and beyond. The femtosecond laser was set at wavelength 980nm to excite green and 1030nm for red fluorescent proteins. Compromise between laser power and gain of a detector also had to be made. Choosing the laser power for eGFP was a challenge as there is no signal during the start of the imaging and the two bands appear in r3 and r5 around 12 hpf and 13 hpf respectively. We optimised the laser power for both mCherry and eGFP signals to set it at first for the whole imaging or it is adjusted around the time of eGFP signal *(krox20)* appearance using remote control during the overnight imaging. We set the temperature in the imaging chamber to 26°C using an OKO-lab system. Along with the heat at the laser focal points, it was expected to be around 28°C in the chamber during the whole imaging period, the ambient temperature for zebrafish embryo growth.

2.1.4.2. Post-imaging

Normal development of the imaged embryo was assessed using a stereo microscope right after imaging and 24 hours later. Data from embryos which exhibited normal morphology were only used for processing. The imaging data was carefully observed to ensure the embryo did not move suddenly during the image acquisition and if the area of interest, hindbrain progenitors and hindbrain domains r3 and r5 with eGFP staining went out of frame during the imaging period. Then the imaging data was uploaded to the workflow for further processing.

Zeiss LSM780-hybride

190828aZ	
Objective	20X 1.0NA Zeiss
x=y	607 µm
z	254 µm (70 µm above the surface)
Voxel volume	1.19x1.19x1µm
∆t	2m33s
Speed	1236 Hz
LASER used Mai tai,	1030nm for mCherry, 980nm for eGFP
Image size	512x512 pixels
Gain	900

Leica SP5

180516aF	
Objective	20X 1.0NA Leica
x=y	596 µm
z	230 µm (70 µm above the surface)
Voxel volume	1.16µm^3
∆t	2m27s
Speed	350 Hz
LASER used	1030nm for mCherry, 980nm for eGFP
Image size	512x512 pixels
Gain	100

Table 2.1: Imaging parameters. a) Zeiss LSM780-hybride b) Leica SP5 systems

2.1.5. Data processing

The uploaded data was processed through the BioEmergences workflow (Faure *et al.*, 2016). Difference of Gaussian (DoG) performs filtering and nuclei centre detection. Using the "Centre select" software, I adjusted three parameters which determine smallest nuclei, biggest nuclei and minimum intensity of the signal to be detected in order to detect correct and maximum nuclei centres at every 30 time steps (over a total of ~300 time steps). And then the parameters were normalised to all the time steps. In this way, digital embryos were obtained. EM, another version of simulated annealing (Sim Ann), nuclei-based tracking algorithm was applied to obtain automated reconstruction of cell lineages (Faure *et al.*, 2016).

To improve the visualization of the nuclei, a new nuclei filtering method was adapted, based on artificial intelligence. I provided images of zebrafish embryo with nuclear staining at around 20 hpf to develop this method. Two images were produced with one at high speed (low quality); and the other with at low speed (high quality) that match at pixel level using Zeiss LSM780 confocal

set up. These images were then used to train an algorithm how to reconstruct the high-quality image from the low quality one. Once it was done, we checked and generalised its learning by providing similar noisy images, ones it never saw, and measured the error with the quality image. Training is done when this error is minimal. This nuclei filtering method improved the raw nuclei signal in my datasets. It allowed manual tracking of cells located at the bottom of the neural plate to greater extend (Figure 2.4).

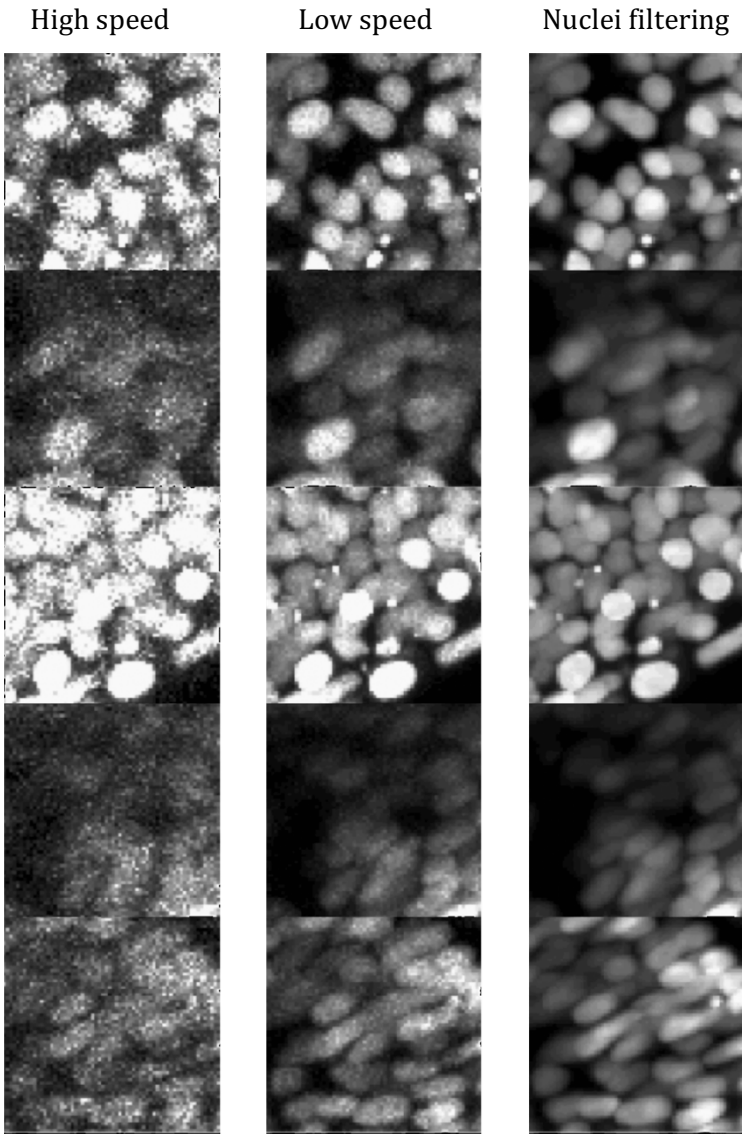

Figure 2. 4. Artificial Intelligence (AI) based nuclei filtering.

Nuclei staining with *H2bmCherry* mRNA injection in one-cell stage embryo imaged at neuroepithelium level at 20 hpf in Zeiss LSM780-hybride confocal at high speed (left), images at lowest speed and maximum quality possible (middle) and the images produced by algorithm based on machine learning developed by Thierry Savy.

2.1.6. Data analysis

MovIT, a custom-made software was used to visualise the raw and digital embryo, annotate, validate, delete and add links of the automated cell tracking obtained. It was further used to perform analysis and extract additional information such as speed, mean value of gravity mass, average neighbour distance, cell lineage tree, cell division rate and their corresponding graphs are made from the values obtained. Images and movies were made using the same software.

Analysis strategy to obtain the hindbrain fate map

- Cell nuclei in r3 and r5 domains were selected with krox20-eGFP membranous expression driven by Krox20 shortly after the rhombomere appearance (Figure 2.5). Each domain was labelled with unique colour and selection. r3 domain is formed earlier than r5, so their selections were done at two different time steps. (Figure 2.5)
- Cell nuclei in r4 region which is located in between r3 and r5 were also selected. r2 and r6 cell nuclei located anterior to r3 and posterior to r5, respectively were selected with certain approximation.
- Using back propagation tool, selected nuclei were back-propagated till the first time step (6-7hpf) along the automated cell tracking.
- Individual links of cells were annotated, validated or corrected.
- Cell division was detected through nuclei shape changes and its distinct dynamics with the oval shape of the nuclei. (Chromosome arrangement). We ensured that the two daughter cells were followed forward till the selection time step.
- Automated tracking was approximately around 96% accurate till around the developmental stage 10hpf. More hand corrections were made at later stages since cells become tightly packed at neural keel and rod stages.
- Cell lineage tree of rhombomere progenitors, r2-r6 was obtained (Figure 2.6).

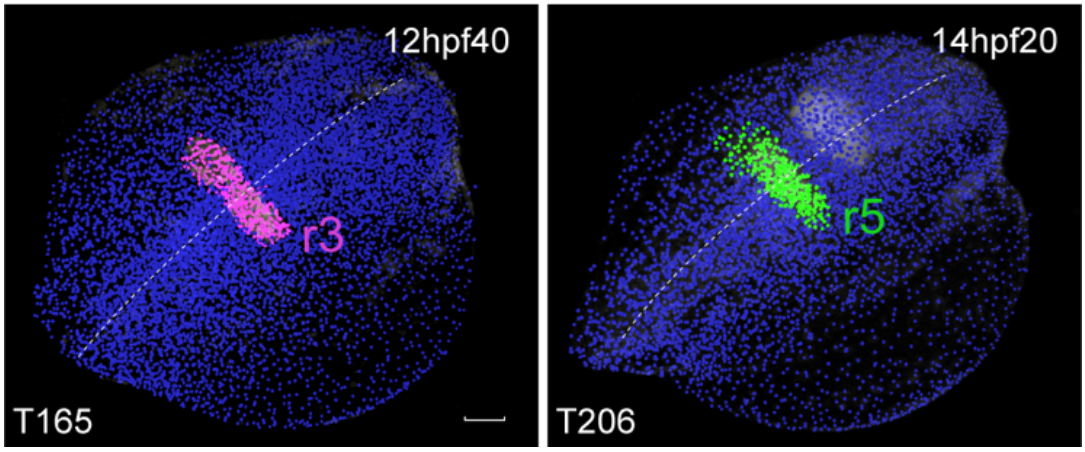

Figure 2. 5. Selection of r3 and r5 cell nuclei.

Digital embryo with nuclei centres in blue, r3 in pink and r5 in green at 12hpf40 and 14hpf20 respectively, superimposed on raw membrane staining in white. Scale bar: 50 μm. T: time step. hpf: hour post fertilisation

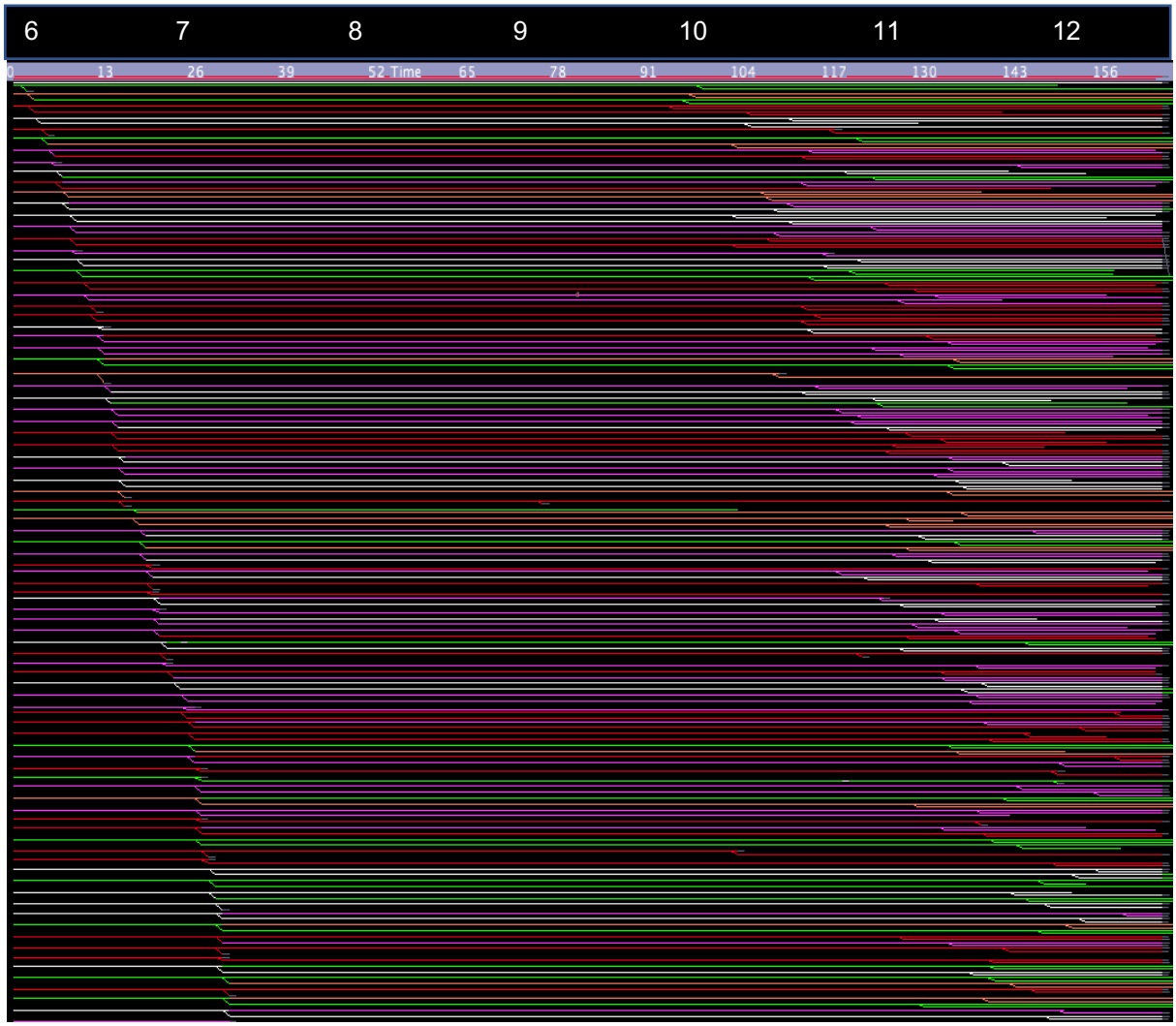

Figure 2. 6. A part of cell lineage tree of hindbrain progenitors (r2-r6).

Lineage tree is obtained from Mov-IT tool after correction and annotation of automated cell tracking. Each line indicates single hindbrain progenitor. Colour code: r2- red, r3- pink, r4- white, r5- green, r6- orange. Branching denotes cell division. The tree is ordered based on first mitosis. Time step is indicated on the second top in grey panel. Hour post-fertilisation (hpf) is indicated on the top panel.

Timing

Embryo Preparation: Injection is performed in the morning. After 4h of incubation, embryo is screened for homogenous staining of H2B-mCherry. At 6 hpf (usually after 7 h of injection time), embryo is mounted in imaging chamber. It takes half an hour to one hour to mount and set up under the microscope.

Imaging: Imaging acquisition is done overnight till ~20 hpf. Experiment is repeated several times to obtain 2-3 exploitable imaging datasets. ~a few months.

Data processing: BioEmergences workflow takes 2 days to process and generate automated cell tracking.

Data Analysis: a) Manual correction: 2-3 months per imaging dataset depending on the quality of the dataset and on the efficiency of the user to perform the tracking correction.

b) A week to extract and analyse several parameters such as speed, mean of gravity mass, cell neighbour distance, cell division rate and others from Mov-IT software.

Data space: The imaging data of over 18 hours from 6-24 hpf can be around 40 GB in leica sp5 and 80 GB in Zeiss LSM780 set ups.

Selected datasets for fate map analysis

Wildtype: ID: 180516aF (fully corrected), 190828aZ (partially corrected), 120302a, 120329a

RA inhibition: ID: 131129a (fully corrected), 200812aF (partially corrected), 200812aZ

Movie 1. 3D raw data rendering. Tg *krox20:eGFP-Hras* from 6 hpf onwards under normal condition injected with H2B-mCherry mRNA.

http://bioemergences.eu/MageshiK/videos/180516aF.mp4

Movie 2. 3D raw data rendering. *krox20:eGFP-Hras* from 6 hpf onwards under normal condition in injected with H2B-mCherry mRNA.

http://bioemergences.eu/MageshiK/videos/190828aZ_t_mix.mp4

Movie 3. 3D raw data rendering. *krox20:eGFP-Hras* from 7 hpf onwards with DEAB treatment injected with H2B-mCherry mRNA.

http://bioemergences.eu/MageshiK/videos/131129a_t_mix.ogg

Movie 4. 3D raw data rendering.*krox20:eGFP-Hras* from 6 hpf onwards with DEAB treatment injected with H2B-mCherry mRNA.

http://bioemergences.eu/MageshiK/videos/200812aF_t_mix.mp4

Movie 5. 3D raw data rendering.*krox20:eGFP-Hras* from 6 hpf onwards with DEAB treatment injected with H2B-mCherry mRNA.

http://bioemergences.eu/MageshiK/videos/200812aZ_t_mix.mp4

Troubleshooting

- The concentration of LMP agarose was tested at a range of 0.4% to 1%. It is fixed to 0.5% as a suitable concentration. The volume of LMP agarose poured on top of the embryo to fix it was chosen to be 20-40 µl. Embryo may be prone to deformation (squeezing) if more volume is used.
- We kept the frame size as minimum as possible 600-700 μm^2 to ensure good spatial resolution for visualisation and automated tracking and at the same time keep hindbrain progenitors in the chosen frame. In the imaging chamber, the embryo is positioned with its shield in the diagonal of the frame to ensure the hindbrain progenitors are in the field of view throughout the imaging period.
- Spatial resolution of nuclei signal is solved by artificial intelligence-based nuclei filtering method.

Advantages of the method

- Imaging chamber is easy to build and maintained at low cost. LMP agarose, as a mounting medium, provides harmless environment to the embryo and also minimises squeezing which enables normal cell movements during gastrulation and neurulation.
- Mounting of the embryo at shield stage is relatively easy compared to unusual light sheet mounting procedure.
- The storage is comparatively less and hence easier processing than light-sheet microscopy.
- Two photon microscopy provides minimal phototoxicity not to interfere with the normal development and also allows imaging at greater depth (rhombomere thickness ~100 µm and more).
- Accuracy of automated cell tracking is high as 96% till around 10hpf with the given spatial and temporal resolution.

Limitations

- The average zebrafish embryo size with the yolk at 6 hpf is 750 µm. Hence with 20X objective, full embryo cannot be imaged in the field of view. The possibility of hindbrain progenitors especially posterior rhombomere progenitors leaving the field of view is high during image acquisition when the shield position is not tilted enough up. Thus, the success of obtaining exploitable datasets is relatively low (10-20%).

- There is a limitation to the acquisition speed which compromises the signal-to-noise ratio. This ratio is always lower in the deeper layers of neuro-epithelium. However, this is almost resolved with our described nuclei filtering tool.
- With the signal-to-noise ratio limitation, automated tracking of the cell in the entire area of interest (hindbrain progenitors r2-r6) throughout the imaging period with high accuracy is not achievable.
- Annotation and manual corrections of around 1000 cells (r2-r6) tracked backwards over 6 hours of development (~200 time steps) takes a lot of time (a month). It is quite laborious. Data analysis is further delayed. Improved tools for automated reconstruction of cell lineages with deep learning would reduce the hand work in near future.

2.2. Local optogenetic restoration of Retinoic Acid (RA) in RA-null embryos

2.2.1. Introduction

To assess the community effect of RA morphogen in hindbrain patterning, we planned to perform local restoration of RA in selective progenitor cells in RA-null background. We reasoned that if there is a community effect, the rescued domain of r5 will be constituted of both restored RA cells and also cells in the neighbourhood (Figure 2.7). In the case of autonomous effect, the rescued domain will be constituted of only restored RA cells. The restored RA cells are followed with the simultaneous conversion of nls-Eos from a green fluorescent protein shifting to red protein upon UV illumination. Photo isomerisation of 13-cis RA to all-trans RA occurs with UV exposure. All-trans RA is the functional isomer of RA during embryogenesis. Therefore, simultaneous conversion of both 13-cis RA and photoconvertible protein, nls-Eos allow us to restore RA in selective cells and track the cells with rescued RA activity over developmental time.

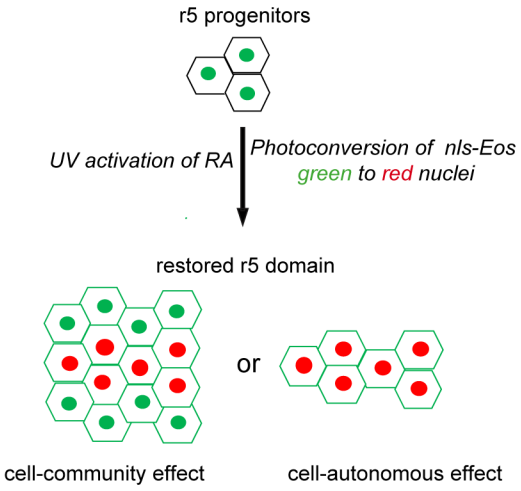

Figure 2. 7. R5 restoration by cell community or cell-autonomous effects.

2.2.2. Material

Zebrafish line	Tg *krox20:eGFP-Hras*
Molecular biology	mMessage mMachine mRNA transcription kit (Invitrogen), plasmid containing the sequence encoding fusion protein, nls-EOS
Chemicals	Embryo medium, Tricaine (Sigma), 0.5% Low melting point agarose (Sigma), Injection needle (glass capillaries 1.0 mm OD) 13-cis RA (Sigma)
Tools	Microinjection of mRNA: Microinjector (Femtojet, Eppendorf), Injection plate at 2% Agarose (Sigma) Imaging chamber: Petri dish, Cover slip, Teflon ring UV lamp
Imaging tools	Mounting and screening: Fluorescent stereo microscope 3D live imaging: Two-photon scanning microscopes (Zeiss LSM780 and Leica sp5) equipped with laser 405nm, 980nm and 1030nm Temperature control system: Okolab H101

2.2.3. Timeline of experiment

Using the photo-isomerisation method, It was shown that restoration of RA in the head region (but not tail) before bud stage rescues hindbrain formation with the read-out of *krox20* expression in r5 (Xu *et al.*, 2012). In our experiment, we first applied global UV illumination at 6hpf with an UV lamp. We observed a rescue of r5 domain at 30hpf (Figure 2.7). Then, only r5 progenitors were locally scanned with laser in UV range (405nm). In order to follow the cells with RA

restoration, we simultaneously converted nls-Eos protein (from a green fluorescent protein shifting to red upon UV illumination).

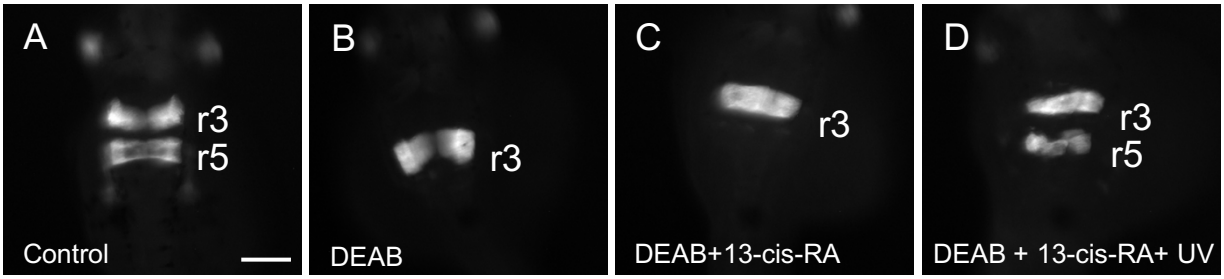

Figure 2. 8. Global UV illumination.

Tg *krox20:eGFP-Hras* embryos showing rhombomere r3 and r5 at 30hpf in A) control embryo B-D) DEAB-treated embryo (10 µM) from 4 hpf and exposed for 5 minutes to 5nM 13-cis RA (B) and illuminated (or not) for1 minute with a UV lamp (C,D). Scale: 100 µm

2.2.4. Standardisation of *13-cis RA* treatment

A series of 13-cis RA concentration from 2nM, 5nM and 10nM were tested on DEAB-treated transgenic embryos. At 10nM 13-cis RA, embryos showed partial rescue of the phenotype, krox20 expression in r5 is 10-30% of the normal expression, without the UV exposure. At 5nM 13-cis RA, there was no rescue observed in the absence of UV. At 5nM 13-cis RA, 1 minute UV illumination resulted in rescue of r5-krox20 expression (30-50% in all embryos. Thus, we opted for 5nM 13-cis RA for further local illumination experiments.

2.2.5. Procedure

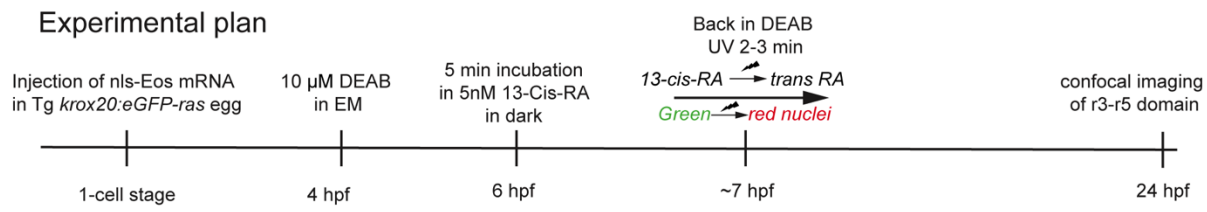

Figure 2. 9. Experiment timeline for local optogenetic restoration of RA.

Each step is given with corresponding stages of embryos.

- Tg *krox20:eGFP-Hras* embryos were collected and injected with 40 ng/µl nls-Eos mRNA. The concentration of mRNA was standardised in order to photoconvert enough nls-Eos shifting to red upon UV exposure. Injected embryos were kept at 28.5 degree until the next step.

- At 4 hpf, embryos were treated with 10μM DEAB and maintained in dark.
- At 6hpf, embryos were washed twice in embryo medium and incubated in 5nm 13-cis RA for 5 minutes in dark.
- Embryos were washed in embryo medium and transferred to 10μM DEAB solution in a new petri dish. From 13-cis RA treatment, the embryos were manipulated in complete dark since very little exposure to light causes conversion of 13-cis RA to all-trans RA.
- Embryos were screened for homogeneous and optimum bright nls-Eos expression in all nuclei using stereo microscope.
- Embryos were mounted in imaging chamber and positioned as explained in previous section to perform 2-photon imaging.
- At around 7hpf, r5 progenitors were specifically located with the help of our established hindbrain fate map, which is approximately 5 layer of cells from the margin in the Zeiss LSM780.
- Located r5 progenitors in oval region are scanned with 405nm laser in bleaching mode on Zeiss LSM 780 set up. Scanning parameters are shown in (Table: 2.2). This also converted nls-Eos from green to red fluorescent protein. Scanning was repeated 5-7times to acquire enough photo conversion. (Figure 2.10)
- Then the embryo was imaged overnight with 2-photon scanning microscopy using Zeiss LSM780 and Leica sp5F set ups

Control: A batch of control embryos were treated as above except that they were not UV illuminated. They were checked the next day for absence of *krox 20* expression in r5.

Zeiss LSM780 (Bleaching mode)	
Start bleaching after #scans	5 out of 20
Repeat Bleach after #scans	5 out of 20
Iterations	10
Stop when intensity drops to	10
Safe bleach for GaAsP	Yes
Cycles	20
Laser power 405nm	20%

Table 2.2: Scanning parameters for UV illumination in confocal microscopy setup.

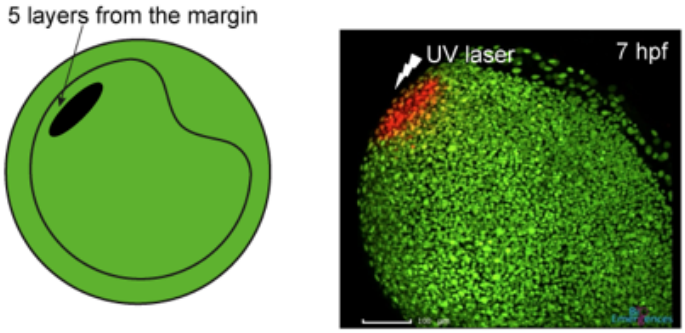

Figure 2. 10. Simultaneous photo conversion of nls-Eos and isomeric conversion of 13-cis RA to all-trans RA in r5 progenitors.

An embryo at 7 hpf is mounted in the imaging chamber in a position suitable for hindbrain imaging. 5 layers were counted from the margin to place the detector on targeted r5 putative progenitors (oval shaped area). UV laser is then used to scan several times in the targeted region. Scale bar: 100 µm.

Notes

- All steps must be performed in complete dark. Embryos in petri dish should always be covered with aluminium foil. Even a little exposure to light can cause enough photo isomerisation of RA to rescue r5 domain, without UV illumination.

- In confocal and two-photon scanning microscopy set ups, brightfield used to locate the embryo under the objective is shielded with a red plate to filter out UV.

3. Results

3.1. Hindbrain fate map and morphogenesis under normal and null-RA conditions

3.1.1. Summary

The current zebrafish CNS fate map at early and late gastrula stages including the hindbrain comes from a study done in 1995 using conventional method, sparse dye labelling that report spatial position of cells. The method involves single cell fluorescein-dextran dye injection at early gastrula stage and scoring their progeny location at later stages using epi-fluorescent microscope. Vertebrate hindbrain is transiently segmented into seven or eight repeated cellular units of segments in the AP axis called rhombomeres. The state of the art lacks cell dynamics of hindbrain progenitors during gastrulation and precision of the hindbrain fate map and their individual rhombomere domains. With the advancement in microscopy techniques, genetic manipulation (transgenesis) and automated cell tracking tools, we aim to provide fate map of zebrafish hindbrain with individual rhombomeres r2- r6 from mid-gastrulation till early neurulation. Our study gives insights into the clonal origin, cell proliferation and movement of hindbrain progenitors during gastrulation. Anterio-posterior and Dorso-ventral organization of the rhombomeres are manifested as early as shield stage. Indeed, rhombomere progenitors exhibit AP segmental organisation along the animal pole-margin axis and dorso-ventral segregation in a proximo-distal axis/distance from the shield. Retinoic acid (RA) forms a morphogen gradient beginning from the presumptive neuroectoderm till the neural tube formation and its inhibition causes progressive loss of posterior hindbrain rhombomeres in a concentration-dependent manner. We study the cellular events such as cell proliferation and cell movement that lead to reported phenotypic defects during early hindbrain morphogenesis by analysing the fate map and progenitor behaviour upon RA inhibition. We identify the rhombomere progenitor domains whose organisation is in correspondence with the position and size of the modified segments i.e the expansion of anterior progenitors' domains. We also observe a delayed convergence movement that is an early consequence of the altered RA gradient. Overall, our analysis on dynamic fate map of hindbrain in DEAB-treated embryos deciphers RA roles in the establishment of the rhombomere progenitor domains' identity at mid-gastrulation and the control of convergence movements of neurectoderm during early stages of neurulation. Further, we restored RA at progenitors' level through optogenetics method around the shield stage in RA-null background and rescued the posterior rhombomere domains which indicates the community effect of the morphogen in the hindbrain morphogenesis.

3.1.2. Manuscript to be submitted to "development"

Segmental organisation of hindbrain progenitors during gastrulation: Implication of RA role in hindbrain patterning at cellular level

Mageshi Kamaraj[1], Thierry Savy[1,2], Balaz Kosa[3], Sophie Desnoulez[1], Adeline Boyeau[1], Karol Mikula[3], Nadine Peyrieras[1,2] and Monique Frain[1,2,*].

Affiliations

[1]Laboratoire BioEmergences (USR3695/FRE2039), Centre National de la Recherche Scientifique, 91198 Gif-sur-Yvette, France.

[2]Laboratoire Matière et Systèmes Complexes (MSC, UMR7057), CNRS, Université de Paris, 75013 Paris, France.

[3]Department of Mathematics and Descriptive Geometry, Slovak University of Technology, 81105 Bratislava, Slovakia.

*Author for correspondence: M.F. (e-mail : monique.frain@cnrs.fr)

Abstract

The current fate map of the zebrafish central nervous system (CNS) at early and late gastrula stages was obtained through sparse lineage tracing. Utilising advanced microscopy imaging of transgenic zebrafish lines and automated image processing tools, we develop a method to reconstruct the cell lineage of rhombomere (r) r2-r6 from mid-gastrulation through early neurulation. We provide a finer and dynamic fate map of zebrafish hindbrain from 6 till 15 hour post fertilisation (hpf). The rhombomere progenitor domains are aligned along the antero-posterior (AP) and dorso-ventral axes as early as the shield stage. Rhombomere progenitor domains exhibit AP organisation parallel to the blastoderm margin. The DV segregation of rhombomeres is set by distribution of the progenitors along the DV axis of the shield stage embryo. Progenitors located at the most dorsal part of the blastoderm will form the ventral domain of rhombomeres. Our study gives insights into the clonal origin, cell proliferation and migration paths of rhombomere progenitors during gastrulation and early neurulation. Retinoic acid morphogen gradient (RA) plays a key role in the specification and patterning of posterior hindbrain. RA inhibition using a chemical inhibitor (DEAB) causes progressive loss of posterior rhombomeres (r5-r7) with corresponding expansion of anterior ones (r3, r4), in a concentration-dependent manner. We study the cellular behaviours that lead to the reported phenotypic defects. We identify the rhombomere progenitor domains whose organisation is in correspondence with the position and size of the modified segments i.e the expansion of anterior progenitors' domains. The cells of the remaining r5 domain which is restricted to the dorsal part of the neural tube, undertake the expected migratory path of dorsal r5 progenitors whereas the

corresponding ventral cells adopt the migratory path of r4 ventral progenitors. We also observe a delayed convergence movement that is an early consequence of the altered RA gradient. Consequently, it results in ectopic neural progenitor accumulations in the dorsal midline and neural tube defects. Overall, the establishment of the dynamic fate map of hindbrain in DEAB-treated embryos deciphers RA roles in the establishment of the rhombomere progenitor domains' identity at mid-gastrulation and the control of convergence movements of neurectoderm during early stages of neurulation. And for the first time, using optogenetic tools, we restored RA in a subset of rhombomere progenitors in zebrafish DEAB-treated embryos and rescued the whole posterior hindbrain which indicates the community effect of RA signalling on target genes and hindbrain morphogenesis.

Introduction

Neural tube, the precursor of brain and spinal cord is constructed from the multi-layered (brain) and single-layered (spinal cord) neural plate cells. The later stages of neural tube construction from neural plate in teleost (zebrafish) differs from other vertebrates including mammalian as it is neither strictly epithelial nor it follows groove formation. During zebrafish gastrulation, dorsal neuro-ectoderm cells from both sides of the embryonic axis undergo convergence and extension (CE) towards the dorsal midline and form neural plate. Neural plate cells undergo mediolateral cell intercalation and extend along the antero-posterior axis and form the neural keel structure, followed by a cylindrical-like solid structure called neural rod. Lumen opens at the apical midline of the rod and forms the neural tube (Schmitz, Papan and Campos-Ortega, 1993). The efficiency of convergence depends on Planar Cell Polarity signalling (Ciruna *et al.*, 2006; Tawk *et al.*, 2007; Quesada-Hernández *et al.*, 2010) and needs coordination with extracellular matrix and underlying mesoderm (Araya *et al.*, 2014; Araya, Carmona-Fontaine and Clarke, 2016).

At late neurulation, hindbrain region undergoes transient segmentation along the AP axis which leads to seven or eight repeated units called rhombomeres. They manifest as visible swellings around 18-20 hpf in zebrafish (Moens and Prince, 2002). Each rhombomere is specified with an unique set of gene expression and results in organization of eight cranial nerves to determine their structure and function (Moens and Prince, 2002; Krumlauf and Wilkinson, 2021). This segmental pattern of hindbrain guides the migration paths of cranial neural crest that emanate from the dorsal part of the hindbrain (Lumsden and Keynes, 1989).

Transparency of early zebrafish embryo makes it an excellent model system for imaging and fate map studies. Dynamic fate maps are necessary to integrate the known genetic regulation

with the morphogenesis process. It gives insight into the tissue deformation and rearrangement processes involved in the formation of complex structures such as brain. Zebrafish CNS fate map was provided by conventional sparse labelling method using fluorescent dyes (Woo and Fraser, 1995). Key insights of zebrafish neurulation about the tissue reorganisation was also investigated (Papan and Campos-Ortega, 1994; Woo and Fraser, 1995; Kozlowski *et al.*, 1997). Cell cycles and clonal strings were examined during the zebrafish CNS using the same method (Kimmel, Warga and Kane, 1994). Cell movements and division orientation were analysed with time-lapse analysis (Concha and Adams, 1998). These studies provided key knowledge of zebrafish CNS formation to greater extend, however the individual cell behaviour of hindbrain progenitors during gastrulation through neurulation was not quantitively studied due to the technical difficulties. Further, it leaves a scope for precision of hindbrain fate map on individual rhombomeres. Thus, the establishment of a precise dynamic fate map of zebrafish hindbrain should decipher the cellular processes underlying its segmental organisation.

The technical advancements in microscopy, image processing and computational tools led to the reconstruction of cell lineages and cell behaviours of whole zebrafish embryo for early stages of development (Keller et al. 2008; Olivier et al., 2010, Faure et al, 2016). Keller's study focused on mesendoderm movements in detail. A more recent study showed the cell behaviours during germ layer formation where global cell movements were examined (Shah *et al.*, 2019). Other studies provided the organization of forebrain and spinal cord morphogenesis in zebrafish (England *et al.*, 2006; Wan *et al.*, 2019). Hindbrain morphogenesis has been described but at late gastrula and early neurulation stages (Hong and Brewster, 2006; Araya *et al.*, 2019). However, cell behaviours of naïve ectoderm cells during the transition to neural plate and neural keel stages at cellular resolution have not been described yet in detail.

Signalling pathways such as RA, Wnt and FGF are involved in the induction of hindbrain segmentation process and various Hox and other key transcription factors work downstream for the individual rhombomere specification and development. RA is synthesized from dietary vitamin-A in paraxial mesoderm and diffuses into the adjacent neuroectoderm at hindbrain and spinal cord level. Cyp26s, which degrades RA are expressed in different time windows that allows the formation of robust and dynamic RA morphogen gradient during hindbrain patterning (Sirbu *et al.*, 2005; White *et al.*, 2007). This activates a set of downstream genes including the main players, *Hox* genes (Parker and Krumlauf, 2020; Bedois, Parker and Krumlauf, 2021). Through the extensive auto- and cross-regulation, the segment-specific gene regulatory network (GRN) establishes discrete segments. RA inhibition, using a chemical inhibitor (DEAB), from 4 hpf leads to expansion of anterior rhombomeres and progressive reduction or

loss of posterior rhombomeres in a concentration-dependent manner (Begemann *et al.*, 2004; Maves and Kimmel, 2005). Defects in the genetic regulation underlying the phenotype has been investigated (Hernandez *et al.*, 2004). The key players of zebrafish posterior hindbrain formation and patterning are including Hox paralog group 3 (in r5-r6) and 4 (in r7), vhnf1 and valentino (val)/kreisler in r5-r6 and krox20 in r5 (Moens and Prince, 2002). RA signaling activates *vhnf1* which cooperates with Fgf signals from r4 to initiate the expression of *val*. Val is required along with vhnf1 and Fgf for *krox20* activation in r5 (Walshe *et al.*, 2002; Hernandez *et al.*, 2004). It should be mentioned that in *val* mutant the r5-r6 region is reduced to a one size segment rX where the expression of *hox* is very low and *krox20* is limited to its dorsal part (Prince, 1998), indicating a mix of cells of distinct identities. The defects in cellular events upon RA inhibition that lead to hindbrain anteriorization and potential cell mixing of some segments, are still unknown and should be elucidated through the establishment of a dynamic fate map.

We imaged the transgenic reporter line, *krox20:eGFP-Hras* that label the odd numbered rhombomeres 3 and 5 with *krox20*-driven eGFP expression in cell membrane from 11 and 12 hpf respectively, with a slight delay compared to endogenous *krox20*. Nuclei staining with H2B-mCherry allows nuclei-based cell tracking. We backtracked the individual rhombomere cells from their formation till 6hpf and obtained the dynamic fate map of individual rhombomeres. Two-photon scanning microscopy provides the advantage of imaging deeper tissue without photobleaching compared to confocal imaging (Pinheiro and Heisenberg, 2020). With the BioEmergences workflow (Faure *et al.*, 2016), the imaging data are processed for automated cell tracking and analysed for the hindbrain progenitors behaviours from mid-gastrulation till early neurulation. Through our established method, further we inhibited the RA signalling using DEAB, a chemical inhibitor from blastula stage and studied the hindbrain progenitors cell behaviours that underlie the anteriorisation phenotype. We also described the consequence of RA inhibition at later stages of neurulation. Using optogenetic tools (Xu *et al.*, 2012), we restored for the first time RA signalling in a subset of rhombomere progenitors in DEAB-treated embryos to study the autonomous and non-autonomous effects of RA on target genes and hindbrain patterning.

Results

AP segmental organization of rhombomeres' progenitors

We established a 3D+time imaging protocol of zebrafish hindbrain formation from mid-gastrulation to early neurulation using two photon microscopy. We used zebrafish transgenic lines constructed in our laboratory on the *casper* background, which is devoid of pigmentation.

krox20:eGFP-Hras drives cell membrane staining in rhombomeres 3 and 5 thanks to cA, an autoregulatory element of *krox20* expression (Chomette *et al.*, 2006). *H2B-mCherry* mRNA injection at the one-cell stage into transgenic eggs provides ubiquitous nuclear staining, instrumental for automated cell tracking (Faure *et al.*, 2016). The 4D image datasets were processed through the BioEmergences workflow by choosing optimal parameters in the Difference of Gaussian and Expectation-Maximization algorithms for image filtering and nucleus detection, and cell tracking respectively which provide an optimized automated cell tracking. We reconstruct the rhombomeres' r2-r6 fate map from mid-gastrulation through early neurulation. Upon obtaining the digital embryos, we superimposed nuclei centres of the whole embryo with the membrane channel, as *eGFP* membrane staining reports r3 and r5 domains. Nuclei centres of r3 and r5 domains in the digital embryo were marked with specific colours with the help of membrane staining at ~ 13 and 14 hpf respectively and were back-tracked till 6hpf stage (Figure 1A,A'). Nuclei centres in r4 domain which lies in between r3 and r5 domains were also marked. We extended our analysis to r2 and r6. The borders of r1/r2 and r6/r7 cannot be identified hence r2 and r6 selection of nuclei are less precise. The number of cells selected for each rhombomere and corrected manually in one-half of the embryo is given (Figure 1I). The position of rhombomeres' r2-r6 progenitors were followed in developing embryo from 6 hpf to early neurulation (Figure 1B-F; movies of progenitors migration in S1). Throughout the course of convergence and extension (CE) movements during gastrulation, we observed no drastic mixing between rhombomere's progenitors indicating a collective flow of cell movements during neuroectoderm convergence as shown with the mean gravity mass paths (Figure 1G). As predicted in (Woo and Fraser, 1995), we observe a segmental organization of r2-r6 progenitors along the animal pole-margin axis at late shield stage that reflect their future AP order in the neural tube. We estimated that the individual rhombomere progenitors occupy distinct domains with a significative overlap 12-18% at their borders at 7 hpf which resolves over time (Figure1H,H',I). We assume that at early mid-gastrulation, the clonal origin of rhombomeres is not yet established and allows more mixing at the borders of adjacent rhombomeres' progenitors population. We notice that the overlap between r5 and r6 is likely underestimated due to the limited number of progenitors analysed.

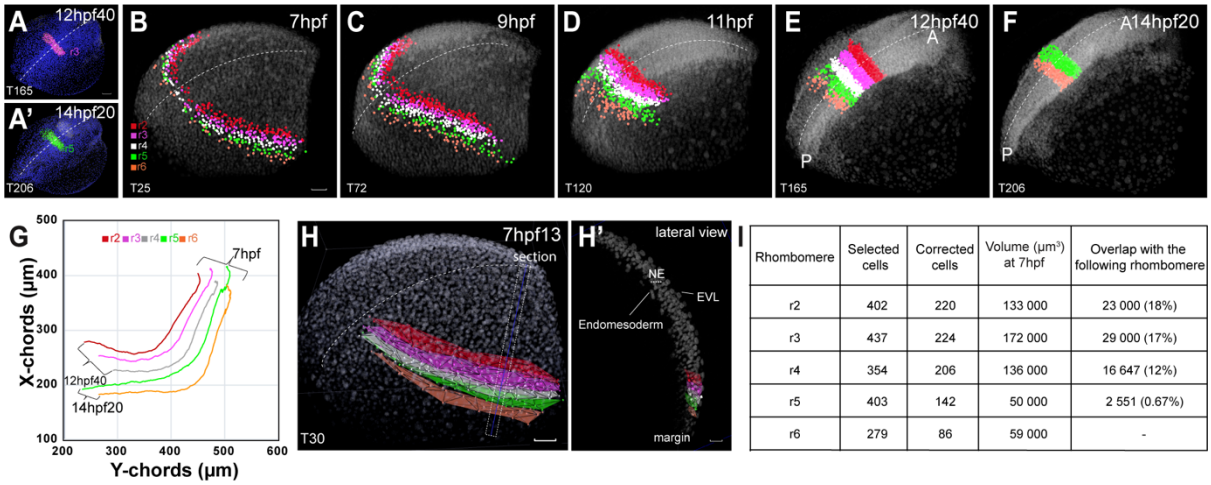

I

Rhombomere	Selected cells	Corrected cells	Volume (µm³) at 7hpf	Overlap with the following rhombomere
r2	402	220	133 000	23 000 (18%)
r3	437	224	172 000	29 000 (17%)
r4	354	206	136 000	16 647 (12%)
r5	403	142	50 000	2 551 (0.67%)
r6	279	86	59 000	-

Figure 1. AP organization of rhombomeres' progenitors during gastrulation.

A,A') Selection of r3 and r5 domains' nuclei at 12hpf40 and 14hpf20 (top and bottom respectively) identified with krox20:eGFP membrane staining (white). Digital embryo with nuclei centres in blue, r3 nuclei centres in pink and r5 in green. B-F) Rhombomere progenitors' position from r2-r6 at 7hpf, 9hpf, 11hpf, 12hpf40 and 14hpf20. Nuclei centres of rhombomere with their colour code, super imposed with imaging raw data. r2-r4 are not labelled in the F panel. Dorsolateral view. Only the right side must be considered since nuclei correction was performed on this half of the digital embryo. G) Gravity mass of rhombomeres' (r2-r6) progenitor population is plotted in XY axis from 7hpf till 14hpf20. H) Individual rhombomere progenitors volume/surface estimated by connecting all nuclei at 7hpf13 in one-half of the embryo. H') lateral view of the section. I) Table indicating the number of selected and corrected cells in individual rhombomere domains analysed in one-half of the embryo and their estimated volume occupied at 7hpf and overlap with the following rhombomere. Time steps (T) indicated bottom left. Dotted line indicates midline. EVL- Enveloping layer. NE- Neuroectoderm. A- Anterior P- Posterior. hpf- hours post fertilization. Scale bar- 50µm in all pictures, H' scale bar- 20µm.

Dorso-ventral segregation of hindbrain progenitor population

It was reported that a dorsal and ventral order in the progenitors within the whole zebrafish hindbrain region exist at 6 and 10 hpf stages (Woo and Fraser, 1995). We analysed in detail the individual rhombomere progenitors. In the reconstructed embryo, cell trajectories of r4 progenitors reveal two population of cells with distinct migration paths observed at 11hpf20 (Figure 2D). The one, labelled in yellow, converges directly to the midline while the other in white migrates caudally. We followed the cells back and forth and identified they give rise to dorsal and ventral domains at neural keel stage, respectively (Figure 2E). At 7 hpf, the progenitors are segregated along the DV axis of the embryo with ventral progenitors located at the most dorsal part of the blastoderm (Figure 2A). Up to 11 hpf these two populations move both medially and anteriorly. Between 11 and 13 hpf, they undertake distinct paths. The ventral progenitors move posteriorly and deeper into the embryo, and then undergo a flanking movement to join in the medial anterior flow while the dorsal progenitors converge directly towards the midline (Figure 2B-E,F)(Movie S2). These cells trajectories recapitulate the neural plate convergence at the midline and internalization to form the neural keel. Dorsal progenitors that are present laterally place themselves on top of medially located ventral progenitors to orchestrate the 3D neural keel structure (Movie S3). Similarly, it was shown that during neural plate-neural keel transition the medial cells form the ventral neural tube and lateral cells form its dorsal part, with lower angle of convergence for medial cells compared to lateral ones (Papan and Campos-Ortega, 1994; Araya *et al.*, 2019). Analysis of speed shows that the dorsal progenitors transiently migrate faster than ventral progenitors towards the midline between 8hpf50 and 10hpf50 (Figure 2A'-E', 2G). This data is in agreement with the increase of speed peaking between yolk plug closure (YPC, 9.5 hpf) and one-somite stage (10.3 hpf) described for lateral cells (Sepich *et al.*, 2000). We also noticed that the dorsal progenitors of posterior rhombomeres move faster than their anterior ones (Figure 2H-J').

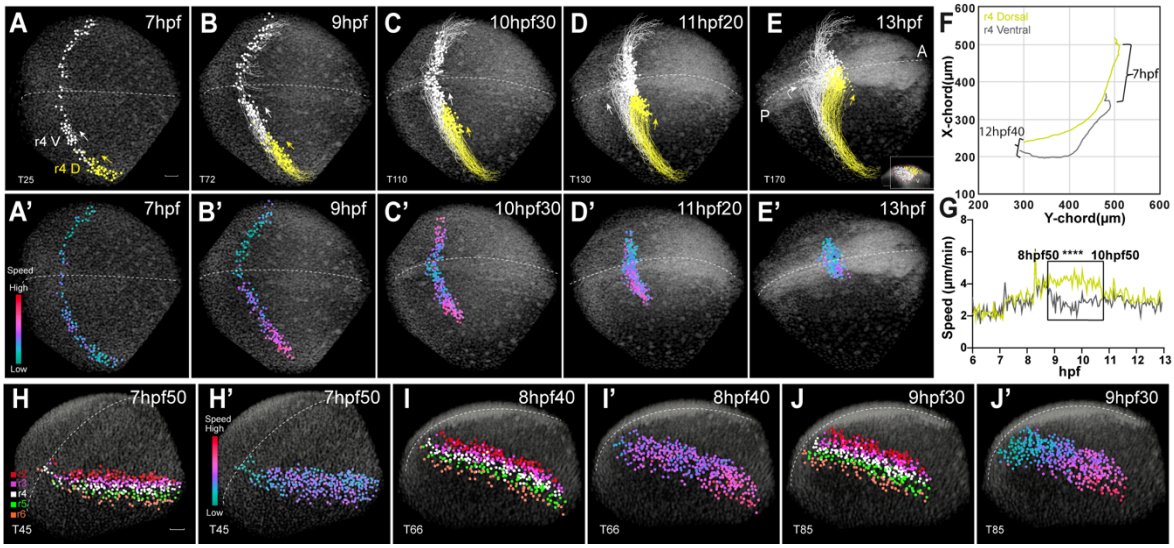

Figure 2. DV organization of rhombomeres' progenitors during gastrulation.

A-E) Rhombomere 4 progenitors trajectories from 7hpf to 13hpf, displayed with Mov-It software. Nuclei centres of dorsal (yellow) and ventral (white) rhombomere, super imposed with raw imaging data. Only the right side must be considered since nuclei correction was performed on this half of the digital embryo. Dorsal view. In E, transverse section of the neural keel is shown bottom right. A'-E') Relative speed of dorsal and ventral progenitors with colour code high-red, low-blue. Dorsal view. F) Gravity mass of dorsal and ventral progenitors of rhombomere 4 is plotted in XY axis from 7hpf. G) Relative speed of dorsal (yellow) and ventral (grey) progenitors of r4 from 6hpf. P=5.8171823800557726e-12. H-J, H'-J') Individual rhombomere progenitors with their colour code along with relative speed at three stages 7hpf50, 8hpf40 and 9hpf30. Lateral view. Time steps (T) indicated bottom left. Dotted line indicates midline. A- Anterior P- Posterior. D- dorsal. V- ventral. hpf- hours post fertilization. Mann Whitney test is performed to test the significance of mean speed of dorsal and ventral cells. Scale bar- 50µm.

Clonal analysis of individual rhombomeres with cell lineage tree

In order to establish the timing of hindbrain cells' commitment to their regional identity, we generated the cell lineage trees of rhombomeres' r2-r6. Nevertheless, the automated reconstruction of cell lineages during early neurulation required more manual/validation due to a much lower lineage score of the workflow than the 96% described for the first three hours of zebrafish embryo development. In the cell lineage tree of r3, we examined at which time point clonal commitment of rhombomere progenitors occurs (Figure 3A; Figure S1 for r4 lineage tree). We found that the clonal origin of individual rhombomeres is achieved at around 8 hpf (Figure 3A,B). This time point is in parallel with transplantation experiments showing regional neural identity commitment occurs at 80% epiboly (8-8.5 h) (Woo and Fraser, 1998). Throughout the embryonic period of development analysed from 6 to 13 hpf, we found that 84-89% of progenitors divide into daughters of same identity (Figure 3C). But at early stages from 6 to 8 hpf, we observed that 40-60% of progenitors contribute to adjacent rhombomeres upon cell division before clonal origin is achieved (Figure 3A; Figure 5G, Control: for r2, 39.5%; for r3, 43.8%; for r4, 63.6%). Progenitors tend to give rise to daughters of flanking rhombomeres but not to alternative rhombomere indicating the cell mixing is limited. After the clonal origin is established, few divisions of progenitors that are predominantly located in the border between contiguous rhombomere progenitors populations could give rise to cells of adjacent rhombomeres due to the challenge faced by the cell intercalations during CE movements to generate the solid neural keel. These cells are known to undergo either cell sorting or cell identity switch to make homogenous segments with sharp boundaries (Xu and Wilkinson, 2013; Calzolari, Terriente and Pujades, 2014). During the 6 hours of embryo development analysed, we observed either one or two cell division(s). Although progenitor cell divisions are asynchronous the two daughters divide within a 20 minutes interval at most. The comparison of cell lineage tree of rhombomeres' r2-r6 indicated the cell cycle length is 4hpf30 +/- 15 minutes in average for all of them as similarly reported (Figure 3D) (Kimmel, Warga and Kane, 1994). There is no difference in the proliferation rate of either individual rhombomeres analysed nor in dorsal versus ventral progenitor populations (not shown).

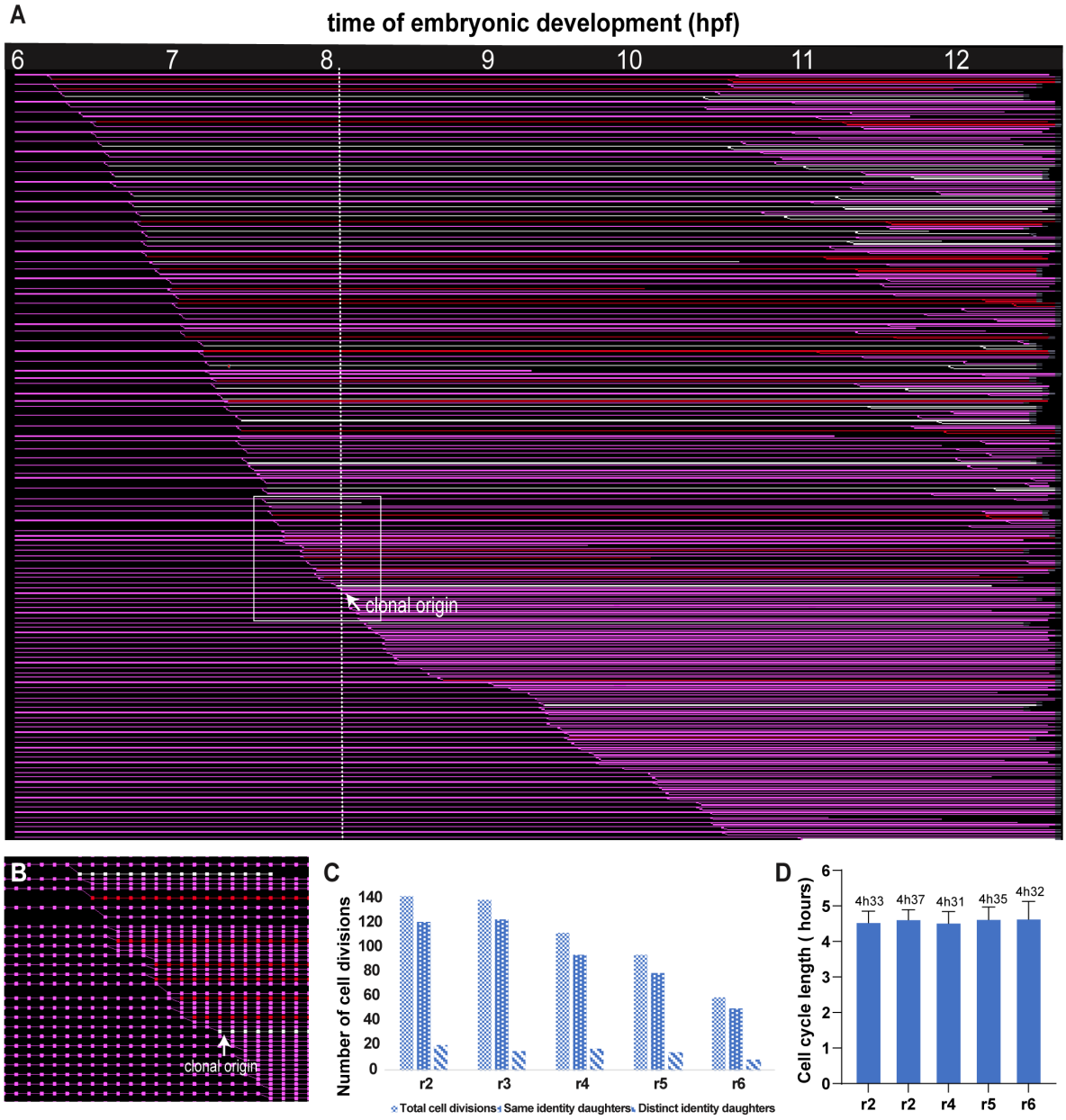

Figure 3. Clonal analysis of rhombomere 3 from cell lineage tree.

A) Flat representation of the reconstructed cell lineage of rhombomere 3 with branches indicating cell division. The x-axis displays the time of embryonic development in hours post-fertilization (hpf). Each line indicates a single hindbrain progenitor. Some cells were not tracked until the end of the sequence, and are depicted as interrupted lines. B) Magnification of the part of the tree in rectangle shown in A, a square corresponds to a cell. r3-pink, r2-red, r4-white. C) Graph indicating total number of cell divisions, number of division leading to two daughters of same rhombomere and of distinct rhombomeres for r2-r6. i.e for r3 progenitor divisions leading to either same r3/r3 or distinct identity daughters: r3/r4 and r3/r2. D) Cell cycle length of r2 to r6 progenitors of developing embryos from 6 to 13 hpf. Number of divisions analysed r2-61, r3-55, r4-60, r5-45, r6-25.

Hindbrain anteriorisation upon RA signalling inhibition

RA which acts in the posterization of neurectoderm is synthesised by RALDH in the mesoderm layer in the vicinity of the margin as early as late blastula stage of zebrafish embryo (Schier and Talbot, 2005). In order to establish the basis for integration of molecular signalling and cell behaviours in hindbrain patterning and in the specification of cell identity, we reconstructed cell lineages in control embryos and in a RA signalling null background in the presence of the drug diethyl-aminobenzaldehyde (DEAB). The DEAB treatment of transgenic *krox20:eGFP-Hras* zebrafish embryos was applied from 4 hpf onwards before the onset of RA activity in the embryo. DEAB treatment at 10 µM ensured the desired hindbrain phenotype characterized by expansion of r3 and r4 and absence of posterior rhombomeres with a reduced r5 in 35% of treated embryos and complete absence of r5 in the rest of the embryos (Maves and Kimmel, 2005)(Figure 4A,A', B, B' and E). Confocal 3D stacks of the embryos in the r3-r5 region were made at 14 and 24 hpf to analyse their distribution in the neural keel and neural tube respectively, upon RA inhibition (Figure 4C, C', D, D'). Segmentation of the domains and their 3D reconstruction showed that the reduced r5 domain restricts to the dorsal part of the neural tube suggesting ventral cells are more sensitive to RA perturbation (Figure 4C',D'). The volume of r3 and r4 domains were both increased ~200% in DEAB-treated embryos at 14hpf stage (Figure 4F). In order to obtain fate map of hindbrain upon RA inhibition, we marked the rhombomeres' r2-r5 nuclei as previously described in control embryo except for the distinctive selection of nuclei with no membrane staining, i.e. eGFP-, in prospective r5 domain (Figure 4G,G'). The position of each progenitor population was shown (Figure 4H-L)(Movie S4). The remaining r5 (eGFP+/krox20+) cells undertook a migratory path that corresponds to dorsal progenitors as expected while the eGFP-/krox20- cells (which are mostly ventral) have their progenitors located within the r4 progenitor domain meaning that more progenitors were specified towards anterior fate than in control embryo. We noticed that the mean path gravity mass of eGFP- cells undertook the migratory path of r4 ventral cells (Figure 4M). Also, the distance between neighbouring cell nuclei remained higher over time in DEAB-treated embryo indicating that RA inhibition caused a retardation in tissue compaction (Figure 4N). Taking it as a read-out for degree of convergence, we report that the delayed convergence of neural progenitors is reduced around 11 hpf, just before neural keel stage. It is well known that convergence movements of the zebrafish neural plate cells are regulated and critical for both tissue internalization and the development of a solid neural keel and neural rod (Tawk *et al.*, 2007; Araya *et al.*, 2014). Further, we analysed the speed of lateral cells and found that the increase of speed is delayed for a shorter period of time (10hpf20-11hpf10) compared to normal embryo (8hpf50-10hpf50) (Figure 40, 2G).

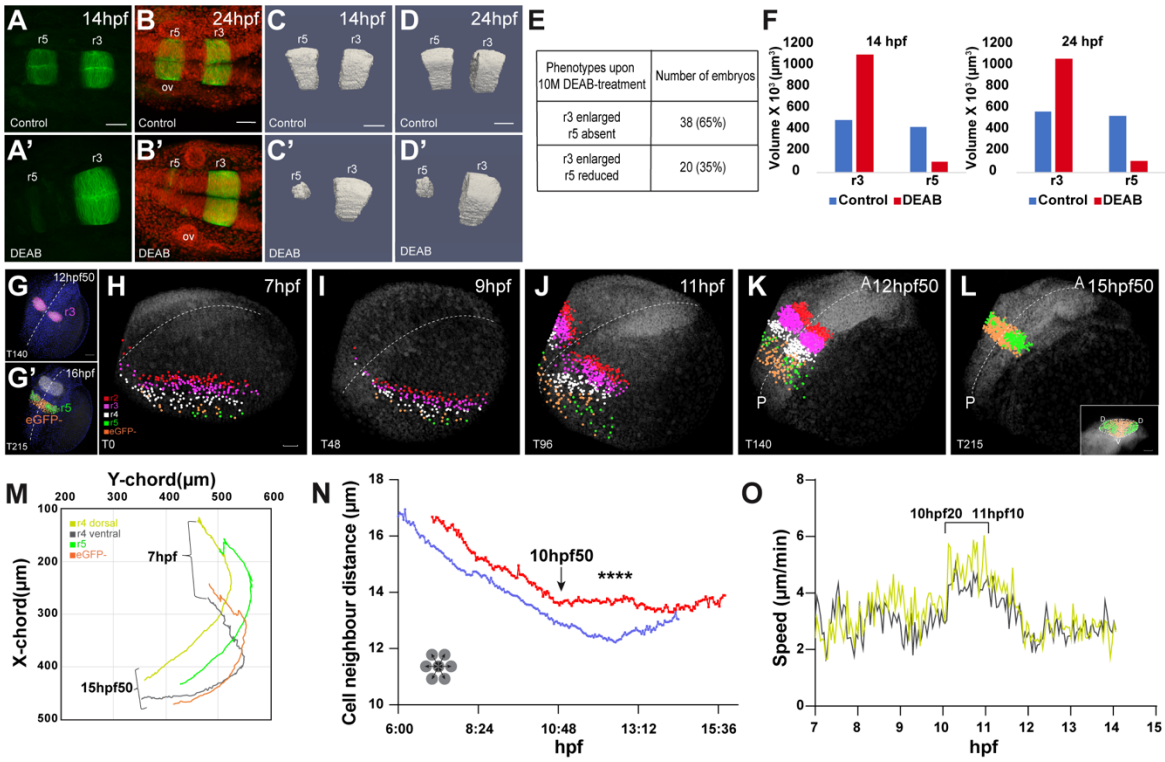

Figure 4. Hindbrain phenotype and fate map upon RA inhibition.

A, A', B, B') Z-projection of confocal images of control and DEAB-treated Tg *krox20:eGFP-Hras* embryos at 14hpf and 24hpf respectively. In B-B', nuclei are stained with mCherry. C,C',D,D') 3D reconstruction of r3 and r5 domains from the confocal imaging through semi-automated segmentation. E) Phenotypes upon 10µM DEAB treatment. F,F') Graphs showing the quantification of volume of r3 and r5 domains from 3D reconstruction in control and DEAB-treated embryo (number of experiments =3). G, G') Selection of r3 and reduced r5 domains' nuclei in DEAB digital embryo at 12hpf50 and 16hpf (top and bottom respectively) identified with *krox20* driven eGFP membrane staining (white). eGFP- nuclei, located ventrally to the r5 cells are selected in G'. DEAB digital embryo with nuclei centres in blue, r3 nuclei centre in pink and r5 in green, eGFP- nuclei centre in orange. H-L) Rhombomere progenitors' position from r2-r5 at 7hpf, 9hpf, 11hpf, 12hpf50 and 15hpf50. Nuclei centres of rhombomere with their colour code, super imposed with raw imaging data. r2-r4 are not coloured in the L panel. In L , transverse section of the neural rod is shown bottom right. Dorso-lateral view. Only the right side must be considered since nuclei correction was performed on this half of the digital embryo. M) Gravity mass of r4 dorsal, r4 ventral, r5 and eGFP- progenitor population is plotted in XY axis from 7hpf. N) Average cell neighbour distance in control (blue) and DEAB-treated (red) embryos during the imaging period. Mann Whitney test is performed to test the significance of difference. P=3.0477602071185435e-16. O) Relative speed of dorsal (yellow) and ventral (grey) progenitors of r4 from 7 to 14 hours of embryonic development. Dotted line indicates midline. A- Anterior, P- Posterior. hpf- hours post fertilization. Scale bar-50µm.

Increase of progenitors specification toward r3 and r4 fate upon RA inhibition

Anteriorisation of hindbrain, i.e expansion of r3-r4 at the expense of posterior ones, upon RA inhibition had been reported in many studies (Begemann *et al.*, 2004; Maves and Kimmel, 2005)(Begemann et al, 2004; Maves and Kimmel, 2005). Through the establishment of hindbrain fate map of DEAB-treated embryo, we deciphered that RA controls convergence movement of rhombomere progenitors and contribute to the specification of posterior progenitors identity from mid-gastrulation. Next, We explored the spatiotemporal features controlling the rhombomere progenitors populations and gather information on population dynamics and lineage relationships. We examined the size of progenitor population of r2, r3 and r4 upon RA inhibition. We found that at mid-gastrulation (7 hpf) the surface area occupied by individual progenitors population is the same between control and DEAB-treated embryos. (Figure 5A,B). But at 8 hpf, the size of r3 and r4 progenitors population became larger whereas the size r2 is not affected upon RA inhibition (Figure 5C,D). It was reported that r2 is not under the control of RA signalling. We examined cell proliferation rate of rhombomere progenitors and found that it remained similar for r2, r3, r4 and r5 indicating that the anteriorisation was not caused through change in proliferation rate (Figure 5F). We next analysed the properties of rhombomere progenitors divisions from 7 to 8 hpf, before the established clonal origin of rhombomere. Progenitors of r3 and r4 tend to give rise to daughters of same rhombomere identity to a greater extend, with 75% and 62.5% of divisions with same identity daughters in DEAB embryo compared to 56.2% and 36.4% in the control, respectively (Figure 5E,G).

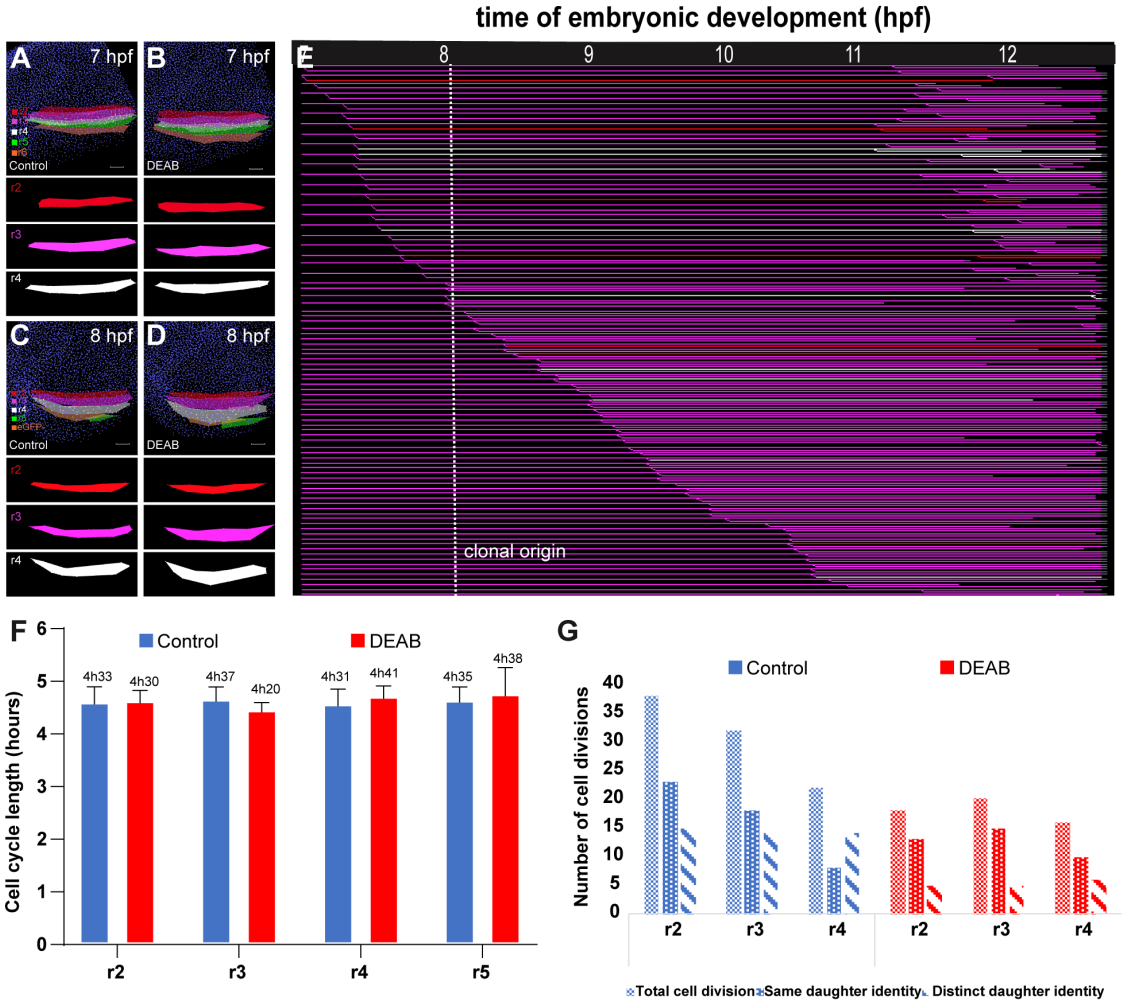

Figure 5. Increase r3 and r4 progenitors division into same identity daughters upon RA inhibition.

A-C) Surface area of rhombomere progenitors in control and DEAB-treated embryos at 7 hpf (A,B) and 8 hpf (C,D) respectively, with their colour code. Bottom: area of r2 (red), r3 (pink) and r4 (white). Scale: 50µm. E) Flat representation of the reconstructed cell lineage tree of r3 in DEAB-treated embryo with branches indicating cell division. The x-axis displays the time of embryonic development in hours post-fertilization (hpf). Each line indicates single hindbrain progenitor (r2 in red, r3 in pink, r4 in white). Interrupted lines indicate that the cells were not tracked further. F) Comparison of cell cycle length of r2, r3, r4 and r5 progenitors in control (Blue) and DEAB-treated (red) embryos. Number of cell divisions analysed in DEAB-treated embryo, r2=27, r3=33, r4=33, r5=5. G) Graphs indicating total number of cell division, number of divisions leading to two daughters of same rhombomere and of distinct rhombomeres i.e for r3 progenitors divisions leading to either same r3/r3 or distinct identity daughters: r3/r4 and r3/r2. The analysis is done before 8 hpf.

Defect in convergence leads to ectopic accumulation of neural progenitors and NTDs

We further examined the impact of impaired movement of convergence of hindbrain progenitors on the morphogenesis of the developing neural tube, upon RA signalling inhibition. Confocal imaging of *krox20:eGFP-Hras* transgenic embryos at 14 hpf shows that the neural keel in DEAB-treated embryos is significantly wider than in control embryos (Figure 6A-C). In addition to this well-known hindbrain phenotypes upon RA inhibition, we observed a dysmorphology in the neural tube lumen at the level of rhombomere 3-5 region in DEAB-treated embryos at 24 hpf (Figure 6D-F). The phenotype appeared to be a spectrum from partial duplication, with ectopic neural progenitors accumulation in the dorsal part of the neural tube, to fully duplicated apical midlines (Figure 6E,F). The lateral section and transverse section of the neural tube revealed a degree of duplicated apical midlines/lumen (Figure 6E',E'',F',F''). The penetrance of the phenotype is higher in the transgenic line established in WT/TÜ background than the other one generated in *casper* background, with 42% and 18% of neural tube defect (NTD) respectively (Figure 6G). The phenotype obtained is reminiscent of *vangl2* zebrafish mutants. Mirror-symmetric C-division which occurs at neural keel and neural rod stages deposits one daughter on each side of neural-axis. This ensures the apical polarity of daughter cells lie at the middle of the tissue. Subsequently apical midline is formed and lumen opens along the apical midline (Tawk *et al.*, 2007; Quesada-Hernández *et al.*, 2010). The delayed convergence is the cause of ectopic C-division in lateral regions of wider neural plate in *vangl2* mutants. This results in formation of duplicated apical midline and consequent duplicated neural tube. As we had previously mentioned, there is a convergence defect in RA-null embryos with the read-out of tissue compaction (Figure 4O). We observed a normal C-division in the DEAB-treated embryos but at lateral regions of the developing neural tube (Figure 6H). Altogether, our data suggests that the observed NT phenotype is due to the delay/defect in convergence.

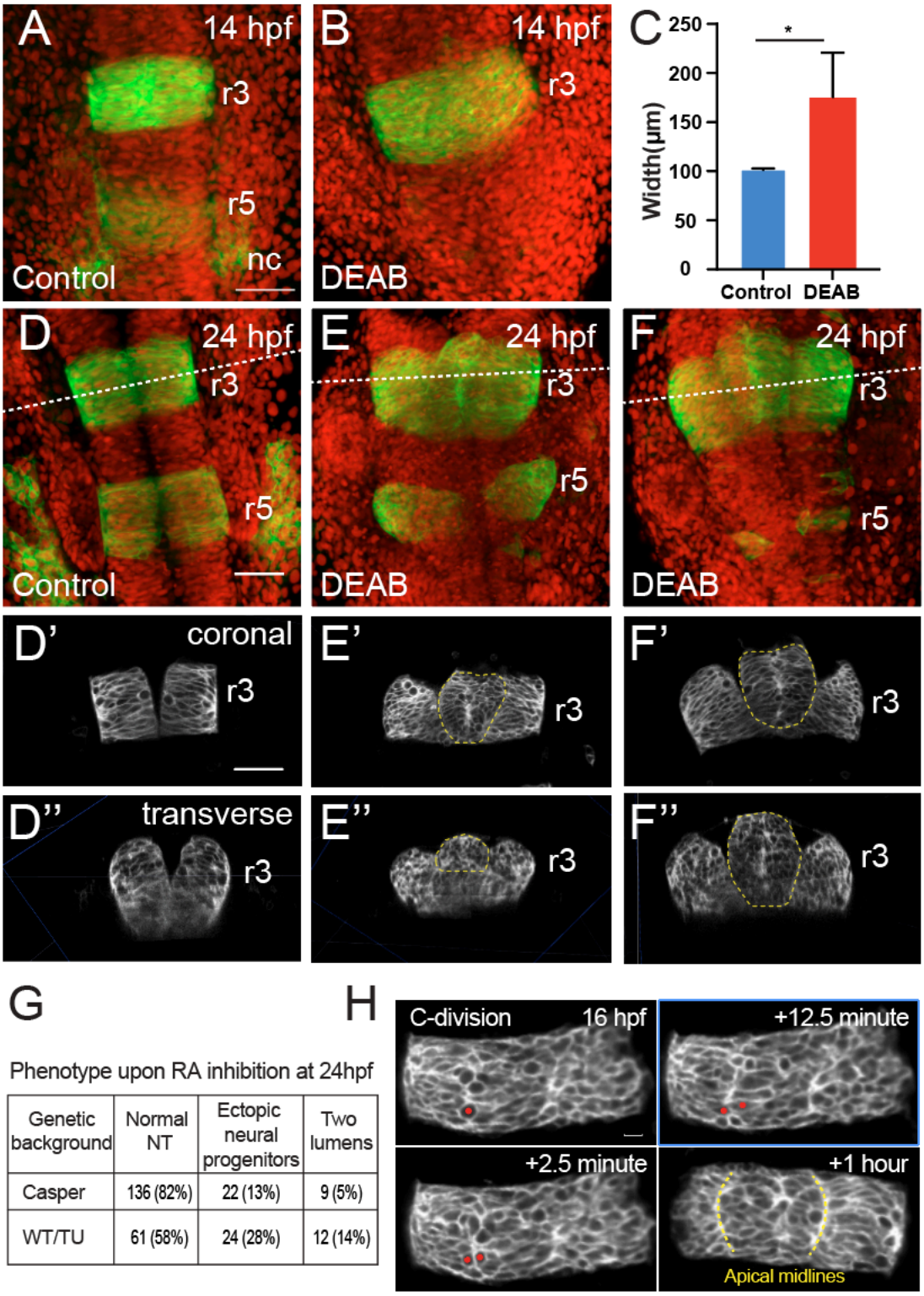

Genetic background	Normal NT	Ectopic neural progenitors	Two lumens
Casper	136 (82%)	22 (13%)	9 (5%)
WT/TU	61 (58%)	24 (28%)	12 (14%)

Figure 6. RA inhibition causes ectopic apical midlines.

Figure 6. RA inhibition causes ectopic apical midlines.

A,B) Z-projection of confocal imaging of Tg *krox20:eGFP-Hras* control and DEAB-treated embryos at 14hpf. nc- neural crest C) Width of neural keel in control and DEAB-treated embryos at 14 hpf. Unpaired student t-test is performed to test the significance of the difference. D-F) Z-projection of confocal imaging of Tg *krox20:eGFP-Hras* control (D) and (E-F) two classes of phenotypes in DEAB-treated embryos at 24hpf. Embryos were injected with *H2B-mCherry* mRNA at one-cell stage. Dotted line in D-F indicates transverse sections through r3 shown in D''-F'' respectively. D'-F', D''-F'') Coronal sections through dorsal part of r3 (D''-F'') and (D''-F'') transverse sections of r3. The ectopic accumulation of neural progenitors has been outlined in panels E'-F' and E''-F''. G) Table scoring the phenotypes in *krox20:eGFP-Hras* transgenic lines established in WT/Tü and *casper* backgrounds upon DEAB treatment. H) Z sections through r3 of 2-photon 4D imaging of DEAB-treated transgenic embryo. Time-lapse sequence shows C-division occurs at two lateral edges of neural keel-neural rod. Red dots indicate the centre of mother and daughter cells. Yellow dotted lines depict apical midlines. Time points are indicated top right. r-rhombomere Scale bar-50µm, H) 20µm.

Rescue of posterior rhombomere with optogenetic restoration of RA in hindbrain progenitors

Optogenetic tools can be used to manipulate RA activity at the single cell level with a high spatiotemporal resolution. In order to tackle the autonomous versus community effect of RA signalling on hindbrain morphogenesis, we made use of the established RA photoactivation method where the biologically inactive 13-cis RA is isomerized to active all-trans RA at the single cell level locally using UV illumination in a null RA background (Xu et al. 2012). It was shown previously that photoactivation must be performed prior to the end of gastrulation to obtain complete rescue of hindbrain (Xu et al. 2012). We first inhibited the RA signalling in *krox20:eGFP-Hras* embryo in the presence of 10μM DEAB from 4 hpf onwards. At 6 hpf, embryos were incubated for 5 minutes in 5nm 13-cis RA (a pulse) (Figure 7A). Then, we restored RA signalling in selected r5 progenitors on one side of the embryo at 7 hpf, by scanning at 405nm for a few minutes (Figure 7B). Our fate map of zebrafish hindbrain was instrumental to target the r5 progenitors precisely. The rescued cells were followed by the simultaneous photoconversion of the fluorescent protein nls-Eos which shifts from green to red nuclei upon UV illumination. We observed a rescue of posterior hindbrain and more specifically the whole r5 domain (Figure 7C,C,D,D'). RA restoration in individual r5 progenitor level caused the rescue of adjacent cells identified with *krox20*-driven membranous eGFP staining suggesting a community effect of RA on *krox20* gene expression and hindbrain morphogenesis.

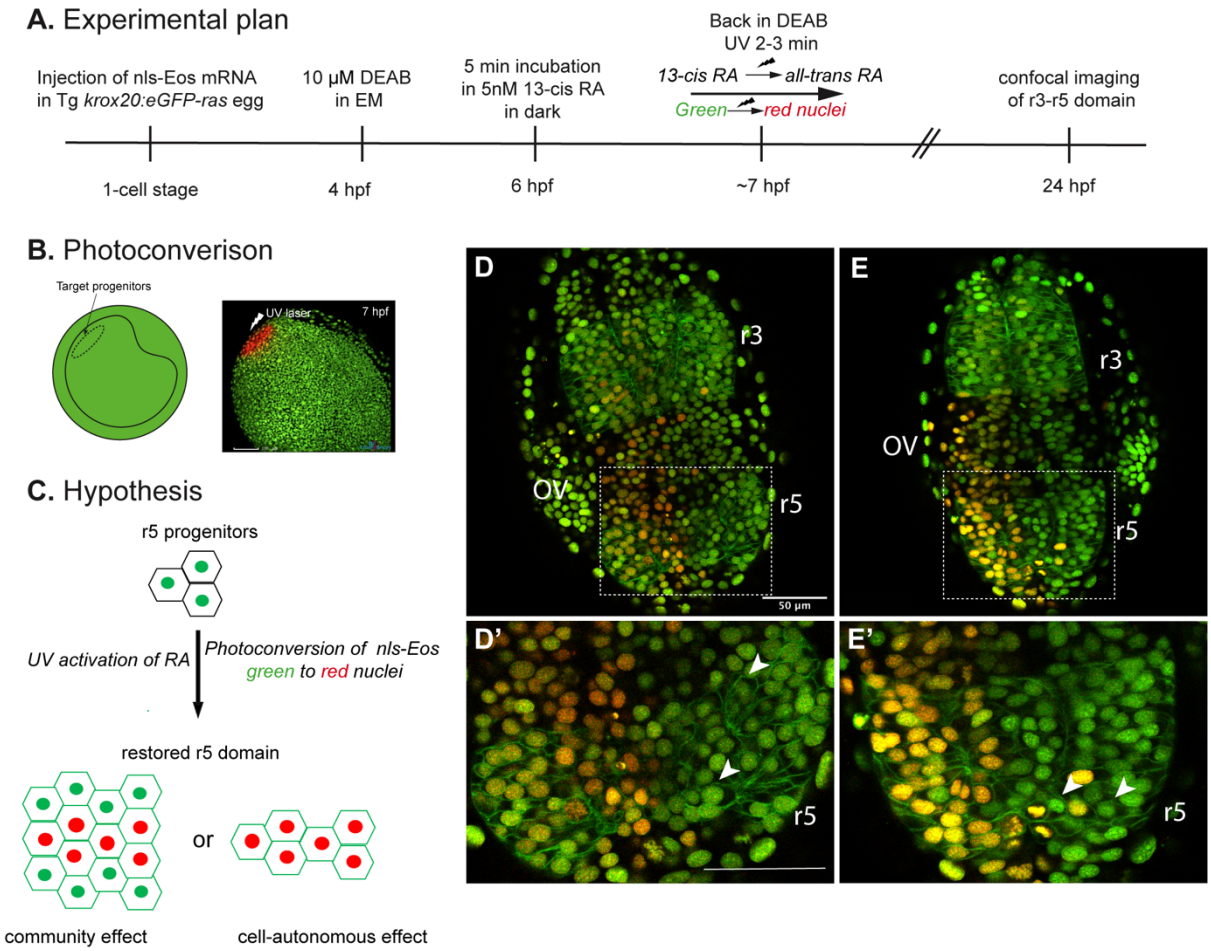

Figure 7. Rhombomere 5 restoration by cell community effect.

A) Timeline of the experiment. B) Tg *krox20:eGFP-Hras* embryo at 6hpf with the simultaneous photoconversion of nls-Eos and photo-isomerization of inactive 13-cis RA to active all-trans RA in targeted r5 progenitor cells mainly. C) Schematic of r5 restoration through cell-community and cell-autonomous effects. D,E) Confocal z-slice of transgenic embryo at 18hpf showing the rescue of rhombomere 5 upon RA restoration in 8 progenitor cells (D) and 12 progenitors cells (E). D',E') Magnified view of the corresponding (D,E).Red nuclei staining identify RA-rescued cells. Arrow heads indicate rescued neighbouring cells with green membrane only.

Discussion

We established a method to study zebrafish hindbrain morphogenesis quantitatively from mid-gastrulation till early neurulation through 3D+time live imaging of hindbrain-specific transgenic embryo. The technical advancement of two-photon scanning microscopy and automated cell tracking tools facilitate such a cellular approach. Quantifying cell behaviour will serve as a basis to build a mechano-genetic model of hindbrain formation *in silico*. Hindbrain rhombomeres start to be specified as early as 8 hpf with their marker gene expression. Thus, this approach can be used to understand the early cell behaviours that lead to hindbrain defects upon gain and loss of various genes' functions during hindbrain morphogenesis.

AP and DV organisation of rhombomere progenitors at the shield stage

We provided a zebrafish hindbrain fate map with greater precision compared to the state-of-the-art by taking advantage of technical advancements (Figure 8) (Woo and Fraser, 1995). Our fate map shows no wavy domains of hindbrain progenitors as predicted in (Woo and Fraser, 1995). However, r1 and r7 domains are not included in our fate map analysis, which may give more overlapping region with midbrain and spinal cord progenitors at anterior and posterior ends respectively. Further, cell behaviours and cell dynamics have been elucidated in the study. Rhombomeres are cell lineages units with polyclonal origin. We demonstrated that clonal commitment of rhombomere progenitors is achieved at around 8 hpf. The defined clonal origin of rhombomere is in agreement with transplantation experiments showing regional neural identity commitment occurs at 80% epiboly (Woo and Fraser, 1995). Neural progenitors (neuroectoderm) undergo orderly movement throughout gastrulation. It is known to be guided by the asymmetric localization of planar cell polarity (PCP) components (Williams and Solnica-Krezel, 2020). Dorsal and ventral progenitors are located more lateral and medial respectively in regard to the embryonic shield. Both populations move in the same direction towards the midline, however at 11 hpf medial cells undergo posterior migration and then follow anterior-ward movement. At the same time, it also undergoes inward movement to internalize. The lateral cells which are far from midline start to speed up and converge directly to the midline. By this way, they place themselves on top of inward moving medial cells. Thus, we showed progenitors undertake distinct migration paths to orchestrate the 3D neural keel structure from 2D neural plate cells with quantitative cell behaviours. Protrusive activity of individual cells during migration is under the control of PCP components and it would be interesting to study the roles of PCP in this differential migration paths of these D and V progenitors during the early neurula stages. The differential migration paths of D and V progenitors were observed in a previous study (Araya *et al.*, 2019). The observed increase in speed of

lateral cells was shown previously using conventional methods which didn't give the exact timing of the increased speed (Sepich *et al.*, 2000; Myers, Sepich and Solnica-Krezel, 2002).

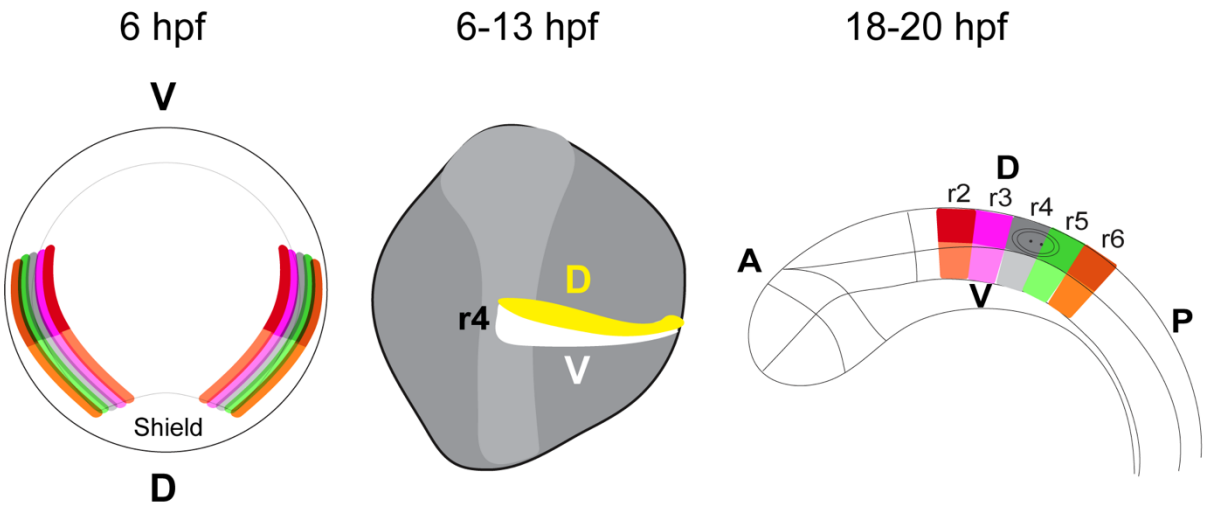

Figure 8. Schematic of zebrafish hindbrain fate map (r2-r6).

Rhombomeres from r2 to r6 are marked in their respective colour code. Shield stage (left) and Neural tube (right). The shaded colours in between two rhombomere progenitor populations, indicate the overlap of the two territories. Ventral progenitors at the shield stage and ventral cells in the neural tube are marked in light colours of their respective dorsal counterparts in dark colours. In the middle, the cell trajectories of the dorsal (yellow) and ventral (white) progenitors of r4 are represented from 6 to 13 hours of embryonic development. D-dorsal, V-ventral, A-Anterior, P-posterior.

RA role in hindbrain patterning

We obtained the hindbrain fate map upon RA inhibition. It showed that the identity switch of progenitors caused the hindbrain anteriorisation but not increased cell proliferation. We found that anterior domains r3 and r4 increased by twice upon DEAB inhibition through volume measurement via semi-automated segmentation and a strong reduction in r5 domain. We measured the cell cycle length of r3 and r4 domains cells in control and DEAB-treated embryos and found no significant change in proliferation rate upon RA inhibition. It strongly suggests that the posterior rhombomere progenitors are acquiring anterior fate due to the shift in RA morphogen gradient and corresponding cell fate.

In our study, we observed that the ventral neural tube is more sensitive to RA inhibition. It has been observed in *val* mutants, the indirect target gene of RA through vhnf1, that the *krox20* expression is restricted to anterior dorsal domain of r5 at 19 hpf and also corresponding to

cells more laterally located in prospective r5 at 11.5 hpf (Prince, 1998). It suggests that the RA may have a differential influence on target gene activation along the trajectory of neural progenitors in the DV axis of the embryo at early-mid gastrula stages. We showed that the progenitors of prospective ventral r5 cells acquired r4 identity upon RA inhibition through back tracking the remaining cells in ventral r5 domain which do not express *krox20*. Over all, our study dissects the phenotypic defect in hindbrain upon RA inhibition.

RA in apical midline formation during neurulation

"Duplicated NT" phenotype upon RA inhibition has not been reported in previous studies. C-division of neural progenitors at neural keel stages has a powerful morphogenetic influence on neural tube organisation. It occurs in response to intrinsic molecular clock rather than depending on the environment (Girdler *et al.*, 2013). Thus, C-divisions could occur on lateral edges of wider neural keel when convergence is slower as observed in *vangl2* mutants (Tawk *et al.*, 2007). We observed a convergence defect in embryos upon RA inhibition. The observed NT phenotype was highly reminiscent of *vangl2 (tri)* mutants (Ciruna *et al.*, 2006; Tawk *et al.*, 2007). In *tri* mutants, the speed of lateral cells is reduced, thus leading to the delayed convergence. We observed the same in embryos upon RA inhibition. We looked for possible link between RA with PCP pathway in the literature. It was shown in *Raldh2-/-* mouse embryos that RA deficiency caused strong downregulation in *Vangl2* and *Fzd3* expression at the level of hindbrain, at E8.25-E8.75 (Tuduce *et al.*, 2009). It can be presumed that RA inhibition causes downregulation of these PCP components during zebrafish gastrulation as well. That results in convergence defects and consequent neural tube dysmorphology. However, the expression pattern of *vangl2* and *fzd3* in zebrafish embryos upon RA inhibition at late gastrula and early neurula stages must be investigated through whole mount *in situ* hybridisation. The exact role of RA in leading to duplicated NT phenotype should be further examined in detail. This would give a perspective for cross-talk between two signalling pathways RA and PCP that are important for cell specification and cell movement respectively. The penetration of NT phenotype differs according to the genetic background of the transgenic lines. Even though the penetrance is not complete, the fact that the phenotype is observed in two distinct lines eliminates the possibility of the influence of regulatory sequences surrounding the integration site of the transgene on the reported phenotype.

Community effect of RA signalling

Morphogen gradients are not just formed through simple diffusion but by active transportation of morphogen molecule through the extracellular matrix at long distances (Rogers and Schier,

2011). To understand the nature of RA morphogen gradient and at which distance it acts in presumptive neuroectoderm, we aimed to restore RA in selective hindbrain progenitors and analysed the followed rescue of posterior rhombomere (r5) domain. Photo-isomerisation of the inactive form 13-cis RA to the active form all-trans-RA was used to develop the spatiotemporal control of RA (Xu *et al.*, 2012). It was shown in the same study that if RA was activated locally at head region before the bud stage, it was possible to rescue the hindbrain defects in DEAB-treated embryos. In our experiment, we restored RA specifically at r5 hindbrain progenitors on one side of the embryo at the shield stage by UV illumination using confocal microscopy. However, we observed the rescue of r5 hindbrain domains on both sides of neural tube AP axis. That indicates the restored RA is sequestered quickly over the long distance and further strengthens that there is a community effect of RA during hindbrain morphogenesis. However, it is important to note that the local activation was not very precise due to the poor axial resolution in confocal microscopy. Photoactivation should be performed using two-photon microscopy in the future to target the progenitor region precisely.

Material and Methods

Zebrafish transgenics and husbandry: Transgenic fish lines, *krox20:eGFP-Hras* were generated in the lab to label developing rhombomere domains r3 and r5 with eGFP targeted to membrane. For this purpose a SalI/ClaI fragment containing GFP-Hras from pCS2/GFP-Hras was sub-cloned into pCR2.1-TOPO to be transferred as a BamHI/NotI fragment in pTol2-cA:GFP construct (Labalette *et al.*, 2011). Transgenic lines were obtained from WT/Tü and *casper* embryos injected at the one-cell stage with the pTol2 constructs together with tol2 transposase mRNA. The zebrafish lines were bred and maintained as described (Westerfield, 2007). Embryos were staged in accordance with (Kimmel *et al.*, 1995).

mRNA preparation and microinjection: *H2B-mCherry* and *nls-Eos* mRNAs were prepared using mMessage mMachine mRNA transcription kit (Invitrogen) and stored in -80˚C. 3-4nl of 75ng/µl H2B-mCherry mRNA was injected in one-cell stage zebrafish embryos. Injection at early one-cell stage into the centre of the cell of the embryo ensured homogenous staining. For optogenetic experiments, 40 ng *nls-Eos* mRNA was injected in one-cell stage embryo. Embryos with homogenous and optimum bright staining were selected around 4 hpf or 6 hpf for live imaging experiments.

Pharmacological treatment: Embryos were incubated with 10µM DEAB from 4 hpf onwards in dark in order to inhibit RA signalling. Fresh dilution was made from a 10mM DEAB stock dissolved in DMSO for each experiment. For optogenetic RA restoration experiments, shield

stage embryos were washed with embryo medium (EM*)* after 10μM DEAB incubation and incubated in 5nM cis-RA for five minutes. Fresh dilutions of 13 cis-RA were made in two steps from 40mM stock in DMSO each time. Control embryos were kept in EM. (all Sigma-Aldrich)

Mounting for hindbrain development imaging: Embryo at 6hpf was dechorionated and mounted in the custom-made imaging chamber on a bed of 0.5% LMP Agarose. The imaging chamber was filled with EM alone or DEAB solution, dissolved in EM for RA inhibition experiments. Tricaine was used at 0.033% in EM to inhibit twitching of embryo at later stages. First, embryo was placed on an agarose bed with animal pole on top and then the shield position is tilted up to 30º angle (1/3rd to the centre of the embryo) and immobilized by pouring 20-30μl of 0.5% LMP agarose on top. This initial position of shield stage embryo ensured that the hindbrain progenitors were inside the field of view throughout the gastrulation and neurulation movements.

Two-photon and confocal microscopy imaging: Leica SP5 and Zeiss LSM780 two-photon microscopes equipped with water immersion 20X/1.0 NA dipping lens objective were used for overnight imaging. Image stacks of 200-250 μm with spatial scaling 1-1.16 μm and with delta T ~2m30s were made continuously for 10 hours and more. 70 μm was scanned above the animal pole to ensure the embryo's growth inside the volume scanned during the imaging period. Embryos were maintained at 28.5°C with the use of OKO-lab heating system (OKO-lab H101 WJC). Only embryos which exhibited normal morphology after imaging were analysed. LSM Zeiss 780 was used for confocal imaging of hindbrain rhombomeres 3-5 at 14 hpf and 24 hpf embryos. Dechorionated embryos were mounted in agarose gel molds. Image stacks 100-120 μm was made at 1024x1024 spatial resolution.

Semi-automated segmentation and 3D reconstruction:

The applied method for 3D image segmentation used surface reconstruction from 3D point cloud data and 3D image information. The available information was combined by the calculation of the distance function to the shape, represented by the point cloud, and the application of the edge detector function to the pre-smoothed 3D image. The method achieved the needed result by implementing a mathematical model and numerical method based on the level set algorithm. In the case of the mentioned data the algorithm was further optimized by using semi-automatically segmented curves in every 2D slice of the 3D image instead of a point cloud data set.

Optogenetic restoration of RA:

Global illumination with UV lamp: UV lamp(365nm) was used to illuminate embryos incubated in 5 nM 13-cis RA (Supp. fig). Local illumination with UV laser: 40 ng/ul of *nls-Eos* mRNA is injected at one-cell stage transgenic embryo. Embryos were treated with 10μM DEAB from 4 hpf onwards. DEAB solution was removed and embryos were incubated in 5nm 13-cis RA for 5 minutes at 6hpf and later transferred back into 10μM DEAB solution. Embryo with homogenous nls-Eos staining was selected and dechorionated using stereo- fluorescent microscope. Embryo was positioned on Teflon mold with animal pole in dorsal view as described above. 20X/1NA objective (Zeiss) was used to locate the r5 progenitor area. With the knowledge from the wildtype embryo, r5 progenitor area is identified approximately and illuminated with 405nm UV laser for 3-4minutes. The simultaneous conversion of nls-Eos from green to red nuclei and biologically inactive 13-cis RA to active all-trans RA allowed us to follow the RA restored cells over time. Note that the bright field of Zeiss microscope was blocked with UV shield and the entire optogenetic part was carried out in at most dark. The method was previously established in (Xu *et al.*, 2012).

Data Analysis:

Raw data was processed through BioEmergences workflow to obtain the automated reconstruction of cell lineages (Faure *et al.*, 2016). Nuclei centres were validated through centre select software and a nuclei-based tracking algorithm Expectation-Maximization (EM) which is the iteration of SimAnn algorithm was applied. The data was visualized, annotated and analysed in Mov-IT, a custom made interface (Faure *et al.*, 2016). Parameters such as gravity mass, average cell neighbour distance, timing of cell division and speed were extracted from Mov-IT software. Mann-whitney and student t-tests were performed to find the significance of compared groups. Images for the publication were made using the same software. Calculations and graphs were made in Excel. Fiji software was used to analyse and present confocal imaging data. Figures were assembled in Adobe illustrator. Graphpad prism and MS excel were used for statistical analysis and representation.

Acknowledgements

We thank Mark E. Hammons and Maxime Comberiati for the assistance of Bio-Emergences workflow and fish facility respectively. We thank Dr Weiting Zhang and Dr David Bensimon for the guidance with optogenetic RA restoration experiments. We are grateful to Dr Paula Alexandre's comments on the manuscript. We thank ImageInLife, European Union's Horizon 2020 research and innovation programme under the Marie Sklodowska-Curie grant agreement No. 721537 for providing PhD funding to MK (2017-2020).

Supplemental figures

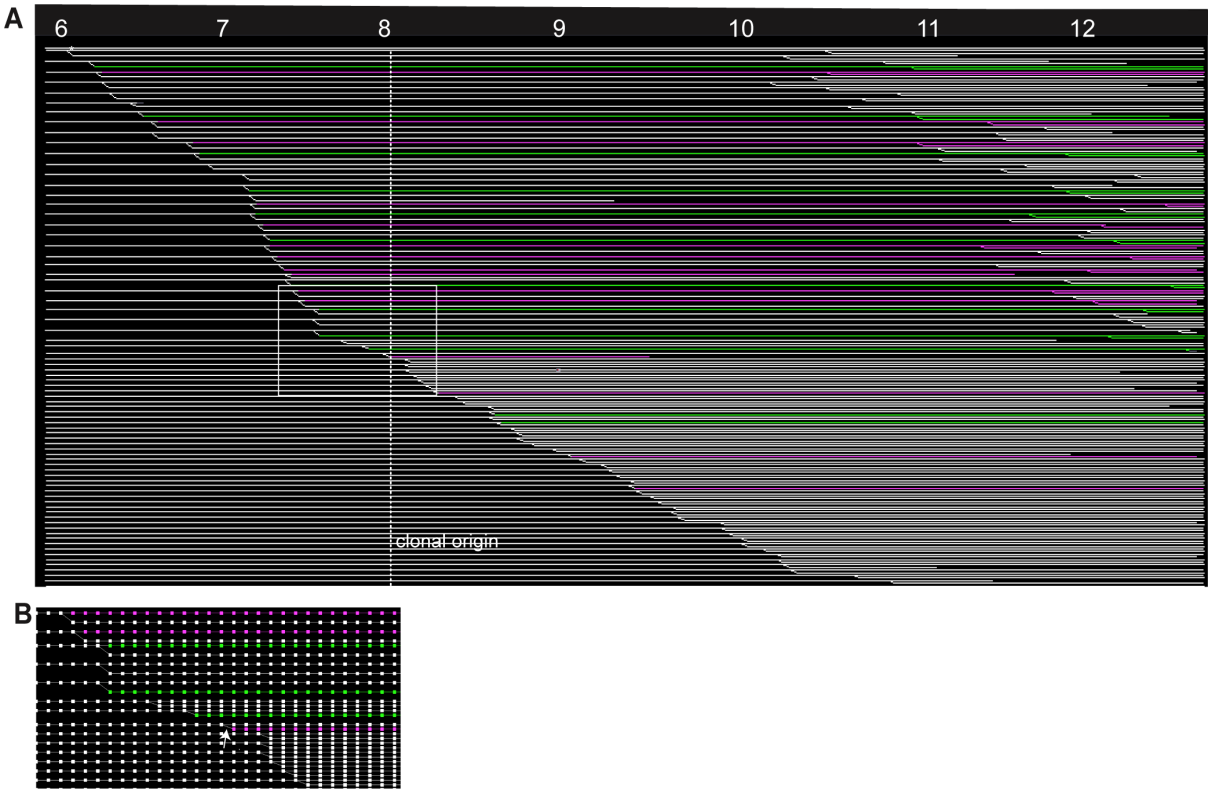

Figure S1. Clonal analysis of rhombomere 4 with cell lineage tree.

A) Flat representation of the reconstructed cell lineage of rhombomere 4 with branches indicating cell division. The x-axis displays the time of embryonic development in hours post-fertilization (hpf). Each line indicates a single hindbrain progenitor. Some cells were not tracked until the end of the sequence, and are depicted as interrupted lines. B) Magnification of the part of the tree in rectangle shown in A, a square corresponds to a cell. White arrow indicates the clonal origin point. r3-pink, r4-white, r5-green.

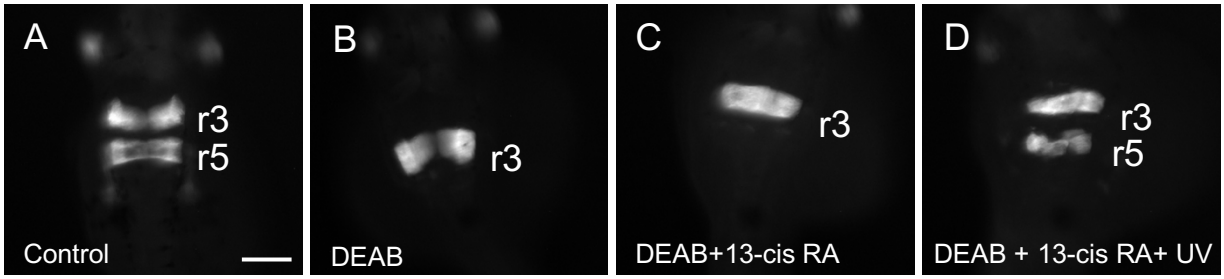

Figure S2. Isomerisation of RA via global UV illumination.

Tg *krox20:eGFP-Hras* embryos showing GFP staining in r3 and r5 at 30hpf in A) control embryo. B-D) DEAB-treated embryo from 4hpf onwards and exposed for 5 minutes to 5nM 13-cis RA (B) and illuminated (or not) for 1 minute with a UV lamp at 7 hpf (C,D). Scale bar: 100 µm.

Supplemental movies

Movie S1. Dynamic fate map of hindbrain (r2-r6) from mid-gastrulation till early neurulation

http://bioemergences.eu/MageshiK/videos/180516aF_annotated.mp4

Movie S2. Construction of dorsal and ventral 3D neural tube (r4) from progenitors domains.

http://bioemergences.eu/MageshiK/videos/180516aF_t_t21383_26.mp4

Movie S3. Transverse view of construction of 3D neural keel.

http://bioemergences.eu/MageshiK/videos/180516aFDVformation.mp4

Movie S4. Hindbrain formation r2-r6 from mid-gastrulation till early neurulation upon RA inhibition.

http://bioemergences.eu/MageshiK/videos/131129a_t_t21406_827.mp4

References

Araya, C. *et al.* (2014) 'Mesoderm is required for coordinated cell movements within zebrafish neural plate in vivo', *Neural Development*, 9(1), p. 9. doi:10.1186/1749-8104-9-9.

Araya, C. *et al.* (2019) 'Cdh2 coordinates Myosin-II dependent internalisation of the zebrafish neural plate', *Scientific Reports*, 9(1), p. 1835. doi:10.1038/s41598-018-38455-w.

Araya, C., Carmona-Fontaine, C. and Clarke, J.D.W. (2016) 'Extracellular matrix couples the convergence movements of mesoderm and neural plate during the early stages of neurulation', *Developmental Dynamics*, 245(5), pp. 580–589. doi:10.1002/dvdy.24401.

Bedois, A.M.H., Parker, H.J. and Krumlauf, R. (2021) 'Retinoic Acid Signaling in Vertebrate Hindbrain Segmentation: Evolution and Diversification', *Diversity*, 13(8), p. 398. doi:10.3390/d13080398.

Begemann, G. *et al.* (2004) 'Beyond the neckless phenotype: influence of reduced retinoic acid signaling on motor neuron development in the zebrafish hindbrain', *Developmental Biology*, 271(1), pp. 119–129. doi:10.1016/j.ydbio.2004.03.033.

Calzolari, S., Terriente, J. and Pujades, C. (2014) 'Cell segregation in the vertebrate hindbrain relies on actomyosin cables located at the interhombomeric boundaries', *The EMBO journal*, 33(7), pp. 686–701. doi:10.1002/embj.201386003.

Chomette, D. *et al.* (2006) 'Krox20 hindbrain cis-regulatory landscape: interplay between multiple long-range initiation and autoregulatory elements', *Development (Cambridge, England)*, 133(7), pp. 1253–1262. doi:10.1242/dev.02289.

Ciruna, B. *et al.* (2006) 'Planar cell polarity signalling couples cell division and morphogenesis during neurulation', *Nature*, 439(7073), pp. 220–224. doi:10.1038/nature04375.

Concha, M.L. and Adams, R.J. (1998) 'Oriented cell divisions and cellular morphogenesis in the zebrafish gastrula and neurula: a time-lapse analysis', *Development (Cambridge, England)*, 125(6), pp. 983–994.

England, S.J. *et al.* (2006) 'A dynamic fate map of the forebrain shows how vertebrate eyes form and explains two causes of cyclopia', *Development (Cambridge, England)*, 133(23), pp. 4613–4617. doi:10.1242/dev.02678.

Faure, E. *et al.* (2016) 'A workflow to process 3D+time microscopy images of developing organisms and reconstruct their cell lineage', *Nature Communications*, 7(1), p. 8674. doi:10.1038/ncomms9674.

Girdler, G.C. *et al.* (2013) 'Developmental time rather than local environment regulates the schedule of epithelial polarization in the zebrafish neural rod', *Neural Development*, 8(1), p. 5. doi:10.1186/1749-8104-8-5.

Hernandez, R.E. *et al.* (2004) 'vhnf1 integrates global RA patterning and local FGF signals to direct posterior hindbrain development in zebrafish', *Development*, 131(18), pp. 4511–4520. doi:10.1242/dev.01297.

Hong, E. and Brewster, R. (2006) 'N-cadherin is required for the polarized cell behaviors that drive neurulation in the zebrafish', *Development*, 133(19), pp. 3895–3905. doi:10.1242/dev.02560.

Keller, P.J. *et al.* (2008) 'Reconstruction of Zebrafish Early Embryonic Development by Scanned Light Sheet Microscopy', *Science*, 322(5904), pp. 1065–1069. doi:10.1126/science.1162493.

Kimmel, C.B. *et al.* (1995) 'Stages of embryonic development of the zebrafish', *Developmental Dynamics: An Official Publication of the American Association of Anatomists*, 203(3), pp. 253–310. doi:10.1002/aja.1002030302.

Kimmel, C.B., Warga, R.M. and Kane, D.A. (1994) 'Cell cycles and clonal strings during formation of the zebrafish central nervous system', *Development (Cambridge, England)*, 120(2), pp. 265–276.

Kozlowski, D.J. *et al.* (1997) 'Regional cell movement and tissue patterning in the zebrafish embryo revealed by fate mapping with caged fluorescein', *Biochemistry and Cell Biology = Biochimie Et Biologie Cellulaire*, 75(5), pp. 551–562.

Krumlauf, R. and Wilkinson, D.G. (2021) 'Segmentation and patterning of the vertebrate hindbrain', *Development*, 148(15). doi:10.1242/dev.186460.

Labalette, C. *et al.* (2011) 'Hindbrain patterning requires fine-tuning of early krox20 transcription by Sprouty 4', *Development*, 138(2), pp. 317–326. doi:10.1242/dev.057299.

Lumsden, A. and Keynes, R. (1989) 'Segmental patterns of neuronal development in the chick hindbrain', *Nature*, 337(6206), pp. 424–428. doi:10.1038/337424a0.

Maves, L. and Kimmel, C.B. (2005) 'Dynamic and sequential patterning of the zebrafish posterior hindbrain by retinoic acid', *Developmental Biology*, 285(2), pp. 593–605. doi:10.1016/j.ydbio.2005.07.015.

Moens, C.B. and Prince, V.E. (2002) 'Constructing the hindbrain: insights from the zebrafish', *Developmental Dynamics: An Official Publication of the American Association of Anatomists*, 224(1), pp. 1–17. doi:10.1002/dvdy.10086.

Myers, D.C., Sepich, D.S. and Solnica-Krezel, L. (2002) 'Bmp Activity Gradient Regulates Convergent Extension during Zebrafish Gastrulation', *Developmental Biology*, 243(1), pp. 81–98. doi:10.1006/dbio.2001.0523.

Papan, C. and Campos-Ortega, J.A. (1994) 'On the formation of the neural keel and neural tube in the zebrafishDanio (Brachydanio) rerio', *Roux's archives of developmental biology: the official organ of the EDBO*, 203(4), pp. 178–186. doi:10.1007/BF00636333.

Parker, H.J. and Krumlauf, R. (2020) 'Chapter Six - A Hox gene regulatory network for hindbrain segmentation', in Peter, I.S. (ed.) *Current Topics in Developmental Biology*. Academic Press (Gene Regulatory Networks), pp. 169–203. doi:10.1016/bs.ctdb.2020.03.001.

Pinheiro, D. and Heisenberg, C.-P. (2020) 'Zebrafish gastrulation: Putting fate in motion', *Current Topics in Developmental Biology*, 136, pp. 343–375. doi:10.1016/bs.ctdb.2019.10.009.

PRINCE, V.E. (1998) 'Hox Genes and Segmental Patterning of the Vertebrate Hindbrain1', *American Zoologist*, 38(4), pp. 634–646. doi:10.1093/icb/38.4.634.

Quesada-Hernández, E. *et al.* (2010) 'Stereotypical Cell Division Orientation Controls Neural Rod Midline Formation in Zebrafish', *Current Biology*, 20(21), pp. 1966–1972. doi:10.1016/j.cub.2010.10.009.

Rogers, K.W. and Schier, A.F. (2011) 'Morphogen gradients: from generation to interpretation', *Annual Review of Cell and Developmental Biology*, 27, pp. 377–407. doi:10.1146/annurev-cellbio-092910-154148.

Schier, A.F. and Talbot, W.S. (2005) 'Molecular Genetics of Axis Formation in Zebrafish', *Annual Review of Genetics*, 39(1), pp. 561–613. doi:10.1146/annurev.genet.37.110801.143752.

Schmitz, B., Papan, C. and Campos-Ortega, J.A. (1993) 'Neurulation in the anterior trunk region of the zebrafish Brachydanio rerio', *Roux's archives of developmental biology*, 202(5), pp. 250–259. doi:10.1007/BF00363214.

Sepich, D.S. *et al.* (2000) 'Role of the zebrafish trilobite locus in gastrulation movements of convergence and extension', *Genesis (New York, N.Y.: 2000)*, 27(4), pp. 159–173. doi:10.1002/1526-968x(200008)27:4<159::aid-gene50>3.0.co;2-t.

Shah, G. *et al.* (2019) 'Multi-scale imaging and analysis identify pan-embryo cell dynamics of germlayer formation in zebrafish', *Nature Communications*, 10(1), p. 5753. doi:10.1038/s41467-019-13625-0.

Sirbu, I.O. *et al.* (2005) 'Shifting boundaries of retinoic acid activity control hindbrain segmental gene expression', *Development*, 132(11), pp. 2611–2622. doi:10.1242/dev.01845.

Tawk, M. *et al.* (2007) 'A mirror-symmetric cell division that orchestrates neuroepithelial morphogenesis', *Nature*, 446(7137), pp. 797–800. doi:10.1038/nature05722.

Tuduce, I.L. *et al.* (2009) '03-P026 Retinoic acid – planar cell polarity crosstalk during neural tube closure', *Mechanisms of Development*, 126, p. S75. doi:10.1016/j.mod.2009.06.079.

Walshe, J. *et al.* (2002) 'Establishment of Hindbrain Segmental Identity Requires Signaling by FGF3 and FGF8', *Current Biology*, 12(13), pp. 1117–1123. doi:10.1016/S0960-9822(02)00899-0.

Wan, Y. *et al.* (2019) 'Single-Cell Reconstruction of Emerging Population Activity in an Entire Developing Circuit', *Cell*, 179(2), pp. 355-372.e23. doi:10.1016/j.cell.2019.08.039.

Westerfield, Monte. (2007) *The zebrafish book : a guide for the laboratory use of zebrafish (Danio rerio)*.

White, R.J. *et al.* (2007) 'Complex Regulation of cyp26a1 Creates a Robust Retinoic Acid Gradient in the Zebrafish Embryo', *PLOS Biology*, 5(11), p. e304. doi:10.1371/journal.pbio.0050304.

Williams, M.L.K. and Solnica-Krezel, L. (2020) 'Cellular and molecular mechanisms of convergence and extension in zebrafish', *Current Topics in Developmental Biology*, 136, pp. 377–407. doi:10.1016/bs.ctdb.2019.08.001.

Woo, K. and Fraser, S.E. (1995) 'Order and coherence in the fate map of the zebrafish nervous system', *Development (Cambridge, England)*, 121(8), pp. 2595–2609.

Xu, L. *et al.* (2012) 'Spatiotemporal manipulation of retinoic acid activity in zebrafish hindbrain development via photo-isomerization', *Development (Cambridge, England)*, 139(18), pp. 3355–3362. doi:10.1242/dev.077776.

Xu, Q. and Wilkinson, D.G. (2013) ‘Boundary formation in the development of the vertebrate hindbrain’, *Wiley Interdisciplinary Reviews. Developmental Biology*, 2(5), pp. 735–745. doi:10.1002/wdev.106.

3.2. The role of FGF signalling in hindbrain morphogenesis

3.2.1. Introduction

The two signalling pathways RA and FGF initiate the division of the hindbrain primordium into a rostral region and a caudal region. The expression of transcription factors such as *hoxb 1b*, *hoxb 1a, vhnf1*, *valentino* and *krox20* will subdivide the caudal part of the hindbrain into r4, r5 and r6. In the zebrafish embryo, fgf3 and fgf8 are co-expressed in the blastoderm margin from 30% epiboly and later in the embryonic shield at 50% epiboly then are detected from 80% epiboly in the presumptive r4 territory before the appearance of the early markers of hindbrain segmentation, hoxb1a, hoxb1b, Vhnf1, valentino/kreisler/MafB and krox20, at the tail bud stage (10hpf). When the hindbrain segments are morphologically established, the *fgf3* transcripts remain restricted to r4, while Fgf8 quickly becomes undetectable in this rhombomere but remains expressed in the isthmus (MHB, midbrain-hindbrain border).

The FGFs (Fgf3 and Fgf8) of r4 and possibly the FGFs (Fgf8 and Fgf4) of the isthmus provide a planar signal to establish the identity of the adjacent hindbrain segments. Indeed, the loss of function experiments show that the loss of one Fgf3 (fgf3-MO) or the other Fgf8 (*ace* mutant, *fgf8-/-*) has a more subtle effect on the patterning of the hindbrain on the other hand in embryos with double mutants / morphants (fgf3-MO; fgf8- or fgf3-MO; fgf8-MO) rhombomers adjacent to r4 are lost (r5, r6) or reduced (r1-r3), while r4 and r7 are maintained (Maves, Jackman and Kimmel, 2002; Walshe *et al.*, 2002). It is well known that the identity of rhombomere segments is established through the differential expression of transcription factors, many under the control of FGFs. In particular, the FGF pathway regulates the expression of the transcription factor Sp51 which is required for the expression of *krox20* in r3, vHNF1 cooperates with Fgf3 and Fgf8 to initiate the expression of *valentine* (*val*) in r5 / r6 which in turn will activate *krox20* in r5 (Sun *et al.*, 2006; Labalette *et al.*, 2011, 2015).

In order to analyse the patterning defects of the hindbrain at the cellular level following the inhibition of the FGF pathway, we perform 3D+time live imaging of embryos treated with SU5402, a competitive inhibitor of the activation of FGFR.

3.2.2. Inhibition of FGF signalling through SU5402 treatment

We established a protocol for inhibiting the FGF pathway by treating embryos with SU5402, an inhibitor of FGF receptor activation (FGFR). Previous work has shown that the FGF signalling pathway required for the regulation of hindbrain patterning acts during a brief period of development, from the 30% epiboly stage to stage 1 somite (Walshe *et al.*, 2002). An early Fgf signal

requirement for hindbrain development was demonstrated with 1 hour inhibition of FGF with SU5402 at 4 to 5 hpf (Roy and Sagerström, 2004). Therefore, we have chosen to carry out the treatment with SU5402 (40µM) of an Tg *krox20: eGFP-Hras* from the "dome" stage (4 hpf) up to 6 hpf and we show that this treatment is sufficient to lead to the expected phenotype, an expression of *krox20* in r3 increased in size, and complete loss (n = 10/28) or strong reduction (n = 18/28) of its expression in r5 (Figure 3.1). A 50% reduction in the size of the otic vesicle with the absence of otolith is systematically observed in all "SU5402" embryos, Fgf3 and Fgf8 being required for induction of the otic placode and vesicle (Kwak *et al.*, 2002; Maroon *et al.*, 2002). Finally, the development of the caudal part of the embryo is affected by treatment with SU5402. At the end of the segmentation period, the somites appear more block-shaped in SU5402-treated embryos similar to *ace* mutant (fgf8-/-) embryos (Reifers *et al.*, 1998), compared to their distinct chevron shape in control embryos.

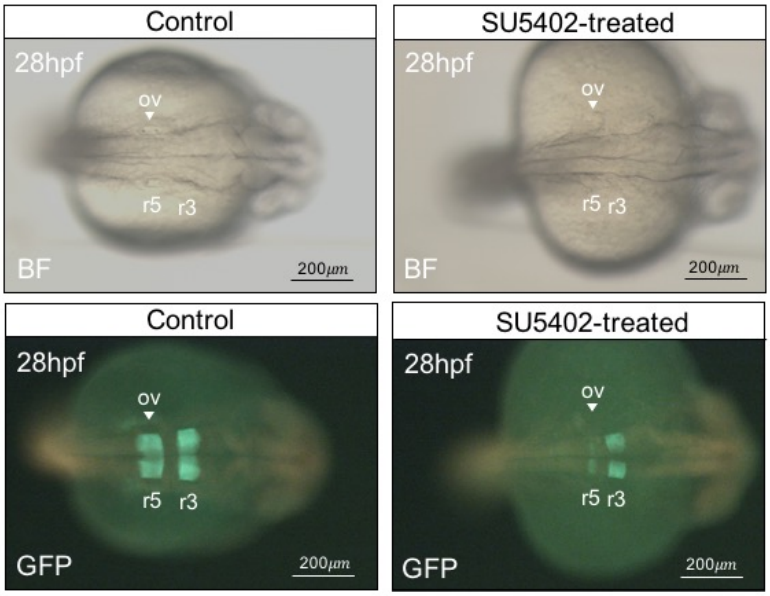

Figure 3. 1. Inhibition of the FGF signalling pathway affects hindbrain patterning.

Dorsal view of Tg *krox20: eGFP-Hras* embryos incubated either in diluted DMSO (left) or SU5402 (right) at 28 hpf development stage, taken with a stereomicroscope: bright field (top panels) and epifluorescence (panels bottom). GFP expression is observed in r3 and r5 in the control embryo while it is reduced in r3 and almost absent in r5 in the SU5402-treated embryo. The arrowhead shows the position of the otic vesicle which is greatly reduced after SU5402 treatment. ov: otic vesicle.

We have thus defined a window of 2 hours of treatment with SU5402 treatment from 4 to 6 hpf as sufficient to lead to the described hindbrain phenotype of FGF signalling inhibition, which will allow us to perform 4D imaging of developing hindbrain from 7hpf onwards. We aim to obtain fate map of hindbrain progenitors and extract measurements of cellular behaviours to elucidate the role of the FGF pathway in the establishment of rhombomeres' identity. In order to examine

the phenotype in detail, 3D stacks were made using two-photon microscopy at 24 hpf after the treatment with SU5402 at 40 µM from 4-6 hpf. As expected, r3 is reduced and r5 is restricted to a thin strip identified with krox20-driven eGFP expression, and r4 is maintained (Figure 3.2).

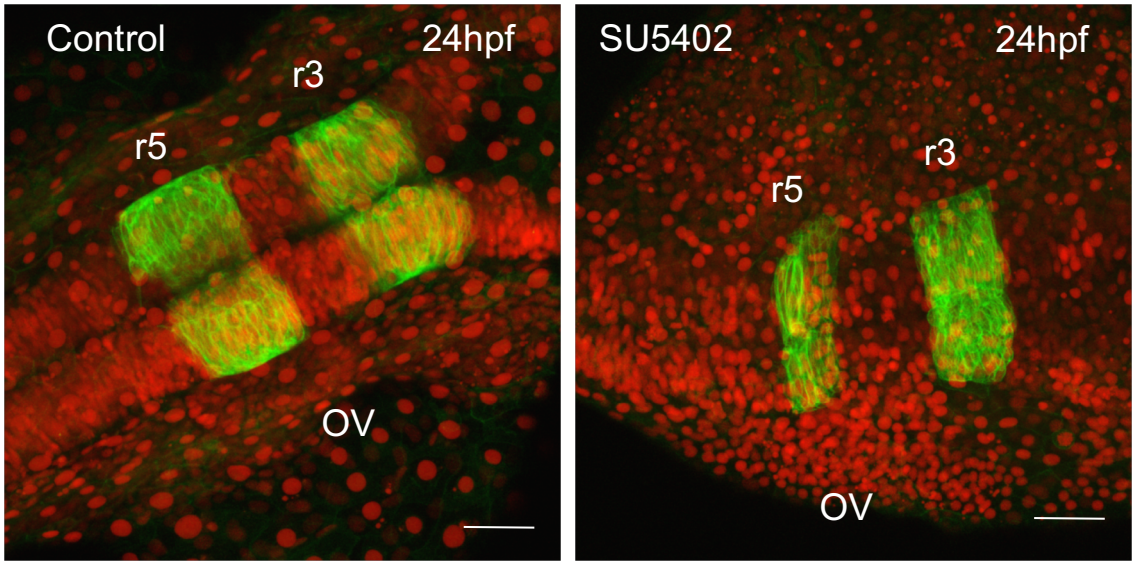

Figure 3. 2. Hindbrain patterning defects upon FGF inhibition.

Tg *krox20: eGFP-Hras* embryos were injected with *H2B-mCherry* mRNA injection. eGFP staining in r3 and r5 cell membrane and mCherry staining in nuclei of whole embryo. Dorsal view of control (left) and SU5402-treated (right) embryos at 24 hpf. r-rhombomere, OV-otic vesicle. Scale bar-50 µm.

3.2.3. 3D+time live imaging of SU5402 embryos

The mounting strategy that we established for WT and DEAB-treated embryos was not apt to capture hindbrain formation in the case of FGF inhibited embryos. FGF is known to affect the convergent-extension during gastrulation (Chung *et al.*, 2005). Under our established mounting, posterior part could not be captured in the field of view during the neural keel and rod stages. Thus, we opted for new mounting strategy of shield-stage embryo. We positioned the embryo with the shield position tilted up in a way yolk takes up 3/4th of the space from dorsal view (Figure 3.3a) In this way, we were able to keep developing rhombomeres 3 and 5 in the field of view. In this new mounting strategy, the scanning depth of the embryo was increased (Figure 3.3b).

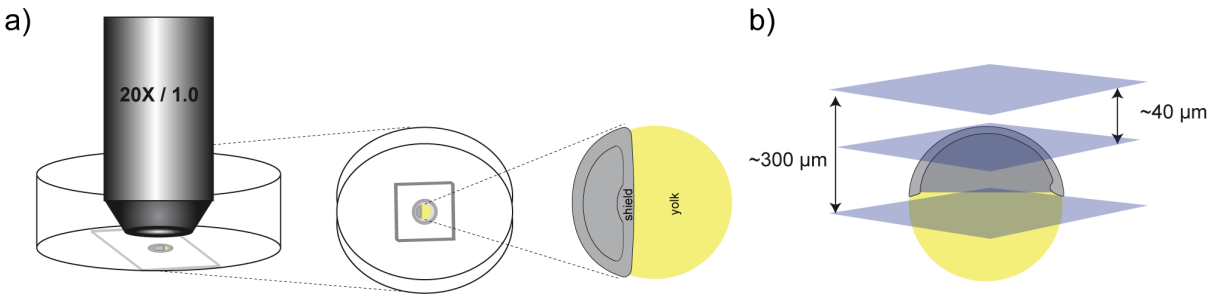

Figure 3. 3. Mounting of shield stage embryo after FGF inhibition.

a) Objective 20X/1NA immersed in embryo medium covering the embryo in the imaging chamber. Position of the shield stage embryo with animal pole on top and tilted up to 140-150 degree angle. b) Schematics of shield stage embryo under scanning.

The 3D+ live imaging movies are attached,

Movie 6: 3D raw data rendering. krox20:eGFP-Hras with SU5402 treatment injected with H2B-mCherry mRNA (ID: 200303aF).

http://bioemergences.eu/MageshiK/videos/200303aF_t_mix.mp4

Movie 7: 3D raw data rendering. krox20:eGFP-Hras with SU5402 treatment injected with H2B-mCherry mRNA (ID: 20313aF).

http://bioemergences.eu/MageshiK/videos/200313aF_t_mix%20%281%29.mp4

3.2.4. Analysis of progenitor cells behaviour

The imaging datasets were processed through BioEmergences workflow. Cells in the r3 and r5 domains were marked and back propagated thanks to automated cell tracking provided by the workflow (Figure 3.4). We observed that the automated cell tracking needs a lot of manual correction. Due to lower krox20:eGFP staining in these datasets the selection of r3 and r5 nuclei in the digital was done at later stages 13hpf40 and 15hpf50 respectively, with a neuroepithelium already much tightly packed. We applied the nuclei filtering tool to improve nuclei signal to facilitate manual correction. However, due to the time constraints, manual correction of automated cell tracking and analysis of the rhombomeres' progenitor population have been delayed.

As FGF affects the gastrulation movements, we aim to analyse the coordinate movements of mesendoderm with overlaying neuroectoderm. We shall determine the relative speed of mesendoderm versus neurectoderm during convergent extension in control (Figure 3.5)(Movie 8) and SU5402-treated embryos.

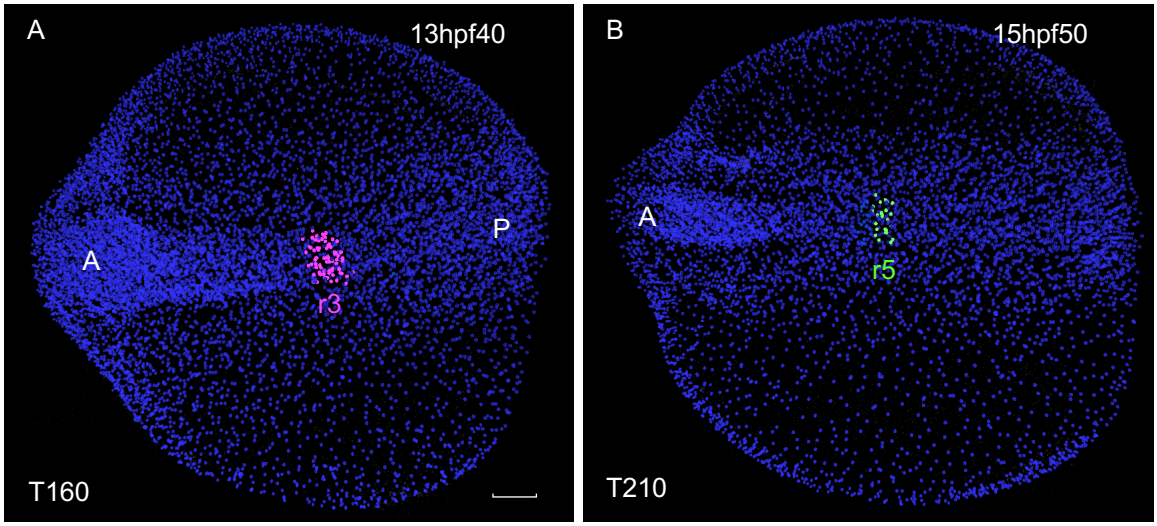

Figure 3. 4. Selection of hindbrain r3 and r5 in embryo upon FGF inhibition.

A,B) Digital embryo with all nuclei centres in blue, r3 nuclei centres in pink and r5 nuclei centres in green at two developmental stages. Time step (T) indicated bottom left. hpf- hour post fertilisation, A-Anterior, P-Posterior, Scale: 50 μm.

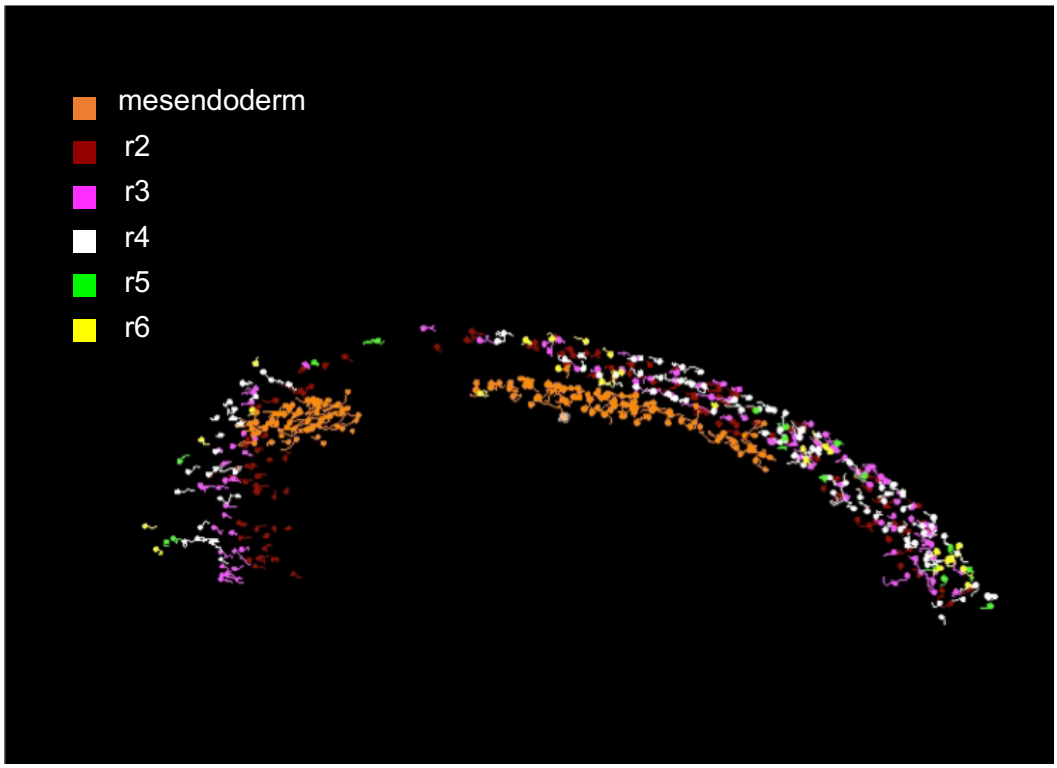

Figure 3. 5. Germ layers' convergence and extension.

Lateral view of mesendoderm (orange) and hindbrain progenitors (r2-red, r3-pink, r4- white, r5-green, r6-yellow) at 7 hpf in control digital embryo.

Movie 8: Movement of mesendoderm and neuroectoderm in WT embryo (ID:180516aF).

http://bioemergences.eu/MageshiK/videos/180516aF_mesendoderm.mp4

Lateral view from 7hpf (T24) till 11hpf20 (T134) and longitudinal view along the AP from 11hpf20 (T134) till 13hpf (T173).

Further, obtaining fate map of rhombomeres' progenitors in SU5402-treated embryo should give insights into hindbrain progenitors behaviour, migration and specification upon FGF inhibition. We shall assess whether the r5-r6 region which is reduced to a one size segment has an undefined "hox-less" identity as observed in val mutant through the examination of migration path of corresponding progenitors.

4. General discussion and perspective

There is a fundamental curiosity on how embryo architects the whole animal body during embryonic development and also how it varies in different species. On the other hand, developmental disorders are a major concern, which affects the human lifespan and lifestyle. Therefore, it is both intriguing and inevitable to study fundamental events in embryonic development under normal and pathological conditions. There are various approaches to study embryonic development. Although, the direct observation of how cells behave and correlate it to the gene function during embryonic development is critical. Segmentation is one of many phenomena used by the multicellular organisms to construct more complex structures. Dividing embryonic field via segmentation is necessary for further specification. Hindbrain, posterior part of developing brain undergoes such event and is highly conserved among vertebrates.

4.1. 3D+time live imaging of hindbrain morphogenesis

Quantifying cell behaviours that underlie morphogenesis is of central importance to our understanding of embryonic development in relation with gene function and regulation. Several animal models serve to understand embryonic development which hold immediate relevance to humans. However, the transparent nature of zebrafish embryos make it a remarkable vertebrate model for understanding cell behaviours and is highly suitable for microscopy. As a step towards that, reconstruction of entire cell lineage for first 24 hours of zebrafish development from early cleavage stages to onset of organogenesis was achieved in 2008 (Keller *et al.*, 2008). The data could be used to dissect various cell behaviours and cell lineages of many regions of the embryo based on morphology. However, the genetic labelling of area of interest is necessary for deeper and precise understanding of their morphogenesis.

In this thesis work, we studied zebrafish hindbrain morphogenesis and its segmentation. We show that the two photon microscopy can be used for long term imaging of hindbrain morphogenesis without the hindrance to embryo growth and health. Previously, zebrafish neurulation has been studied from late gastrula through neurula stages (Papan and Campos-Ortega, 1994; Hong and Brewster, 2006; Araya *et al.*, 2019). In our study, following cells from gastrulation through early neurulation gives an overview of the cell behaviour during embryonic development such as continuous trajectories. One of the limitations in previous studies is that the ventral layers of neural keel and rod stages were not imaged at good resolution. Here, using two-photon microscopy we were able to image as well as track them with automated cell tracking provided by the BioEmergences workflow, complemented by manual correction.

However, live imaging is a challenge and the success rate of obtaining exploitable datasets is very low. We generated many imaging datasets which could not be exploited due to limited spatial resolution and movement of embryo during the imaging period. With the improved machine learning based segmentation and filtering tools, we expect to exploit the datasets in the near future. On the other hand, 2-photon light sheet microscopy would be a better choice to achieve suitable spatial resolution for lineage tracing. It requires commercialisation of advanced light sheet microscopy setups and a solution to handle big data for routine usage.

With our established protocol, a few changes in mounting procedure and using other reporter transgenic lines can be done to obtain fate map of other subdivisions in the zebrafish CNS such as MHB, forebrain and spinal cord. Perturbation of other signalling and transcription factors involved in hindbrain morphogenesis and consequent alteration in cell behaviours can be studied with this approach. Key segmentation genes such as *vhnf1*, *val*, *krox20* and various *Hox* are expressed as early as 8hpf and are good candidates for studies involving 3D+time imaging. Therefore, this would shed light on their function in cell behaviour underlying hindbrain segmentation.

4.2. Dynamic fate map of r2-r6 rhombomeres

Fate map studies provide the remodelling of cell and tissue organisation during embryonic development. It has been shown in mice, chick and zebrafish that rhombomere are cell lineage units. Such analysis has been performed in zebrafish at later stages from 12 hpf and demonstrated that cells do not cross between rhombomeres once boundaries are formed (Calzolari, Terriente and Pujades, 2014). Here, we show the formation of segments from very early progenitor domains till organ morphogenesis i.e. individual rhombomeres. We have provided the zebrafish hindbrain dynamic fate map from late shield stage (7 hpf) which gives finer precision of hindbrain progenitors compared to the state of the art, utilising high-resolution microscopy techniques and automated tracking algorithm. Although the description of fate map and cell movements have been predicted in the previous study (Woo and Fraser, 1995), we show for the first time the morphogenesis of early hindbrain at cellular resolution from mid-gastrulation through early neurulation. Our data shows that segmental organisation of rhombomere are evident as early as the shield stage. We also show the elegant construction of dorsal and ventral parts of neural tube from neuroectoderm cells which is achieved in part through differential trajectories of their respective progenitors. The underlying molecular mechanism of varying degree of distinct migrational paths of dorsal and ventral progenitors from 10-13 hpf needs to be further examined. Furthermore, the speed of dorsal progenitors is increased during a transient period to facilitate 3D construction of neural tube. PCP signalling components are known to regulate the speed of lateral cells (Sepich

et al., 2000; Jessen *et al.*, 2002). Further analysis such as the expression pattern of various components of PCP would elucidate the cellular mechanism. Individual rhombomere fate map is obtained, thus further provides insights into the clonal origin of individual rhombomeres. We established that clonal commitment of individual rhombomere is achieved at around 8 hpf. The mixing of progenitor cells at the border of contiguous rhombomeres progenitors is observed before 8 hpf but at a low 20%. The directed and collective migration of neuroectoderm cells allow less mixing of the progenitors during convergence and extension. Previous work proposed that cells are committed to hindbrain identity and hindbrain progenitors acquire regional identity as a group by 8 hpf, through transplantation experiments (Woo and Fraser, 1998). However, challenges due to cell intercalation leads to little mixture of cells with different identity at borders. Cell sorting plays a major role in making sharp boundaries with homogenous segment. Cell identity switch of intermingled progenitors also contribute to the homogeneous segment.

4.3. Computational modelling of hindbrain morphogenesis

(Collaboration with Joel Dokmegang, Centre for Advanced Computational Science, Manchester Metropolitan University, Manchester, UK)

The study of multicellular development is grounded in two complementary domains: cell biomechanics, which examines how physical forces shape the embryo, and genetic regulation and molecular signalling, which concern how cells determine their states and behaviours. Integrating both sides into a unified framework is crucial to fully understand the self-organized dynamics of morphogenesis. We aim to study the mechanical drivers of rhombomere cells robust trajectories by considering their motion in the broader context of the global structural reorganization events that underlie zebrafish neurulation. During zebrafish neurulation, cells from lateral regions migrate towards the dorsal midline, creating a depression that leads to the folding of the neural plate and the formation of the neural tube. It has been established that in early stages of zebrafish development, coordinated movements of cells are similar to fluid flows (Pastor-Escuredo *et al.*, 2021). We expect that a deeper understanding of the mechanics of this global fluid-like behavior will reveal insights into the morphogenesis of rhombomeres in the early zebrafish.

By leveraging cell tracking data provided by the *BioEmergences* workflow, we are able to compute key mechanical indicators that are suitable to describe the observed cellular behaviours. Of particular interest is the characterization of the singularities (sources, sinks, vortices) emerging from collective cell migration and the understanding of how they influence this fluid-like movement. In order to identify these singularities, we plan to decompose the velocity field associated with cell movements into a divergence-free component and a curl-free component based on the

Helmholtz-Hodge decomposition, as is often the case in the study of fluid flows (Bhatia *et al.*, 2013). Analyzing these fields in isolation from one another is expected to yield an in-depth description of the cellular movements leading to rhombomere formation.

Because cell velocity fields directly derived from raw tracking data can be very noisy, we compute instead a smoothed velocity field as input for our decomposition. A smoothed velocity field as described in (Pastor-Escuredo *et al.*, 2021) has the additional advantage that it satisfies the differentiability constraints required by the Helmholtz-Hodge method. Here, for every cell, a velocity is calculated by taking the weighted average through space and time of its first and second order ring of neighbors. Preliminary data shows the time evolution of this vector field at the surface of the developing embryo (Appendix figure 3).

4.4. RA role in hindbrain morphogenesis

Retinoic acid, a Vitamin A derivative is essential for embryonic development. Both the deficiency and over dose of Vitamin A during pregnancy cause various health issues in both mother and infant. Studies on animal models have shown that RA is necessary for various organ formation. It is a potent teratogen that causes many developmental defects including neural tube closure defects (Copp and Greene, 2010). Many mice mutants of components in RA signalling pathway such as *Raldh2-/-*, *Cyp26A-/-* and RAR causes neural tube defects, exencephaly and spina bifida. At molecular level, retinoic acid acts as a morphogen which determines distinct cell fate depending on the concentration threshold. We aimed to understand the cellular events that lead to hindbrain anteriorisation phenotype observed in zebrafish embryos upon RA inhibition. We investigated the cellular events, cell proliferation and cell movements from the dynamic fate map under RA-null condition. We identified the progenitor domains whose organisation is in correspondence with the position and size of the modified segments i.e the expansion of anterior progenitors' domains. Our data shows that in a normal embryo, a small percentage of progenitors give rise to daughters cells of distinct neighbouring rhombomeres before clonal origin is set and occurring at the interface between individual rhombomeres. In the case of RA inhibition, more cells tend to acquire anterior rhombomere identity resulting in a reduced total number of individual progenitors domains (4 instead of 7) with the absence of r5, r6 and r7. We observed that the percentage of progenitors giving rise to daughters of distinct rhombomeres dropped tremendously and this could be an indirect consequence of the lower number of individual rhombomeres due to the expansion of r3 and r4.

In our study, We found that the ventral hindbrain progenitors are more sensitive to RA perturbation. In *Val* mutants, *krox20* is restricted to dorsal domains of r5 (Prince *et al.*, 1998). Val is under the direct regulatory control of RA. Such similar observation under RA inhibition indicates the mis-specification of cells with distinct molecular identity acquisition. We find that the convergence is delayed upon RA inhibition with the read out of tissue compaction. Consequently we observe neural tube dysmorphology in 20-40% embryos in the transgenic lines, which were established in *casper* and WT/Tü backgrounds. This is highly reminiscent of *vangl2* mutants in which the convergence is delayed. PCP signalling gives polarity to cells during convergence extension. Delayed convergence leads to wider neural plate. C-division which is intrinsic time dependent activity occurs in lateral region of neural plate and leads to dual apical midline formation and consequently duplicated neural tube. We further looked for the cross talk between RA and PCP pathways. It is shown in *Raldh2-/-* mouse embryos, vangl2 and fzd3 which are necessary for PCP signalling are strongly downregulated in the hindbrain and spinal cord at E8.25-E8.75 (Tuduce *et al.*, 2009). This possible link explains the observed phenotype in embryos upon RA inhibition in zebrafish. The expression pattern of Vangl2 and Fzd3 should be investigated in DEAB-treated embryos through either in-situ hybridisation or in transgenic reporter lines specific for these genes or to study their distribution by injecting *GFP-VANGL2* mRNA (Love, Prince and Jessen, 2018). Our data suggests that there is a conserved mechanism of RA and PCP crosstalk that regulate CE movements during mice and zebrafish gastrulation. This would also show how two signalling molecules interact during cell fate and cell movement.

We demonstrated the community effect of RA through optogenetic tools. The long range effect of RA on target gene activation is strengthened with our observation of complete rescue of r5 rhombomere domain following the restoration of RA signalling in progenitors on one side of zebrafish embryo. Further, we planned to follow the cells with restored RA and the surrounding cells how they make the rescued r5 domain. The optogenetic RA restoration at the almost single cell level can be harnessed to understand the role of RA in other organogenesis as RA plays vast roles during embryogenesis and beyond. UV illumination with one-photon (405nm) gives spatio-temporal control. However, due to poor axial resolution, cells located along the axial length will also be illuminated. In order to have more precise spatial control, we plan to perform two-photon illumination. The two-photon UV illumination was demonstrated in the previous study of the D. Bensimon's laboratory that developed these optogenetic tools (Zhang *et al.*, 2018; Hamouri *et al.*, 2019).

4.4. FGF role in hindbrain patterning

FGF plays regulatory roles at two different times during hindbrain patterning. The later role has been well established in several studies (Maves, Jackman and Kimmel, 2002; Walshe *et al.*, 2002). At early stage, FGF is necessary and should be activated before 5 hpf for expression for many hindbrain patterning genes (Roy and Sagerström, 2004). We show that the FGF inhibition from 4 to 6 hpf is sufficient to perturb hindbrain patterning. We observe the reduction of r3 and r5 in those embryos. FGF is known to regulate convergent extension movements of mesoderm. Thus, FGF inhibition of zebrafish embryo at 4-6 hpf affects the extension of AP body plan. This perturbed our imaging strategy but we were able to opt for new mounting position of shield stage embryo in order to capture hindbrain development. Imaging datasets obtained upon FGF inhibition would be exploited to understand the role of FGF in gastrulation movements by analysing the coordinated movement of mesendoderm and ectoderm, analysing various parameters such as speed, directional movements and others. The imaging data collected upon FGF perturbation can be explored in detail to understand the FGF role in hindbrain formation at cellular level by obtaining the fate map of individual rhombomeres.

FGF is known to be a short range morphogen. To assess the community or autonomous effect of FGF signalling on targets genes, we plan to use the activation of a *UAS:fgf8-T2A-CFP* transgene under the control of *Gal4-ERT2* driven by ubiquitin regulatory sequences and the UV-mediated uncaging of cyclofen-OH (a photostable analog of the original estrogen receptor ligand, tamoxifen) in FGF morphants (Appendix Figure 2). FGF inhibition is achieved through injection of morpholino fgf3 and fgf8 injection at one-cell stage. We will assess the phenotypic consequences of FGF8 signalling restoration in rhombomere progenitors. The FGF8 activation strategy is transient and will be less temporally precise than RA activation because of the delay in protein expression. Further, we speculate that the rescue of posterior rhombomere domains will be limited as FGF is known to act at a short range.

4.5. Perspective

Single-cell sequencing and *in toto* imaging are forefront technologies to understand descriptive embryogenesis (Wallingford, 2019). Single-cell sequencing has now become routinely used at various stages of development and huge data are generated (Farrell *et al.*, 2018; Wagner *et al.*, 2018). The laboratory of D. Wilkinson has established the single-cell transcriptome atlas of the developing zebrafish which reveal new candidate regulators of cell differentiation in the hindbrain and provide a valuable resource for future functional investigations (Tambalo, Mitter and

Wilkinson, 2020). The clearly defined regions of hindbrain rhombomeres in normal and pathological condition (obtained in our study) will be instrumental to perform segment-specific RNA sequencing at very early stages before the morphological appearance of segments. As John Wallingford quotes “The precise and dynamic registration of gene expression changes with the constant changes in each cell's position in the embryo will unleash the true power of single-cell transcriptomics of a developing organism” (Wallingford, 2019). Thus, our approach with technical advancements will help integrate the various domains such as cell behaviour, gene regulation and mechanical forces for the complete understanding of hindbrain morphogenesis (embryogenesis).

5. Appendix

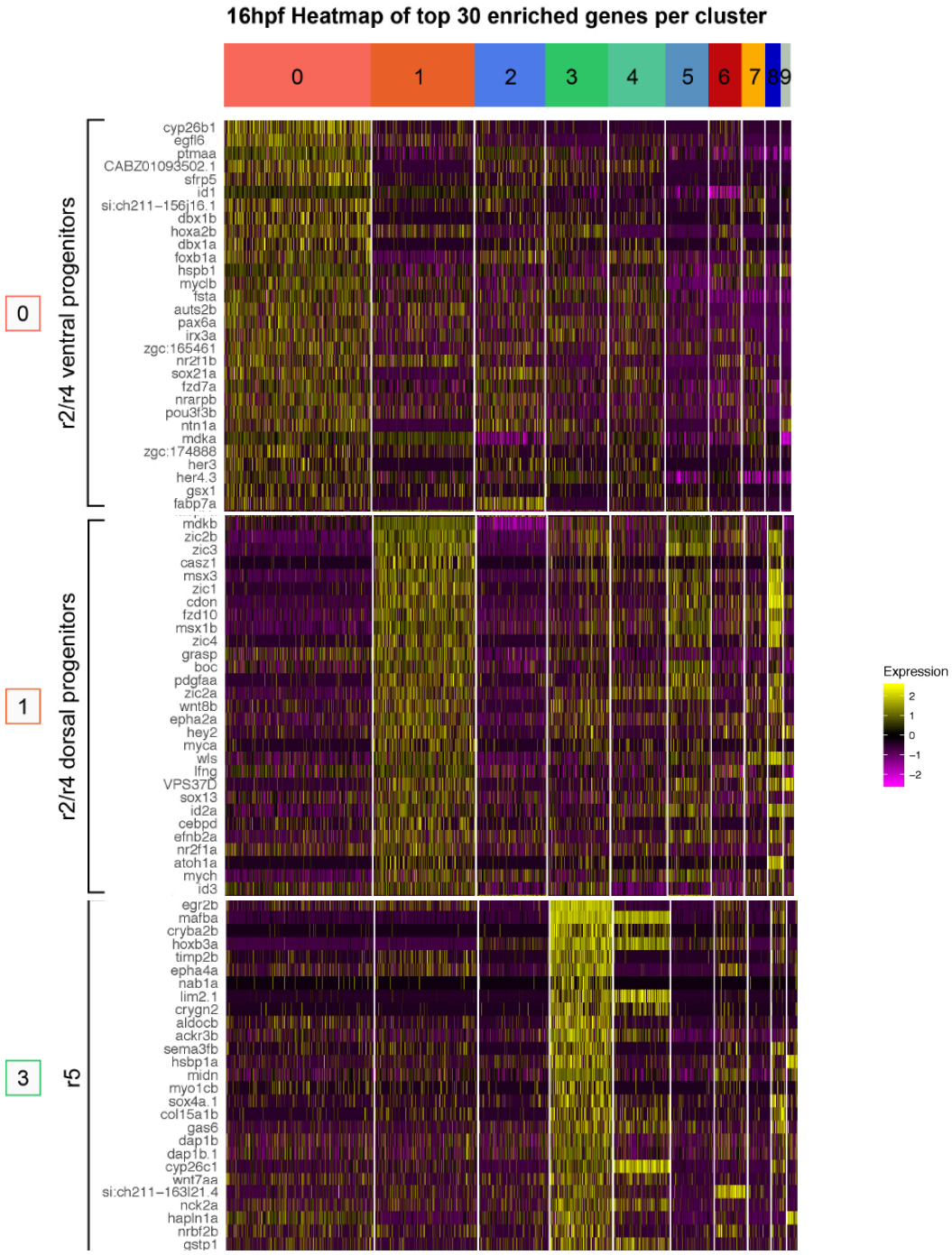

Figure 1: Heatmap of the top 30 significant markers per cluster at 16 hpf.

Full heatmap of the top 30 significant markers per cluster (with 9 clusters in total). Figure from (Tambalo, Mitter and Wilkinson, 2020).

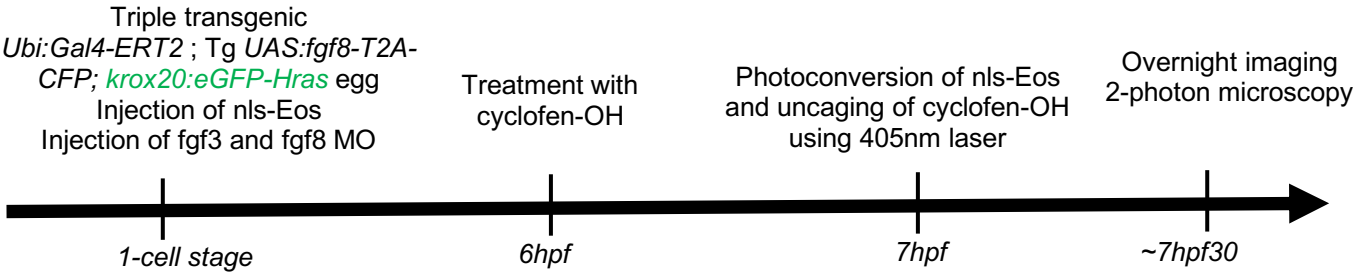

Figure 2: : Experimental plan to assess community effect of FGF activity during hindbrain patterning.

Triple transgenic embryos were made by crossing double transgenic animals Ubi:Gal4-ERT2 ; Tg UAS:fgf8-T2A-CFP with Tg *krox20: eGFP-Hras* fishes. Injection of fgf3 and fgf8 morpholinos at one-cell stage embryo will inhibit the FGF signalling. At 6 hpf, embryos will be treated with caged-Cyclofen-OH. R5 progenitors will be targeted and scanned with UV laser with one-photon microscope. Following that, embryos will be imaged overnight to follow the rescued cells.

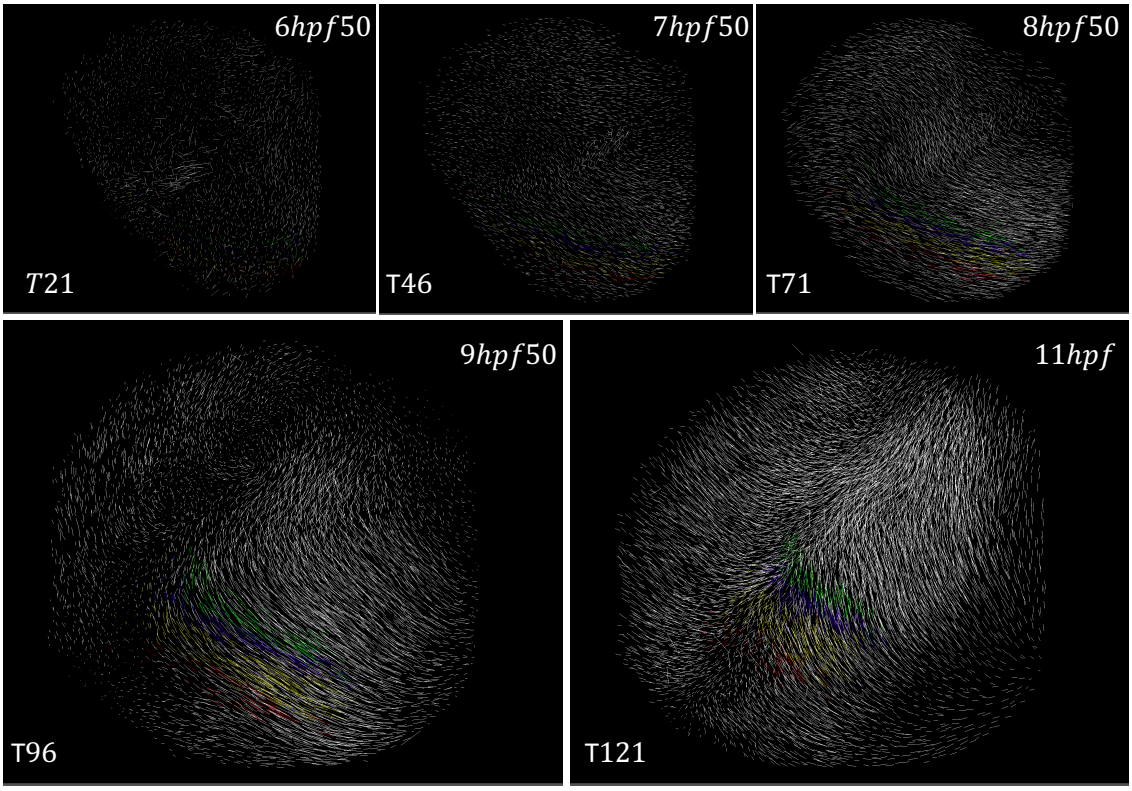

Figure 3: Velocity field vector during hindbrain segmentation.

Plots of the evolution through time of the smoothed vector field at the surface of the embryo. The oblique bars represent the velocity vectors (direction and magnitude) associated with each cell and are drawn at the position of the cell. The colours red, yellow, blue and green represent different rhombomere population. Here, the collective movement of cells, and of rhombomeres in particular, towards the dorsal midline to form the neural tube is shown. hpf-hour post fertilisation, T-time step.

Bibliography

Addison, M. *et al.* (2018) 'Cell Identity Switching Regulated by Retinoic Acid Signaling Maintains Homogeneous Segments in the Hindbrain', *Developmental Cell*, 45(5), pp. 606-620.e3. doi:10.1016/j.devcel.2018.04.003.

Alexander, T., Nolte, C. and Krumlauf, R. (2009) 'Hox genes and segmentation of the hindbrain and axial skeleton', *Annual Review of Cell and Developmental Biology*, 25, pp. 431–456. doi:10.1146/annurev.cellbio.042308.113423.

Amat, F. *et al.* (2014) 'Fast, accurate reconstruction of cell lineages from large-scale fluorescence microscopy data', *Nature Methods*, 11(9), pp. 951–958. doi:10.1038/nmeth.3036.

Amin, S. *et al.* (2015) 'Hoxa2 Selectively Enhances Meis Binding to Change a Branchial Arch Ground State', *Developmental Cell*, 32(3), pp. 265–277. doi:10.1016/j.devcel.2014.12.024.

Amores, A. *et al.* (1998) 'Zebrafish hox clusters and vertebrate genome evolution', *Science (New York, N.Y.)*, 282(5394), pp. 1711–1714. doi:10.1126/science.282.5394.1711.

Amoyel, M. *et al.* (2005) 'Wnt1 regulates neurogenesis and mediates lateral inhibition of boundary cell specification in the zebrafish hindbrain', *Development (Cambridge, England)*, 132(4), pp. 775–785. doi:10.1242/dev.01616.

Araya, C. *et al.* (2014) 'Mesoderm is required for coordinated cell movements within zebrafish neural plate in vivo', *Neural Development*, 9(1), p. 9. doi:10.1186/1749-8104-9-9.

Araya, C. *et al.* (2016) 'Coordinating cell and tissue behavior during zebrafish neural tube morphogenesis', *Developmental Dynamics: An Official Publication of the American Association of Anatomists*, 245(3), pp. 197–208. doi:10.1002/dvdy.24304.

Araya, C. *et al.* (2019) 'Cdh2 coordinates Myosin-II dependent internalisation of the zebrafish neural plate', *Scientific Reports*, 9(1), p. 1835. doi:10.1038/s41598-018-38455-w.

Araya, C., Carmona-Fontaine, C. and Clarke, J.D.W. (2016) 'Extracellular matrix couples the convergence movements of mesoderm and neural plate during the early stages of neurulation', *Developmental Dynamics*, 245(5), pp. 580–589. doi:10.1002/dvdy.24401.

Bao, Z. *et al.* (2006) 'Automated cell lineage tracing in Caenorhabditis elegans', *Proceedings of the National Academy of Sciences of the United States of America*, 103(8), pp. 2707–2712. doi:10.1073/pnas.0511111103.

Basu, S. and Sachidanandan, C. (2013) 'Zebrafish: a multifaceted tool for chemical biologists', *Chemical Reviews*, 113(10), pp. 7952–7980. doi:10.1021/cr4000013.

Bedois, A.M.H., Parker, H.J. and Krumlauf, R. (2021) 'Retinoic Acid Signaling in Vertebrate Hindbrain Segmentation: Evolution and Diversification', *Diversity*, 13(8), p. 398. doi:10.3390/d13080398.

Begemann, G. *et al.* (2001) 'The zebrafish neckless mutation reveals a requirement for raldh2 in mesodermal signals that pattern the hindbrain', *Development (Cambridge, England)*, 128(16), pp. 3081–3094.

Begemann, G. *et al.* (2004) 'Beyond the neckless phenotype: influence of reduced retinoic acid signaling on motor neuron development in the zebrafish hindbrain', *Developmental Biology*, 271(1), pp. 119–129. doi:10.1016/j.ydbio.2004.03.033.

Behrndt, M. *et al.* (2012) 'Forces driving epithelial spreading in zebrafish gastrulation', *Science (New York, N.Y.)*, 338(6104), pp. 257–260. doi:10.1126/science.1224143.

Benninger, R.K.P. and Piston, D.W. (2013) 'Two-photon excitation microscopy for the study of living cells and tissues', *Current Protocols in Cell Biology*, Chapter 4, p. Unit 4.11.1-24. doi:10.1002/0471143030.cb0411s59.

Bhatia, H. *et al.* (2013) 'The Helmholtz-Hodge Decomposition—A Survey', *IEEE Transactions on Visualization and Computer Graphics*, 19(8), pp. 1386–1404. doi:10.1109/TVCG.2012.316.

Biswas, S., Emond, M.R. and Jontes, J.D. (2010) 'Protocadherin-19 and N-cadherin interact to control cell movements during anterior neurulation', *The Journal of Cell Biology*, 191(5), pp. 1029–1041. doi:10.1083/jcb.201007008.

Bruce, A.E.E. and Heisenberg, C.-P. (2020) 'Mechanisms of zebrafish epiboly: A current view', *Current Topics in Developmental Biology*, 136, pp. 319–341. doi:10.1016/bs.ctdb.2019.07.001.

Buckingham, M.E. and Meilhac, S.M. (2011) 'Tracing Cells for Tracking Cell Lineage and Clonal Behavior', *Developmental Cell*, 21(3), pp. 394–409. doi:10.1016/j.devcel.2011.07.019.

Buckley, C.E. *et al.* (2013) 'Mirror-symmetric microtubule assembly and cell interactions drive lumen formation in the zebrafish neural rod', *The EMBO journal*, 32(1), pp. 30–44. doi:10.1038/emboj.2012.305.

Calzolari, S., Terriente, J. and Pujades, C. (2014) 'Cell segregation in the vertebrate hindbrain relies on actomyosin cables located at the interhombomeric boundaries', *The EMBO journal*, 33(7), pp. 686–701. doi:10.1002/embj.201386003.

Cambronero, F. *et al.* (2020) 'Inter-rhombomeric interactions reveal roles for fibroblast growth factors signaling in segmental regulation of EphA4 expression', *Developmental Dynamics: An Official Publication of the American Association of Anatomists*, 249(3), pp. 354–368. doi:10.1002/dvdy.101.

Cayuso, J. *et al.* (2019) 'Actomyosin regulation by Eph receptor signaling couples boundary cell formation to border sharpness', *eLife*. Edited by M.E. Bronner, F.M. Rijli, and R. Krumlauf, 8, p. e49696. doi:10.7554/eLife.49696.

Chandrasekhar, A. (2004) 'Turning heads: development of vertebrate branchiomotor neurons', *Developmental Dynamics: An Official Publication of the American Association of Anatomists*, 229(1), pp. 143–161. doi:10.1002/dvdy.10444.

Chomette, D. *et al.* (2006) 'Krox20 hindbrain cis-regulatory landscape: interplay between multiple long-range initiation and autoregulatory elements', *Development (Cambridge, England)*, 133(7), pp. 1253–1262. doi:10.1242/dev.02289.

Chung, H.A. *et al.* (2005) 'FGF signal regulates gastrulation cell movements and morphology through its target NRH', *Developmental Biology*, 282(1), pp. 95–110. doi:10.1016/j.ydbio.2005.02.030.

Ciruna, B. *et al.* (2006) 'Planar cell polarity signalling couples cell division and morphogenesis during neurulation', *Nature*, 439(7073), pp. 220–224. doi:10.1038/nature04375.

Clarke, J. (2009) 'Role of polarized cell divisions in zebrafish neural tube formation', *Current Opinion in Neurobiology*, 19(2–3), pp. 134–138. doi:10.1016/j.conb.2009.04.010.

Clarke, J.D.W. and Tickle, C. (1999) 'Fate maps old and new', *Nature Cell Biology*, 1(4), pp. E103–E109. doi:10.1038/12105.

Concha, M.L. and Adams, R.J. (1998) 'Oriented cell divisions and cellular morphogenesis in the zebrafish gastrula and neurula: a time-lapse analysis', *Development (Cambridge, England)*, 125(6), pp. 983–994.

Cooke, J. *et al.* (2001) 'Eph signalling functions downstream of Val to regulate cell sorting and boundary formation in the caudal hindbrain', *Development*, 128(4), pp. 571–580. doi:10.1242/dev.128.4.571.

Cooke, J.E., Kemp, H.A. and Moens, C.B. (2005) 'EphA4 is required for cell adhesion and rhombomere-boundary formation in the zebrafish', *Current biology: CB*, 15(6), pp. 536–542. doi:10.1016/j.cub.2005.02.019.

Copp, A.J. and Greene, N.D.E. (2010) 'Genetics and development of neural tube defects', *The Journal of pathology*, 220(2), pp. 217–230. doi:10.1002/path.2643.

Corda, G. and Sala, A. (2017) 'Non-canonical WNT/PCP signalling in cancer: Fzd6 takes centre stage', *Oncogenesis*, 6(7), pp. e364–e364. doi:10.1038/oncsis.2017.69.

Couly, G. *et al.* (1998) 'Determination of the identity of the derivatives of the cephalic neural crest: incompatibility between Hox gene expression and lower jaw development', *Development (Cambridge, England)*, 125(17), pp. 3445–3459.

Cunningham, T.J. and Duester, G. (2015) 'Mechanisms of retinoic acid signalling and its roles in organ and limb development', *Nature reviews. Molecular cell biology*, 16(2), pp. 110–123. doi:10.1038/nrm3932.

Dimitri, Fabrèges. *et al.* (2018) 'Control of the proportion of inner cells by asymmetric divisions and the ensuing resilience of cloned rabbit embryos', *Development (Cambridge, England)*, 145(8). doi:10.1242/dev.152041.

Davey, C.F. and Moens, C.B. (2017) 'Planar cell polarity in moving cells: think globally, act locally', *Development*, 144(2), pp. 187–200. doi:10.1242/dev.122804.

Dobbs-McAuliffe, B., Zhao, Q. and Linney, E. (2004) 'Feedback mechanisms regulate retinoic acid production and degradation in the zebrafish embryo', *Mechanisms of Development*, 121(4), pp. 339–350. doi:10.1016/j.mod.2004.02.008.

Doniach, T. (1995) 'Basic FGF as an inducer of anteroposterior neural pattern', *Cell*, 83(7), pp. 1067–1070. doi:10.1016/0092-8674(95)90133-7.

Dorey, K. and Amaya, E. (2010) 'FGF signalling: diverse roles during early vertebrate embryogenesis', *Development (Cambridge, England)*, 137(22), pp. 3731–3742. doi:10.1242/dev.037689.

Driever, W. *et al.* (1994) 'Zebrafish: genetic tools for studying vertebrate development', *Trends in Genetics*, 10(5), pp. 152–159. doi:10.1016/0168-9525(94)90091-4.

Duester, G. (2008) 'Retinoic Acid Synthesis and Signaling during Early Organogenesis', *Cell*, 134(6), pp. 921–931. doi:10.1016/j.cell.2008.09.002.

Dyballa, S. *et al.* (2017) 'Distribution of neurosensory progenitor pools during inner ear morphogenesis unveiled by cell lineage reconstruction', *eLife*. Edited by T.T. Whitfield, 6, p. e22268. doi:10.7554/eLife.22268.

England, S.J. *et al.* (2006) 'A dynamic fate map of the forebrain shows how vertebrate eyes form and explains two causes of cyclopia', *Development (Cambridge, England)*, 133(23), pp. 4613–4617. doi:10.1242/dev.02678.

England, S.J. and Adams, R.J. (2007) 'Building a dynamic fate map', *BioTechniques*, 43(1 Suppl), pp. 20–24. doi:10.2144/000112510.

Eswarakumar, V.P., Lax, I. and Schlessinger, J. (2005) 'Cellular signaling by fibroblast growth factor receptors', *Cytokine & Growth Factor Reviews*, 16(2), pp. 139–149. doi:10.1016/j.cytogfr.2005.01.001.

Farrell, J.A. *et al.* (2018) 'Single-cell reconstruction of developmental trajectories during zebrafish embryogenesis', *Science (New York, N.Y.)*, 360(6392), p. eaar3131. doi:10.1126/science.aar3131.

Faure, E. *et al.* (2016) 'A workflow to process 3D+time microscopy images of developing organisms and reconstruct their cell lineage', *Nature Communications*, 7(1), p. 8674. doi:10.1038/ncomms9674.

Frank, D. and Sela-Donenfeld, D. (2019) 'Hindbrain induction and patterning during early vertebrate development', *Cellular and Molecular Life Sciences*, 76(5), pp. 941–960. doi:10.1007/s00018-018-2974-x.

Fraser, S., Keynes, R. and Lumsden, A. (1990) 'Segmentation in the chick embryo hindbrain is defined by cell lineage restrictions', *Nature*, 344(6265), pp. 431–435. doi:10.1038/344431a0.

Garcia-Bellido, A., Ripoll, P. and Morata, G. (1973) 'Developmental Compartmentalisation of the Wing Disk of Drosophila', *Nature New Biology*, 245(147), pp. 251–253. doi:10.1038/newbio245251a0.

Gavalas, A. (2002) 'ArRAnging the hindbrain', *Trends in Neurosciences*, 25(2), pp. 61–64. doi:10.1016/S0166-2236(02)02067-2.

Gebo, D.L. (1988) 'Vertebrate paleontology and evolution. By Robert L. Carroll, New York: W.H. Freeman and Company. 1988. xiv + 698 pp., figures, appendix, index. $52.95 (cloth)', *American Journal of Physical Anthropology*, 77(1), pp. 135–135. doi:10.1002/ajpa.1330770119.

Geldmacher-Voss, B. *et al.* (2003) 'A 90-degree rotation of the mitotic spindle changes the orientation of mitoses of zebrafish neuroepithelial cells', *Development (Cambridge, England)*, 130(16), pp. 3767–3780. doi:10.1242/dev.00603.

Gilland, E. and Baker, R. (1993) 'Conservation of neuroepithelial and mesodermal segments in the embryonic vertebrate head', *Acta Anatomica*, 148(2–3), pp. 110–123. doi:10.1159/000147530.

Girdler, G.C. *et al.* (2013) 'Developmental time rather than local environment regulates the schedule of epithelial polarization in the zebrafish neural rod', *Neural Development*, 8(1), p. 5. doi:10.1186/1749-8104-8-5.

Golding, J.P. *et al.* (2000) 'Defects in pathfinding by cranial neural crest cells in mice lacking the neuregulin receptor ErbB4', *Nature Cell Biology*, 2(2), pp. 103–109. doi:10.1038/35000058.

Golding, J.P., Dixon, M. and Gassmann, M. (2002) 'Cues from neuroepithelium and surface ectoderm maintain neural crest-free regions within cranial mesenchyme of the developing chick', *Development (Cambridge, England)*, 129(5), pp. 1095–1105.

Gould, A., Itasaki, N. and Krumlauf, R. (1998) 'Initiation of rhombomeric Hoxb4 expression requires induction by somites and a retinoid pathway', *Neuron*, 21(1), pp. 39–51. doi:10.1016/s0896-6273(00)80513-9.

Graham, A. *et al.* (2014) 'What can vertebrates tell us about segmentation?', *EvoDevo*, 5(1), p. 24. doi:10.1186/2041-9139-5-24.

Guignard, L. *et al.* (2020) 'Contact area-dependent cell communication and the morphological invariance of ascidian embryogenesis', *Science (New York, N.Y.)*, 369(6500), p. eaar5663. doi:10.1126/science.aar5663.

Gutzman, J.H. and Sive, H. (2010) 'Epithelial relaxation mediated by the myosin phosphatase regulator Mypt1 is required for brain ventricle lumen expansion and hindbrain morphogenesis', *Development*, 137(5), pp. 795–804. doi:10.1242/dev.042705.

Hall, B.K. (2000) 'The neural crest as a fourth germ layer and vertebrates as quadroblastic not triploblastic', *Evolution & Development*, 2(1), pp. 3–5. doi:10.1046/j.1525-142x.2000.00032.x.

Halloran, M.C. *et al.* (2000) 'Laser-induced gene expression in specific cells of transgenic zebrafish', *Development (Cambridge, England)*, 127(9), pp. 1953–1960.

Hamouri, F. *et al.* (2019) 'Optical control of protein activity and gene expression by photoactivation of caged cyclofen', *Methods in Enzymology*, 624, pp. 1–23. doi:10.1016/bs.mie.2019.04.009.

von der Hardt, S. *et al.* (2007) 'The Bmp Gradient of the Zebrafish Gastrula Guides Migrating Lateral Cells by Regulating Cell-Cell Adhesion', *Current Biology*, 17(6), pp. 475–487. doi:10.1016/j.cub.2007.02.013.

Hatta, K., Tsujii, H. and Omura, T. (2006) 'Cell tracking using a photoconvertible fluorescent protein', *Nature Protocols*, 1(2), pp. 960–967. doi:10.1038/nprot.2006.96.

Heisenberg, C.P. *et al.* (2000) 'Silberblick/Wnt11 mediates convergent extension movements during zebrafish gastrulation', *Nature*, 405(6782), pp. 76–81. doi:10.1038/35011068.

Hernandez, R.E. *et al.* (2004) 'vhnf1 integrates global RA patterning and local FGF signals to direct posterior hindbrain development in zebrafish', *Development*, 131(18), pp. 4511–4520. doi:10.1242/dev.01297.

Hernandez, R.E. *et al.* (2007) 'Cyp26 Enzymes Generate the Retinoic Acid Response Pattern Necessary for Hindbrain Development', *Development (Cambridge, England)*, 134(1), pp. 177–187. doi:10.1242/dev.02706.

Heyman, I., Kent, A. and Lumsden, A. (1993) 'Cellular morphology and extracellular space at rhombomere boundaries in the chick embryo hindbrain', *Developmental Dynamics: An Official Publication of the American Association of Anatomists*, 198(4), pp. 241–253. doi:10.1002/aja.1001980402.

Higashijima, S., Hotta, Y. and Okamoto, H. (2000) 'Visualization of cranial motor neurons in live transgenic zebrafish expressing green fluorescent protein under the control of the islet-1 promoter/enhancer', *The Journal of Neuroscience: The Official Journal of the Society for Neuroscience*, 20(1), pp. 206–218.

Holtzman, N.G. *et al.* (2016) 'Learning to Fish with Genetics: A Primer on the Vertebrate Model Danio rerio', *Genetics*, 203(3), pp. 1069–1089. doi:10.1534/genetics.116.190843.

Hong, E. and Brewster, R. (2006) 'N-cadherin is required for the polarized cell behaviors that drive neurulation in the zebrafish', *Development*, 133(19), pp. 3895–3905. doi:10.1242/dev.02560.

Houle, M. *et al.* (2000) 'Retinoic Acid Regulation of Cdx1: an Indirect Mechanism for Retinoids and Vertebral Specification', *Molecular and Cellular Biology*, 20(17), pp. 6579–6586.

Howe, K. *et al.* (2013) 'The zebrafish reference genome sequence and its relationship to the human genome', *Nature*, 496(7446), pp. 498–503. doi:10.1038/nature12111.

Hunt, P. and Krumlauf, R. (1991) 'Deciphering the Hox code: clues to patterning branchial regions of the head', *Cell*, 66(6), pp. 1075–1078. doi:10.1016/0092-8674(91)90029-x.

Irizarry, J. and Stathopoulos, A. (2021) 'Dynamic patterning by morphogens illuminated by cis-regulatory studies', *Development (Cambridge, England)*, 148(2), p. dev196113. doi:10.1242/dev.196113.

Jessen, J.R. *et al.* (2002) 'Zebrafish trilobite identifies new roles for Strabismus in gastrulation and neuronal movements', *Nature Cell Biology*, 4(8), pp. 610–615. doi:10.1038/ncb828.

Jimenez-Guri, E. *et al.* (2010) 'Clonal Analysis in Mice Underlines the Importance of Rhombomeric Boundaries in Cell Movement Restriction during Hindbrain Segmentation', *PLOS ONE*, 5(4), p. e10112. doi:10.1371/journal.pone.0010112.

Joshi, J., Rubart, M. and Zhu, W. (2020) 'Optogenetics: Background, Methodological Advances and Potential Applications for Cardiovascular Research and Medicine', *Frontiers in Bioengineering and Biotechnology*, 7, p. 466. doi:10.3389/fbioe.2019.00466.

Karlstrom, R.O. and Kane, D.A. (1996) 'A flipbook of zebrafish embryogenesis', *Development (Cambridge, England)*, 123, p. 461.

Kayam, G. *et al.* (2013) 'A novel role for Pax6 in the segmental organization of the hindbrain', *Development*, 140(10), pp. 2190–2202. doi:10.1242/dev.089136.

Keller, P.J. *et al.* (2008) 'Reconstruction of Zebrafish Early Embryonic Development by Scanned Light Sheet Microscopy', *Science*, 322(5904), pp. 1065–1069. doi:10.1126/science.1162493.

Keller, P.J. (2013) 'Imaging Morphogenesis: Technological Advances and Biological Insights', *Science*, 340(6137), p. 1234168. doi:10.1126/science.1234168.

Keller, R.E. (1975) 'Vital dye mapping of the gastrula and neurula of Xenopus laevis. I. Prospective areas and morphogenetic movements of the superficial layer', *Developmental Biology*, 42(2), pp. 222–241. doi:10.1016/0012-1606(75)90331-0.

Kerszberg, M. and Wolpert, L. (1998) 'Mechanisms for Positional Signalling by Morphogen Transport: a Theoretical Study', *Journal of Theoretical Biology*, 191(1), pp. 103–114. doi:10.1006/jtbi.1997.0575.

Kiecker, C. and Lumsden, A. (2005) 'Compartments and their boundaries in vertebrate brain development', *Nature Reviews Neuroscience*, 6(7), pp. 553–564. doi:10.1038/nrn1702.

Kilian, B. *et al.* (2003) 'The role of Ppt/Wnt5 in regulating cell shape and movement during zebrafish gastrulation', *Mechanisms of Development*, 120(4), pp. 467–476. doi:10.1016/S0925-4773(03)00004-2.

Kimelman, D. and Martin, B.L. (2012) 'Anterior–posterior patterning in early development: three strategies', *WIREs Developmental Biology*, 1(2), pp. 253–266. doi:10.1002/wdev.25.

Kimmel, C.B. *et al.* (1995) 'Stages of embryonic development of the zebrafish', *Developmental Dynamics: An Official Publication of the American Association of Anatomists*, 203(3), pp. 253–310. doi:10.1002/aja.1002030302.

Kimmel, C.B., Sepich, D.S. and Trevarrow, B. (1988) 'Development of segmentation in zebrafish', *Development (Cambridge, England)*, 104 Suppl, pp. 197–207.

Kimmel, C.B., Warga, R.M. and Kane, D.A. (1994) 'Cell cycles and clonal strings during formation of the zebrafish central nervous system', *Development (Cambridge, England)*, 120(2), pp. 265–276.

Kimmel, C.B., Warga, R.M. and Schilling, T.F. (1990) 'Origin and organization of the zebrafish fate map', *Development*, 108(4), pp. 581–594. doi:10.1242/dev.108.4.581.

Knecht, A.K. and Bronner-Fraser, M. (2002) 'Induction of the neural crest: a multigene process', *Nature Reviews. Genetics*, 3(6), pp. 453–461. doi:10.1038/nrg819.

Köster, R.W. and Fraser, S.E. (2004) 'Time-lapse microscopy of brain development', *Methods in Cell Biology*, 76, pp. 207–235. doi:10.1016/s0091-679x(04)76011-2.

Kozlowski, D.J. *et al.* (1997) 'Regional cell movement and tissue patterning in the zebrafish embryo revealed by fate mapping with caged fluorescein', *Biochemistry and Cell Biology = Biochimie Et Biologie Cellulaire*, 75(5), pp. 551–562.

Krumlauf, R. and Wilkinson, D.G. (2021) 'Segmentation and patterning of the vertebrate hindbrain', *Development*, 148(15). doi:10.1242/dev.186460.

Krzic, U. *et al.* (2012) 'Multiview light-sheet microscope for rapid in toto imaging', *Nature Methods*, 9(7), pp. 730–733. doi:10.1038/nmeth.2064.

Kudoh, T., Wilson, S.W. and Dawid, I.B. (2002) 'Distinct roles for Fgf, Wnt and retinoic acid in posteriorizing the neural ectoderm', *Development (Cambridge, England)*, 129(18), pp. 4335–4346.

Kwak, S.-J. *et al.* (2002) 'An expanded domain of fgf3 expression in the hindbrain of zebrafish valentino mutants results in mis-patterning of the otic vesicle', *Development*, 129(22), pp. 5279–5287. doi:10.1242/dev.129.22.5279.

Labalette, C. *et al.* (2011) 'Hindbrain patterning requires fine-tuning of early krox20 transcription by Sprouty 4', *Development*, 138(2), pp. 317–326. doi:10.1242/dev.057299.

Labalette, C. *et al.* (2015) 'Molecular dissection of segment formation in the developing hindbrain', *Development (Cambridge, England)*, 142(1), pp. 185–195. doi:10.1242/dev.109652.

Lawrence, P.A. (1973) 'Maintenance of Boundaries between Developing Organs in Insects', *Nature New Biology*, 242(114), pp. 31–32. doi:10.1038/newbio242031a0.

Le Douarin, N. (1973) 'A biological cell labeling technique and its use in expermental embryology', *Developmental Biology*, 30(1), pp. 217–222. doi:10.1016/0012-1606(73)90061-4.

Le Douarin, N. and Kalcheim, C. (1999) *The Neural Crest*. 2nd edn. Cambridge: Cambridge University Press (Developmental and Cell Biology Series). doi:10.1017/CBO9780511897948.

Lemon, W.C. and McDole, K. (2020) 'Live-cell imaging in the era of too many microscopes', *Current Opinion in Cell Biology*, 66, pp. 34–42. doi:10.1016/j.ceb.2020.04.008.

Love, A.M., Prince, D.J. and Jessen, J.R. (2018) 'Vangl2-dependent regulation of membrane protrusions and directed migration requires a fibronectin extracellular matrix', *Development (Cambridge, England)*, 145(22), p. dev165472. doi:10.1242/dev.165472.

Lowery, L.A. and Sive, H. (2004) 'Strategies of vertebrate neurulation and a re-evaluation of teleost neural tube formation', *Mechanisms of Development*, 121(10), pp. 1189–1197. doi:10.1016/j.mod.2004.04.022.

Lumsden, A. (1990) 'The cellular basis of segmentation in the developing hindbrain', *Trends in Neurosciences*, 13(8), pp. 329–335. doi:10.1016/0166-2236(90)90144-Y.

Lumsden, A. and Keynes, R. (1989) 'Segmental patterns of neuronal development in the chick hindbrain', *Nature*, 337(6206), pp. 424–428. doi:10.1038/337424a0.

Lumsden, A., Sprawson, N. and Graham, A. (1991) 'Segmental origin and migration of neural crest cells in the hindbrain region of the chick embryo', *Development (Cambridge, England)*, 113(4), pp. 1281–1291.

Maître, J.-L. *et al.* (2012) 'Adhesion Functions in Cell Sorting by Mechanically Coupling the Cortices of Adhering Cells', *Science*, 338(6104), pp. 253–256. doi:10.1126/science.1225399.

Malin-Mayor, C. *et al.* (2021) *Automated Reconstruction of Whole-Embryo Cell Lineages by Learning from Sparse Annotations*, p. 2021.07.28.454016. doi:10.1101/2021.07.28.454016.

Manzanares, M. *et al.* (2001) 'Independent regulation of initiation and maintenance phases of Hoxa3 expression in the vertebrate hindbrain involve auto- and cross-regulatory mechanisms', *Development*, 128(18), pp. 3595–3607. doi:10.1242/dev.128.18.3595.

Maroon, H. *et al.* (2002) 'Fgf3 and Fgf8 are required together for formation of the otic placode and vesicle', *Development*, 129(9), pp. 2099–2108. doi:10.1242/dev.129.9.2099.

Martik, M.L. and Bronner, M.E. (2017) 'Regulatory logic underlying diversification of the neural crest', *Trends in genetics : TIG*, 33(10), pp. 715–727. doi:10.1016/j.tig.2017.07.015.

Mason, I. (2007) 'Initiation to end point: the multiple roles of fibroblast growth factors in neural development', *Nature Reviews Neuroscience*, 8(8), pp. 583–596. doi:10.1038/nrn2189.

Maves, L., Jackman, W. and Kimmel, C.B. (2002) 'FGF3 and FGF8 mediate a rhombomere 4 signaling activity in the zebrafish hindbrain', *Development (Cambridge, England)*, 129(16), pp. 3825–3837.

Maves, L. and Kimmel, C.B. (2005) 'Dynamic and sequential patterning of the zebrafish posterior hindbrain by retinoic acid', *Developmental Biology*, 285(2), pp. 593–605. doi:10.1016/j.ydbio.2005.07.015.

McClintock, J.M. *et al.* (2001) 'Consequences of Hox gene duplication in the vertebrates: an investigation of the zebrafish Hox paralogue group 1 genes', *Development*, 128(13), pp. 2471–2484. doi:10.1242/dev.128.13.2471.

McDole, K. *et al.* (2011) 'Lineage mapping the pre-implantation mouse embryo by two-photon microscopy, new insights into the segregation of cell fates', *Developmental biology*, 355(2), pp. 239–249. doi:10.1016/j.ydbio.2011.04.024.

McDole, K. *et al.* (2018) 'In Toto Imaging and Reconstruction of Post-Implantation Mouse Development at the Single-Cell Level', *Cell*, 175(3), pp. 859-876.e33. doi:10.1016/j.cell.2018.09.031.

McMahon, A. *et al.* (2008) 'Dynamic analyses of Drosophila gastrulation provide insights into collective cell migration', *Science (New York, N.Y.)*, 322(5907), pp. 1546–1550. doi:10.1126/science.1167094.

Megason, S.G. and Fraser, S.E. (2007a) 'Imaging in Systems Biology', *Cell*, 130(5), pp. 784–795. doi:10.1016/j.cell.2007.08.031.

Megason, S.G. and Fraser, S.E. (2007b) 'Imaging in Systems Biology', *Cell*, 130(5), pp. 784–795. doi:10.1016/j.cell.2007.08.031.

Metzis, V. *et al.* (2018) 'Nervous System Regionalization Entails Axial Allocation before Neural Differentiation', *Cell*, 175(4), pp. 1105-1118.e17. doi:10.1016/j.cell.2018.09.040.

Moen, E. *et al.* (2019) 'Accurate cell tracking and lineage construction in live-cell imaging experiments with deep learning', *bioRxiv*, p. 803205. doi:10.1101/803205.

Moens, C.B. *et al.* (1998) 'Equivalence in the genetic control of hindbrain segmentation in fish and mouse', *Development*, 125(3), pp. 381–391. doi:10.1242/dev.125.3.381.

Moens, C.B. and Prince, V.E. (2002) 'Constructing the hindbrain: insights from the zebrafish', *Developmental Dynamics: An Official Publication of the American Association of Anatomists*, 224(1), pp. 1–17. doi:10.1002/dvdy.10086.

Myers, D.C., Sepich, D.S. and Solnica-Krezel, L. (2002) 'Bmp Activity Gradient Regulates Convergent Extension during Zebrafish Gastrulation', *Developmental Biology*, 243(1), pp. 81–98. doi:10.1006/dbio.2001.0523.

Neveu, P. *et al.* (2008) 'A caged retinoic acid for one- and two-photon excitation in zebrafish embryos', *Angewandte Chemie (International Ed. in English)*, 47(20), pp. 3744–3746. doi:10.1002/anie.200800037.

Nguyen, H. *et al.* (2019) '3D + Time Imaging and Image Reconstruction of Pectoral Fin During Zebrafish Embryogenesis', *Methods in Molecular Biology (Clifton, N.J.)*, 2040, pp. 135–153. doi:10.1007/978-1-4939-9686-5_8.

Niederreither, K. *et al.* (2000) 'Retinoic acid synthesis and hindbrain patterning in the mouse embryo', *Development (Cambridge, England)*, 127(1), pp. 75–85.

Olivier, N. *et al.* (2010) 'Cell lineage reconstruction of early zebrafish embryos using label-free nonlinear microscopy', *Science (New York, N.Y.)*, 329(5994), pp. 967–971. doi:10.1126/science.1189428.

Ornitz, D.M. and Itoh, N. (2001) 'Fibroblast growth factors', *Genome Biology*, 2(3), p. reviews3005.1. doi:10.1186/gb-2001-2-3-reviews3005.

Oxtoby, E. and Jowett, T. (1993) 'Cloning of the zebrafish krox-20 gene (krx-20) and its expression during hindbrain development', *Nucleic Acids Research*, 21(5), pp. 1087–1095. doi:10.1093/nar/21.5.1087.

Pantazis, P. and Supatto, W. (2014) 'Advances in whole-embryo imaging: a quantitative transition is underway', *Nature Reviews Molecular Cell Biology*, 15(5), pp. 327–339. doi:10.1038/nrm3786.

Papan, C. and Campos-Ortega, J.A. (1994) 'On the formation of the neural keel and neural tube in the zebrafishDanio (Brachydanio) rerio', *Roux's archives of developmental biology: the official organ of the EDBO*, 203(4), pp. 178–186. doi:10.1007/BF00636333.

Parker, H.J., Bronner, M.E. and Krumlauf, R. (2014) 'A Hox regulatory network of hindbrain segmentation is conserved to the base of vertebrates', *Nature*, 514(7523), pp. 490–493. doi:10.1038/nature13723.

Parker, H.J., Bronner, M.E. and Krumlauf, R. (2016) 'The vertebrate Hox gene regulatory network for hindbrain segmentation: Evolution and diversification: Coupling of a Hox gene regulatory network to hindbrain segmentation is an ancient trait originating at the base of vertebrates', *BioEssays: News and Reviews in Molecular, Cellular and Developmental Biology*, 38(6), pp. 526–538. doi:10.1002/bies.201600010.

Parker, H.J. and Krumlauf, R. (2020) 'Chapter Six - A Hox gene regulatory network for hindbrain segmentation', in Peter, I.S. (ed.) *Current Topics in Developmental Biology*. Academic Press (Gene Regulatory Networks), pp. 169–203. doi:10.1016/bs.ctdb.2020.03.001.

Pastor-Escuredo, D. *et al.* (2021) 'Unraveling the embryonic fate map through the mechanical signature of cells and their trajectories'. doi:10.21203/rs.3.rs-333921/v1.

Pastor-Escuredo, D. and del Álamo, J.C. (2020) 'How Computation Is Helping Unravel the Dynamics of Morphogenesis', *Frontiers in Physics*, 8, p. 31. doi:10.3389/fphy.2020.00031.

Pd, N. (1999) 'The neural induction process; its morphogenetic aspects', *The International journal of developmental biology*, 43(7). Available at: https://pubmed.ncbi.nlm.nih.gov/10668971/ (Accessed: 31 January 2022).

Peterson, B.W. (1979) 'Reticulospinal Projections to Spinal Motor Nuclei', *Annual Review of Physiology*, 41(1), pp. 127–140. doi:10.1146/annurev.ph.41.030179.001015.

Pinheiro, D. and Heisenberg, C.-P. (2020) 'Chapter Twelve - Zebrafish gastrulation: Putting fate in motion', in Solnica-Krezel, L. (ed.) *Current Topics in Developmental Biology*. Academic Press (Gastrulation: From Embryonic Pattern to Form), pp. 343–375. doi:10.1016/bs.ctdb.2019.10.009.

Polevoy, H. *et al.* (2019) 'New roles for Wnt and BMP signaling in neural anteroposterior patterning', *EMBO Reports*, 20(6), p. e45842. doi:10.15252/embr.201845842.

Prin, F. *et al.* (2014) 'Hox proteins drive cell segregation and non-autonomous apical remodelling during hindbrain segmentation', *Development (Cambridge, England)*, 141(7), pp. 1492–1502. doi:10.1242/dev.098954.

PRINCE, V.E. (1998) 'Hox Genes and Segmental Patterning of the Vertebrate Hindbrain1', *American Zoologist*, 38(4), pp. 634–646. doi:10.1093/icb/38.4.634.

Prince, V.E. *et al.* (1998) 'Zebrafish hox genes: expression in the hindbrain region of wild-type and mutants of the segmentation gene, valentino', *Development (Cambridge, England)*, 125(3), pp. 393–406.

Pujades, C. (2020) 'The multiple functions of hindbrain boundary cells: Tinkering boundaries?', *Seminars in Cell & Developmental Biology*, 107, pp. 179–189. doi:10.1016/j.semcdb.2020.05.002.

Qiu, Y. *et al.* (2021) 'Multiple morphogens and rapid elongation promote segmental patterning during development', *PLOS Computational Biology*, 17(6), p. e1009077. doi:10.1371/journal.pcbi.1009077.

Quesada-Hernández, E. *et al.* (2010) 'Stereotypical Cell Division Orientation Controls Neural Rod Midline Formation in Zebrafish', *Current Biology*, 20(21), pp. 1966–1972. doi:10.1016/j.cub.2010.10.009.

Reifers, F. *et al.* (1998) 'Fgf8 is mutated in zebrafish acerebellar (ace) mutants and is required for maintenance of midbrain-hindbrain boundary development and somitogenesis', *Development (Cambridge, England)*, 125(13), pp. 2381–2395.

Riley, B.B. *et al.* (2004) 'Rhombomere boundaries are Wnt signaling centers that regulate metameric patterning in the zebrafish hindbrain', *Developmental Dynamics: An Official Publication of the American Association of Anatomists*, 231(2), pp. 278–291. doi:10.1002/dvdy.20133.

Rocha, M. *et al.* (2020) 'Neural crest development: insights from the zebrafish', *Developmental Dynamics: An Official Publication of the American Association of Anatomists*, 249(1), pp. 88–111. doi:10.1002/dvdy.122.

Roehl, H. and Nüsslein-Volhard, C. (2001) 'Zebrafish pea3 and erm are general targets of FGF8 signaling', *Current biology: CB*, 11(7), pp. 503–507. doi:10.1016/s0960-9822(01)00143-9.

Rogers, K.W. and Müller, P. (2020) 'Optogenetic approaches to investigate spatiotemporal signaling during development', *Current Topics in Developmental Biology*, 137, pp. 37–77. doi:10.1016/bs.ctdb.2019.11.009.

Rogers, K.W. and Schier, A.F. (2011) 'Morphogen gradients: from generation to interpretation', *Annual Review of Cell and Developmental Biology*, 27, pp. 377–407. doi:10.1146/annurev-cellbio-092910-154148.

Rohrschneider, M.R., Elsen, G.E. and Prince, V.E. (2007) 'Zebrafish Hoxb1a regulates multiple downstream genes including prickle1b', *Developmental Biology*, 309(2), pp. 358–372. doi:10.1016/j.ydbio.2007.06.012.

Roszko, I. *et al.* (2015) 'A dynamic intracellular distribution of Vangl2 accompanies cell polarization during zebrafish gastrulation', *Development (Cambridge, England)*, 142(14), pp. 2508–2520. doi:10.1242/dev.119032.

Roy, N.M. and Sagerström, C.G. (2004) 'An early Fgf signal required for gene expression in the zebrafish hindbrain primordium', *Brain Research. Developmental Brain Research*, 148(1), pp. 27–42. doi:10.1016/j.devbrainres.2003.10.005.

Schier, A.F. and Talbot, W.S. (2005) 'Molecular Genetics of Axis Formation in Zebrafish', *Annual Review of Genetics*, 39(1), pp. 561–613. doi:10.1146/annurev.genet.37.110801.143752.

Schilling, T.F. and Kimmel, C.B. (1994) 'Segment and cell type lineage restrictions during pharyngeal arch development in the zebrafish embryo', *Development*, 120(3), pp. 483–494. doi:10.1242/dev.120.3.483.

Schmitz, B., Papan, C. and Campos-Ortega, J.A. (1993) 'Neurulation in the anterior trunk region of the zebrafish Brachydanio rerio', *Roux's archives of developmental biology*, 202(5), pp. 250–259. doi:10.1007/BF00363214.

Schneider-Maunoury, S. *et al.* (1993) 'Disruption of Krox-20 results in alteration of rhombomeres 3 and 5 in the developing hindbrain', *Cell*, 75(6), pp. 1199–1214. doi:10.1016/0092-8674(93)90329-O.

Schneider-Maunoury, S. *et al.* (1997) '[Role of the Krox-20 gene in the development of rhombencephalon]', *Comptes Rendus Des Seances De La Societe De Biologie Et De Ses Filiales*, 191(1), pp. 91–94.

Sepich, D.S. *et al.* (2000) 'Role of the zebrafish trilobite locus in gastrulation movements of convergence and extension', *Genesis (New York, N.Y.: 2000)*, 27(4), pp. 159–173. doi:10.1002/1526-968x(200008)27:4<159::aid-gene50>3.0.co;2-t.

Shah, G. *et al.* (2019) 'Multi-scale imaging and analysis identify pan-embryo cell dynamics of germlayer formation in zebrafish', *Nature Communications*, 10(1), p. 5753. doi:10.1038/s41467-019-13625-0.

Sharma, P. *et al.* (2019) 'Single cell dynamics of embryonic muscle progenitor cells in zebrafish', *Development*, 146(14). doi:10.1242/dev.178400.

Shimozono, S. *et al.* (2013) 'Visualization of an endogenous retinoic acid gradient across embryonic development', *Nature*, 496(7445), pp. 363–366. doi:10.1038/nature12037.

Simões-Costa, M. and Bronner, M.E. (2015) 'Establishing neural crest identity: a gene regulatory recipe', *Development (Cambridge, England)*, 142(2), pp. 242–257. doi:10.1242/dev.105445.

Sirbu, I.O. *et al.* (2005) 'Shifting boundaries of retinoic acid activity control hindbrain segmental gene expression', *Development*, 132(11), pp. 2611–2622. doi:10.1242/dev.01845.

Sivak, J.M., Petersen, L.F. and Amaya, E. (2005) 'FGF signal interpretation is directed by Sprouty and Spred proteins during mesoderm formation', *Developmental Cell*, 8(5), pp. 689–701. doi:10.1016/j.devcel.2005.02.011.

Smutny, M. *et al.* (2017) 'Friction forces position the neural anlage', *Nature cell biology*, 19(4), pp. 306–317. doi:10.1038/ncb3492.

Solnica-Krezel, L. and Sepich, D.S. (2012) 'Gastrulation: making and shaping germ layers', *Annual Review of Cell and Developmental Biology*, 28, pp. 687–717. doi:10.1146/annurev-cellbio-092910-154043.

Strnad, P. *et al.* (2016) 'Inverted light-sheet microscope for imaging mouse pre-implantation development', *Nature Methods*, 13(2), pp. 139–142. doi:10.1038/nmeth.3690.

Sturgeon, K. *et al.* (2011) 'Cdx1 refines positional identity of the vertebrate hindbrain by directly repressing Mafb expression', *Development (Cambridge, England)*, 138(1), pp. 65–74. doi:10.1242/dev.058727.

Sugawara, K., Cevrim, C. and Averof, M. (2021) *Tracking cell lineages in 3D by incremental deep learning*, p. 2021.02.26.432552. doi:10.1101/2021.02.26.432552.

Sun, Z. *et al.* (2006) 'Sp5l is a mediator of Fgf signals in anteroposterior patterning of the neuroectoderm in zebrafish embryo', *Developmental Dynamics*, 235(11), pp. 2999–3006. doi:10.1002/dvdy.20945.

Suster, M.L. *et al.* (2009) 'Transgenesis in zebrafish with the tol2 transposon system', *Methods in Molecular Biology (Clifton, N.J.)*, 561, pp. 41–63. doi:10.1007/978-1-60327-019-9_3.

Takacs, C.M. and Giraldez, A.J. (2016) 'miR-430 regulates oriented cell division during neural tube development in zebrafish', *Developmental Biology*, 409(2), pp. 442–450. doi:10.1016/j.ydbio.2015.11.016.

Tambalo, M., Mitter, R. and Wilkinson, D.G. (2020) 'A single cell transcriptome atlas of the developing zebrafish hindbrain', *Development (Cambridge, England)*, 147(6), p. dev184143. doi:10.1242/dev.184143.

Tawk, M. *et al.* (2007) 'A mirror-symmetric cell division that orchestrates neuroepithelial morphogenesis', *Nature*, 446(7137), pp. 797–800. doi:10.1038/nature05722.

Thisse, B. and Thisse, C. (2005) 'Functions and regulations of fibroblast growth factor signaling during embryonic development', *Developmental Biology*, 287(2), pp. 390–402. doi:10.1016/j.ydbio.2005.09.011.

Tinevez, J.-Y. *et al.* (2017) 'TrackMate: An open and extensible platform for single-particle tracking', *Methods (San Diego, Calif.)*, 115, pp. 80–90. doi:10.1016/j.ymeth.2016.09.016.

Torbey, P. *et al.* (2018) 'Cooperation, cis-interactions, versatility and evolutionary plasticity of multiple cis-acting elements underlie krox20 hindbrain regulation', *PLOS Genetics*, 14(8), p. e1007581. doi:10.1371/journal.pgen.1007581.

Trainor, P.A. (2003) 'Making Headway: The Roles of Hox Genes and Neural Crest Cells in Craniofacial Development', *The Scientific World Journal*, 3, pp. 240–264. doi:10.1100/tsw.2003.11.

Trinh, L.A. and Fraser, S.E. (2015) 'Chapter Twenty-one - Imaging the Cell and Molecular Dynamics of Craniofacial Development: Challenges and New Opportunities in Imaging Developmental Tissue Patterning', in Chai, Y. (ed.) *Current Topics in Developmental Biology*. Academic Press (Craniofacial Development), pp. 599–629. doi:10.1016/bs.ctdb.2015.09.002.

Tsai, T.Y.-C. *et al.* (2020) 'An adhesion code ensures robust pattern formation during tissue morphogenesis', *Science*, 370(6512), pp. 113–116. doi:10.1126/science.aba6637.

Tuduce, I.L. *et al.* (2009) '03-P026 Retinoic acid – planar cell polarity crosstalk during neural tube closure', *Mechanisms of Development*, 126, p. S75. doi:10.1016/j.mod.2009.06.079.

Tümpel, S., Wiedemann, L.M. and Krumlauf, R. (2009) 'Chapter 8 Hox Genes and Segmentation of the Vertebrate Hindbrain', in *Current Topics in Developmental Biology*. Academic Press (Genes), pp. 103–137. doi:10.1016/S0070-2153(09)88004-6.

Vaage, S. (1969) 'The segmentation of the primitive neural tube in chick embryos (Gallus domesticus). A morphological, histochemical and autoradiographical investigation', *Ergebnisse Der Anatomie Und Entwicklungsgeschichte*, 41(3), pp. 3–87.

Veldman, M.B. and Lin, S. (2008) 'Zebrafish as a Developmental Model Organism for Pediatric Research', *Pediatric Research*, 64(5), pp. 470–476. doi:10.1203/PDR.0b013e318186e609.

Villoutreix, P. *et al.* (2016) 'An integrated modelling framework from cells to organism based on a cohort of digital embryos', *Scientific Reports*, 6(1), p. 37438. doi:10.1038/srep37438.

Voltes, A. *et al.* (2019) 'Yap/Taz-TEAD activity links mechanical cues to progenitor cell behavior during zebrafish hindbrain segmentation', *Development*, 146(14). doi:10.1242/dev.176735.

Wagner, D.E. *et al.* (2018) 'Single-cell mapping of gene expression landscapes and lineage in the zebrafish embryo', *Science (New York, N.Y.)*, 360(6392), pp. 981–987. doi:10.1126/science.aar4362.

Wallingford, J.B. (2019) 'The 200-year effort to see the embryo', *Science*, 365(6455), pp. 758–759. doi:10.1126/science.aaw7565.

Walshe, J. *et al.* (2002) 'Establishment of Hindbrain Segmental Identity Requires Signaling by FGF3 and FGF8', *Current Biology*, 12(13), pp. 1117–1123. doi:10.1016/S0960-9822(02)00899-0.

Wan, Y. *et al.* (2019) 'Single-Cell Reconstruction of Emerging Population Activity in an Entire Developing Circuit', *Cell*, 179(2), pp. 355-372.e23. doi:10.1016/j.cell.2019.08.039.

Wan, Y., McDole, K. and Keller, P.J. (2019) 'Light-Sheet Microscopy and Its Potential for Understanding Developmental Processes', *Annual Review of Cell and Developmental Biology*, 35(1), pp. 655–681. doi:10.1146/annurev-cellbio-100818-125311.

Wang, Q. *et al.* (2017) 'Cell Sorting and Noise-Induced Cell Plasticity Coordinate to Sharpen Boundaries between Gene Expression Domains', *PLOS Computational Biology*, 13(1), p. e1005307. doi:10.1371/journal.pcbi.1005307.

Warga, R.M. and Kimmel, C.B. (1990) 'Cell movements during epiboly and gastrulation in zebrafish', *Development (Cambridge, England)*, 108(4), pp. 569–580.

Wassef, M.A. *et al.* (2008) 'Rostral hindbrain patterning involves the direct activation of a Krox20 transcriptional enhancer by Hox/Pbx and Meis factors', *Development (Cambridge, England)*, 135(20), pp. 3369–3378. doi:10.1242/dev.023614.

Westerfield, Monte. (2007) *The zebrafish book : a guide for the laboratory use of zebrafish (Danio rerio)*.

White, R.J. *et al.* (2007) 'Complex Regulation of cyp26a1 Creates a Robust Retinoic Acid Gradient in the Zebrafish Embryo', *PLOS Biology*, 5(11), p. e304. doi:10.1371/journal.pbio.0050304.

White, R.J. and Schilling, T.F. (2008) 'How degrading: Cyp26s in hindbrain development', *Developmental Dynamics*, 237(10), pp. 2775–2790. doi:10.1002/dvdy.21695.

White, R.M. *et al.* (2008) 'Transparent adult zebrafish as a tool for in vivo transplantation analysis', *Cell Stem Cell*, 2(2), pp. 183–189. doi:10.1016/j.stem.2007.11.002.

Wiellette, E.L. and Sive, H. (2003) 'vhnf1 and Fgf signals synergize to specify rhombomere identity in the zebrafish hindbrain', *Development (Cambridge, England)*, 130(16), pp. 3821–3829. doi:10.1242/dev.00572.

Wilkinson, D.G. *et al.* (1989) 'Segment-specific expression of a zinc-finger gene in the developing nervous system of the mouse', *Nature*, 337(6206), pp. 461–464. doi:10.1038/337461a0.

Wilkinson, D.G. (2018) 'Establishing sharp and homogeneous segments in the hindbrain', *F1000Research*, 7, p. F1000 Faculty Rev-1268. doi:10.12688/f1000research.15391.1.

Williams, M.L.K. and Solnica-Krezel, L. (2020) 'Cellular and molecular mechanisms of convergence and extension in zebrafish', *Current Topics in Developmental Biology*, 136, pp. 377–407. doi:10.1016/bs.ctdb.2019.08.001.

Wizenmann, A. and Lumsden, A. (1997) 'Segregation of rhombomeres by differential chemoaffinity', *Molecular and Cellular Neurosciences*, 9(5–6), pp. 448–459. doi:10.1006/mcne.1997.0642.

Wolf, S., Wan, Y. and McDole, K. (2021) 'Current approaches to fate mapping and lineage tracing using image data', *Development*, 148(18). doi:10.1242/dev.198994.

Woo, K. and Fraser, S.E. (1995) 'Order and coherence in the fate map of the zebrafish nervous system', *Development (Cambridge, England)*, 121(8), pp. 2595–2609.

Woo, K. and Fraser, S.E. (1997) 'Specification of the Zebrafish Nervous System by Nonaxial Signals', *Science*, 277(5323), pp. 254–257. doi:10.1126/science.277.5323.254.

Woo, K. and Fraser, S.E. (1998) 'Specification of the hindbrain fate in the zebrafish', *Developmental Biology*, 197(2), pp. 283–296. doi:10.1006/dbio.1998.8870.

Woo, K., Shih, J. and Fraser, S.E. (1995) 'Fate maps of the zebrafish embryo', *Current Opinion in Genetics & Development*, 5(4), pp. 439–443. doi:10.1016/0959-437X(95)90046-J.

Woodworth, M.B., Girskis, K.M. and Walsh, C.A. (2017) 'Building a lineage from single cells: genetic techniques for cell lineage tracking', *Nature reviews. Genetics*, 18(4), pp. 230–244. doi:10.1038/nrg.2016.159.

Wu, Y. *et al.* (2011) 'Inverted selective plane illumination microscopy (iSPIM) enables coupled cell identity lineaging and neurodevelopmental imaging in Caenorhabditis elegans', *Proceedings of the National Academy of Sciences*, 108(43), pp. 17708–17713. doi:10.1073/pnas.1108494108.

Xu, L. *et al.* (2012) 'Spatiotemporal manipulation of retinoic acid activity in zebrafish hindbrain development via photo-isomerization', *Development (Cambridge, England)*, 139(18), pp. 3355–3362. doi:10.1242/dev.077776.

Xu, Q. *et al.* (1999) 'In vivo cell sorting in complementary segmental domains mediated by Eph receptors and ephrins', *Nature*, 399(6733), pp. 267–271. doi:10.1038/20452.

Xu, Q. and Wilkinson, D.G. (2013) 'Boundary formation in the development of the vertebrate hindbrain', *Wiley Interdisciplinary Reviews. Developmental Biology*, 2(5), pp. 735–745. doi:10.1002/wdev.106.

Yang, X. *et al.* (2002) 'Cell movement patterns during gastrulation in the chick are controlled by positive and negative chemotaxis mediated by FGF4 and FGF8', *Developmental Cell*, 3(3), pp. 425–437. doi:10.1016/s1534-5807(02)00256-3.

Zhang, F., Nagy Kovács, E. and Featherstone, M.S. (2000) 'Murine hoxd4 expression in the CNS requires multiple elements including a retinoic acid response element', *Mechanisms of Development*, 96(1), pp. 79–89. doi:10.1016/s0925-4773(00)00377-4.

Zhang, M. *et al.* (1994) 'Ectopic Hoxa-1 induces rhombomere transformation in mouse hindbrain', *Development (Cambridge, England)*, 120(9), pp. 2431–2442.

Zhang, W. *et al.* (2018) 'Control of Protein Activity and Gene Expression by Cyclofen-OH Uncaging', *ChemBioChem*, 19(12), pp. 1232–1238. doi:10.1002/cbic.201700630.

Zhang, Y. *et al.* (2020) 'Lineage tracing: technology tool for exploring the development, regeneration, and disease of the digestive system', *Stem Cell Research & Therapy*, 11(1), p. 438. doi:10.1186/s13287-020-01941-y.

Žigman, M. *et al.* (2011) 'Zebrafish Neural Tube Morphogenesis Requires Scribble-Dependent Oriented Cell Divisions', *Current biology : CB*, 21(1), pp. 79–86. doi:10.1016/j.cub.2010.12.005.

Zigman, M. *et al.* (2014) 'Hoxb1b controls oriented cell division, cell shape and microtubule dynamics in neural tube morphogenesis', *Development (Cambridge, England)*, 141(3), pp. 639–649. doi:10.1242/dev.098731.

université PARIS-SACLAY
ÉCOLE DOCTORALE
Signalisations et réseaux intégratifs en biologie (BIOSIGNE)

Titre : Dynamique cellulaire et régulation génétique de la morphogenèse du cerveau postérieur du poisson zèbre

Mots clés : Embryogenèse, Rhombencephale, Segmentation, Carte du destin, Acide rétinoïque, Imagerie 3D+temps

Résumé : Au cours du développement embryonnaire, le cerveau est classiquement divisé en trois unités fonctionnelles et anatomiques, à savoir le cerveau antérieur, moyen et postérieur. Le cerveau postérieur utilise la segmentation comme stratégie pour organiser les nerfs crâniens et les flux de cellules de la crête neurale. La segmentation transitoire du cerveau postérieur conduit à 7/8 unités cellulaires répétées le long de l'axe antéro-postérieur (AP) appelés rhombomères (r). Ce processus conservé au cours de l'évolution établit le plan de la tête des vertébrés. Les mécanismes moléculaires sous-jacents à la segmentation du cerveau postérieur ont été largement étudiés. Notre objectif est d'étudier la formation des r au niveau cellulaire chez le poisson zèbre, un modèle vertébré star de la biologie. Nous avons besoin de la carte précise du destin et de la dynamique cellulaire qui mène du domaine des progéniteurs à l'organe. La carte actuelle du destin du système nerveux central du poisson aux stades précoce et tardif de la gastrula a été publiée en 1995. Elle a été obtenue par une reconstruction partielle du lignage grâce à un colorant fluorescent. La frontière précise des domaines de progéniteurs des r et les dynamiques cellulaire qui façonnent le cerveau postérieur sont inconnues. En utilisant l'imagerie par microscopie de pointe de poissons transgéniques et des outils de traitement d'image automatisés, nous avons reconstruit le lignage de r2-r6 de la mi gastrulation à la neurulation précoce. Nous fournissons une carte du destin plus fine et dynamique du cerveau postérieur de 6 à 15hpf. Les domaines de progéniteurs sont alignés le long des axes AP et dorso-ventral (DV) dès le stade du bouclier embryonnaire. Ils présentent une organisation AP parallèle à la marge du blastoderme. La ségrégation DV des r est établie par une distribution des progéniteurs le long de l'axe DV tel que ceux situés dans la partie dorsale du blastoderme vont former le domaine ventral des r. Notre étude donne un aperçu de l'origine clonale, de la prolifération cellulaire et des voies de migration des progéniteurs au cours de la mise en place du rhombencéphale.
Nous avons exploré le rôle des voies de signalisation de l'acide rétinoïque (AR) et du facteur de croissance des fibroblastes (FGF) dans la morphogenèse du cerveau postérieur. On pense que les gradients des morphogènes AR et FGF spécifient et modèlent les ébauches du cerveau postérieur en sept segments d'identités distinctes. L'inhibition de l'AR à l'aide de drogue entraîne une perte progressive des r postérieurs, dépendante de sa concentration. De même, il y a une perte d'expression de leurs marqueurs moléculaires. On suppose que l'expansion des r antérieurs se fait au détriment des postérieurs. Nous ne savons pas comment la morphogenèse des domaines de progéniteurs conduit à ce défaut. Nous avons établi la carte dynamique du destin du cerveau postérieur de l'embryon AR nul. L'organisation des domaines de progéniteurs est en correspondance avec la position et la taille des segments modifiés, i.e. l'expansion des domaines des progéniteurs antérieurs. De plus, le mouvement de convergence des cellules est retardé ce qui est une conséquence précoce du gradient AR altéré. Il en résulte des accumulations ectopiques de progéniteurs neuraux et des anomalies du tube neural. Notre phénotype rappelle celui du mutant *trilobite* de *Vangl2* acteur dans la voie de signalisation de polarité cellulaire planaire (PCP). Il a été montré dans l'embryon de souris *Raldh2-/-* que le déficit en AR provoque une forte inhibition de *Vangl2* et *Fzd3* au niveau du cerveau postérieur et de la moelle épinière. Dans l'ensemble, nos données suggèrent que les défauts du tube neural dans l'embryon AR nul sont dus à l'altération de la signalisation PCP. De plus, nous avons démontré l'effet de communauté de l'AR sur les gènes cibles et la morphogenèse du cerveau postérieur par la restauration optogénétique du morphogène dans l'embryon vivant.

Title : Cell dynamics and genetic regulation of zebrafish hindbrain morphogenesis

Keywords : Embryogenesis, Hindbrain, Segmentation, Fate map, Retinoic acid, 3D+time imaging

Abstract : The brain is often considered the most complex organ. During embryonic development, the brain is classically divided into three functional and anatomical units namely, fore, mid and hindbrain. Hindbrain, the posterior part utilises segmentation as a strategy to organise its diverse range of cranial nerves and the streams of neural crest cells. The transient segmentation of hindbrain leads to 7/8 repeated cellular units of segments in the antero-posterior axis (AP) called rhombomeres. Hindbrain segmentation patterns the head and is conserved among vertebrates. Molecular mechanisms that underlie hindbrain segmentation have been vastly investigated. We aim to study the formation of the rhombomeres at cellular level in zebrafish, a vertebrate model at the forefront of developmental biology. We need the precise fate map and the cell dynamics that lead from the progenitors' domains to the organ. The current fate map of the zebrafish central nervous system (CNS) at early and late gastrula stages was published in 1995. It was obtained through sparse lineage tracing with a fluorescent dye. The precise border of the rhombomere progenitor domains and the cell dynamics that shape the hindbrain are unknown. Utilising advanced microscopy imaging of transgenic zebrafish lines and automated image processing tools, we developed a method to reconstruct the cell lineage of rhombomeres r2-r6 from mid-gastrulation through early neurulation. We provide a finer and dynamic fate map of zebrafish hindbrain from 6hpf till 15hpf. The rhombomere progenitor domains are aligned along the AP and dorso-ventral (DV) axes as early as the shield stage. Rhombomere progenitor domains exhibit AP organisation parallel to the blastoderm margin. The DV segregation of the rhombomeres is set by distribution of the progenitors along the DV axis at the shield stage. Progenitors located at the most dorsal part of the blastoderm will form the ventral domain of the rhombomeres. Our study gives insights into the clonal origin, cell proliferation and migration paths of hindbrain's rhombomere progenitors throughout the early steps of the organ morphogenesis.
We used our method to explore the role of the signalling pathways Retinoic acid (RA) and Fibroblast Growth Factor (FGF) in hindbrain morphogenesis RA and FGF morphogen gradients are thought to specify and pattern the hindbrain primordia into seven segments with different identities. RA inhibition upon drug treatment leads to progressive loss of posterior rhombomeres in a concentration dependent manner. Concomitantly, there is a loss of expression of their molecular markers. It is presumed the expansion of anterior rhombomeres happens at the expense of the posterior ones. How the morphogenesis of the progenitor domains leads to this phenotypic defect is not known. We investigate the cellular events, cell proliferation and cell movements from the dynamic fate map under RA-null condition. We identified the progenitor domains whose organisation is in correspondence with the position and size of the modified segments i.e. the expansion of anterior progenitors' domains. We also observed a delayed convergence movement that is an early consequence of the altered RA gradient. Consequently, it results in ectopic neural progenitor accumulations and neural tube defects. Our phenotype is reminiscent of the *trilobite* mutant of *vangl2,* that is a component of planer cell polarity (PCP) pathway. It was shown in mouse *Raldh2-/-* embryo that RA deficiency causes a strong downregulation of *Vangl2* and *Fzd3* at the level of hindbrain and spinal cord. Altogether our data suggests that neural tube defects in zebrafish RA-null embryo is due to the alteration in the PCP signalling. We demonstrated the community effect of RA signalling on target genes and hindbrain morphogenesis. Optogenetic restoration of RA in r5 progenitors at mid-gastrulation on one half of the embryo rescued the whole posterior rhombomere formation.